



Hassan Awadat Salem

**RESEARCH OF THE RELEVANT  
TEMPERATURES FOR THE DESIGN OF  
PAVEMENT CONSTRUCTIONS ON THE  
DESERT ROADS IN LIBYA**

Dissertation submitted to the University of Novi Sad,  
Faculty of Technical Sciences,  
in partial fulfillment of the requirements for the degree of  
Doctor of Philosophy, Civil Engineering

**Novi Sad (2015)**



**UNIVERSITY NOVI SAD**  
FACULTY OF TECHNICAL  
SCIENCES



**RESEARCH OF THE RELEVANT TEMPERATURES  
FOR THE DESIGN OF PAVEMENT CONSTRUCTIONS  
ON THE DESERT ROADS IN LIBYA**

**ИСТРАЖИВАЊЕ МЕРОДАВНИХ  
ТЕМПЕРАТУРА ЗА ПРОЈЕКТОВАЊЕ КОЛОВОЗНИХ  
КОНСТРУКЦИЈА ПУСТИЊСКИХ ПУТЕВА У  
ЛИБИЈИ**

Dissertation submitted to the University of Novi Sad,  
Faculty of Technical Sciences,  
in partial fulfillment of the requirements for the degree of  
Doctor of Philosophy, Civil Engineering

Candidate:


*Hassan Awadat Salem*

Mentors:

*Uzelac Đorđe*

*Matić Bojan*

## Novi Sad (2015)

	<b>UNIVERSITY OF NOVI SAD • FACULTY OF TECHNICAL SCIENCES</b> 21000 NOVI SAD, Trg Dositeja Obradovića 6
<b>КЉУЧНА ДОКУМЕНТАЦИЈСКА ИНФОРМАЦИЈА</b>	

Accession number, <b>ANO</b> :	
Identification number, <b>INO</b> :	
Document type, <b>DT</b> :	Elaborate of PhD Thesis
Type of record, <b>TR</b> :	
Contents code, <b>CC</b> :	Doctor Thesis
Author, <b>AU</b> :	Msc. Hassan Awadat Salem
Mentor, <b>MN</b> :	Prof. Djordje Uzelac, PhD, CE Asst. Prof. Bojan Matić, PhD, CE
Title, <b>TI</b> :	Research of the relevant temperatures for the design of pavement constructions on the desert roads in Libya
Language of text, <b>LT</b> :	English
Language of abstract, <b>LA</b> :	Serbian, English
Country of publication, <b>CP</b> :	Serbia
Locality of publication, <b>LP</b> :	Vojvodina
Publication year, <b>PY</b> :	2015
Publisher, <b>PB</b> :	University of Novi Sad, Faculty of Technical Sciences
Publication place, <b>PP</b> :	21000 Novi Sad, Trg Dositeja Obradovića 6
Physical description, <b>PD</b> : <small>(chapters/pages/ref./tables/pictures/graphs/appendixes)</small>	7 chapters, 244 pages, 64 references, 214 tables, 83 figures, 16 appendixes
Scientific field, <b>SF</b> :	Civil Engineering
Scientific discipline, <b>SD</b> :	Roads
Subject/Key words, <b>S/KW</b> :	Pavement, temperatures, predicting, model, asphalt, SHRP, LTPP, PG, Libya
<b>UC</b>	
Holding data, <b>HD</b> :	
Note, <b>N</b> :	

Abstract, <b>AB</b> :	<p>Asphalt pavements form an important, integral part of any transportation system. The structural capacity of the hot mix asphalt concrete layers depends on many factors including its temperature. Moreover, temperature can be a major contributor to several types of distress. Therefore, temperature is a significant factor that affects the performance and life span of a pavement. The Libyan road network expanded at a phenomenal pace from approximately 10,000 km of paved roads in 1980, to more than 34,000 km in 2010. The study area is located on the southern of Libya at latitude between (24°17'N) and (30°11'N) in the desert of Libya. With the recent SHRP and LTTP research findings, it was necessary to investigate the applicability of the models developed from these research studies to the study area region's environmental conditions and more generally to the rest Libya desert reigns. This research presents the investigations undertaken to develop models to predict high and low asphalt pavement temperatures in study area regions. A pavement monitoring station was set-up at the regions to monitor air, pavement temperatures in different depth, wind speed and solar radiation. Data were collected for 365 days. Daily minimum and maximum temperatures were recorded. A regression analysis was used to develop the minimum and maximum pavement temperature models, using air temperature, wind speed and solar radiation. This research presents a new model for predicting maximum and minimum of pavement layers temperature based on data collected by installed pavement monitoring station. The study area was divided into different "performance grade zones" – zones with different extreme temperatures for bitumen "PG" gradation - on the basis of previous 10 years temperature data collected from 10 weather stations. Also a temperature and "PG" zoning map has been proposed to be implemented in Libya desert area.</p>	
Accepted by the Scientific Board on, <b>ASB</b> :	SB of Faculty of Technical Sciences: SB of University:	
Defended on, <b>DE</b> :		
Defended Board, <b>DB</b> :	President:	Prof. Milinko Vasić, PhD
	Member:	Prof. Vlastimir Radonjanin, PhD, CE
	Member:	Prof. Mitar Đogo, PhD, CE
	Member:	Prof. Drađan Lukić, PhD, CE
	Member, Mentor:	Prof. Đorđe Uzelac, PhD, CE
	Member, Mentor:	Ass. Prof. Bojan Matić, PhD, CE
		Menthor's sign



УНИВЕРЗИТЕТ У НОВОМ САДУ ● ФАКУЛТЕТ ТЕХНИЧКИХ НАУКА  
21000 НОВИ САД, Трг Доситеја Обрадовића 6

## КЉУЧНА ДОКУМЕНТАЦИЈСКА ИНФОРМАЦИЈА

Редни број, <b>РБР:</b>	
Идентификациони број, <b>ИБР:</b>	
Тип документације, <b>ТД:</b>	Елаборат докторске дисертације
Тип записа, <b>ТЗ:</b>	
Врста рада, <b>ВР:</b>	Докторска теза
Аутор, <b>АУ:</b>	Хасан Авадат Салем
Ментор, <b>МН:</b>	Проф. др Ђорђе Узелац, диг Доц. др Бојан Матић, диг.
Наслов рада, <b>НР:</b>	Истраживање меродавних температура за пројектовање коловозних конструкција пустињских путева у Либији
Језик публикације, <b>ЈП:</b>	Енглески
Језик извода, <b>ЈИ:</b>	Српски и енглески
Земља публикавања, <b>ЗП:</b>	Србија
Уже географско подручје, <b>УГП:</b>	Војводина
Година, <b>ГО:</b>	2015
Издавач, <b>ИЗ:</b>	Факултет техничких наука
Место и адреса, <b>МА:</b>	Трг Доситеја Обрадовића 6
Физички опис рада, <b>ФО:</b> (поглавља/страна/ цитата/табела/слика/графика/прилога)	7 поглавља, 244 страна, 64 цитата, 214 табела, 83 слика и графика, 16 прилога
Научна област, <b>НО:</b>	Грађевинарство
Научна дисциплина, <b>НД:</b>	Саобраћајнице
Предметна одредница/Кључне речи, <b>ПО:</b>	Коловоз, температура, предвиђање, асфалт, модел, SHRP, LTPP, PG, Либија
<b>УДК</b>	
Чува се, <b>ЧУ:</b>	
Важна напомена, <b>ВН:</b>	

Извод, ИЗ:	<p>Асфалтни коловози чине важан, интегрални деосваког транспортног система. Носивост слојева од асфалтних мешавина зависи од више фактора, укључујући температуру. Штавише, температура асфалта може бити главни фактор код развоја неких оштећења па зато има велики утицај на перформансе и животни век коловоза. Мрежа либијских путева се развијала великом брзином од око 10 000 km путева са савременим застором 1980. године до више од 34 000 km у 2010-ој години. Студија је спроведена у либијској пустињи, у јужном делу Либије, на географским ширинама између 24°17'N и 30°11'N. Моделе развијене у оквиру истраживачких програма SHRP и LTPP било је потребно проверити у амбијенталним условима какви су у подручју обухваћеном Студијом, односно генерално, у пустињском делу Либије. Овај истраживачки одухват чине истраживања спроведена у циљу формирања модела за предвиђање високих и ниских температура асфалтног коловоза у предметном региону. Успостављене су мониторинг станице за праћење температуре ваздуха, температуре коловоза на различитим дубинама, брзине ветра и сунчевог зрачења. Подаци су прикупљени за 365 дана. Снимљене су максималне и минималне дневне температуре, а затим је извршена регресиона анализа за моделирање максималне и минималне температуре коловоза на основу температуре ваздуха, брзине ветра и сунчевог зрачења. Истраживањем је формиран нови модел за предвиђање минималне и максималне температуре у слојевима коловозне конструкције заснован на подацима прикупљеним помоћу мониторинг станица. Подручје које је било предмет истраживања, подељено је на 10 "PG" зона – према различитим екстремним температурама за PG градацију битумена – на основу десетогодишњих података прикупљених са 10 климатолошких станица. Накрају се предлаже мапа са температурним, односно "PG" зонама либијске пустиње.</p>															
Датум прихватања теме, ДП:	<p>ННВ Факултета техничких наука: ННВ Универзитета:</p>															
Датум одбране, ДО:																
Чланови комисије, КО:	<table border="1"> <tr> <td data-bbox="659 1245 794 1272">Председник:</td> <td data-bbox="794 1245 1201 1272">Проф. др Милинко Васић</td> </tr> <tr> <td data-bbox="659 1272 794 1299">Члан:</td> <td data-bbox="794 1272 1201 1299">Проф. др Властимир Радоњанин</td> </tr> <tr> <td data-bbox="659 1299 794 1326">Члан:</td> <td data-bbox="794 1299 1201 1326">Проф. др Митар Ђого</td> </tr> <tr> <td data-bbox="659 1326 794 1352">Члан:</td> <td data-bbox="794 1326 1201 1352">Проф. др Драган Лукић</td> </tr> <tr> <td data-bbox="659 1352 794 1379">Члан, ментор:</td> <td data-bbox="794 1352 1201 1379">Проф. др Ђорђе Узелац</td> </tr> <tr> <td data-bbox="659 1379 794 1444">Члан, ментор:</td> <td data-bbox="794 1379 1201 1444">Доц. др Бојан Матић</td> </tr> </table>	Председник:	Проф. др Милинко Васић	Члан:	Проф. др Властимир Радоњанин	Члан:	Проф. др Митар Ђого	Члан:	Проф. др Драган Лукић	Члан, ментор:	Проф. др Ђорђе Узелац	Члан, ментор:	Доц. др Бојан Матић	<table border="1"> <tr> <td data-bbox="1201 1245 1479 1379">Потпис ментора</td> </tr> <tr> <td data-bbox="1201 1379 1479 1444"></td> </tr> </table>	Потпис ментора	
Председник:	Проф. др Милинко Васић															
Члан:	Проф. др Властимир Радоњанин															
Члан:	Проф. др Митар Ђого															
Члан:	Проф. др Драган Лукић															
Члан, ментор:	Проф. др Ђорђе Узелац															
Члан, ментор:	Доц. др Бојан Матић															
Потпис ментора																

# **RESEARCH OF THE RELEVANT TEMPERATURES FOR THE DESIGN OF PAVEMENT CONSTRUCTIONS ON THE DESERT ROADS IN LIBYA**

**Hasan Awadat Salem**

## **ABSTRACT**

Asphalt pavements form an important and integral part of any transportation system. The structural capacity of the hot mix asphalt concrete layers depends on many factors including its temperature. Moreover temperature can be a major contributor to several types of distress. Therefore temperature is a significant factor that affects the performance and life span of a pavement.

The Libyan road network expanded at a phenomenal pace from approximately 10,000 km of paved roads in 1980 to more than 34,000 km in 2010. The study area is located in the southern desert region of Libya at latitudes between (24°17'N) and (30°11'N). With the recent SHRP and LTTP research findings, it was necessary to investigate the applicability of the models developed from these research studies to the study area region's environmental conditions and more generally to the rest Libya desert reigns.

This research presents the investigations undertaken to develop models to predict high and low asphalt pavement temperatures in study area regions. A pavement monitoring station was set-up at the regions to monitor air, pavement temperatures in different depth, wind speed and solar radiation. Data were collected for 365 days.

Daily minimum and maximum temperatures were recorded. Regression analysis was used to develop the minimum and maximum pavement temperature models, using air temperature, wind speed and solar radiation.

This research presents a new model for predicting maximum and minimum of pavement layers temperature based on data collected by installed pavement monitoring station. The study area was divided into different "performance grade zones" – zones with different extreme temperatures for bitumen "PG" gradation - on the basis of previous 10 years temperature data collected from 10 weather stations. Also a temperature and "PG" zoning map has been proposed to be implemented in the Libyan desert area.

**Keywords:** pavement, temperature, predicting, asphalt, SHRP, LTTP, PG, Libya

# ИСТРАЖИВАЊЕ МЕРОДАВНИХ ТЕМПЕРАТУРА ЗА ПРОЈЕКТОВАЊЕ КОЛОВОЗНИХ КОНСТРУКЦИЈА ПУСТИЊСКИХ ПУТЕВА У ЛИБИЈИ

Хасан Авадат Салем

## РЕЗИМЕ

Асфалтни коловози чине важан, интегрални део сваког транспортног система. Носивост слојева од асфалтних мешавина зависи од више фактора, укључујући температуру. Штавише, температура асфалта може бити главни фактор код развоја неких оштећења па зато има велики утицај на перформансе и животни век коловоза.

Мрежа либијских путева се развијала великом брзином од око 10 000 км путева сасавременим застором 1980. Године довише од 34 000 км у 2010-ој години. Студија је спроведена у Либијској пустињи, у јужном делу Либије, на географским ширинама између 24°17'N и 30°11'N. Моделе развијене у оквиру истраживачких програма SHRP и LTPP било је потребно проверити у амбијенталним условима какви су у подручју обухваћеном студијом, односно генерално, у пустињском делу Либије.

Овај истраживачки подухват чине истраживања спроведена у циљу формирања модела за предвиђање високих и ниских температура асфалтног коловоза у предметном региону. Успостављене су мониторинг станице за праћење температуре ваздуха, температуре коловоза на различитим дубинама, брзине ветра и сунчевог зрачења. Подаци су прикупљени за 365 дана.

Снимљене су максималне и минималне дневне температуре а затим је извршена регресиона анализа за моделирање максималне и минималне температуре коловоза на основу температуре ваздуха, брзине ветра и сунчевог зрачења.

Истраживањем је формиран нови модел за предвиђање минималне и максималне температуре у слојевима коловозне конструкције заснован на подацима прикупљеним помоћу мониторинг станица. Подручје које је било предмет истраживања, подељено је на 10 "PG" зона – премаразличитим екстремним температурама за PG градацију битумена – на основу десетогодишњих података прикупљених са 10 климатолошких станица. На крају се предлаже мапа са температурним, односно "PG" зонама Либијске пустиње.

**Кључне речи:** коловоз, температура, предвиђање, асфалт, SHRP, LTPP, PG, Либија



## **ACKNOWLEDGEMENTS**

Firstly and foremost, I would like to express my gratitude to Almighty Allah S.W.T. for giving me the guidance and strength in completing this PhD thesis with success.

I also would like to extent my greatest thanks to all those who gave me the possibility to complete this thesis. First and foremost, I would like to express my sincere gratitude to my supervisor Prof. Dr Djordje Uzelac for his advice, comments, guidance, support and encouragement during the completion of my study.

Special thanks are dedicated to Associate Prof. Dr. Bojan Matić, my co-supervisor for sharing his ideas and information with me.

Furthermore, I am also indebted to Prof. Zagorka Lozanov Crvenković (Department of Mathematics and Informatics, Faculty of Sciences, Novi Sad University), whose assistance enable me to complete this project. This work would not have been possible without their outmost capability and intelligence.

I also would like to thank all other parties, those who have involved directly or indirectly in making this research a very great success.

Finally, to my beloved family and friends, especially to my parents, heartiest gratitude and thanks for your encouragement, inspiration and support.

Thanks for all the kindness. May the Almighty Allah S.W.T. bless us and be with us all the time.

# TABLE OF CONTENTS

<b>ABSTRACT</b> .....	i
<b>РЕЗУМЕ</b> .....	ii
<b>ACKNOWLEDGEMENTS</b> .....	iii
Table of contents.....	iv
Appendixes (CD) .....	viii
List of tables.....	x
List of figures.....	xxii
<b>Chapter 1 INTRODUCTION</b> .....	1
1.1 Background.....	2
1.2 Study area.....	3
1.2.1 Climate.....	4
1.2.2 Pavement temperature prediction .....	6
1.3 Problem statement.....	6
1.4 Methodology .....	6
1.4 Objectives of research.....	8
1.5 Research Hypotheses .....	9
1.6 Scope of research .....	9
<b>Chapter 2 BACKGROUND</b> .....	10
2.1 Pavement Temperature Prediction Models.....	10
2.2 Energy balance in asphaltic pavements .....	17
2.3 Solar radiation.....	18
2.4 Aging due to temperatures and solar radiation .....	19
2.5 Radiation theory (energy equilibrium).....	19
2.5.1 Solar Radiation.....	20
2.6 Radiation emitted by pavement surface.....	23
2.6.1 Conduction Energy .....	23
2.6.2 Convection Energy.....	23
2.7 Pavement temperature prediction .....	24
2.8 Performance grade of bitumen (PG).....	24

2.9 Analysis of SHRP models.....	26
2.10 Applications of pavement temperature prediction.....	34
2.11 FHWA integrated climatic model.....	36
2.12 Considerations on prediction accuracy.....	38
2.13 Determination of Performance Grade according to Superpavemethod.....	38
<b>Chapter 3 LIBYA ENVIRONMENT AND CLIMATE CONDITIONS .....</b>	<b>41</b>
3.1 General.....	41
3.2 Weather classifications .....	41
3.3 Libya road materials .....	42
3.4.1 Weather related data .....	44
3.5 Deterioration of the Libyan desert road network.....	45
3.6 Types of distress in Libya desert roads.....	45
3.6.2 Cracking.....	46
3.6.3 Alligatoring.....	47
3.6.4 Edge Cracks .....	48
3.6.4 Rutting.....	49
3.7 Pavement temperature parameters related to thermal stress and durability.....	49
3.8 Field instrumentation and data collection system.....	50
3.8.1 Zones and stations.....	50
3.8.2 Description of data collection system .....	51
3.8.3 Description of study area .....	52
3.9 Temperatures monitoring at the Libya desert stations.....	54
<b>Chapter 4 DATA PRESENTATION AND ANALYSIS .....</b>	<b>55</b>
4.1 General.....	55
4.1.1 Pavement Temperature Monitoring System .....	55
4.1.2 Climatological Monitoring System.....	55
4.2 Thermocouple placements .....	55
4.3 Analysis of results with respect to pavement structural configuration .....	57
2.3.1 Cumulative solar radiation calculation .....	64
4.4 Pavement temperature prediction .....	66

4.5 Linear modeling for daily pavement temperature prediction incorporating air temperature .....	67
4.5.1 Relationship with the air temperature .....	67
4.5.2 Relationship with air temperature and day of the year .....	76
4.5.3 Relationship with air temperature and wind speed .....	87
4.5.4 Relationship with air temperature, and cumulative solar radiation .....	95
4.5.5 Relationship with air temperature, day of the year, and cumulative solar radiation .	104
4.5.6 Relationship with air temperature, cumulative solar radiation and wind speed .....	114
4.5.7 Evaluation of the models with air temperature .....	114
4.6 Pavement temperature prediction models incorporating air temperature and the distance from the surface (depth).....	121
4.6.1 Relationship with air temperature and the distance from the surface (depth) .....	121
4.6.2 Relationship with daily air temperature, distance from the surface, and day of the year .....	125
4.6.3 Relationship with air temperature, the depth from the surface and cumulative solar radiation .....	129
4.6.4 Relationship with air temperature, the distance from the surface, day of the year and cumulative solar radiation .....	133
4.6.5 Evaluation of the models including air temperature and the distance from the surface .....	136
4.7 Linear modeling for daily pavement temperature prediction incorporating surface (C1) temperature .....	139
4.7.1 Relationship with the surface temperature.....	139
4.7.2 Relationship with the surface temperature and day of the year .....	147
4.7.3 Relationship with surface temperature and wind speed.....	154
4.7.4 Relationship with surface temperature, and cumulative solar radiation .....	160
4.7.5 Relationship with surface temperature, day of the year, and cumulative solar radiation .....	167
4.7.6 Evaluation of the models with surface temperature.....	171
4.8 Pavement temperature prediction models incorporating surface (C1) temperature and the distance from the surface (depth).....	177
4.8.1 Relationship with surface temperature and the distance from the surface (depth) ....	177
4.8.2 Relationship with surface temperature, depth from the surface, and day of the year	181

4.8.3 Relationship with surface temperature, depth from the surface and cumulative solar radiation .....	185
4.8.4 Models including wind speed .....	188
4.6.5 Relationship with surface temperature, the distance from the surface, day of the year and cumulative solar radiation and latitude .....	189
4.8.5 Evaluation of the models including surface temperature and depth from the surface	191
4.9 Comparison of model developed for Libyan Desert with SHRP and LTPP models .....	194
<b>Chapter 5 PERFORMANCE GRADE OF BITUMEN ON LIBYAN DESERT .....</b>	<b>197</b>
5.1 Introduction.....	197
5.2 Superpaveperformance grading (PG system) .....	197
5.3 Binder Specifications .....	197
5.4 Pavement Temperature by SHRPIS THAT MODEL USED FOR COMPARATION IN CH 4.9??? Maybe this should be moved to chapter 4.9? .....	200
5.4.1 High Temperature Models .....	200
5.4.2 Low temperature models.....	201
5.5 Temperature database for Libyan desert.....	202
5.6 Temperature data analysis.....	202
5.6.1 Project pavement temperature models based on data collected in 2012–2013.....	204
5.6.2 Project pavement temperatures predicted on air temperature data collected from year 2000 to year 2009.....	206
5.6.3 Libyan Desert road PG mapping.....	228
<b>Chapter 6 SUMMARY AND CONCLUSIONS .....</b>	<b>231</b>
6.1 Findings -temperature .....	232
6.2 Findings - PG .....	234
6.3 Conclusions – temperature.....	234
6.4 Conclusions – PG.....	237
<b>Chapter 7 RECOMMENDATIONS .....</b>	<b>239</b>
<b>REFERENCES.....</b>	<b>240</b>

## **Appendixes (CD)**

Appendix A	Figures of the distributions of maximum and minimum air and pavement temperature for four depths for different locations for whole study period
Appendix B	Descriptive statistics for maximal and minimal temperatures for different locations
Appendix C	Daily maximal and minimal temperatures for 30 <sup>th</sup> of June 2012 and 30 <sup>th</sup> of December 2012 and matrix plots for different locations
Appendix D	Predicting daily maximal and minimal pavement temperatures as a linear function of maximal and minimal air temperatures for different locations
Appendix E	Predicting daily maximal and minimal pavement temperatures as a linear function of maximal and minimal air temperatures and the day of the year for different locations
Appendix F	Predicting daily maximal and minimal pavement temperatures as a linear function of: <ol style="list-style-type: none"><li>1. Air temperature and wind speed</li><li>2. Air temperature and cumulative solar radiation</li></ol> for different locations
Appendix G	Predicting daily maximal and minimal pavement temperatures as a linear function of maximal and minimal air temperatures, the day of the year and the wind speed for different locations
Appendix H	Figures of actual maximum and minimum daily pavement temperature at different depths versus predicted from the model including the air temperature and the day of the year, for different locations
Appendix I	Relationship of maximal pavement temperatures with air temperature, depth from the surface, day of the year and cumulative solar radiation
Appendix J	Figures of actual maximum and minimum daily pavement temperature versus predicted from the model including the air temperature, depth from the surface and the day of the year, at different locations
Appendix K	Predicting daily maximal and minimal pavement temperatures as a linear function of maximal and minimal surface temperatures for different locations

Appendix L	Predicting daily maximal and minimal pavement temperatures as a linear function of maximal and minimal surface temperatures and the day of the year for different locations
Appendix M	Predicting daily maximal and minimal pavement temperatures as a linear function of maximal and minimal surface temperatures and the wind speed for different locations. 1. Surface temperature and wind speed 2. Surface temperature and cumulative solar radiation for different locations
Appendix N	Figures of actual maximum and minimum daily pavement temperature at different depths versus predicted from the model including the surface temperature and the day of the year, for different locations
Appendix O	Relationship of maximal pavement temperatures with surface temperature, depth from the surface, day of the year and cumulative solar radiation.
Appendix P	Figures of actual maximum and minimum daily pavement temperature versus predicted from the model including the surface temperature, depth from the surface and the day of the year, at different locations

## List of tables

Table 1.1 Weather station locations and climate regions .....	4
Table 1.2 Technical Specification of data logger .....	7
Table 1.3 The structures of stations that were recorded by sensors.....	8
Table 2.1 Specification of asphalt layers, depending on the PG (Kennedy T. et al., 1994) .....	39
Table 3.1 Latitude and longitude of the locations of the selected station for the study.....	52
Table 4.1 The typical layers of roads in roads stations.....	56
Table 4.2 The descriptive statistics for maximal daily temperatures for station Al-Jufroh .....	59
Table 4.3 The descriptive statistics for minimal daily temperatures for station Al-Jufroh .....	59
Table 4.4 Cumulative solar radiations at eight locations, at 15 <sup>th</sup> of January and 15 <sup>th</sup> of June...	64
Table 4.5 Parameters of the model for predicting daily pavement temperature from daily air temperature at the Al-Jufroh location .....	68
Table 4.6 Parameters of the model for predicting pavement temperatures when including air temperature and latitude.....	74
Table 4.7 Latitudes and longitudes of the stations.....	74
Table 4.8 Characteristics of the model for predicting maximal daily C1 temperature from maximal daily air temperature and day of the year at the Brak location. ....	78
Table 4.9 Characteristics of the model for predicting maximal daily C2 temperature from maximal daily air temperature and day of the year at the Brak location .....	78
Table 4.10 Characteristics of the model for predicting maximal daily C3 temperature from maximal daily air temperature and day of the year at the Brak location .....	79
Table 4.11 Characteristics of the model for predicting maximal daily C4 temperature from maximal daily air temperature and day of the year at the Brak location .....	79
Table 4.12 Characteristics of the model for predicting minimal daily C1 temperature from minimal daily air temperature and day of the year at the Brak location.....	81
Table 4.13 Characteristics of the model for predicting minimal daily C2 temperature from minimal daily air temperature and day of the year at the Brak location.....	81
Table 4.14 Characteristics of the model for predicting minimal daily C3 temperature from minimal daily air temperature and day of the year at the Brak location.....	81
Table 4.15 Characteristics of the model for predicting minimal daily C4 temperature from minimal daily air temperature and day of the year at the Brak location.....	82
Table 4.16 Characteristics of the model for predicting maximal daily C1 temperature from maximal daily air temperature and day of the year for all locations.....	84
Table 4.17 Characteristics of the model for predicting maximal daily C2 temperature from maximal daily air temperature and day of the year for all locations.....	84
Table 4.18 Characteristics of the model for predicting maximal daily C3 temperature from maximal daily air temperature and day of the year for all locations.....	85



Table 4.19	Characteristics of the model for predicting maximal daily C3 temperature from maximal daily air temperature and day of the year for all locations.....	85
Table 4.20	Characteristics of the model for predicting minimal daily C1 temperature from minimal daily air temperature and day of the year for all locations .....	86
Table 4.21	Characteristics of the model for predicting minimal daily C2 temperature from minimal daily air temperature and day of the year for all locations .....	86
Table 4.22	Characteristics of the model for predicting minimal daily C3 temperature from minimal daily air temperature and day of the year for all locations .....	86
Table 4.23	Characteristics of the model for predicting minimal daily C4 temperature from minimal daily air temperature and day of the year for all locations .....	87
Table 4.24	Characteristics of the model for predicting maximal daily C1 temperature from maximal daily air temperature and the wind speed for the Awbari location .....	88
Table 4.25	Characteristics of the model for predicting maximal daily C2 temperature from maximal daily air temperature and the wind speed for the Awbari location .....	88
Table 4.26	Characteristics of the model for predicting maximal daily C3 temperature from maximal daily air temperature and the wind speed for the Awbari location .....	89
Table 4.27	Characteristics of the model for predicting maximal daily C4 temperature from maximal daily air temperature and the wind speed for the Awbari location .....	89
Table 4.28	Characteristics of the model for predicting minimal daily C1 temperature from minimal daily air temperature and wind speed for Awbari location.....	90
Table 4.29	Characteristics of the model for predicting minimal daily C2 temperature from minimal daily air temperature and wind speed for the Awbari location.....	90
Table 4.30	Characteristics of the model for predicting minimal daily C3 temperature from minimal daily air temperature and wind speed for the Awbari location.....	90
Table 4.31	Characteristics of the model for predicting minimal daily C4 temperature from minimal daily air temperature and wind speed for the Awbari location.....	90
Table 4.32	Characteristics of the model for predicting maximal daily C1 temperature from maximal daily air temperature and wind speed for all locations .....	92
Table 4.33	Characteristics of the model for predicting maximal daily C2 temperature from maximal daily air temperature and wind speed for all locations .....	92
Table 4.34	Characteristics of the model for predicting maximal daily C3 temperature from maximal daily air temperature and wind speed for all locations .....	93
Table 4.35	Characteristics of the model for predicting maximal daily C4 temperature from maximal daily air temperature and wind speed for all locations .....	93
Table 4.36	Characteristics of the model for predicting minimal daily C1 temperature from minimal daily air temperature and wind speed for all locations.....	94
Table 4.37	Characteristics of the model for predicting minima daily C2 temperature from minimal daily air temperature and wind speed for all locations.....	94
Table 4.38	Characteristics of the model for predicting minimal daily C3 temperature from minimal daily air temperature and wind speed for all locations.....	95

Table 4.39	Characteristics of the model for predicting minima daily C4 temperature from minimal daily air temperature and wind speed for all locations .....	95
Table 4.40	Cumulative solar radiations at eight locations for January 15 <sup>th</sup> and June 15 <sup>th</sup> .....	96
Table 4.41	Characteristics of the model for predicting maximal daily C1 temperature from maximal daily air temperature and cumulative solar radiation for the Awjilah location .....	96
Table 4.42	Characteristics of the model for predicting maximal daily C2 temperature from maximal daily air temperature and cumulative solar radiation for the Awjilah location .....	97
Table 4.43	Characteristics of the model for predicting maximal daily C3 temperature from maximal daily air temperature and cumulative solar radiation for the Awjilah location .....	97
Table 4.44	Characteristics of the model for predicting maximal daily C4 temperature from maximal daily air temperature and cumulative solar radiation for the Awjilah location .....	97
Table 4.45	Characteristics of the model for predicting minimal daily C1 temperature from minimal daily air temperature and cumulative solar radiation for the Awjilah location .....	98
Table 4.46	Characteristics of the model for predicting minimal daily C2 temperature from minimal daily air temperature and cumulative solar radiation for the Awjilah location. ....	98
Table 4.47	Characteristics of the model for predicting minimal daily C3 temperature from minimal daily air temperature and cumulative solar radiation for the Awjilah location .....	99
Table 4.48	Characteristics of the model for predicting minimal daily C4 temperature from minimal daily air temperature and cumulative solar radiation for the Awjilah location .....	99
Table 4.49	Characteristics of the model for predicting maximal daily C1 temperature from maximal daily air temperature and cumulative solar radiation for all locations.....	100
Table 4.50	Characteristics of the model for predicting maximal daily C2 temperature from maximal daily air temperature and cumulative solar radiation for all locations.....	101
Table 4.51	Characteristics of the model for predicting maximal daily C3 temperature from maximal daily air temperature and cumulative solar radiation for all locations.....	101
Table 4.52	Characteristics of the model for predicting maximal daily C4 temperature from maximal daily air temperature and cumulative solar radiation for all locations.....	101
Table 4.53	Characteristics of the model for predicting minimal daily C1 temperature from minimal daily air temperature and cumulative solar radiation for all locations .....	102
Table 4.54	Characteristics of the model for predicting minimal daily C2 temperature from minimal daily air temperature and cumulative solar radiation for all locations .....	103
Table 4.55	Characteristics of the model for predicting minimal daily C3 temperature from minimal daily air temperature and the cumulative solar radiation for all locations .....	103
Table 4.56	Characteristics of the model for predicting minimal daily C4 temperature from minimal daily air temperature and cumulative solar radiation for all locations .....	103
Table 4.57	Characteristics of the model for predicting maximal daily C1 temperature from maximal daily air temperature, the day of the year, and cumulative solar radiation for the Al Qatrun location.....	105

Table 4.58 Characteristics of the model for predicting maximal daily C2 temperature from maximal daily air temperature, the day of the year and cumulative solar radiation for the Al Qatrun location.....	105
Table 4.59 Characteristics of the model for predicting maximal daily C3 temperature from maximal daily air temperature, the day of the year, and wind speed for the Al Qatrun location.....	106
Table 4.60 Characteristics of the model for predicting maximal daily C4 temperature from maximal daily air temperature, the day of the year, and cumulative solar radiation for the Al Qatrun location.....	106
Table 4.61 Characteristics of the model for predicting minimal daily C1 temperature from minimal daily air temperature, the day of the year, and cumulative solar radiation for the Al Qatrun location.....	107
Table 4.62 Characteristics of the model for predicting minimal daily C2 temperature from minimal daily air temperature, the day of the year, and cumulative solar radiation for the Al Qatrun location.....	108
Table 4.63 Characteristics of the model for predicting minimal daily C3 temperature from minimal daily air temperature, the day of the year, and cumulative solar radiation for the Al Qatrun location.....	108
Table 4.64 Characteristics of the model for predicting minimal daily C4 temperature from minimal daily air temperature, the day of the year, and cumulative solar radiation for the Al Qatrun location.....	109
Table 4.65 Characteristics of the model for predicting maximal daily C1 temperature from maximal daily air temperature, the day of the year and cumulative solar radiation for all locations. ....	110
Table 4.66 Characteristics of the model for predicting maximal daily C2 temperature from maximal daily air temperature, the day of the year, and cumulative solar radiation for all locations. ....	110
Table 4.67 Characteristics of the model for predicting maximal daily C3 temperature from maximal daily air temperature, the day of the year, and cumulative solar radiation for all locations. ....	111
Table 4.68 Characteristics of the model for predicting maximal daily C4 temperature from maximal daily air temperature, the day of the year, and cumulative solar radiation for all locations. ....	111
Table 4.69 Characteristics of the model for predicting minimal daily C1 temperature from minimal daily air temperature, the day of the year, and cumulative solar radiation for all locations. ....	112
Table 4.70 Characteristics of the model for predicting minimal daily C2 temperature from minimal daily air temperature, the day of the year, and cumulative solar radiation for all locations. ....	113

Table 4.71 Characteristics of the model for predicting minimal daily C3 temperature from minimal daily air temperature, the day of the year, and cumulative solar radiation for all locations. ....	113
Table 4.72 Characteristics of the model for predicting minimal daily C4 temperature from minimal daily air temperature, the day of the year, and cumulative solar radiation for all locations. ....	114
Table 4.73 Adjusted R <sup>2</sup> and standard errors for different models which are based on the data from all locations. ....	115
Table 4.74 Characteristics of the model for predicting maximal daily pavement temperatures from maximal daily air temperature and depth from the surface at the Al Jufroh location. ....	122
Table 4.75 Characteristics of the model for predicting minimal daily pavement temperatures from minimal daily air temperature and depth from the surface at the Al Jufroh location. ....	123
Table 4.76 Characteristics of the model for predicting maximal daily pavement temperatures from maximal daily air temperature, depth from the surface, and latitude. ....	124
Table 4.77 Characteristics of the model for predicting minimal daily pavement temperatures from minimal daily air temperature, depth from the surface and latitude. ....	125
Table 4.78 Characteristics of the model for predicting maximal daily pavement temperatures from maximal daily air temperature, the day of the year, and depth from the surface at the Al Jufroh location. ....	126
Table 4.79 Characteristics of the model for predicting minimal daily pavement temperatures from minimal daily air temperature, the day of the year, and depth from the surface at the Al Jufroh location. ....	127
Table 4.80 Characteristics of the model for predicting maximal daily pavement temperatures from maximal daily air temperature, distance from the surface, the day of the year and latitude. ....	128
Table 4.81 Characteristics of the model for predicting minimal daily pavement temperatures from minimal daily air temperature, distance from the surface, the day of the year, and latitude. ....	129
Table 4.82 Characteristics of the model for predicting maximal daily pavement temperatures from maximal daily air temperature, cumulative solar radiation, and distance from the surface at the Al Jufroh location. ....	130
Table 4.83 Characteristics of the model for predicting minimal daily pavement temperatures from minimal daily air temperature, cumulative solar radiation and distance from the surface at the Al Jufroh location. ....	131
Table 4.84 Characteristics of the model for predicting maximal daily pavement temperatures from maximal daily air temperature, distance from the surface, cumulative solar radiation and latitude. ....	132
Table 4.85 Characteristics of the model for predicting minimal daily pavement temperatures from minimal daily air temperature, depth from the surface, cumulative solar radiation and latitude. ....	133

Table 4.86 Characteristics of the model for predicting maximal daily pavement temperatures from maximal daily air temperature, distance from the surface, day of the year, cumulative solar radiation and latitude.....	134
Table 4.87 Characteristics of the model for predicting minimal daily pavement temperatures from minimal daily air temperature, depth from the surface, day of the year, cumulative solar radiation and latitude.....	135
Table 4.88 Adjusted R <sup>2</sup> and standard errors for different models which are based on the data from all locations. ....	136
Table 4.89 Parameters of the model for predicting daily maximal and minimal pavement temperature from daily maximal and minimal surface temperature at the Al-Jufroh location...	139
Table 4.90 Parameters of the model for predicting pavement temperature from the surface temperature at the Al-Jufroh location. ....	144
Table 4.91 Characteristics of the model for predicting maximal daily C2 temperature from maximal daily surface temperature and day of the year at the Brak location.....	148
Table 4.92 Characteristics of the model for predicting maximal daily C3 temperature from maximal daily surface temperature and day of the year at the Brak location.....	148
Table 4.93 Characteristics of the model for predicting maximal daily C4 temperature from maximal daily surface temperature and day of the year at the Brak location.....	148
Table 4.94 Characteristics of the model for predicting minimal daily C2 temperature from minimal daily surface temperature and day of the year at the Brak location. ....	149
Table 4.95 Characteristics of the model for predicting minimal daily C3 temperature from minimal daily surface temperature and day of the year at the Brak location. ....	150
Table 4.96 Characteristics of the model for predicting minimal daily C4 temperature from minimal daily surface temperature and day of the year at the Brak location. ....	150
Table 4.97 Characteristics of the model for predicting maximal daily C2 temperature from maximal daily surface temperature and day of the year for all locations. ....	152
Table 4.98 Characteristics of the model for predicting maximal daily C3 temperature from maximal daily surface temperature and day of the year for all locations. ....	152
Table 4.99 Characteristics of the model for predicting maximal daily C3 temperature from maximal daily surface temperature and day of the year for all locations. ....	153
Table 4.100 Characteristics of the model for predicting minimal daily C2 temperature from minimal daily surface temperature and day of the year for all locations. ....	153
Table 4.101 Characteristics of the model for predicting minimal C3 temperature from minimal daily surface temperature and day of the year for all locations. ....	154
Table 4.102 Characteristics of the model for predicting minimal daily C4 temperature from minimal daily surface temperature and day of the year for all locations.....	154
Table 4.103 Characteristics of the model for predicting maximal daily C2 temperature from maximal daily surface temperature and the wind speed for the Awbari location.....	155
Table 4.104 Characteristics of the model for predicting maximal daily C3 temperature from maximal daily surface temperature and wind speed for the Awbari location.....	155

Table 4.105 Characteristics of the model for predicting maximal daily C4 temperature from maximal daily surface temperature and wind speed for the Awbari location.....	156
Table 4.106 Characteristics of the model for predicting minimal daily C2 temperature from minimal daily surface temperature and the wind speed for the Awbari location. ....	156
Table 4.107 Characteristics of the model for predicting minimal daily C3 temperature from minimal daily surface temperature and wind speed for the Awbari location. ....	157
Table 4.108 Characteristics of the model for predicting minimal daily C4 temperature from minimal daily surface temperature and wind speed for the Awbari location. ....	157
Table 4.109 Characteristics of the model for predicting maximal daily C2 temperature from maximal daily surface temperature and wind speed for all locations. ....	158
Table 4.110 Characteristics of the model for predicting maximal daily C3 temperature from maximal daily surface temperature and wind speed for all locations. ....	158
Table 4.111 Characteristics of the model for predicting maximal daily C4 temperature from maximal daily surface temperature and wind speed for all locations. ....	159
Table 4.112 Characteristics of the model for predicting minimal daily C2 temperature from minimal daily surface temperature and wind speed for all locations.....	159
Table 4.113 Characteristics of the model for predicting minimal C3 temperature from minimal surface temperature and wind speed for all locations. ....	160
Table 4.114 Characteristics of the model for predicting minimal daily C4 temperature from minimal daily surface temperature and wind speed for all locations.....	160
Table 4.115 Cumulative solar radiations at eight locations, on 15 <sup>th</sup> of January and 15 <sup>th</sup> of June. ....	161
Table 4.116 Characteristics of the model for predicting maximal daily C2 temperature from maximal daily surface temperature and cumulative solar radiation for the Awjilah location. ...	161
Table 4.117 Characteristics of the model for predicting maximal daily C3 temperature from maximal daily surface temperature and cumulative solar radiation for the Awjilah location. ...	162
Table 4.118 Characteristics of the model for predicting maximal daily C4 temperature from maximal daily surface temperature and cumulative solar radiation for the Awjilah location. ...	162
Table 4.119 Characteristics of the model for predicting minimal daily C2 temperature from minimal daily surface temperature and cumulative solar radiation for the Awjilah location....	163
Table 4.120 Characteristics of the model for predicting minimal daily C3 temperature from minimal daily surface temperature and cumulative solar radiation for the Awjilah location....	163
Table 4.121 Characteristics of the model for predicting minimal C4 temperature from minimal daily surface temperature and cumulative solar radiation for the Awjilah location. ....	163
Table 4.122 Characteristics of the model for predicting maximal C2 daily temperature from maximal daily surface temperature and cumulative solar radiation for all locations. ....	164
Table 4.123 Characteristics of the model for predicting maximal daily C3 temperature from maximal daily surface temperature and cumulative solar radiation for all locations. ....	165
Table 4.124 Characteristics of the model for predicting maximal daily C4 temperature from maximal daily surface temperature and cumulative solar radiation for all locations. ....	165

Table 4.125 Characteristics of the model for predicting minimal daily C2 temperature from minimal daily surface temperature and cumulative solar radiation for all locations. ....	166
Table 4.126 Characteristics of the model for predicting minimal daily C3 temperature from minimal daily surface temperature and cumulative solar radiation for all locations. ....	166
Table 4.127 Characteristics of the model for predicting minimal daily C4 temperature from minimal daily surface temperature and cumulative solar radiation for all locations. ....	166
Table 4.128 Characteristics of the model for predicting maximal daily C2 temperature from maximal daily surface of the pavement temperature, the day of the year, and cumulative solar radiation and latitude. ....	168
Table 4.129 Characteristics of the model for predicting maximal daily C3 temperature from maximal daily surface of the pavement temperature, the day of the year, and cumulative solar radiation and latitude. ....	168
Table 4.130 Characteristics of the model for predicting maximal daily C4 temperature from maximal daily surface of the pavement temperature, the day of the year, and cumulative solar radiation and latitude. ....	169
Table 4.131 Characteristics of the model for predicting minimal daily C2 temperature from minimal daily surface of the pavement temperature, the day of the year, and cumulative solar radiation and latitude. ....	170
Table 4.132 Characteristics of the model for predicting minimal daily C3 temperature from minimal daily surface of the pavement temperature, the day of the year, and cumulative solar radiation and latitude. ....	170
Table 4.133 Characteristics of the model for predicting minimal daily C4 temperature from minimal daily surface of the pavement temperature, the day of the year, and cumulative solar radiation and latitude. ....	170
Table 4.134 Adjusted R <sup>2</sup> and standard errors for different models based on the data from all locations. ....	172
Table 4.135 Characteristics of the model for predicting maximal daily pavement temperatures from maximal daily surface temperature and depth from the surface at the Al Jufroh location. ....	177
Table 4.136 Characteristics of the model for predicting minimal daily pavement temperatures from minimal daily surface temperature and depth from the surface at the Al Jufroh location. ....	178
Table 4.137 Characteristics of the model for predicting maximal daily pavement temperatures from maximal daily surface temperature and depth from the surface for all locations. ....	180
Table 4.138 Characteristics of the model for predicting minimal daily pavement temperatures from minimal daily surface temperature and depth from the surface for all locations. ....	181
Table 4.139 Characteristics of the model for predicting maximal daily pavement temperatures from maximal daily surface temperature, the day of the year, and depth from the surface at the Al Jufroh location. ....	182

Table 4.140 Characteristics of the model for predicting minimal daily pavement temperatures from minimal daily surface temperature, the day of the year, and depth from the surface at the Al Jufroh location. ....	183
Table 4.141 Characteristics of the model for predicting maximal daily pavement temperatures from maximal daily surface temperature, depth from the surface, day of the year, and latitude. ....	184
Table 4.142 Characteristics of the model for predicting minimal daily pavement temperatures from minimal daily surface temperature, depth from the surface, day of the year, and latitude. ....	185
Table 4.143 Characteristics of the model for predicting maximal daily pavement temperatures from maximal daily surface temperature, cumulative solar radiation and depth from the surface at the Al Jufroh location. ....	186
Table 4.144 Characteristics of the model for predicting minimal daily pavement temperatures from minimal daily surface temperature, cumulative solar radiation and depth from the surface at the Al Jufroh location. ....	186
Table 4.145 Characteristics of the model for predicting maximal daily pavement temperatures from maximal daily surface temperature, depth from the surface, cumulative solar radiation, and latitude. ....	187
Table 4.146 Characteristics of the model for predicting minimal daily pavement temperatures from minimal daily surface temperature, depth from the surface, cumulative solar radiation, and latitude. ....	188
Table 4.147 Characteristics of the model for predicting maximal daily pavement temperatures from maximal daily surface temperature, distance from the surface, day of the year, cumulative solar radiation and latitude. ....	190
Table 4.148 Characteristics of the model for predicting minimal daily pavement temperatures from minimal daily surface temperature, depth from the surface, day of the year, cumulative solar radiation and latitude. ....	191
Table 4.149 Adjusted $R^2$ and standard errors for different models which are based on the data from all locations. ....	192
Table 5.1 Penetration and viscosity grading system. ....	198
Table 5.2 Binder grades as specified in Superpave specifications. ....	200
Table 5.3 Summary of weather stations. ....	202
Table 5.4 Maximum of seven day average of maximal daily temperatures and minimum of minimal daily temperatures for different locations, for year 2012–2013. ....	203
Table 5.5 Maximum of maximal daily temperatures for different locations for the year 2012–2013. ....	204
Table 5.6 Regression models for maximal pavement temperatures for the Al Jufroh location. ....	207
Table 5.7 Regression models for minimal pavement temperatures for the Al Jufroh location. ....	207
Table 5.8 Maximum of seven-day average of predicted maximal daily temperatures and minimum of minimal daily temperatures from year 2000 to year 2009, year 2012/2013, for the Al Joufroh location. ....	208



Table 5.9 Maximum of predicted maximal daily temperatures for years 2000–2009 and 2012 for the Al Joufroh location.....	208
Table 5.10 Descriptive statistics for data for 11 years at the Al Jufroh location.....	209
Table 5.11 Values of standard normal distribution for 50%, 85%, 95%, 98% and 99.9% level of reliability. ....	210
Table 5.12 Reliability data for PG Al Jufroh.....	210
Table 5.13 PG for different levels of reliability for the Al Jufroh location. ....	210
Table 5.14 Regression models for maximal pavement temperatures for the Al Kufrah location. ....	211
Table 5.15 Regression models for minimal pavement temperatures for the Al Kufrah location. ....	211
Table 5.16 Maximum of seven-day average of predicted maximal daily temperatures and minimum of minimal daily temperatures from year 2000 to year 2009 and year 2012–2013, for the Al Kufrah location. ....	211
Table 5.17 Maximum of predicted maximal daily temperatures for years 2000–2009 and 2012 for the Al Kufrah location.....	212
Table 5.18 Descriptive statistics for data for 11 years at the Al Kufrah location.....	212
Table 5.19 Reliability data for PG at the Al Kufrah location. ....	213
Table 5.20 PG for different level of reliability for the Al Jufroh location.....	213
Table 5.21 Regression models for maximal pavement temperatures for the Al Qatrun location. ....	213
Table 5.22 Regression models for minimal pavement temperatures for the Al Qatrun location. ....	213
Table 5.23 Maximum of seven-day average of predicted maximal daily temperatures and minimum of minimal daily temperatures from year 2000 to year 2009, year 2012–2013, for the Al Qatrun location.....	214
Table 5.24 Maximum of predicted maximal daily temperatures for years 2000–2009 and 2012 for the Al Qatrun location. ....	214
Table 5.25 Descriptive statistics for data for 11 years at the Al Qatrun location.....	215
Table 5.26 Reliability data for PG at the Al Qatrun location. ....	215
Table 5.27 PG for different level of reliability for the Al Qatrun location.....	215
Table 5.28 Regression models for maximal pavement temperatures for the Awbari location..	216
Table 5.29 Regression models for minimal pavement temperatures for the Awbari location. ...	216
Table 5.30 Maximum of seven-day average of predicted maximal daily temperatures and minimum of minimal daily temperatures from year 2000 to year 2009, year 2012–2013, for the Awbari location.....	216
Table 5.31 Maximum of predicted maximal daily temperatures for years 2000–2009 and 2012 for the Al Joufroh location.....	217
Table 5.32 Descriptive statistics for data for 11 years at the Al Jufroh location.....	217
Table 5.33 Reliability data for PG at the Awbari location. ....	218

Table 5.34 PG for different level of reliability for the Awbari location.....	218
Table 5.35 Regression models for maximal pavement temperatures for the Awjilah location.	218
Table 5.36 Regression models for minimal pavement temperatures for the Awjilah location...	218
Table 5.37 Maximum of seven-day average of predicted maximal daily temperatures and minimum of minimal daily temperatures from year 2000 to year 2009, year 2012–2013, for the Awjilah location.....	219
Table 5.38 Maximum of predicted maximal daily temperatures for years 2000–2009 and 2012 for the Al Joufroh location.....	219
Table 5.39 Descriptive statistics for data for 11 years at the Al Jufroh location.....	220
Table 5.40 Reliability data for PG at the Awjilah location.....	220
Table 5.41 PG for different levels of reliability for the Al Jufroh location.....	220
Table 5.42 Regression models for maximal pavement temperatures for the Al Jufroh location.	221
Table 5.43 Regression models for minimal pavement temperatures for the Al Jufroh location.	221
Table 5.44 Maximum of seven-day average of predicted maximal daily temperatures and minimum of minimal daily temperatures from year 2000 to year 2009, year 2012–2013, for the Brak location.....	221
Table 5.45 Maximum of predicted maximal daily temperatures for years 2000–2009 and 2012 for the Brak location. ....	222
Table 5.46 Descriptive statistics for data for 11 years at the Brak location. ....	222
Table 5.47 Reliability data for PG at the Brak location.....	223
Table 5.48 PG for different levels of reliability for the Brak location. ....	223
Table 5.49 Regression models for maximal pavement temperatures for the Ghadamis location.....	223
Table 5.50 Regression models for minimal pavement temperatures for the Ghadamis location.....	223
Table 5.51 Maximum of seven-day average of predicted maximal daily temperatures and minimum of minimal daily temperatures from year 2000 to year 2009, year 2012–2013, for the Ghadamis location. ....	224
Table 5.52 Maximum of predicted maximal daily temperatures for years 2000–2009 and 2012 for the Al Joufroh location.....	224
Table 5.53 Descriptive statistics for data for 11 years at the Ghadamis location.....	225
Table 5.54 Reliability data for PG at the Ghadamis location. ....	225
Table 5.55 PG for different level of reliability for the Ghadamis location.....	225
Table 5.56 Regression models for maximal pavement temperatures for the Ghat location. ....	226
Table 5.57 Regression models for minimal pavement temperatures for the Ghat location.....	226
Table 5.58 Maximum of seven-day average of predicted maximal daily temperatures and minimum of minimal daily temperatures from year 2000 to year 2009, year 2012–2013, for the Ghat location.....	226
Table 5.59 Maximum of predicted maximal daily temperatures for years 2000–2009 and 2012 for the Ghat location. ....	227

Table 5.60 Descriptive statistics for data for 11 years at the Ghat location. ....	227
Table 5.61 Reliability data for PG at the Ghat location.....	228
Table 5.62 PG for different level of reliability for the Ghat location. ....	228
Table 5.63 PG for pavement temperatures at the surface, for eight locations. ....	228
Table 5.64 PG for pavement temperatures at 3 cm depth for eight locations.....	229
Table 5.65 PG for pavement temperatures at 8 cm depth for eight locations.....	229
Table 5.66 PG for pavement temperatures at 15 cm depth for eight locations.....	229

## List of figures

Figure 1.1 Libya's road network. (Source Ezilion maps) .....	2
Figure 1.2 Map of Libyan climate (Source: <a href="http://fanack.com/en/countries/libya/basic-facts/geography-and-climate/">http://fanack.com/en/countries/libya/basic-facts/geography-and-climate/</a> ) .....	5
Figure 1.3 Temperature Data Logger Picture ( source: HUATO Company General Catalogue)...	7
Figure 2.1 Energy balance on the surface of the pavement. (William Herb, Mihai Marasteanu and Heinz G. Stefan, 2006).....	17
Figure 2.2 The effects of temperature and solar radiation on pavement .....	19
Figure 2.3 Definition of solar and surface angles (Kreith, 1986) .....	22
Figure 2.4 Explanation of PG symbol.....	39
Figure 3.1 Geographic and climatic location of Libya. ....	42
Figure 3.2 Temperature variations in south region in Libya. ....	44
Figure 3.3 Raveling distress in Libyan roads characteristic .....	46
Figure 3.4 Block cracking distress in Libyan roads.....	46
Figure 3.5 Longitudinal and transverse cracking distress in Libyan roads.....	47
Figure 3.6 Alligator cracking distress in Libyan roads.....	47
Figure 3.7 Alligator cracks in Libya roads .....	48
Figure 3.8 Edge damages in Libya roads.....	48
Figure 3.9 Road damages in Libya roads.....	49
Figure 3.10 Rutting distresses ( <a href="http://www.pavementinteractive.org/article/rutting/">http://www.pavementinteractive.org/article/rutting/</a> ) .....	49
Figure 3.11 Road damages in Libya roads.....	50
Figure 3.12 Libya stats map (Source Ezilion maps) .....	51
Figure 3.13 Location of the study area station (Source Ezilion maps).....	52
Figure 4.1 Pavement layers and thermocouples locations .....	56
Figure 4.2 Maximal daily temperatures at Bark during the study period (1.3.2012.- 4.3.2013.) .	57
Figure 4.3 Minimal daily temperatures at Brak during the study period (1.3.2012.- 4.3.2013.)..	58
Figure 4.4 Box plot of maximal daily temperatures the Al-Jufroh location.....	60
Figure 4.5 Box plot of minimal daily temperatures at the Al-Jufroh location.....	61
Figure 4.6 Air and pavement temperatures at four depths at the Brak location for June 30, 2012. .....	62
Figure 4.7 Air and pavement temperatures at four depths at Brak location for .....	62
Figure 4.8 Relationship between maximal daily air and pavement temperatures at the Brak location.....	63
Figure 4.9 Relationship between minimal daily air and pavement temperatures at the Brak location.....	63
Figure 4.10 Air, pavement temperatures and solar radiation at Ghat on 30 <sup>th</sup> and 31 <sup>st</sup> of December 2012.....	65
Figure 4.11 Air, pavement temperatures and solar radiation at the Ghat location 5 <sup>th</sup> and 6 <sup>th</sup> June 2012.....	65

Figure 4.12 Cumulative solar radiations at the Ghat location during one year .....	66
Figure 4.13 Maximal daily temperature at layer C1 versus the maximal daily air temperature at the Al-Jufroh location .....	69
Figure 4.14 Maximal daily temperature at layer C2 versus the maximal daily air temperature at the Al-Jufroh location .....	69
Figure 4.15 Maximal daily temperature at layer C3 versus the maximal daily air temperature at the Al-Jufroh location .....	70
Figure 4.16 Maximal daily temperature at layer C4 versus the maximal daily air temperature at the Al-Jufroh location .....	70
Figure 4.17 Minimal daily temperature at layer C1 versus the minimal daily air temperature at the Al-Jufroh location .....	71
Figure 4.18 Minimal daily temperature at layer C2 versus the minimal daily air temperature at the Al-Jufroh location .....	71
Figure 4.19 Minimal daily temperature at layer C3 versus the minimal daily air temperature at the Al-Jufroh location .....	72
Figure 4.20 Minimal daily temperature at layer C4 versus the minimal daily air temperature at the Al-Jufroh location .....	72
Figure 4.21 Maximal daily C1 temperatures for all locations as a function of maximum daily air temperature and latitude .....	75
Figure 4.22 Minimal daily C1 temperatures for all locations as a function of maximum daily air temperature and latitude .....	75
Figure 4.23 C1 maximal daily temperature as a function of the day of the year for the Brak station .....	76
Figure 4.24 C1 minimal daily temperature as a function of the day of the year for the Brak station .....	77
Figure 4.25 Maximal daily C1 temperature as a function of maximal daily air temperature and the day of the year for the Brak station .....	80
Figure 4.26 Minimal daily C1 temperature as a function of minimal daily air temperature and the day of the year for the Brak station .....	82
Figure 4.27 Actual maximal daily pavement temperature at C1 depth versus predictions from the model including maximal daily air temperature, latitude, the day of the year, and cumulative solar radiation at the Al Jufroh location. ....	117
Figure 4.28 Actual maximal daily pavement temperature at C2 depth versus predictions from the model including maximal daily air temperature, latitude, the day of the year, and cumulative solar radiation at the Al Jufroh location. ....	118
Figure 4.29 Actual maximal daily pavement temperature at C3 depth versus predictions from the model including maximal daily air temperature, latitude, the day of the year, and cumulative solar radiation at the Al Jufroh location. ....	118

Figure 4.30 Actual maximal daily pavement temperature at C4 depth versus predictions from the model including maximal daily air temperature, latitude, the day of the year, and cumulative solar radiation at the Al Jufroh location. ....	119
Figure 4.31 Actual minimal daily pavement temperature at C1 depth versus predictions from the model including minimal daily air temperature, latitude, the day of the year, and cumulative solar radiation at the Al Jufroh location. ....	119
Figure 4.32 Actual minimal daily pavement temperature at C2 depth versus predictions from the model including minimal daily air temperature, latitude, the day of the year, and cumulative solar radiation at the Al Jufroh location. ....	120
Figure 4.33 Actual minimal daily pavement temperature at C3 depth versus predictions from the model including minimal daily air temperature, latitude, the day of the year, and cumulative solar radiation at the Al Jufroh location. ....	120
Figure 4.34 Actual minimal daily pavement temperature at C4 depth versus predictions from the model including minimal daily air temperature, latitude, the day of the year, and cumulative solar radiation at the Al Jufroh location. ....	121
Figure 4.35 Actual maximal daily pavement temperature and predicted maximal daily pavement temperatures from the model including maximal daily air temperature, distance from the surface, and day of the year at the Al-Jufroh location.....	138
Figure 4.36 Actual minimal daily pavement temperature and predicted minimal daily pavement temperatures from the model including minimal daily air temperature, distance from the surface and day of the year at the Al Jufroh location. ....	138
Figure 4.37 Maximal daily temperature at layer C2 versus the maximal daily surface temperature at the Al-Jufroh location. ....	140
Figure 4.38 Maximal daily temperature at layer C3 versus the maximal daily surface temperature at the Al-Jufroh location. ....	141
Figure 4.39 Maximal daily temperature at layer C4 versus the maximal daily surface temperature at the Al-Jufroh location. ....	141
Figure 4.40 Minimal daily temperature at layer C2 versus the minimal daily surface temperature at the Al-Jufroh location. ....	142
Figure 4.41 Minimal daily temperature at layer C3 versus the minimal daily surface temperature at the Al-Jufroh location. ....	142
Figure 4.42 Minimal daily temperature at layer C4 versus the minimal daily surface temperature at the Al-Jufroh location. ....	143
Figure 4.43 Maximal daily C2 temperatures for all locations as a function of the maximal daily surface temperature and latitude. ....	144
Figure 4.44 Maximal daily C3 temperatures for all locations as a function of the maximal daily surface temperature and latitude. ....	145
Figure 4.45 Maximal daily C4 temperatures for all locations as a function of the maximal daily surface temperature and latitude. ....	145

Figure 4.46 Minimal daily C2 temperatures for all locations as a function of the minimal daily surface temperature and latitude. ....	146
Figure 4.47 Minimal daily C3 temperatures for all locations as a function of the minimal daily surface temperature and latitude. ....	146
Figure 4.48 Minimal daily C4 temperatures for all locations as a function of the minimal daily surface temperature and latitude. ....	147
Figure 4.49 Maximal daily C2 temperature as a function of maximal daily surface temperature and the day of the year for the Brak station. ....	149
Figure 4.50 Minimal daily C2 temperature as a function of minimal daily surface temperature and the day of the year for the Brak station. ....	151
Figure 4.51 Actual maximal daily pavement temperature at C2 layer and predictions from the model including the maximal daily surface temperature, cumulative solar radiation and the day of the year at the Al-Jufroh location. ....	174
Figure 4.52 Actual maximal daily pavement temperature at C3 depth versus predictions from the model including maximal daily surface temperature, cumulative solar radiation and the day of the year at the Al-Jufroh location. ....	174
Figure 4.53 Actual maximal daily pavement temperature at C4 depth versus predictions from the model including maximal daily surface temperature, cumulative solar radiation and the day of the year at the Al-Jufroh location. ....	175
Figure 4.54 Actual minimal daily pavement temperature at C2 depth versus predictions from the model including minimal daily surface temperature and the day of the year at the Al Jufroh location. ....	175
Figure 4.55 Actual minimal daily pavement temperature at C3 depth versus predictions from the model including minimal daily surface temperature, cumulative solar radiation and the day of the year at the Al Jufroh location. ....	176
Figure 4.56 Actual minimal daily pavement temperature at C4 depth versus predictions from the model including minimal daily surface temperature, cumulative solar radiation and the day of the year at the Al Jufroh location. ....	176
Figure 4.57 Actual maximal daily pavement temperature and predicted values from the model including maximal daily surface temperature, depth from the surface and day of the year at the Al-Jufroh location. ....	193
Figure 4.58 Actual minimal daily pavement temperature and predicted values from the model including maximal daily surface temperature, depth from the surface and day of the year at the Al Jufroh location. ....	194
Figure 4.59 Comparison between daily minimum surface pavement temperature prediction model and SHRP and LTPP models at the Ghat location. ....	195
Figure 4.60 Comparison between daily maximum surface pavement temperature prediction model and SHRP and LTPP models. ....	196
Figure 5.1 Graphical comparison of two binders meeting penetration and viscosity grading specification. ....	199

Figure 6.1 PG temperature zoning across Libya's desert area for wearing course layer .....	237
Figure 6.2 PG temperature zoning across Libya's desert area for binder course layer .....	238



## Chapter 1 INTRODUCTION

Asphalt pavements form an integral part of any transportation system. The structural capacity of the hot mix asphalt concrete layers depends on many factors including its temperature. Temperature can also be a major contributor to several types of distresses. Therefore, temperature is a significant factor that affects the performance and life span of a pavement.

The Libyan road network expanded at a phenomenal pace from approximately 1500 km of paved roads in 1970 to more than 34,000 km in 2010. Presently, the road construction program is still under way in all regions of Libya. The main function of these roads is to connect the cities, towns and villages as possible throughout the country so; it is necessary to have roads with excellent pavement from structural and functional point of view.

The road network density is generally satisfactory, the total length of Libya's paved road network is about 34,000 km (2010), of which about 15,000 km main roads, the secondary and agricultural road network is about at 18,000 km.

The unpaved network is about 3,000 km long, there is also a network of seasonal tracks about 50,000 km. Figure 1.1 shows Libya's road network. The highway network is classified into four main roadway types:

- Expressways: Roads arteries outside municipal borders linking the cities and regions with two carriage ways and at least four lanes (two lanes or more in each direction).
- Main roads: Roadways linking cities and regions, or serving cities within municipal boundaries, there are single carriageway roads for good paved standard or dual carriage ways with two lanes in each direction.
- Secondary roads: These link district centers and villages.
- Agricultural roads: Roads linking agricultural land and farms with markets.

Two main strategic highways have been planned for Libya's road network. One of them, the North-South highway, is almost completed. The other is the East-West highway, which will run from the Tunisian border up to the Egyptian border. This is a two-lane highway in each direction; it is fully access controlled with a speed limit of 130 km/hour. It is planned up to international standards and will be part of the Maghreb highway, which runs from Morocco to Egypt as well as being part of the Mediterranean road system.



Figure 1.1 Libya's road network. (Source Ezilion maps)

## 1.1 Background

A significant factor that affects the performance and life span of a pavement is the influence of temperature. Temperature can contribute to certain common types of asphalt pavement distresses such as permanent deformation or rutting (typically associated with high temperature environments), bleeding, and thermal cracking (associated with low temperature environments). The Strategic Highway Research Program (SHRP) established the Long-term Pavement Monitoring Program (LTPP) program in 1987 to support a broad range of pavement performance analyses leading to improved engineering tools to design, construct, and manage pavements (Diefenderfer, *et al.* 2002).

The Seasonal Monitoring Program (SMP) was established as an element of LTPP in 1991 to measure and evaluate the effects of temperature and moisture variations on pavement performance and validate the available models (Mohesni, 1998; Diefenderfer, *et al.* 2002). From the initial SHRP testing and SMP data, several pavement temperature models were developed to assist in the proper selection of the asphalt binder performance grade (PG) (Mohesni, 1998; Mohesni and Symons, 1998a; Mohesni and Symons, 1998b; Lukanen, 1998; Diefenderfer, *et al.* 2002). Solaimanian and Kennedy (1993) proposed an analytical model based on the theory of heat and energy transfer. Shao *et al.* (1997) also developed a procedure based on heat transfer theory to estimate pavement temperatures. Regression models based on other sets of data were developed (Bosscher *et al.* 1998; Marshall *et al.* 2001). A simulation model was developed to calculate temperatures during summer conditions based on the heat transfer models developed by Solaimanian and Kennedy (Hermansson, 2000 and 2001; Diefenderfer, *et al.* 2002).

Al-Abdul Wahhab et al. (1994) conducted a study in two regions in Saudi Arabia to manually measure pavement temperatures in different pavement sections. The study concluded that the extreme pavement temperatures in arid environment ranged between 3 and 72°C, while in coastal areas, the temperature ranged between 4 and 65°C. In another study, Al-Abdul Wahhab *et al.* (1997) recommended five performance graded binder zones for the whole Gulf area. The study also proposed modification of the currently used binders to suit the proposed grades.

Libya as well as the desert area, in general, possesses a different environment from that of North America and the Gulf area. The applicability of the recent SHRP and LTPP developments in the United States to Libya's or the desert area's environmental conditions needed to be evaluated.

The Strategic Highway Research Program (SHRP), conducted in the United States and Canada between 1987 and 1992, resulted in a new approach to asphalt mix design (Superpave). The new approach includes a grading system for asphalt binder, called performance grading (PG), that proposes a two-number system intended to insure that the proper asphalt binder is used with resistance to pavement rutting in hot temperatures and with resistance to cracking in cold temperatures. The two numbers in the new approach represent the expected maximum high and minimum low asphalt temperatures, based on local climatic data for the hottest and coldest times of the year.

A significant number of departments of transportation across the United States and Canada either have already implemented, or are in the process of implementing, the Superpave design. However, implementation of Superpave raises questions with respect to pavement temperature estimations since the new performance grading method for asphalt binders appears to modify the asphalt operational temperature range, and thus further limits availability of asphalt that meets the prescribed criteria. One concern associated with this implementation is the cost since both asphaltic cement and aggregate costs may be higher for Superpave mixes due to limited sources or increased processing than for normal agency mix designs. Also, performance grading requirements either may require modifications in the asphalt or simply further constrain the available crude oil sources. In either case, the cost of asphalt may increase by as much as 30 percent over conventional agency implementations. The Superpave performance grading requirements for lower asphalt layers - including the binder and base courses, and the appropriate binder selection for hot mix asphalt recycling, calls for a detailed understanding of the temperature profile in pavements.

## **1.2 Study area**

A pavement monitoring station was established at eight stations in the Libyan desert to monitor air, pavement temperatures, wind speed and solar radiation. Table 1.1 shows the weather station locations and climatic regions. Data were collected for 365 days. Daily minimum and maximum

temperatures were recorded. Regression analysis was used to develop the low pavement temperature model. Stepwise regression was used to develop high temperature models using air temperature, solar radiation, and duration of solar radiation as independent variables.

Table 1.1 Weather station locations and climate regions

Location	Climatic Region	Latitude & Longitude	Elevation	Max temp	Min temp	Precipitation (per year)
Kufra	Desert	24°13'N 23°18'E	435 m	46	-5	1 mm
Ghadames	Desert	30°08' N 9°30' E	360	42.5	2	2mm
Brak	Desert	27°32' N 14°16' E	349	46	-2	2mm
Ghat	Desert	24°59'N 10°11'E	710	48	-2	0.5mm
Wuddan	Desert	29°02'N 16°00'E	288	45	1	1mm
Awbari	Desert	26°46'N 12°57'E	468	46	-3	0.5mm
Al Qatrun	Desert	24°56'N 15°03'E	479	48	-2	0.5mm
Ojalah	Desert	29°08' N 21°33' E	49	42	2	1.5mm

### 1.2.1 Climate

The Mediterranean and the Sahara together have a large influence on the climate. The Greek historian Herodotus wrote, in the 5th century BCE: 'In the higher parts of Libya, it is always summer', and this is still true. Along the coast there is a Mediterranean climate with hot summers and mild winters. Tripoli has an average winter temperature of 14°C. In early summer temperatures reach 30°C, with high humidity. In July and August the temperature can reach 40°C. From October till March, rain falls along the coast.

The highlands, such as Jebel Algarbi and Jebel Akhdar, are generally cooler. In winter, the temperatures sometimes fall below freezing. Snow falls occasionally; Jebel Algarbi was snow-covered in 1994. In the interior, the climate becomes dryer, and the desert is extremely arid.

Temperatures can reach 50°C in summer, and nighttime temperatures drop drastically. On the coast, the wind usually blows from the northeast or north, hot in summer and colder in winter. In spring and fall, a hot, dry, dust-laden wind called ghibli blows over the country. This south wind

lasts from one to four days, and the dust storms and sandstorms it raises often affect the countries north of the Mediterranean. The winds have eroded the Libyan mountain ranges, as exemplified in the Tibesti Mountains.

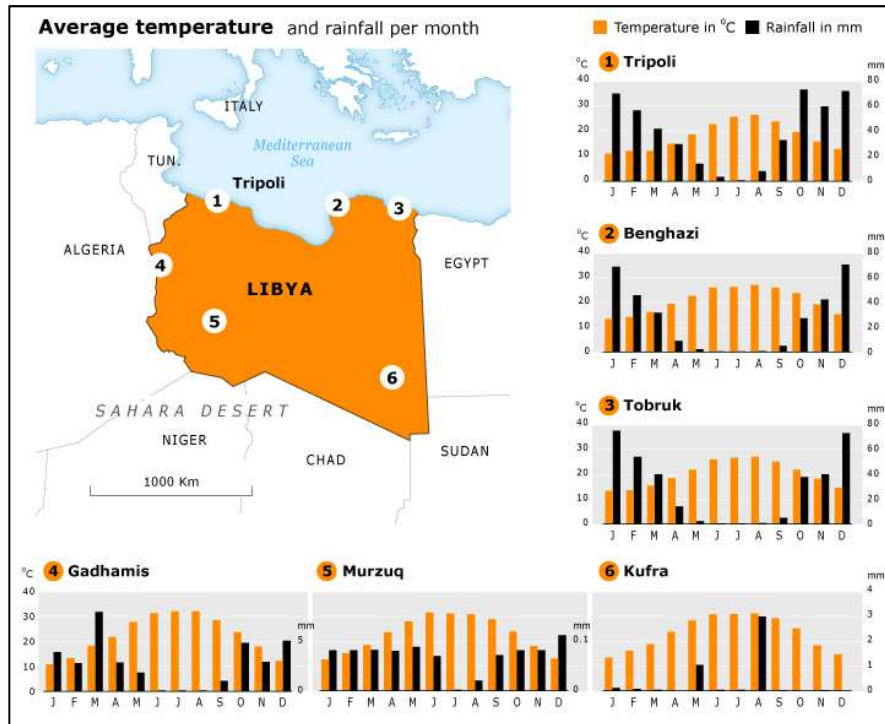


Figure 1.2 Map of Libyan climate (Source: <http://fanack.com/en/countries/libya/basic-facts/geography-and-climate/>)

Libya is located in a hot and arid climatic region characterized by high variation in daily temperatures, high solar radiation, low humidity, low precipitation, wind and dust storms (Table 1.1). Asphalt pavement roads are the main and only source of the Libyan overland transportation system for most passengers and goods. Though the design life for Libyan roads is 20 years, the harsh climate leads to rapid deterioration and reduced service life. The tendency for the asphalt binder to harden and age under atmospheric influences has been known and studied for many years. High solar radiation with the presence of oxygen accelerates and increases the physical, chemical, and photochemical processes in the asphalt binder. The pavement in midday of summer season can be heated by solar radiation to more than 70°C, but it may cool down in some extreme cases to freezing temperatures during night. This swinging and fluctuation of solar radiation and temperatures induces thermal stresses and causes fast aging in the asphalt pavement layers. Therefore, thermal cracking becomes a problem.

### **1.2.2 Pavement temperature prediction**

Flexible pavements comprise a majority of the primary highways in Libya. These primary roads are subjected to heavy loading that can cause significant damage to the hot-mix asphalt (HMA) pavements. As HMA is a viscoelastic material, the structural or load-carrying capacity of the pavement varies with temperature. Thus, to determine in-situ strength characteristics of flexible pavement, it is necessary to predict the temperature distribution within the HMA layers. The majority of previously published research on pavement temperature prediction has consisted of predicting the annual maximum or minimum pavement temperature so as to recommend a suitable asphalt binder performance grade.

To determine the pavement temperature profile, the influence of the air temperature and seasonal changes must be understood so that the effects of heating and cooling trends within the pavement structure can be quantified. Recent investigations have shown that it is possible to model daily pavement maxima and minima temperature by knowing the maximum or minimum air temperatures, the depth at which the pavement temperature is desired, and the day of the year of appearance of extreme temperatures at a particular location. (Diefenderfer, 2002).

### **1.3 Problem statement**

Previous research has investigated prediction of pavement temperatures mainly due to changes in air temperature for pavement design purposes. However, the equations predicting pavement temperature from air temperature has been based on early theoretical and experimental studies performed worldwide, but not covering desert area like Libiyan Desert, with its particular climate conditions.

The current asphalt binder specifications in Libya are based on the bitumen Penetration Grade: penetration test is performed at 25°C. Penetration is an empirical measure of the consistency that is used as an empirical indicator of the rutting and fatigue susceptibility of asphalt binder, and is not related to pavement performance. The new approach, involved through SHRP Investigation program, with Superpave method for asphalt mixture design, has include number of parameters for ambiental impacts on pavement, with detailed anayse of temperatures. But model is under the question for implementation in special desert areas.

### **1.4 Methodology**

Eight climatic regions of Libya's desertarea were identified for this research. These are located between 18° and 29°latitude, with dimensions nearly 1500km \* 900km and include: Kufra, Ghadames, Brak, Ghat, Wuddan, Awbari, Al Qatrunand Ojalah.

Eight stations, one representing each of the climatic regions, were chosen and the weather data for each location were obtained from the Libyan National Climatic Database Center. The weather data included 10 years of daily maximum and minimum temperatures, daily average percent sunshine, daily average rainfall, and daily average wind speed for each location. A monitoring station was set-up to collect data on air temperature, wind speed, solar radiation and pavement temperatures at various depths. The enclosure was mounted on an instrumentation tower. The data logger was operated by a solar battery.

For this study, the sensors (HUATIO S300 ) SERIES TEMPERATURE DATA LOGGER was used to record temperatures of different depths of asphalt pavement in different locations. S300 Series temperature humidity logger HUATO Digital temperature and humidity logger is widely used in the engineering purposes medical industry, electronic industry, food industry, the transport industry, the meteorological industry, textile industry, HVAC refrigeration, file management, agricultural research, biochemistry lab as well as hospitality industry and food and beverage business. Table 1.2 shows the technical specification of data logger and the figure 1.3 presents the picture of data logger.

Table 1.2 Technical Specification of data logger

Temperature accuracy	$\pm 0.3C$
Humidity accuracy	$\pm 3\%$
Recording volume	43000
Temperature measurement range	-40-85C
Logging interval	2S-24H



Figure 1.3 Temperature Data Logger Picture (source: HUATO Company General Catalogue)

Data were analyzed using the statistical package Statistica 12 (StatSoft Inc., Tulsa, OK, USA), university license for Novi Sad University.

Table 1.3 The structures with layer thickness of stations that temperatures were recorded by sensors.

Station Name	Material Designation	Wearing course (cm)	Binder course (cm)	Base course (cm)	Natural subgrade
Kufra	AC	5	9	20	---
Ghadams	AC	5	9	20	---
Brak	AC	5	9	20	---
Ghat	AC	5	9	20	---
Wuddan	AC	5	9	20	---
Ubari	AC	5	9	20	---
Algatron	AC	5	9	20	---
Ojalah	AC	5	9	20	---

## 1.4 Objectives of research

The objective of this research is to develop a model to determine pavement temperature from air temperature for special desert conditions. This model should accurately describe the effects of seasonal variation on pavement temperature in desert conditions and be able to accurately predict temperatures within the HMA layers. To achieve this, the following needs to be accomplished:

- Study the relationship between air temperature and pavement temperature at several depths within the pavement;
- Develop a regression equation to predict temperature at several depths within the pavement based on air temperature;
- Quantify the effects of seasonal variations and pavement location on pavement temperature using parameters such as date or solar radiation to develop a predictive model;
- Develop a PG MAP (Performance Grade Map) of Libya's roads located in the desert area, determine the PG of bitumen used in Libya, and make a comparative study between PG Map and bitumen used up to now in the study area. .

The overall objective is to improve the design and construction of roads in Libya through:

- Defining zones in Libya's desert areas with a different climate (temperature);
- Determining a model of temperature propagation through pavement and correlation between air temperature, road surface temperatures in the characteristic depth (in the individual layers);



- Defining the recommended design temperature for the individual layers of asphalt and some desert areas and linking these data with the appropriate type of bitumen with the PG gradation;
- Mapping Libya's desert areas and dividing them into zones designated by the recommended applicable temperature (i.e., the required performance of bitumen and asphalt mixtures).

## **1.5 Research Hypotheses**

The general hypotheses in this research:

For desert areas, such as the Sahara region, existing models for pavement “project temperatures” prediction are not very reliable, and could be improved through investigations with well-defined procedures and appropriate assumptions and instrumentation, using in field measurements and existing climate data for the Sahara region. This would be the basis for reliable temperature model development and PG mapping (according PG bitumen gradation) of the Sahara desert area.

## **1.6 Scope of research**

To achieve the objectives of this study, research was performed as part of the ongoing studies for recording air and pavement temperatures in Libya. Instrumentation was installed to allow for quantitative measurement of the pavement response due to ambient environmental conditions.

This thesis is organized as follows: Chapter 2 presents a theory of temperature and radiation influences on a flexible pavement and presents previously developed pavement temperature prediction models (STATE OF THE ART). Chapter 3 describes the environmental monitoring portion of the research conducted on the Libyan Road Network. Details of pavement temperature research are given. Chapters 4 and 5 present data and analysis. Chapter 6 presents the summary and conclusions of the research, and Chapter 7 offers recommendations for further study.

## **Chapter 2 BACKGROUND**

To develop and calibrate the pavement performance and temperature prediction models of pavement, it is necessary to know the available methods used for pavement temperature evaluation models and prediction. The approaches used for pavement temperature prediction models are summarized in this chapter.

### **2.1 Pavement Temperature Prediction Models**

Roadways constructed using hot-mix asphalt (HMA) are complex to characterize in terms of their in-situ performance due to the nature of the material. HMA is a viscoelastic material; that is it exhibits the properties of both a viscous and an elastic material. At low temperatures, HMA acts as an elastic solid where low amounts of applied strain are recoverable and thus permanent deformation is not likely to occur until this low strain limit is surpassed. However, at high temperatures, HMA acts as a viscous fluid in which the material will begin to flow with an applied strain. These variations in temperature related performance show why it is important to consider the in-situ properties of HMA during its laboratory evaluation.

The temperature within a section of pavement varies due to several factors. The most important is ambient temperature. Next is solar radiation (especially during the summer months). Following these, in lesser significance are wind speed and relative humidity. The ambient temperature will vary with season and location. Solar radiation is an important factor to consider when trying to describe or predict the pavement temperature profile. As the earth revolves about its axis of rotation, different areas of the planet receive differing amounts of radiation. During the summer months, this radiation is greater due to the fact that the surface of the earth at that location is closer to being perpendicular to the sun than during the winter months. In addition, there are seasonal effects that must be considered. During the summer months, the temperature of the ground will tend to increase (even at depths up to 1m) and this heat can be conducted to upper layers following the first law of thermodynamics. Thus, seasonal effects are nearly as important to consider as daily environmental fluctuations. (Diefenderfer, 2002)

Extensive research on flexible pavement prediction models has been carried out in many different climate areas of the world. Pioneering research in the field of asphalt pavement temperatures was done by Barber (1957). Barber attempted to correlate pavement surface temperatures and temperatures at 3.5in depths with standard weather report information. The weather parameters used were wind speed, precipitation, air temperature, and solar radiation. The pavement was considered to be a semi-infinite mass in contact with air. Baber (1957) observed that pavement temperature fluctuations measured in Hybla Valley, Vir, roughly followed a sine curve within a period of one day. The research showed that when solar radiation was included in

the analyses with air temperature, the sine curve approximation provided estimates of asphalt surface temperatures. (Yavuzturk and Ksaibati,2002)

Straub et al. (1968) studied asphalt pavements in the northern climate of New York. The study considered both 6 in and 12 in thick dense graded pavement at various depths. A computer model was developed to predict pavement temperature based on air temperature and solar radiation. The study showed that surface temperature measurements must be made at the surface to achieve a good correlation with solar radiation received at the site. Straub stated the temperatures at various depths of an asphalt pavement are independent of the thickness of the flexible pavement. He indicated that solar radiation had greater effect on surface temperatures than air temperatures.

Southgate and Deen (1969) developed a method of adjusting pavement deflection measurements to a reference mean pavement temperature using a five-day air temperature history. A linear relationship was found between pavement temperatures at a given depth and the sum of the surface temperature and the five-day mean air temperature history. A model validation was performed using data from Arizona and New York.

Rumney and Jimenez (1971) conducted a study of pavement temperatures in the southwest United States, near Tucson, Ariz. In this hot desert climate, maximum pavement temperatures are a main concern to pavement engineers. Researchers were looking for a practical tool for predicting maximum surface temperatures. The study collected pavement temperatures at various depths, as well as corresponding surface temperature and rate of incident solar radiation. From this data set, correlations were developed that predicted pavement temperatures for a given set of air temperatures and solar radiation intensities. Sets of curves were developed for pavement temperatures at 2 in and 4 in depths.

Pavement temperatures are of concern for pavement engineers in many climates worldwide. In South Africa, the primary consideration is the maximum pavement temperature in the upper levels of pavement. Williamson (1971) developed a model adapting a FORTRAN IV. This model used finite-difference techniques to predict temperatures at various depths over a short period of time, usually a day. Inputs for the model included climatic parameters as well as the thermal properties of the pavement. A series of sensitivity analyses was performed investigating the impact of the radioactivity of the pavement material, pavement density, and possible errors in the measurements of incident radiation, initial temperature boundary conditions, and air temperature. This study showed that variation in other items, such as emissive power, convection coefficient, and thermal conductivity, had marginal effects on temperature. In addition, the model was validated using case studies. Data for model validation was collected from 8 in thick asphalt pavement and a Portland cement concrete pavement section in Pretoria. Actual temperatures and predicted temperatures were plotted versus time for various 24-hour periods.

The results showed a good correlation between predicted and measured temperatures. However, neither precipitation nor humidity effects were considered in the model. Also studied were the differences in temperature of pavements painted white versus naturally colored asphalt pavement and surface temperatures of cement treated base that were sheltered from direct sunlight versus those exposed.

Christson and Andereson (1972) investigated the response of asphalt pavements to low temperature climatic environments. A computer model was developed that used a numerical finite difference method to predict the thermal regime in pavement systems. Christson and Andereson used a one-dimensional, transient approach in a homogeneous pavement to solve resulting energy balance equations with an implicit scheme. Input variables were the meteorological data, such as the air temperature, solar radiation, cloud cover and wind velocity, structural and physical properties including the geometry of asphalt pavements and thermo-physical properties of asphalt materials. Comparison between predicted temperatures throughout the asphalt pavement and measured temperatures showed excellent agreement at the Alberta, Canada test site. (Yavuzturk and Ksaibati, 2002)

In Norway, Noss (1973) studied pavement temperatures related to frost penetration in subgrades. Using weather and pavement temperature data collected at the Vormsund Test Road, multivariate regression analyses were performed to predict the difference between air temperature and pavement temperature during cold winters. This boundary condition could then be used to calculate frost depth. The parameters included in regression analyses were 30-year mean air temperature (i.e., normal air temperature), relative difference between the normal air temperature and the recorded temperature, precipitation, wind velocity, cloud cover, relative humidity, and absorbed global radiation at the surface. Regression coefficients were calculated for various months.

Berg (1974) investigated the accuracy of individual balance components and total energy balance at the surface of pavement sections constructed with Portland cement concrete. Experimental data were obtained from a section located at Lebanon Regional Airport in Lebanon, N.H. The surface energy balance approach included heat transfer due to incident and short reflected short-wave radiation, long-wave radiation emitted by the atmosphere and the earth's surface, convection, conduction into the air and ground, evaporation and condensation on the surface, and infiltration of moisture into the ground. The study concluded that a surface energy balance approach was not sufficient to estimate frost and thaw depths within 15% of measured depths.

Wilson (1975) used data collected from four pavement sections laid next to the Alconbury By-Pass in the United Kingdom. The study also considered solar radiation for cloudless skies. Data collected on one such rare day were compared to the predicted values. Since published values for solar radiation and the thermal properties of the pavement material were used, the model yielded

results with limited accuracy. In addition, an empirical approach was tried. In this study, daily pavement temperatures were represented as sine function. Temperature variation with depth was accounted for by applying a factor that reduced the amplitude of the sine curve with increasing depth. The method provided the greatest accuracy during the warming period at the surface, but had decreasing accuracy with increasing depth.

Dempsey et al (1987) developed a climatic database for the State of Illinois. This database was derived from weather station records in 23 locations in and near the state. Maps were developed showing areas of equal percent sunshine and wind speed. A table of average weekly high and low air temperatures was also produced. Using this new database, combined with the heat transfer model developed years earlier, several new applications could be made. In one application, pavement temperatures were computed with the heat transfer model and climate data. A regression analysis was run to establish a relationship between pavement temperatures and Mean Monthly Air Temperatures (MMAT). This information could then be used for selection of the proper asphalt concrete modulus value to be used in pavement design. The heat transfer model together with input from the climate database produced the dependency of pavement temperatures on MMAT which compared well to published correlations by the Asphalt Institute. The new tools also were used to predict temperature profiles in PCCP for a given date, time, and location. (Yavuzturk and Ksaibati, 2002).

Wolfe et al. (1987) suggested a “simple” predictive method based on heat transfer equations to determine the cooling rate of a freshly laid asphaltic mat under a given set of environmental conditions. The method was developed to help pavement engineers decide whether to proceed with construction on a daily basis. Research indicated that the cooling rates of mats of sufficient thickness can be slow enough to permit satisfactory compaction even under rather adverse weather conditions and temperatures.

Huber et al. (1989) adapted a computer program originally created to predict long-term permafrost thawing over a period of years. The focus of the research was to develop methods for the prediction of pavement thaw onset so that the time allowable for use of heavy trucks for logging during the winter could be maximized.

Hsieh et al. (1989) developed computer models for predicting temperatures in concrete pavements and rain water infiltration into soil and sub grades due to weather changes. The models use an implicit finite difference scheme that employs spatial factorization to implement the solution as an alternating-direction implicit sequence. The model utilizes a series of TMY (typical meteorological Year) weather databases pertaining to various climate conditions. The significance of the study is that a three-dimensional numerical modeling approach was used coupled with moisture diffusion into pavement. An experimental validation of the model was

attempted using data from sunny and cloud covered days in Miami and Orlando, Fla. (Mohseni, 1998).

The advent of the SHRP steered research in a slightly different direction. The performance-type specifications developed for asphalt cements required that a certain grade of asphalt binder perform over a given range of temperatures. For pavement engineers, knowing the upper and lower temperatures a pavement would be exposed to became important. Solaimanian and Kennedy (1993) made an effort to develop a simple way for pavement engineers to determine these critical temperature extremes. Their study indicated that the difference between maximum pavement temperatures and maximum air temperatures was a function of latitude. A parabolic equation was developed that describes this relationship well. Using a known value of latitude, the maximum expected surface temperature could be approximated. The study also recommended using the lowest expected surface temperature as the lowest expected pavement temperature for design. A third order polynomial corollary equation was suggested to predict pavement temperatures at various depths (Bosscher et al., 1998; Lukanen et al., 1998; Mohseni and Symons, 1998a and 1998b).

Another study to predict effective asphalt layer temperatures was conducted by Inge and Kim (1995), who developed a database approach for the estimation of asphalt concrete mid-depth temperature. The method represents improvements over the AASHTO method for the temperature correction procedure deflections in that air temperatures for the previous five days are not needed, allowing quicker computations. Additionally, the heating and cooling cycles of asphalt pavements are taken into account. The research also studied an alternative temperature prediction model known as the BELLS equation to validate temperature prediction at one-third asphalt depths (Liao et al., 2008).

Lukanen et al. (1998) suggested a probabilistic method for asphalt binder selection based on pavement temperatures. The study developed an empirical prediction model based on simple regression analysis to relate the seven-day average high air temperature to the seven-day average high pavement temperature. The analyses used data from SHRP obtained in Canada and the United States as well as data from LTPP-SMP. Temperature prediction of the empirical model was compared to existing prediction relationships including an asphalt pavement heat flow model (Mohseni, 1998).

Mohseni (1998) proposed revisions to the SHRP performance grading system for asphalt selection, specifically for low temperature applications. The study, based on data from the LTPP-SMP, presents a revised model for determining the low and high temperature component of Superpave performance-based binders. The study compares existing models and resulting performance grades with the proposed approach. However, the temperature limits used for the PG binder specification are pavement temperatures and not air temperatures. Thus, expressions were developed to determine the pavement temperature from the air temperature. The current

expression used for the PG grading is given in equations below and it is referred to as the SHRP models. (Mohseni, 1998).

Bosscher et al. (1998) conducted a study on six test sections on US-53 in Trempealeau County, Wis., by using different performance-graded asphalt binders to validate the superpave pavement temperature algorithm and the binder specification limits. The analysis was focused on development of a statistical model for estimation of low and high pavement temperatures from meteorological data. The model was compared to the superpave recommended model and to the more recent model recommended by the LTPP program. Although the temperature data analyses indicated a strong agreement between the new statistical model and LTPP model for the estimation of low pavement design temperatures, LTPP and superpave models both underestimated the high pavement temperatures at air temperatures higher than 30°C. The temperature data analyses also showed that there are significant differences between standard deviation and air temperatures and the standard deviation of pavement temperatures. The study raised questions about the accuracy of the reliability estimates used in the current Superpave recommendations (Yavuzturk and Ksaibati,2002)

Maintenance decision support system (MDSS) research (Mahoney and Myers 2003; Pisano, Stern, and Mahoney 2005) has shown that predicting weather and road conditions requires weather data at an hourly resolution to properly characterize rapidly changing conditions associated with sunrise, sunset, frontal passages, and precipitation episodes. Road temperature models are particularly sensitive to the solar cycle, as road temperatures rise and fall quickly at dawn and dusk, respectively. The temporal resolution of weather model data provided by the NWS is only three hours. Therefore, anyone using the standard NWS models will only be able to provide forecast information at this temporal resolution. They may provide hourly output by interpolating, but the true resolution will remain three hours. It is likely that the NWS will eventually disseminate selected weather parameters at hourly resolution, but the timeframe for this is unclear.

Liao et al. (2011) developed a temperature prediction model for flexible pavement of freeways in Taiwan. Using thermocouples embedded at 20-mm distance in depth, temperature profiles were determined for 24-hr periods covering seasonal variations. Pavement temperature predictions made by the BELLS model revealed that, at pavement temperature higher than 40°C, the model tends to underestimate pavement temperatures. Considering the climatic characteristics in Taiwan, the air temperature at testing time is used in the model. Also, a single sine function on a 24-hr clock system is used to simplify the predicting equation. The proposed pavement temperature model shows a good correlation between measured and predicted temperatures and has a coefficient of determination around 0.92.

Matić et al, (2011) formulated new models for predicting minimum and maximum pavement surface temperatures in Serbia using regression equations, in dependence on the ambient air

temperature. Furthermore, model validation has been conducted. Based on the correlation coefficient, standard model deviation and the mean absolute error (MAE) and standard deviation of error (SDE) between measured and predicted pavement temperatures, they concluded that the models predict pavement surface temperatures well and that they can be utilized for calculations in analyzing air temperature influence on a pavement structure.

On validating the model for pavement temperature prediction according to the Superpave methodology and in relation to the measured temperatures, the conclusion is that the model does not predict pavement temperature with adequate accuracy.

The model predicting maximum temperatures in the pavement surface was presented by the following equation:

$$Y_{p,max} = 0,065567 + 1,268887 \cdot X_{a,max}. \quad (2.1)$$

Standard model deviation is 3,0016. Correlation coefficient is 0,972651.

The model predicting minimum temperatures in the pavement surface was presented by the following equation:

$$Y_{p,min} = 0,318933 + 1,10967 \cdot X_{a,min}. \quad (2.2)$$

Standard model deviation is 1,8569. Correlation coefficient is 0,980397,

where

$Y_{p,max}$  = predicted maximum daily surface pavement temperature (°C);

$X_{a,max}$  = measured maximum daily air temperature (°C);

$Y_{p,min}$  = predicted minimum daily surface pavement temperature (°C); and

$X_{a,min}$  = measured maximum daily air temperature (°C).

Yuan Xun Zheng et al., 2011, *Advanced Materials Research*, 243-249, 506 presented a kind of new model correlates air and pavement temperatures in bituminous pavement. Based on abundant measured temperature data in Henan Province, China, distribution laws in asphalt concrete pavement temperature is studied detailed and the dependency between air and pavement temperature is discussed by the method of regression analysis and the prediction models of asphalt pavement temperature are established. He found that the Comparisons between measured and predicted asphalt pavement temperatures indicate that the models are equipped with comprehensive applicability and excellent accuracy.

Bojan Matic (2013) presented a new model for predicting minimum surface pavement temperature based on data collected by Road Weather Information System (RWIS) in Serbia in the period from 2010 to 2012 (Matic B., Awadat H.S., Matic D., Uzelac Dj., 2012).

$$Y_{p,min} = 0,910 \cdot X_{a,min} - 0,415 \quad (2.3)$$



where

$Y_{p,min}$  = predicted minimum daily pavement surface temperature; and

$X_{a,min}$  = minimum daily air temperature.

## 2.2 Energy balance in asphaltic pavements

The temperature profile in an asphaltic pavement is affected directly by the thermal environmental conditions to which it is exposed. The primary modes of heat transfer are incident solar radiation, thermal and long-wave radiation between the pavement surface and the sky, convection due to heat transfer between the pavement surface and the fluid (air or water) that is in contact with the surface, and conduction inside the pavement as shown in figure 2.1.

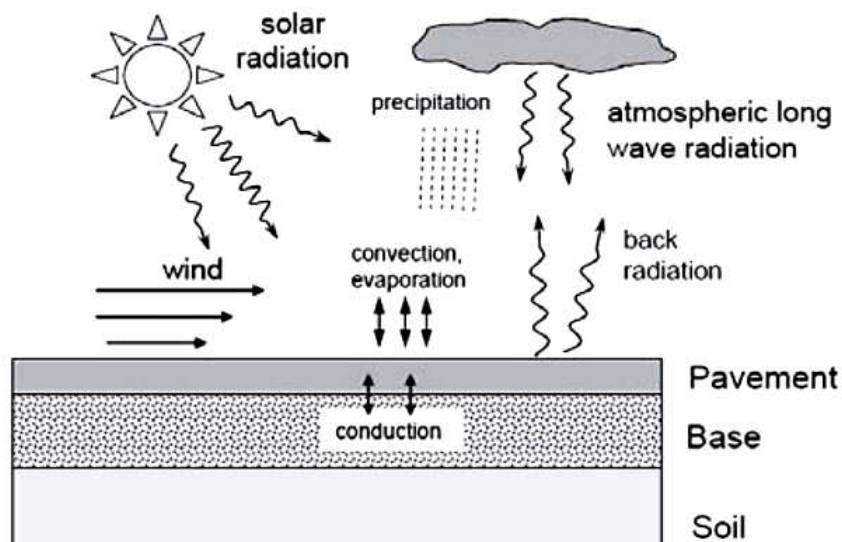


Figure 2.1 Energy balance on the surface of the pavement.(William Herb, Mihai Marasteanu and Heinz G. Stefan, 2006)

The intensity of solar radiation (direct and diffuse) is dependent on diurnal cycles, the location of the sun in the sky and the incident angle between the surface and sun's rays. The solar radiation results in direct and diffuse heat gain on the pavement through absorption of solar energy by the pavement. The convection heat flux is a function of fluid velocity and direction, and it is affected primarily by wind velocity and direction on the surface. As the convection heat transfer coefficient increases due to higher velocities and opportune wind directions, the convective heat flux also increases. Thus, at relatively high wind velocities, a convective cooling of the surface occurs when the temperature of the wind is lower than the temperature of the pavement surface. The direction of the heat transfer due to thermal and long-wave radiation is away from the pavement since deep sky temperatures typically are significantly lower than pavement surface temperatures (Yavuzturk and Ksaibati, 2002).

The surface energy balance on a pavement requires that the sum of all heat gains through the surface of the pavement must be equal to the heat conducted in the pavement. The direction of the heat flux due to convection and thermal radiation is a function of the temperature difference between the pavement surface and the bulk fluid/sky temperatures. In cases where the sky temperature and the bulk fluid temperature are lower than the pavement surface temperature, a cooling of the surface occurs while the surface might simultaneously be heated through incident solar radiation. Thus, depending on the magnitudes of individual heat fluxes, a heating or a cooling of the pavement takes place. An adiabatic bottom surface can be assumed for sufficiently thick pavements stipulating no heat transfer between the pavement and sub-grade layers. Similarly, side surfaces of the pavement (pavement edges) are considered to be adiabatic for sufficiently large horizontal expansions since spatial temperature changes in the vertical direction will be much greater than horizontal changes at pavement edges, and any heat transfer through pavement edge surfaces can be neglected. In this study, a pavement of 730 cm width approximating a two-lane pavement of 50 cm depth and infinitely long length is considered. The length of the pavement is of interest since it affects directly the convective heat flux on the surface (Yavuzturk and Ksaibati, 2002).

### **2.3 Solar radiation**

The solar radiation going through the atmosphere is partially absorbed by its constituents, partially reflected back to space and partially diffused, with the remaining reaching the ground as direct solar radiation. On a planetary scale, 17% of solar radiation is absorbed by the atmosphere, 30% is reflected by the constituents of the atmosphere, and 53% reaches the surface of the earth, 31% of it as direct solar radiation and 22% as diffuse radiation (Shaltout et al., 2001).

Libya lies between a subtropical high pressure cell and the equatorial low pressure cell. We have mentioned that its climate is located in a harsh, hot, and arid region, where, about 88% of the area is considered to be desert. The daily average solar radiation on a horizontal plane is 7.1 kWh/m<sup>2</sup>/day in the coastal region, and 8.1 kWh/m<sup>2</sup>/day in the southern region, with average sun duration of more than 3500 hours per year (Saleh, 2001).

Libya's weather is mostly clear and sunny; thus, there is a high potential for solar energy. The intensity of the incoming solar energy varies widely and significantly over the 24-hour period and as well as over the course of the year. For example, in the Ghat location, radiation ranges from about zero during night to its maximum of about 1300 watts per square meter W/m<sup>2</sup>. In the (middle of the day). It is known that solar radiation can be transmitted through empty space. The above-mentioned fluctuations of solar energy between day and night, and over the year, which causes daily air temperatures to rise and fall in addition to the high absorption coefficient of asphalt binder to solar radiation, leads the upper layers of the pavement to be rapidly effected

and deteriorated. Therefore, prior to introducing the influence of solar radiation on asphalt pavement layers, we introduce hereafter, the cumulative solar radiation for Libyan road pavement and climate conditions.

## 2.4 Aging due to temperatures and solar radiation

The aging of bitumen is a process of change in the bitumen properties due to hardening and changes in the bitumen structure and composition. The presence of oxygen, ultra-violet, and temperature, in addition to dry wind storms, lead to rapid loss of the volatile material in the bitumen, resulting in a decrease of penetration and an increase of the softening point and penetration index (PI). Short-term aging is influenced by the source of the bitumen used, the chemical composition, type of mixture, mixing process temperature and time. Long-term aging is related mainly to the bitumen hardening due to the effect of environmental conditions on the road pavement, which is known as road hardening.

Long-term aging happens more on the surface of the pavement due to the presence of oxygen and the temperature variation is more likely to occur at the surface; aging decreases as the depth of the pavement increases. In-service aging, which occurs when the asphalt (bitumen) reacts with the oxygen in the atmosphere by oxidation, is also affected by air voids, bitumen content and bitumen type or source of bitumen.



Figure 2.2 The effects of temperature and solar radiation on pavement

Aging of bitumen is one of the major factors influencing the performance of the pavement, where the bitumen is subjected to a wide range of temperatures during storage, mixing, and laying, which is known as short-term aging, and in service life, which is known as long-term aging.

## 2.5 Radiation theory (energy equilibrium)

This section presents the current theory on heat transfer in a layered pavement system.

(Diefenderfer, *et al.* 2002)

Considering the earth as a black body radiator system, the net rate of heat flow in and out of the system,  $q_{net}$ , can be expressed as the following:

$$q_{net} = q_s + q_a + q_t \pm q_c \pm q_k - q_r \quad (2.4)$$

where

$q_s$  = energy absorbed from direct (solar) radiation;

$q_a$  = energy absorbed from diffuse radiation (radiation reflected by the atmosphere);

$q_t$  = energy absorbed from terrestrial radiation;

$q_c$  = energy transferred by convection;

$q_k$  = energy transferred by conduction; and

$q_r$  = energy emitted through outgoing radiation.

The energy absorbed from direct solar radiation, and which is reflected by the atmosphere ( $q_s$  and  $q_a$ ), is positive for the surface of a body on the surface of the earth, such as a pavement. The terrestrial radiation component ( $q_t$ ) can be considered to be zero for a pavement since it is defined as the radiation that is absorbed by a body above the surface of the earth. The energy transferred by convection ( $q_c$ ) is defined as the transfer of energy from a solid surface to a fluid (in this case the air above the pavement). The convection term is positive if energy is transferred from the pavement to the air in the case that the pavement surface possesses a higher temperature. The convection term will be negative if the air temperature is higher than the pavement surface temperature. Conduction energy will be positive if the heat is transferred from within the pavement to the pavement surface (i.e., when the surface is cooler). A negative sign is used when the pavement surface is warmer than the pavement below the surface. Outgoing radiation from the pavement surface is always given with a negative sign.

### 2.5.1 Solar Radiation

Due to the high surface temperature of the sun (approximately 6000°K), radiation of high frequency, or shortwave radiation, is emitted. Part of this radiation from the sun can be scattered by clouds or moisture in the atmosphere. Thus, there are two types of shortwave radiation, direct and diffuse. Diffuse shortwave radiation is that which is scattered or diffused by the atmosphere or by particles in the atmosphere. Direct shortwave radiation is that which is not scattered by the atmosphere or by particles in the atmosphere. The relative percentages of direct and diffuse radiation making up the total shortwave radiation are dependent upon the weather and local environmental conditions. On a cloudless day, the percentage of direct shortwave radiation is higher. Bosscher et al. (1998) measured the solar radiation using a pyranometer and obtained values in Wisconsin of approximately 500 W/m<sup>2</sup> (winter) and 1200 W/m<sup>2</sup> (summer). The energy received as direct solar radiation,  $q_s$ , can be expressed as the following:

$$q_s = \alpha_s R_i \quad (2.5)$$

where

$\alpha_s$  is the solar surface absorptivity, and

$R_i$  is the incident solar radiation.

The surface absorptivity depends upon the wavelength of the radiation received, which is dependent upon the surface temperature of the radiator. Solaimanian and Kennedy (1995) report a typical  $\alpha_s$  range as 0.85 to 0.93. The incident solar radiation is defined as the radiation received by a body parallel to the surface of the earth. However, radiation from the sun is not always perpendicular to a specific surface, thus, the incident solar radiation is defined as the following:

$$R_i = R_n \cos(i) \quad (2.6)$$

where

$R_n$  = radiation received by a body which is placed normal to the direction of the sun, and

$i$  = angle between the normal to the surface and the direction of the sun.

The value of  $R_n$  can be calculated from the solar constant,  $R_0$  which is given as  $1394W/m^2$ . The solar constant is defined as the solar energy incident upon a surface that is perpendicular to the direction of the sun located at the outer edges of the earth's atmosphere. However, gases, moisture, and suspended particles in the atmosphere together reflect approximately 26% of the incoming solar radiation (insulation) back into space.

The solar energy received at the earth's surface depends upon the time of day, season, and location on the planet. The value of  $R_n$  is given as the following:

$$R_n = R_0 \cdot \tau_a^m \quad (2.7)$$

where

$\tau_a$  = transmission coefficient for a unit air mass;

$m$  = relative air mass, defined as the ratio of the actual path length to the shortest path length  $\approx 1/\cos(z)$ ; and

$z$  = zenith angle (angle between the zenith and the direction of the sun).

The transmission coefficient, according to Kreith (1986), ranges from 0.81 on a clear day to 0.62 on a cloudy day. A value of 0.7 can be used as an average. In addition, the value of the transmission coefficient is higher in the summer than in the winter due to higher moisture content. The zenith angle depends on the latitude ( $\varphi$ ), the time of day, and the solar declination ( $\delta_s$ ). The time is expressed in terms of an hour angle ( $h$ ) that is defined as the angle through which the earth turns to bring the sun directly overhead a particular location. The hour angle ( $h$ ) is defined as being zero at local noon. The zenith angle ( $z$ ) can be found from the following:

$$\cos(z) = \sin(\varphi) * \sin(\delta_s) + \cos(\delta_s) * \cos(h) * \cos(\varphi). \quad (2.8)$$

For a horizontal surface,  $\cos(i) = \cos(z)$ , however, if the surface is tilted at an angle  $\psi$  (as shown in Figure 2.3, it can be determined from the following:

$$\frac{R_i}{R_n} = \cos(i) = \cos(z - \psi) - \sin(z) * \sin(\psi) + \sin(z) * \cos(\psi) * \sin |A - \beta| \quad (2.9)$$

where

$\psi$  = angle of tilt from the horizontal.

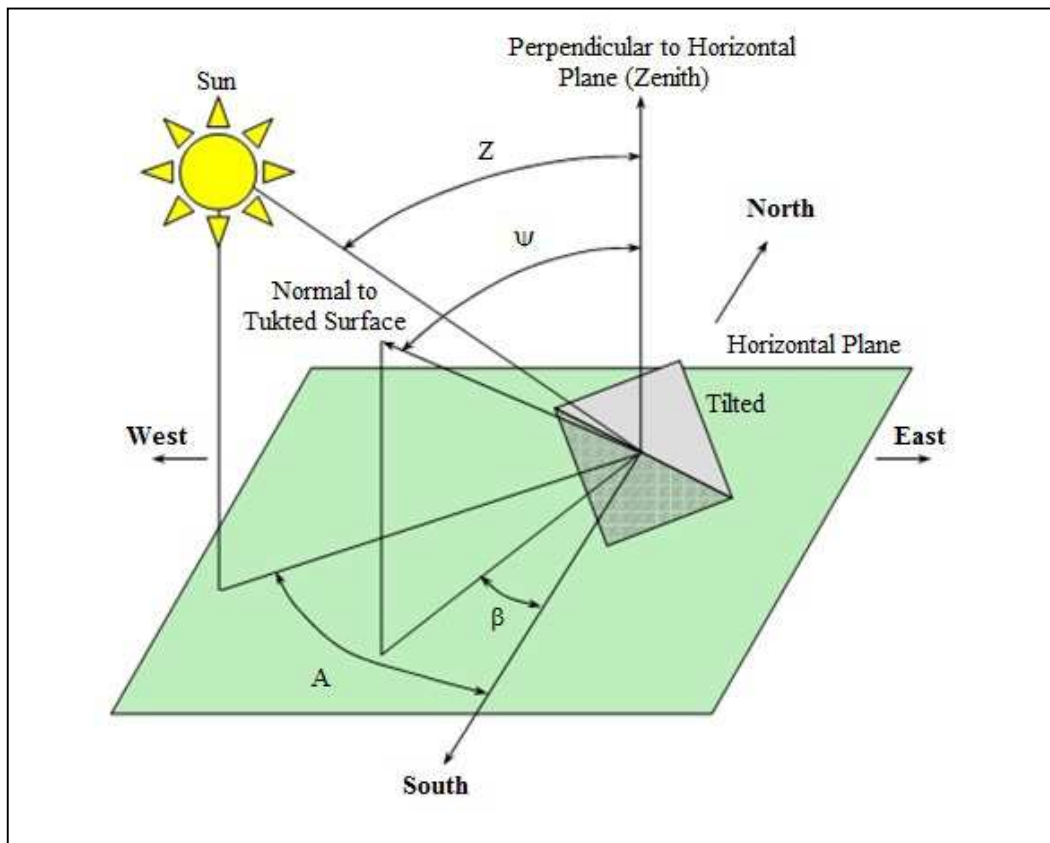


Figure 2.3 Definition of solar and surface angles (Kreith, 1986)

where

A = azimuth of the sun; and

$\beta$  = angle between the south meridian and the normal to the surface measured westward along the horizon.

Solaimanian and Kennedy (1993) report that the zenith angle can be approximated at locations of latitude greater than  $22^\circ$  between the months of May and August (at local noon time) as the following:

$$Z = \text{latitude} - 20 \text{ degrees} \quad (2.10)$$

The radiation received by the pavement that is reflected from the atmosphere as longwave radiation,  $q_a$ , can be calculated as the following:

$$q_a = \varepsilon_a \cdot \sigma \cdot T_{air}^4 \quad (2.11)$$

where

$\varepsilon_a$  = atmospheric emissivity, assumed to be 0.7 for a cloudless day;

$\sigma$  = Stefan-Boltzman constant =  $5.68 \times 10^{-8}$  (W/m<sup>2</sup>K<sup>4</sup>); and

$T_{air}$  = the air temperature (°K).

## 2.6 Radiation emitted by pavement surface

Any heat transfer by radiation will involve both emissivity (ability of a surface to emit radiation as compared to a black body) and absorptivity (ability of a surface to absorb radiation) component. It has been reported that the emissivity and the absorptivity to solar radiation for asphaltic materials is identical at approximately 0.93 (Solaimanian and Kennedy, 1993). Solaimanian and Kennedy (1993) state that the outgoing (longwave) radiation,  $q_r$ , can be expressed in W/m<sup>2</sup> (using the black body assumption) from the Stefan-Boltzman Law as the following:

$$q_r = \varepsilon_p \cdot \sigma \cdot T_s^4 \quad (2.12)$$

where

$\varepsilon_p$  = pavement emissivity; and

$T_s$  = surface temperature (°K).

### 2.6.1 Conduction Energy

The conduction of thermal energy within the pavement can be expressed as the following:

$$q_k = -k \frac{T_d - T_s}{d} \quad (2.13)$$

where

$k$  = thermal conductivity;

$T_s$  = surface temperature (°C);

$d$  = depth (m); and

$T_d$  = temperature at depth  $d$  (°C).

### 2.6.2 Convection Energy

The rate of heat flow by convection to the air surrounding the pavement can be expressed as follows:

$$q_c = h_c (T_s - T_{air}) \quad (2.14)$$

where

$h_c$  = the surface coefficient of heat transfer;

$T_s$  = surface temperature (°K); and

$T_{air}$  = air temperature (°K).

The coefficient of heat transfer depends upon the surface geometry of the pavement, the wind velocity, and physical properties of the air.

## **2.7 Pavement temperature prediction**

Using results from the LTPP and SMP studies, civil engineers have a higher probability of specifying an asphalt binder that can withstand the effects of vehicular loading at different temperatures regardless of location. More than 3,000 pavement sites throughout North America were fitted with instruments to measure responses of the pavement due to vehicular loading and environmental conditions. The LTPP sites were chosen so that a wide variety of pavement types, structural designs, and environmental factors could be analyzed. As a result of this work, the Superpave method was developed. Not only did this mix design protocol include new methods of evaluating HMA and asphalt binder in the laboratory, but it also included a new way to specify asphalt binder for field projects based on environmental conditions (temperature) experienced at different areas within the United States and Canada. Under the current Superpave protocol, asphalt binder is specified in terms of the expected minimum air temperature and maximum seven-day average air temperature. These air temperatures are used to estimate the temperature experienced by the pavement. Through the estimation of yearly high and low pavement temperatures, a proper binder can be selected in terms of the PG designation. (Diefenderfer, *et al.* 2002)

## **2.8 Performance grade of bitumen (PG)**

Selection of the appropriate binder for different areas of the United States is performed using a set of performance-based equations under the SHRP Superpave Binder PG System. This PG system is intended to ensure that the appropriate binder is used in locations with different environmental conditions. A database was developed in which environmental data from 6092 weather stations in the United States and Canada can be used to determine the seven-day average high air temperature and the one-day low air temperature for any location (Ali and Lopez, 1996). However, the temperature limits used for the PG binder specifications are pavement temperatures and not air temperatures. Thus, expressions were developed to determine the pavement temperature from the air temperature. The current expressions used for the PG grading are given in Equations 2.15 through 2.18 and will be referred to herein as the SHRP models. Equation 2.15 gives the high pavement temperature for the surface of a pavement as the following:



$$T_{s(max)} = T_{a(max)} - 0.00618 * \Phi^2 + 0.2289 * \Phi + 24.4 \quad (2.15)$$

where

$T_{s(max)}$  = maximum pavement temperature at the surface (°C);

$T_{a(max)}$  = seven-day average maximum air temperature (°C); and

$\Phi$  = latitude of the desired location (degrees).

Equation 2.16 yields the high pavement temperature with depth as the following:

$$T_{pav(max)} = T_{s(max)} * (1 - 0.063 * d^2 - 0.007 * d^3) \quad (2.16)$$

where

$T_{pav(max)}$  = maximum pavement temperature at depth  $d$  (°F);

$T_{s(max)}$  = maximum pavement temperature at the surface (°F); and

$d$  = depth from surface (in).

The low pavement temperature at the surface is given as being equal to the low air temperature, expressed as the following:

$$T_{s(min)} = T_{a(min)} \quad (2.17)$$

where

$T_{s(min)}$  = minimum pavement temperature at the surface (°C); and

$T_{a(min)}$  = minimum one-day air temperature (°C).

The minimum pavement temperature at any depth is given as the following:

$$T_{pav(min)} = T_{a(min)} + 0.051 * d - 0.000063 * d^2 \quad (2.18)$$

where  $T_{pav(min)}$  = minimum pavement temperature at depth  $d$ .

Equations 2.15 and 2.17 are based on research performed by Solaimanian and Kennedy (1993).

In addition to the above expressions, updated versions of the SHRP models have been developed (Mohseni, 1998; Mohseni and Symons, 1988a and 1988b) based on current LTPP data, referred to herein as the LTPP models. Equations 2.19 through 2.22 were developed from additional data obtained after the previously published SHRP work. To determine the maximum pavement temperature at any depth, the following expression is given:

$$T_{d(max)} = (T_{s(max)} + 17.8) * (1 - 2.48 * 10^{-3}d + 1.1 * 10^{-5}d^2 - 2.4 * 10^{-8}d^3) - 17.8 \quad (2.19)$$

where

$T_{d(max)}$  = maximum pavement temperature (°C) at depth =  $d$ ; and

$d$  = depth (mm).

As an expression for the maximum pavement temperature, at a depth of 20mm, Equation 2.19 simplifies to the following:

$$T_{20(max)} = 0.955 * T_{s(max)} - 0.8 . \quad (2.20)$$

The minimum pavement surface temperature is found using the minimum air temperature, shown as the following:

$$T_{s(min)} = 0.859 * T_{a(min)} + 1.7 \quad (2.21)$$

To determine the minimum pavement temperature with depth, the following expression is given:

$$T_{d(min)} = T_{s(min)} + 5.1 \times 10^{-2}d - 6.3 \times 10^{-5}d^2 \quad (2.22)$$

where  $T_{d(min)}$  is the minimum pavement temperature ( $^{\circ}\text{C}$ ). at depth = d.

It is important to keep in mind that these models were developed to calculate annual minimum and maximum pavement temperatures for the purpose of binder specification and not for daily pavement temperature analysis.

## 2.9 Analysis of SHRP models

Many researchers have investigated the initial SHRP models to determine the appropriateness of these expressions (Ali and Lopez, 1996; Robertson, 1997; Mohseni and Symons, 1988a; Bosscher et al., 1998; Lukanen, et al., 1998). These studies point out that several erroneous assumptions about the physical nature of pavement temperature arise when employing the heat flow model. Equation (2.23) considers the earth as a black body radiator system in which the net rate of heat flow in and out of the system,  $q_{net}$ , can be expressed as the following:

$$q_{net} = q_s + q_a + q_t \pm q_c \pm q_k - q_r \quad (2.23)$$

where

$q_s$  = energy absorbed from direct (solar) radiation;

$q_a$  = energy absorbed from diffuse radiation (radiation reflected by the atmosphere);

$q_t$  = energy absorbed from terrestrial radiation;

$q_c$  = energy transferred by convection;

$q_k$  = energy transferred by conduction; and

$q_r$  = energy emitted through outgoing radiation.

Mohseni and Symons (1998a and 1998b) presented analysis using the updated data to make comparisons with the initial SHRP models. Their interest was in discussing differences between observed data and the SHRP models. The authors performed statistical analysis on the pavement

temperature data in order to determine which physical factors had the most influence on the pavement temperature. (Diefenderfer, *et al.* 2002)

In the SHRP model it was determined that the air temperature, latitude, and depth from the surface were the most significant factors. This updated data was used for the development of a revised low-temperature model that consisted of 411 data points. The air and pavement temperatures ranged from 4.6 to 41.5°C and 13 to 33°C, respectively. The location of the sensors ranged from 0 to 150mm in depth from the pavement surface. The latitude of the pavement sites varied between approximately 24°59'N. The variables of low air temperature, latitude, and depth were found to have the most influence on the low pavement temperature. The relationship between air and pavement temperatures was found to be linear and it was also found that air temperature was the most influential variable in the model. A latitude variable was found to vary nonlinearly with pavement temperature. Through trial and error, the variable latitude-squared was found to be more significant. A third variable, depth from the pavement surface, was found to have a weak correlation with the pavement temperature. Therefore, the terms depth-squared and  $\log(\text{depth}+25)$  were considered with  $\log(\text{depth}+25)$  providing a better fit.

Mohseni and Symmons analyzed SMP data using Equation 2.24 (depth,  $d = 25\text{mm}$ ) and found that the low pavement temperatures were approximately 10°C warmer than the air temperature at a low air temperature of -40°C and approximately 5°C warmer than the air temperature at a low air temperature of -5°C. In light of these differences, it was proposed to develop a new model to be able to predict the low pavement temperature at various depths. The variables that were considered to have a significant effect on low pavement temperature are low air temperature, latitude, and depth. It was shown that the relationship between low air temperature and low pavement temperature is of a linear nature; a nonlinear relationship exists between low pavement temperature and both latitude and depth. (Diefenderfer, *et al.* 2002)

From this analysis, Mohseni and Symons developed a revised set of temperature prediction equations. These equations termed here the revised LTPP models. Equation 2.24 gives the revised LTPP low pavement temperature model as the following:

$$T_{pav} = -1.56 + 0.72 * T_{air} - 0.004 * \Phi^2 + 6.26 \log(d + 25) \quad (2.24)$$

where

$T_{pav}$  = low pavement temperature below the surface (°C); and

$T_{air}$  = low air temperature (°C).

When the residuals (difference between actual pavement temperature and predicted temperature using Equation 2.24) were plotted versus the significant terms, no obvious trend was found and the error appeared to be evenly distributed across the temperature range. A standard error of 2.1°C was reported. Again, this revised model calculates an annual low pavement temperature.

It was reported that in determining the design pavement temperature (such as when using the Superpave binder selection), two types of errors are present: an error based on model prediction, and an error associated with the mean air temperature. To account for these errors, the standard deviation of the mean air temperature and root mean square error (RMSE) of the model is incorporated into Equation 2.24 and thus Equation 2.25 is presented as follows:

$$T_{pav} = -1.56 + 0.72 * T_{air} - 0.004 * \Phi^2 + 6.26 \log(d + 25) - z \sqrt{4.4 + 0.52\sigma_{air}^2} \quad (2.25)$$

where  $\sigma_{air}$  is the standard deviation of the mean low air temperature (°C), and  $z$  is obtained from the standard normal distribution for the desired area under the normal distribution curve. Equation 2.24 is sufficient to determine the low pavement temperature having 50% reliability. However, Equation 2.25 allows the calculation of the low pavement temperature with a higher reliability by subtracting the error from the 50% reliability expression. The error portion of Equation 2.25 can be expressed in terms of the standard deviation of the mean air temperature ( $\sigma_{air}$ ) and the standard error estimate of the model ( $\sigma_{model}$ ).

The variability in calculating the low pavement temperature can be written in terms of both of these errors as the following:

$$\sigma_{pav} = \sqrt{\sigma_{model}^2 + (0.72\sigma_{air})^2} \quad (2.26)$$

Substituting the standard error estimate of the model (2.1°C) into the pavement temperature variability, the error term (Equation 2.26) can be written independently as: features

$$\varepsilon = z \sqrt{4.4 + 0.52\sigma_{air}^2} \quad (2.27)$$

Mohseni and Symons (1998a) also presented a revised high temperature model. Again, the variables to be included were air temperature, latitude, and depth from the surface. The correlation between pavement temperature and air temperature was again found to be linear and was also the strongest correlation of the three variables. The relationship between latitude and pavement temperature was also found to be strong but was of a nonlinear nature. Through trial and error, the term latitude-squared was found to be the most significant variable incorporating latitude. Depth from the surface was also found to have a strong nonlinear correlation with pavement temperature. The terms depth-squared and  $\log(\text{depth}+25)$  were considered with the second term providing a better fit. The revised high-temperature is given as follows:

$$T_{pav} = 54.32 + 0.78 * T_{air} - 0.0025 * \Phi^2 + 15.14 \log(d + 25) - z \sqrt{9 + 0.61\sigma_{air}^2} \quad (2.28)$$

The standard error was given as 3.0 and an  $R^2$  of 0.76 was reported.

Following this, Mohseni and Symons (1998b) investigated the effects of different estimated pavement temperatures on binder selection using the revised LTPP and the SHRP models. One randomly selected weather station was chosen from each state or province in the United States and Canada and the two models were compared. The original SHRP model indicated that a PG 76-10 and a PG 82-10 binder would be specified for a 50% and a 98% reliability, respectively. However, using the revised LTPP model, the binder grades were given as 70-10 and 82-10 for 50% and 98% reliability, respectively. For all eight randomly selected weather stations, it was seen that the revised LTPP model specified binders one or two grades higher than the original SHRP model in estimating the low temperature binder specification. When comparing all 7801 weather stations in the SHRP program, the revised LTPP model specified a higher low temperature binder grade than the original SHRP model for 76% and 85% of the weather station sites for 50% and 98% reliability, respectively. The comparisons between the SHRP data and the LTPP models are discussed in more detail in Mohseni (1998). The low temperature model presented by Mohseni and Symons (Equation 2.24) has recently been incorporated into a revised Superpave standard.

Robertson (1997) developed a model to estimate the low temperature binder specification based on data obtained from Canadian Strategic Highway Research Program (C-SHRP) projects. This study also included a method that allows the user to select the reliability of the estimated pavement temperature. As part of his investigation, Robertson listed some observations about the pavement temperatures under study:

- the maximum and minimum ground temperatures occur sometime after the summer and winter solstices, respectively;
- the pavement temperature range tends to decrease in coastal areas since the capacity for heat absorption of water is much greater than for land;
- winter pavement temperatures vary over a smaller range and they vary more slowly than air temperatures;
- the lowest pavement temperature is warmer than the lowest air temperature;
- the difference between low air and low pavement temperatures is larger for areas having lower air temperatures; and
- almost all thermally related cracking occurs between November and February.

In addition to the above statements, Robertson (1997) developed a linear relationship between air and pavement temperatures for seven Canadian sites having a pavement thickness greater than 100mm. The model covers an expected minimum air temperature range from -32 to -48°C. The resulting regression model is given as follows:

$$T_s = 0.749T_a \quad (2.29)$$

where  $T_s$  and  $T_a$  represent the minimum pavement surface temperature (°C) and the minimum air temperature (°C), respectively. Robertson reports that this model, developed from 653 data

points, has a standard error equal to 1.5°C and an R<sup>2</sup> of 0.95. A design equation, allowing the user to specify the desired reliability is presented as follows:

$$T_{design} = 0.749(T_{air} - n\sigma_{air}) - 1.5n \quad (2.30)$$

where

$T_{design}$  = winter pavement (surface) design temperature (°C);

$T_{air}$  = mean of minimum air temperatures at the pavement site (°C);

$\sigma_{air}$  = standard deviation of the minimum air temperature (°C); and

$n$  = multiplier associated with the desired reliability (1.28 for 99%, 1.00 for 97.5%, 0.76 for 95%, and 0.48 for 90%).

Lukanen et al. (1998) presents a summary of comparisons between the initial SHRP temperature model (heat flow model) and three models independently developed by Han (as discussed by Lukanen et al., 1998; Mohseni 1998; and Robertson 1997), using data from the SMP. Han utilized the same dataset used by Mohseni to develop the revised LTPP models; however, slightly different results were obtained. Han's model for the maximum pavement temperature is given as follows:

$$T_{d(max)} = 0.52 + 6.225\Phi - 0.15\Phi^2 + 0.0011\Phi^3 + 0.28T_{a(max)} - 8.37LN(d + 40). \quad (2.31)$$

The standard error for Han's maximum pavement temperature equation was given as 2.2°C using 70 data points. Han's model for the minimum pavement temperature is given as follows:

$$T_{d(min)} = -0.14 - 1.7\Phi - 0.06\Phi^2 - 0.0007\Phi^3 + 0.69 * T_{a(min)} + 4.12LN(d + 100). \quad (2.32)$$

The standard error for Hans's minimum pavement temperature equation was given as 2.6°C using 71 data points. The standard error for Mohseni's maximum pavement temperature model was given as 3.0°C based on 309 data points. The standard error for Mohseni's minimum pavement temperature model was given as 2.1°C based on 411 data points. (Diefenderfer, *et al.* 2002)

Robertson's work, as discussed earlier, was prompted by previous research at C-SHRP, suggesting that the initial minimum temperature prediction model offered by SHRP was too severe (i.e., the pavement temperature was actually warmer than the prediction). Differences between Mohseni's model (and thus Han's also) and Robertson's work may have resulted since although hourly temperature data was available at the time, Robertson's concurrent study did not utilize it since it was suggested that he might not have known of its recent availability. Thus, Robertson used only daily minimum temperatures to develop his model (Equation 2.29). Observing the differences between the models, it is seen that Robertson's model does not account for latitude. The latitude variable was seen as less significant with the C-SHRP data since the latitudes for the projects under study are greater than 45°N and thus the air temperature

is the predominant factor. If Robertson's model were to be compared with Han's model, it would require a latitude input of approximately 47°N.

In addition, Lukanen et al. (1998) present their own maximum and minimum pavement temperature prediction models based on an expanded set of SMP data. At the time this paper was published (1998), data from an additional 15 sites had been added to the SMP first loop (the data used by Mohseni and Han). The models presented by Lukanen et al. (1998) were taken from two summer seasons and one winter season. For each test site, only one annual maximum and one annual minimum were used to develop the models. Lukanen's model for predicting maximum pavement temperature is presented as follows:

$$T_{d(max)} = 0.47 + 5.717\phi - 0.1276\phi^2 + 0.0008121\phi^3 + 0.3078 * T_{a(max)} - 8.602LN(d + 40) . \quad (2.33)$$

Lukanen et al. (1998) reported that the standard error for this model is 2.7°C and is based on 113 data points. Lukanen's model for predicting minimum pavement temperatures is presented as follows:

$$T_{d(min)} = -0.15 - 1.9\phi + 0.06\phi^2 - 0.0007\phi^3 + 0.59 * T_{a(min)} + 5.2LN(d + 100). \quad (2.34)$$

The standard error for this model is reported to be 2.4°C and is also based on 113 data points. Lukanen also suggested that the temperature profile models could be used to estimate the temperature at different depths within the pavement to determine the appropriate PG binder selection for the asphalt within the base courses of the pavement.

In a study incorporating an independent dataset from a field study in Wisconsin, Bosscher et al. (1998) described a pavement section instrumented with thermistors to monitor pavement temperature down to a depth of 101.6mm. Models were developed and compared to the original SHRP and the revised LTPP pavement temperature models. Findings presented by Bosscher include that solar radiation values of 500 W/m<sup>2</sup> and 1200 W/m<sup>2</sup> were typical for winter and summer, respectively. Conclusions include that during the night, when air temperatures are typically the lowest; the pavement temperature was always found to be higher than the air temperature (probes were installed at a depth of 6.4mm from the surface). The surface layer always experienced the largest temperature fluctuation (compared to the other pavement layers) that coincided with daily changes in air temperature. Also, significant differences exist between the standard deviation of the pavement temperature and the air temperature.

Bosscher developed a model that gave the daily minimum pavement temperature with daily minimum air temperature as the only input. Although the model correlated well with a linear relationship, the standard error of estimate was reported to be 2.71°C, too high by the author's reasoning. To improve this model, other factors were included to reduce the standard error. The total solar radiation intensity for the previous 24 hours and the average hourly freezing index of

the air temperature for the previous three days were included. The total solar radiation ( $\text{W}/\text{m}^2$ ) was recorded for the 24 hours prior to the time in which the minimum pavement temperature occurred. The hourly freezing index of the air temperature is calculated by summing the hourly air temperatures below  $0^\circ\text{C}$  during the 72 hours preceding the minimum pavement temperature and dividing this total by 72 (total number of hours in three days). The result of these two values when multiplied was taken to the 0.25 power for use in the model equation. This fourth root factor was based on the theory that any blackbody radiator (whose temperature is greater than absolute zero) radiates heat at a rate that is proportional to the fourth power of the absolute temperature (Kreith, 1986). In addition to these factors, the inclusion of the average air temperature of the previous 24-hour period improved the error of the prediction model to between  $1.25$  and  $1.9^\circ\text{C}$ . To further improve pavement temperature prediction, a step approach, employing different models over different air temperature ranges, was incorporated. Two models, predicting the pavement temperature at a depth of  $6.4\text{mm}$ , are given as follows:

$$T_{p(\min)6.4} = 0.3768 + 0.687 * T_{a(\min)} \quad (2.35)$$

$$T_{p(\min)6.4} = -1.001 + 0.422 * T_{a(\min)} + 0.359 * T_{a-01} \quad (2.36)$$

where  $T_{a(\min)}$  and  $T_{a-01}$  are the minimum air temperature for the day in which the pavement minimum is being predicted and the average air temperature for the 24 hrs preceding the time of the pavement low temperature, respectively.

Bosscher et al. (1998) were also interested in determining the pavement temperature as it varied with depth in relationship to the low air temperature. An expression for determining the temperature at depth,  $d$  (mm), is given as follows:

$$T_{d(\min)} = T_{p(\min)6.4} - [(0.00123 * T_{p(\min)6.4}) * (d - 6.4)] + 0.01416 * (d - 6.4). \quad (2.37)$$

The authors go on to state that the data used to develop the above expression do not include time as a factor in determining the pavement depth. Thus, it was assumed that the minimum temperature within each layer occurs simultaneously (an assumption incorporated into the heat flow theory used in the original SHRP models). It was also noted that the above expression is only valid for estimating pavement temperatures when the air temperature is less than  $-5^\circ\text{C}$ . Since the analysis performed under SHRP assumes that the low temperature occurs at the surface of the pavement, Equations 2.35 and 2.36 can be substituted into Equation 2.38, respectively, to yield:

$$T_{s(\min)} = 0.286 + 0.692 * T_a \quad (2.38)$$

$$T_{s(\min)} = -1.102 + 0.425 * T_a + 0.362 * T_{a-01} \quad (2.39)$$

The authors again state that Equations 2.38 and 2.39 are best suited for air temperatures less than  $-5^\circ\text{C}$ .



Following this, Bosscher et al. (1998) compared the developed prediction models to the existing SHRP and revised LTPP models. When considering low pavement temperatures, the SHRP models consider the most severe or coldest low pavement temperature to occur at the surface of the pavement. That is, the temperature at this location is equal to the low air temperature at that time. The revised LTPP models incorporate regression analysis that is presented in Mohseni (1998). When comparing the SHRP model, the revised LTPP model and equations (2.35) and (2.36) for predicting pavement temperature at a depth of 6.4mm to the actual pavement temperature at 6.4mm, the standard error (in °C) was found to be 2.409, 1.719, 1.655, and 1.226, respectively, for air temperatures less than -5°C. The authors concluded that the developed models (equations (2.35) and (2.36) and the LTPP models) show good agreement between actual pavement temperatures at 6.4mm depth and predicted pavement temperatures at 6.4mm depth. However, according to Bosscher et al. (1998), the SHRP models did not show good agreement between actual pavement temperatures at 6.4 mm depth and predicted pavement temperatures at 6.4 mm depth. Bosscher et al. (1998) reported that the SHRP models predicted the pavement temperature at 6.4mm depth to be significantly lower than the measured pavement temperature at the same depth. This difference ranged from approximately 3°C to 14°C at measured pavement temperatures of -5°C to -30°C, respectively. (Diefenderfer, *et al.* 2002)

The standard deviation of the pavement temperature versus the standard deviation of the air temperature is also important to consider. The Superpave binder selection protocol assumes that the standard deviations are equal for both the pavement temperature and the air temperature. Bosscher et al. (1998) showed that this was not the case for either high or low temperatures. Thus, the assumptions used to determine the reliability of the binder grade selection are erroneous. The standard deviations were calculated from monthly averages of the daily minimum and maximum air and pavement temperatures. Data for the maximum temperature portion were taken from the three hottest months for each summer. It was shown that the standard deviation for the maximum pavement temperature is much higher than the standard deviation of the maximum air temperature. However, at lower temperatures this trend is reversed; the minimum pavement temperature standard deviation is much lower than the minimum air temperature standard deviation. Equations for determining the standard deviation of the pavement temperatures based on the standard deviation of the air temperatures are given as equations (2.40) and (2.41) for minimum and maximum temperatures, respectively. (Diefenderfer, *et al.* 2002)

$$SD_{p(min)} = 1.170 + 0.6422 * SD_{a(min)} \quad (2.40)$$

$$SD_{p(max)} = 1.694 + 1.2733 * SD_{a(max)} \quad (2.41)$$

where

$SD_p$  = standard deviation of the pavement temperature; and

$SD_a$  = standard deviation of the air temperatures.

Equations (2.40) and (2.41) are given by Bosscher et al. (1998) as valid for pavement surface temperatures below 0°C and above 40°C, respectively.

When predicting maximum pavement temperatures at different pavement sites, Solaimanian and Kennedy (1993) state that latitude is an influential component. For areas in the United States, states of lower latitude will receive more direct radiation per hour in the summer than states of higher latitude. The greater amount of radiation will manifest itself as a larger difference between maximum air temperature and maximum temperature within the pavement. Solaimanian and Kennedy state that for project sites sharing the same latitude, the difference between maximum air temperature and maximum pavement temperature is nearly constant, varying only upon radiation, conduction, and convection. An expression was developed to yield the difference between air and pavement temperatures as a function of latitude as the following:

$$\Delta T = -0.0062\Phi^2 + 0.2289\Phi + 24.38 \quad (2.42)$$

where

$\Delta T$  = difference between maximum air and maximum pavement temperatures (°C); and

$\Phi$  = latitude (degrees).

Solaimanian and Kennedy (1993) also state that at lower latitudes, the difference between air and pavement temperatures can be up to approximately 26°C when the air temperature varies between 24 and 42°C. At a latitude of 60°, the difference can reach approximately 15°C. The authors also discuss prediction of pavement temperature with depth. However, they only state that the form of this equation should be quadratic where the input variable is the surface temperature. No mention of factors, including a seasonal adjustment, is offered.

## **2.10 Applications of pavement temperature prediction**

Up to this point, the research mentioned previously has focused on maximum or minimum air temperatures for predicting the annual maximum or minimum pavement temperatures for the purpose of binder selection. Studying the daily changes in pavement temperature poses a problem of similar nature; however, prediction becomes a more complicated task. Climatologic factors affect the analysis now as much as engineering principles. While the basic theories previously discussed hold true, yearly climatic cycles begin to exert their influence on the pavement temperature. For example, while the air temperature may be identical for two dates, the distribution of temperatures within the pavement may be vastly different if the two dates are many months apart. In an effort to model this variance, Hermansson (2000 and 2001) presents a simulation-based prediction model to monitor the diurnal temperature changes in the pavement during the summer months. The models follow the concepts discussed by Salaimanian and

Kennedy (1993) and utilize data from LTPP sites in the United States and from sites in Sweden.(Diefenderfer, *et al.* 2002)

Park et al. (2001) developed a model that could be used to predict pavement temperatures given the surface temperature and time of day for use with FWD analysis. Huang (1993) lists the pavement temperature and the local climate as significant factors influencing the deflection of the pavement system. The development of Park's model was performed by collecting temperatures using retrofitted (added to the pavement after construction) thermocouples and measuring the temperature of mineral oil in holes of various depths in six flexible pavements in Michigan. A regression-based model was developed using 197 data points and compared with data from SMP sites in seven other states (Colorado, Connecticut, Georgia, Nebraska, Minnesota, South Dakota, and Texas). The developed model is given as follows:

$$T_z = T_{surf} + (-0.3451z - 0.432z^2 + 0.00196z^3) * \sin(-6.3252t + 5.0967) \quad (2.43)$$

where

$T_z$  = temperature at depth  $z$  (°C);

$T_{surf}$  = temperature at the surface (°C);

$z$  = depth from surface (cm);

$\sin$  = sine function (radians); and

$t$  = time of temperature measurement in fraction of day (i.e., 1:30PM = 13.5/24 = 0.5625 days).

The model was validated over a surface temperature range of -28.4 to 53.7°C and a depth range of 14 to 27.7cm. A  $R^2$  value better than 90% was reported and a temperature prediction band of  $\pm 4^\circ\text{C}$  was given. After validating the model with data from SMP sites across the United States, the authors suggested that this model could be adopted for all seasons and other climatic areas. Marshall et al. (2001) present another recent temperature prediction model for use with FWD analysis. Four flexible pavements in Tennessee were instrumented with thermistors during construction or during reconstruction at mid-depth in the asphalt surface and base layers. The data collected from the four sites were used to develop the following regression based model:

$$T_d = 0.95 + 0.892 * T_s + (\log d - 1.25) * (1.83 \sin\left(\frac{2\pi}{18} A\right) - 0.448T_s + 0.621 * T_{avg}) + 0.042 * T_s * \sin\left(\frac{2\pi}{18} B\right) \quad (2.44)$$

where

$T_d$  = pavement temperature at mid-layer depth (°C);

$T_s$  = surface temperature measured with infrared sensor (°C);

$T_{avg}$  = average of high and low temperature of preceding day (°C);

$d$  = mid-layer depth (mm); and

A and B are variables defined as

$$A = \begin{cases} t_d + 9.5 & \text{if } 0 \leq t_d < 5 \\ -4.5 & \text{if } 5 \leq t_d < 11 \\ t_d - 15.5 & \text{if } 11 \leq t_d < 24 \end{cases} \quad B = \begin{cases} t_d + 9.5 & \text{if } 0 \leq t_d < 3 \\ -4.5 & \text{if } 3 \leq t_d < 9 \\ -13.5 & \text{if } 9 \leq t_d < 24 \end{cases}$$

The authors state that the above model gives good agreement between predicted and actual mid-layer temperatures over a range of 5 to 45°C.

Ovik et al. (1999) present an analysis of temperature data from the MnRoad test site in Minnesota. The goal for these researchers was to quantify the relationships between climatic factors and pavement mechanical properties for use in mechanistic-empirical pavement design. A falling weight deflectometer was employed to measure the mechanical response of pavements to load at various times of the year. Data from the instrumented roadway gave the pavement temperature. The measured temperature data was compared with an equation presented in Andersland and Anderson (1978) and is given as follows:

$$T(x, t) = T_{mean} + Ae^{-x\sqrt{\frac{2\pi}{P\alpha}}} \sin\left(\frac{2\pi}{P} * t - x\sqrt{\frac{2\pi}{P\alpha}}\right) \quad (2.45)$$

where

$T(x, t)$  = temperature at depth, x and time, t (°C);

x = depth from surface (m);

$T_{mean}$  = average temperature at surface (°C);

A = maximum temperature amplitude =  $T_{max} - T_{mean}$  (°C);

$\omega = \frac{2\pi}{P} = \frac{2\pi}{365}$ ;

P = period or recurrence cycle;

$\alpha$  = thermal diffusivity, assumed to be 0.121 m<sup>2</sup>/day; and

t = time measured from when the surface temperature passes through  $T_{mean}$  (days).

The authors reported that equation (2.44) gave close approximations to the actual measured temperature at the MnRoad site. In addition, Birgisson et al. (2000) utilize data from the MnRoad project to compare predicted pavement temperatures and base course moisture contents using the FHWA Integrated Climatic Model. The authors reported good correlations between predicted and actual values. The model presented by Ovik et al. (1999) are given as to be used in predicting a daily pavement temperature and not an hourly distribution as are the models presented by (Park et al. 2001) and Marshall et al. 2001).

## 2.11 FHWA integrated climatic model

An integrated model was developed through research between FHWA and Texas Transportation Institute (TTI) (Lytton et al., 1993) to provide a comprehensive model encompassing all factors

contributing to environmental effects on pavements. The climatic model is made up of several components: the Precipitation Model, the Infiltration and Drainage Model, the Climatic-Materials-Structural Model, and the Frost Heave/Thaw Settlement Model. These components are then combined to perform an overall analysis of the pavement and subgrade. The user can add detailed climatic information for specific sites, or employ the provided average data for nine climatic zones in the United States.

The model was developed to utilize historical data to give an average expected result of climatic conditions. The Precipitation Model is a statistical database of precipitation events for various climatic areas of the United States. Through this model, the user may determine the probability of rain occurring during certain time periods and the historically based amount of precipitation that can be expected. The historical data is based on 30 years of observations from the National Oceanic and Atmospheric Administration (NOAA) first order weather stations. This model provides input to the Infiltration and Drainage Model. One assumption for this model is that all precipitation occurs in the form of rain. No allowances for snow, sleet, etc. are made. Thus, according to this assumption, at mean monthly temperatures less than  $-1^{\circ}\text{C}$ , infiltration of moisture ceases. The Infiltration and Drainage Model, developed at Texas A&M University, allows for drainage analysis of saturated base courses, design based on an empirical assessment of the drainage characteristics for the base course materials, and analysis of infiltration of moisture into the base course and subgrade moduli from data obtained from the Precipitation Model. The Climatic-Materials-Structural Model, developed at the University of Illinois, incorporates weather related data to calculate pavement temperature profile, changes in stiffness of asphalt courses, and resilient modulus and Poisson's ratio of base courses. Inputs into this model include percent sunshine, wind speed, air temperature, solar radiation, pavement geometry, and pavement material properties.

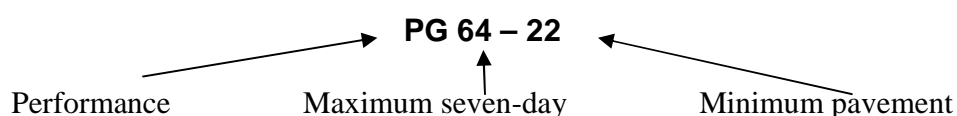
The Frost Heave/Thaw Settlement Model, developed at the Army Corps of Engineers Cold Region Research and Engineering Laboratory, deals with heat and moisture flow within soils. The soil temperature is derived from the CMS model estimates for pavement temperature, thus estimates of frost depth can also be made. A study of the effectiveness and sensitivity of the integrated climatic model was performed by Solaimanian and Bolzan (1993). The sensitivity of various parameters was analyzed, including: air temperature, percent sunshine, solar radiation, and pavement emissivity, absorptivity, and thermal conductivity. The effectiveness was analyzed by comparing outputs from the model with measured pavement temperatures from various sites in the United States and Canada during summer and winter conditions. The variables listed above were estimated. The predicted values tended to underestimate the actual pavement temperatures by 4 to 18%. However, below a depth of approximately 50mm the prediction improved. The surface temperature, based on the air temperature, was predicted within  $1.1^{\circ}\text{C}$ . The authors suggested that additional testing needed to be undertaken for better approximations to thermal values (emissivity, absorptivity, and thermal conductivity). (Diefenderfer, *et al* 2002)

## 2.12 Considerations on prediction accuracy

It may be unavoidable to have some discrepancy between predicted and measured pavement temperature values due to the number of variables that could be considered. The number of these input variables will depend upon a balance of the accuracy and the complexity of the model. One important topic that merits discussion (albeit brief in this work) when considering the accuracy of temperature prediction is the measurement of surface temperature. This is not such an arbitrary quantity that a thermometer at ground level can accurately measure it. Many of the aforementioned models utilize air temperature, surface temperature, or both in their prediction. In fact, Geiger (1965) dedicates an entire volume to the treatment of this topic. Factors that can influence the surface temperature include: solar radiation, air temperature, wind speed, cloud cover, time of day, distance from the surface, and physical properties of the material at the surface (Solaimanian and Kennedy, 1993). Not only are there atmospheric effects to consider, but also the pavement itself presents many variables that can influence the movement of thermal energy. Factors such as color (especially when discussing surface absorptivity), percent voids, moisture content, and orientation to the horizontal may also be important to consider when discussing thermal energy within a pavement structure.(Diefenderfer, *et al.* 2002)

## 2.13 Determination of Performance Grade according to Superpave method

Pavement surface temperature can be determined either by direct measurement or calculated using air temperature and other factors. A model for designing asphalt pavements called Superpave (Superior Performing Asphalt Pavement) has been created after many years of research (LTTP - Long-Term Pavement Performance and SMP - Seasonal Monitoring Program) of behavior of pavement due to traffic load and environmental conditions. According to the method of Superpave, asphalts are designed according to the expected minimum air temperature and maximum seven-day average annual temperature. An appropriate asphalt-binder is based on estimates of annual high and low temperatures and a defined PG x-y (Performance Grade, Figure 2.4) (Kennedy T. et al., 1994). Symbol (PG x-y) is used to determine asphalts depending on the pavement temperature. PG - Performance Grade x - high pavement design temperature y - low pavement design temperature. (Matić et.al 2011)



grade

average annual  
temperature

temperature

Figure 2.4 Explanation of PG symbol

Selecting an appropriate binder for different locations is determined using a series of equations defined by SHRP Superpave Binder System. PG system attempts to indicate the appropriate layers of asphalt-binder depending on the temperature. (Matić et.al 2011)

Table 2.1 Specification of asphalt layers, depending on the PG (Kennedy T. et al., 1994)

Performance Graded Asphalt Binder Specification (from AASHTO MP 1)																																					
Performance Grade	PG 46			PG 52				PG 58				PG 64				PG 70				PG 76				PG 82													
Average 7-day Maximum Pavement Design Temperature, °C <sup>a</sup>	< 46			< 52				< 58				< 64				< 70				< 76				< 82													
Minimum Pavement Design Temperature, °C <sup>a</sup>	-34	-40	-46	-10	-16	-22	-28	-34	-40	-46	-16	-22	-28	-34	-40	-10	-16	-22	-28	-34	-40	-10	-16	-22	-28	-34	-10	-16	-22	-28	-34						
ORIGINAL BINDER																																					
Flash Point Temp, T 48, Minimum (°C)	230																																				
Viscosity, ASTM D 4402 <sup>b</sup> Maximum, 3 Pa*s, Test Temp, °C	135																																				
Dynamic Shear, TP 5: <sup>c</sup> G*/sin $\delta$ , Minimum, 1.00 kPa Test Temp @ 10 rad/s, °C	46			52				58				64				70				76				82													
ROLLING THIN FILM OVEN RESIDUE (T 240)																																					
Mass Loss, Maximum, percent	1.00																																				
Dynamic Shear, TP 5: <sup>c</sup> G*/sin $\delta$ , Minimum, 2.20 kPa Test Temp @ 10 rad/s, °C	46			52				58				64				70				76				82													
PRESSURE AGING VESSEL RESIDUE (PP 1)																																					
PAV Aging Temperature, °C <sup>d</sup>	90			90				100				100				100 (110)				100 (110)				100 (110)													
Dynamic Shear, TP 5: <sup>c</sup> G*/sin $\delta$ , Maximum, 5000 kPa Test Temp @ 10 rad/s, °C	10	7	4	25	19	16	13	10	7	25	22	19	16	13	31	28	25	22	19	16	34	31	28	25	22	19	37	34	31	28	25	40	37	34	31	28	
Physical Hardening <sup>e</sup>																																					
Creep Stiffness, TP 1 Determine the critical cracking temperature as described in PP 42	-24	-30	-36	0	-6	-12	-18	-24	-30	-36	-6	-12	-18	-24	-30	0	-6	-12	-18	-24	-30	0	-6	-12	-18	-24	-30	0	-6	-12	-18	-24	0	-6	-12	-18	-24
Direct Tension, TP 3 Determine the critical cracking temperature as described in PP 42	-24	-30	-36	0	-6	-12	-18	-24	-30	-36	-6	-12	-18	-24	-30	0	-6	-12	-18	-24	-30	0	-6	-12	-18	-24	-30	0	-6	-12	-18	-24	0	-6	-12	-18	-24

a. Pavement temperatures are estimated from air temperatures using an algorithm contained in the LTPP Bind program, may be provided by the specifying agency, or by following the procedures as outlined in MP 2 and PP 28.


b. This requirement may be waived at the discretion of the specifying agency if the supplier warrants that the asphalt binder can be adequately pumped and mixed at temperatures that meet all applicable safety standards.

c. For quality control of unmodified asphalt binder production, measurement of the viscosity of the original asphalt cement may be used to supplement dynamic shear measurements of G\*/sin $\delta$  at test temperatures where the asphalt is a Newtonian fluid.

d. The PAV aging temperature is based on simulated climatic conditions and is one of three temperatures 90°C, 100°C or 110°C. The PAV aging temperature is 100°C for PG 58- and above, except in desert climates, where it is 110°C.

e. Physical hardening – TP 1 is performed on a set of asphalt beams according to Section 12, except the conditioning time is extended to 24 hours  $\pm$  10 minutes at 10°C above the minimum performance temperature. The 24-hour stiffness and *m*-value are reported for information purposes only.

f. G\*/sin $\delta$  = high temperature stiffness and G\*/sin $\delta$  = intermediate temperature stiffness



Way of calculating pavement temperatures, according to the Superpave method, based on air temperature is as follows:

- convert average 7-day maximum air temperature to pavement surface temperature;
- calculate 7-day maximum pavement temperature at design depth;
- convert minimum air temperature to minimum pavement surface temperature;
- calculate minimum pavement temperature at design depth (Kennedy T. et al., 1994).

The method allows the estimation of the pavement surface temperature and the temperature at specified depths from the surface. The average seven-day maximum pavement design temperature is the average of the highest daily pavement temperatures for 7 warmest consecutive days in a year. Minimum annual pavement temperature is the lowest temperature in a year. The

design depth for calculation of maximum pavement temperature used in the Superpave system is 20 mm below the top of the pavement layer. When considering, for example, a 50-mm thick surface mixture over a base mixture, a design depth for the surface mixture is 20 mm below the pavement surface. Design depth for the base mixture is 20 mm below the top of the base mixture, that is, 70 mm below the pavement surface (Kennedy T. et al., 1994).



## **Chapter 3 LIBYA ENVIRONMENT AND CLIMATE CONDITIONS**

### **3.1 General**

Libya is located in a hot and arid climatic region characterized by high variation in daily temperatures, high solar radiation, low humidity, low rainfall intensity, wind and dust storms. Asphalt pavement roads are the main and only source of the Libyan overland transportation system for most passengers and goods. Most of Libya's deteriorated roads pass through the Libyan desert. While Libyan roads have an expected design life of 20 years, these roads do not last so long due to the hot, arid climate, which produces aging, rapid deterioration and a reduction of service life. The tendency for the asphalt binder to harden and age under atmospheric influences has been known and studied for many years. High solar radiation in Libya's hot and arid climate, along with the presence of oxygen, accelerates and increases the physical, chemical, and photochemical processes in the asphalt binder. Additionally, swinging and fluctuation a fluctuation of daily solar radiation and temperature—pavement in the summer can reach more than 70°C during the day and yet be freezing at night—induces thermal stresses and causes fast aging in the asphalt pavement layers. Therefore, deterioration in the form of thermal cracking is a problem.

### **3.2 Weather classifications**

The hot-arid climate is characteristic of regions lying mostly between 15° and 45° both north and south. The severe conditions of hot dry climates markedly complicate construction and call for special architectural treatments, design approaches, and construction practices to make durable buildings and other structures (Stoll and Evstratov 1987). Generally asphalt pavement roads are the main and only source of the Libyan overland transportation system for most passengers and goods. These roads are without traffic control system or limitations to the loading. There is also lack of exact and accurate traffic information relating to axle loads and traffic growth trends in Libya. The estimated number of equivalent standard axle load (8.2 tons), the repetition reaches or exceeds 2 500 000 EAL, medium to heavy traffic (Roffa 2000).

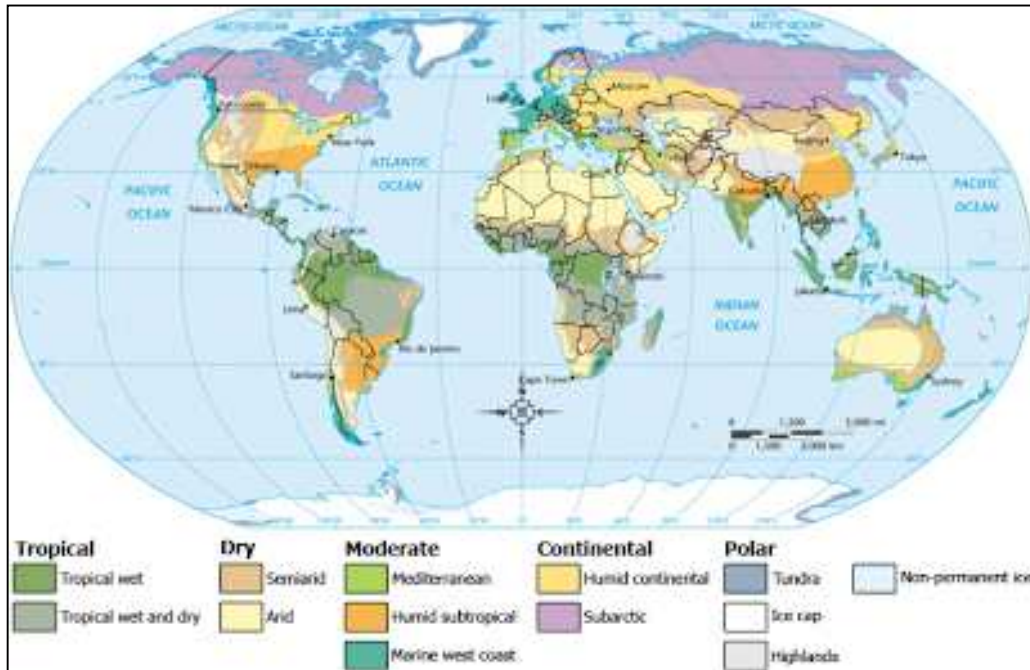


Figure 3.1 Geographic and climatic location of Libya.  
 (Source: [http://en.wikipedia.org/wiki/Geographical\\_zone](http://en.wikipedia.org/wiki/Geographical_zone))

Most of Libya's main roads pass through different geological formations and are located between 24° and 30°. The most deteriorated roads pass through the Libyan desert, which is characterized by high variation in daily temperatures, high solar radiation, low humidity, low rainfall intensity, wind and dust storms. Although the usual mode of failure expected in this geographical location is deformation (rutting), it has been seen that the main mode of pavement deterioration is cracking failure. This type of pavement failure is seen in many highways in the Libyan desert, (e.g., Waddan-Sebha highway, Brak bête-Brak, Waddan-Zellah, and Ajdabiya-ALKufra highway).

### 3.3 Libya road materials

The asphalt cement (bitumen) binder used in Libyan roads is semi-solid asphalt (AC 60/70), which is recommended by the general road department of Libya and produced by Azzawia Oil Refining Company. Bituminous mixture pavement regarded as linear visco-elastic materials, where the bitumen plays the major part for the viscous properties, while, the mineral substances are responsible for the elastic properties. The viscous property plays a large part in asphalt pavement performance and deterioration, the cracking and deterioration of asphalt pavement layers due to the consequence of several causes like, material fatigue, shrinkage, sub grade rutting, ageing due to environment influences and poor construction quality, etc.

Particularly, in Libyan road deterioration, we expect that the hot arid climate plays a predominant role, leading to a much faster aging process in the bituminous binder than observed in other regions. The high solar radiation in the region with presence of oxygen accelerates and increases the asphalt binder physical, chemical, and photochemical processes.

### **3.4 Climate conditions**

Libya is located in a hot and arid climatic region with high temperatures and low humidity in summer. In the desert, the mean annual duration of sunshine is about 11 hours daily, and the temperature is over 25°C for about seven months of the year (Roffa 2005). The ambient temperature, (the absolute temperature) is in excess of 40°C, the daily average temperature in the hottest month is over 20°C. The extreme maximum temperature in summer exceeds 52°C, and the extreme low temperature in winter reaches below freezing (-6 °C). The hottest recorded world temperature was in Libya on September 13, 1922, which was 58 °C. Azizia is which lies at about 32.53 °N 13.02 °E, and a height above sea level about 112 m / 367 feet, and only about 50 km far from the seaside. The rainfall in the Libyan Desert is not uniform and does not last long; its annual intensity is as low as 0–10 mm.

Mean annual relative humidity is about 30 to 50 %. The dry wind and dust storms are very severe and impact both structures and humans (Roffa 2002). The well known scorching wind called the "gibli"(a hot, very dry, sand-laden wind) can raise the temperatures in a matter of hours to between 40°C and 50°C. The under study road sections passing through this region are subjected to long hot summers (over 100 days a year). The above-mentioned climate not only causes human discomfort but also building materials deterioration. This hot arid environmental condition has its hard impact and influences on the asphalt pavement mixtures, leading to fast and rapid hardening and aging. Figure 3.2 shows the temperature variation along the months of the year. As the asphalt pavement binder ages (oxidation of the organic materials and sublimation of volatile fractions), the pavement loses its durability and becomes intolerant, and behave as rigid pavement and owes its strength to friction between the mineral component alone.

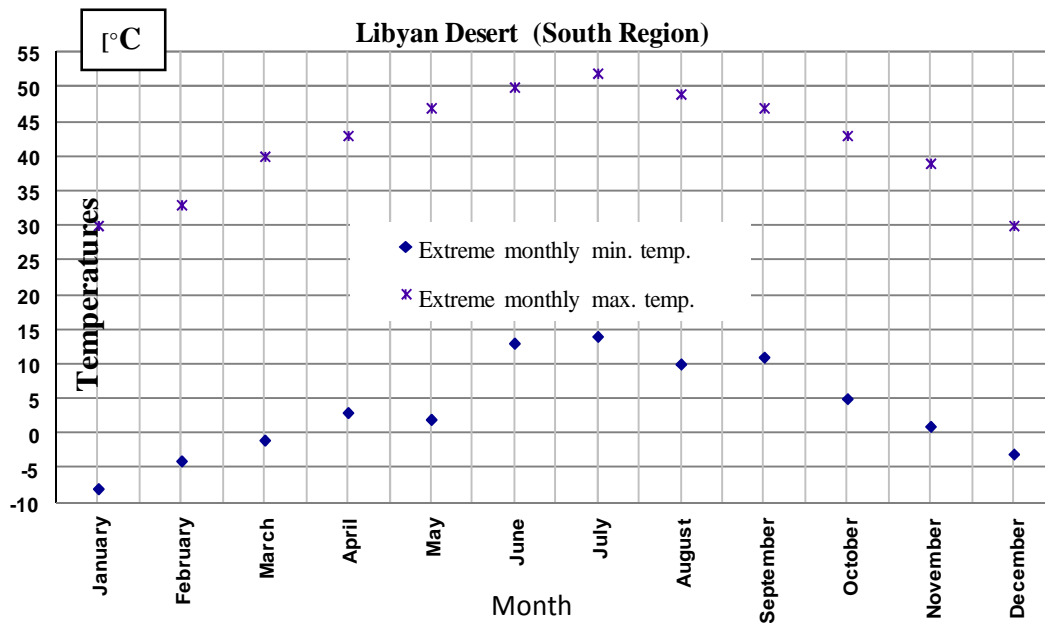


Figure 3.2 Temperature variations in south region in Libya.

### 3.4.1 Weather related data

To accomplish the climatic analysis required for incremental damage accumulation, the following five weather-related parameters are required:

- Hourly air temperature
- Hourly precipitation
- Hourly wind speed
- Hourly percentage sunshine (used to define cloud cover)
- Hourly relative humidity
- Solar radiation

The air temperature is required by the heat balance equation in the Enhanced Integrated Climatic Model EICM for calculations of long wave radiation emitted by the air and for the convective heat transfer from surface to air. Both computations are explained in detail later in this chapter. In addition to the heat calculations, the temperature data is used to define the frozen/thawing periods within the analysis time frame and to determine the number of freeze-thaw cycles.

Heat fluxes resulting from precipitation and infiltration into the pavement structure have not been considered in formulating the surface heat flux boundary conditions. The role of precipitation under these circumstances is not entirely clear, and methods to incorporate it in the energy balance have not been attempted. However, precipitation is needed to compute infiltration

for rehabilitated pavements and aging processes. Furthermore, the precipitation that falls during a month when the mean temperature is less than the freezing temperature of water is assumed to fall as snow.

Wind speed is required in the computations of the convention heat transfer coefficient at the pavement surface. The percentage of sunshine is needed for the calculations of heat balance at the surface of the pavement.

### **3.5 Deterioration of the Libyan desert road network**

A road pavement continuously deteriorates under the combined action of traffic and the environment. The ability of the road to satisfy the demands of traffic and the environment over its design life is called its performance. The most common indicators of pavement performance are: fatigue cracking, surface rutting, riding quality, and skid resistance. The change in the value of these performance indicators over time is referred to as deterioration.

Libya's road network has been considerably expanded since 1978. At that time, Libya had only about 8,800 kilometers of roads, of which perhaps one-half were paved. However, by 1985 Libya had between 23,000 and 25,600 kilometers of paved roads. Surfaced roads existed between the north and the southern oases of Al Kufrah, Marzuq, and Sabha. By 1999 Libya had an estimated total road network of 83,200 kilometers, of which 47,590 kilometers were paved. These roads helped much to end the isolation of remote settlements. In particular, the agricultural projects underway in the desert oases have benefited from the more efficient crop marketing made possible by these roads. The National General Company for Roads oversees all new construction and maintenance. The key road in Libya is the 1,822-kilometer national coastal highway. It runs from the border with Tunisia to the Egyptian border and passes through Tripoli and Benghazi. About two-thirds of Libya's roads have a bitumen surface or have at least been treated with bitumen.

Pavement cracking and rutting are two of the most critical distress types manifested on flexible pavements, and they often dominate the overall pavement condition. Generally, most of desert roads damages apparts without surface deformation, meaning there is no luck of bearing capacity, and main causes are the environmental coditions with material properties.

### **3.6 Types of distress in Libya desert roads**

Cracking and rutting are two of the major problems of the Libyan road network. The following pictures were taken on Libyan roads by the author.

### 3.6.1 Raveling

Heat from the sun's ultra-violet rays causes the liquid asphalt in pavement to oxidize and become brittle as shown in figure 3.3. The weight of vehicles causes the surface to crumble at the point of contact between the tires and the pavement. Water then washes away the dry, crumbled aggregate, diminishes pavement thickness, and reveals a rough rocky appearance



Figure 3.3 Raveling distress in Libyan roads characteristic

### 3.6.2 Cracking

Variation in temperature and expansive soils cause pavement to expand and contract. Cracking causes the pavement surface to divide into rectangular pieces. Longitudinal (expansion) cracks run parallel to the roadway or along curb lines. Transverse cracks (block cracking) run perpendicular to centerline and are a sign of age. Figure 3.4–3.6 show the types of cracking. These cracks indicate that the pavement has lost flexibility and needs major reconstruction.



Figure 3.4 Block cracking distress in Libyan roads



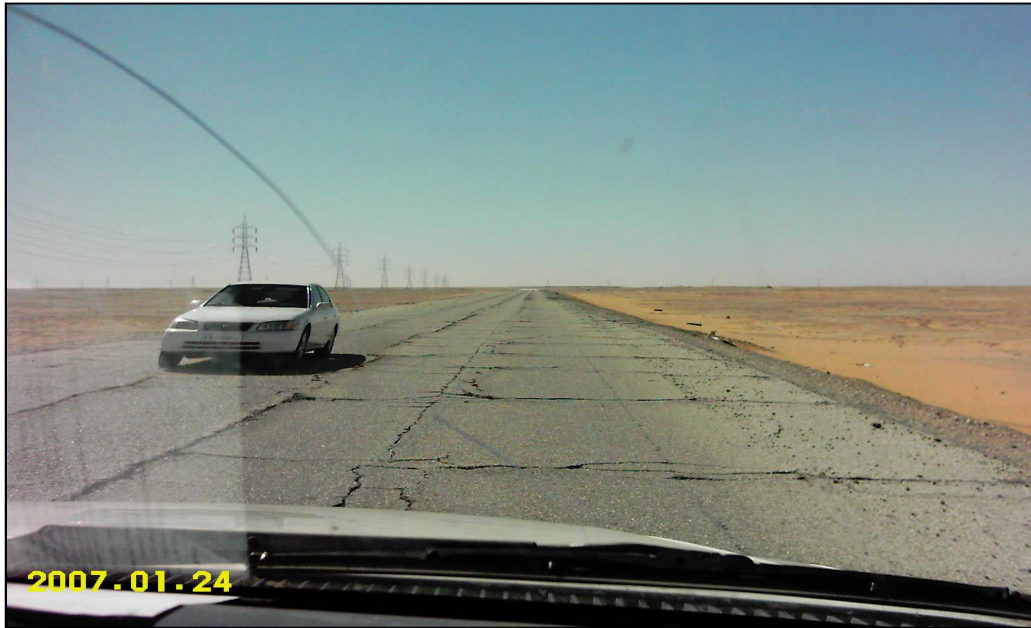


Figure 3.5 Longitudinal and transverse cracking distress in Libyan roads



Figure 3.6 Alligator cracking distress in Libyan roads

### 3.6.3 Alligating

As a load associated structural failure, alligator cracking often occurs because of weakness in the surface, base or sub grade; a surface or base that is too thin; or poor drainage. Alligating spreads through the pavement, breaking the pavement into even smaller pieces and eventually forming potholes as the loose pieces are thrown off to the side.





Figure 3.7 Alligator cracks in Libya roads

### 3.6.4 Edge Cracks

Edge cracks travel along the edge of the pavement. They are commonly caused by poor drainage conditions and lack of support at the pavement edge.



Figure 3.8 Edge damages in Libya roads





Figure 3.9 Road damages in Libya roads

### 3.6.4 Rutting

Pavement rutting is one of the most common and destructive pavement distresses being observed in flexible pavements, which is primarily due to axle loads that exceed the legal limit and high ambient temperatures. Poor mix design is also a cause of rutting. Rutting is characterized by permanent deformation of the pavement. It generally develops during the hot seasons when the asphalt is softer. It can be identified by ruts on the wheel path,



Figure 3.10 Rutting distresses (<http://www.pavementinteractive.org/article/rutting/> )

### 3.7 Pavement temperature parameters related to thermal stress and durability

The following parameters that characterize pavement temperatures are of interest in the context of pavement durability.

- 1) The average pavement temperature affects both the tensile/compressive stress level and the mechanical material properties.
- 2) The temperature gradient over the pavement thickness produces bending stresses, which are a concern for rigid pavement (concrete) but of less importance for flexible pavement (asphalt). Nonetheless, it should be recognized that temperature and stress gradients may be higher at or near the surface than over the thickness of the pavement.
- 3) The diurnal amplitude of pavement temperature is important for pavement fatigue analysis.
- 4) The time rate of change of temperature is of interest because fast temperature changes give the material less time for plastic creep, and therefore should give higher stress levels.



Figure 3.11 Road damages in Libya roads

### 3.8 Field instrumentation and data collection system

#### 3.8.1 Zones and stations

Libya can be divided into two main weather zones: the Mediterranean sea and the desert. From the weather map, we can see that most of Libya is located in the desert. Before installing the sensors in the stations, we selected the zones located in the desert. The map below presents all the Libyan regions, and it is listed as:

- |             |                     |                   |
|-------------|---------------------|-------------------|
| 1. Zwarah   | 9. Marj             | 17. Al Wahat      |
| 2. Zawiya   | 10. Jabal al Akhdar | 18. Ghat          |
| 3. Jafara   | 11. Derna           | 19. Wadi al Hayaa |
| 4. Tripoli  | 12. Butnan          | 20. Sabha         |
| 5. Murqub   | 13. Nalut           | 21. Murzuq        |
| 6. Misrata  | 14. Jabal al Gharbi | 22. Kufra         |
| 7. Sirte    | 15. Wadi al Shatii  |                   |
| 8. Benghazi | 16. Jufra           |                   |

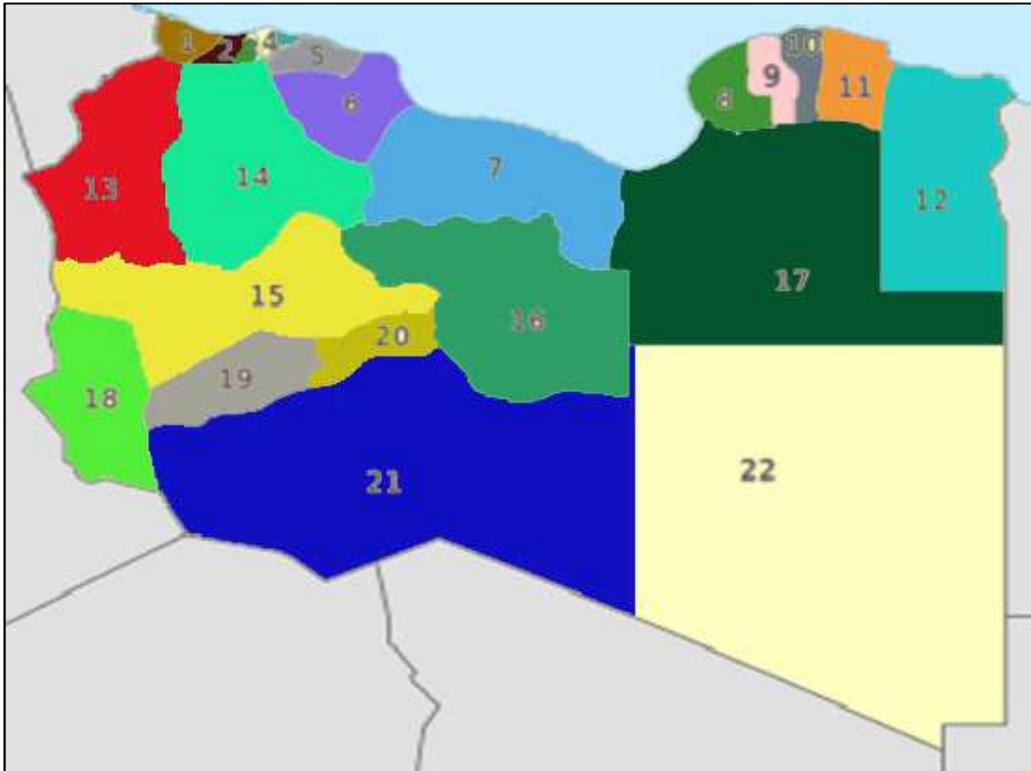


Figure 3.12 Libya stats map (Source Ezilion maps)

### 3.8.2 Description of data collection system

The data collection system provides pavement temperature and climatologically monitoring. Eight test sections were selected for the pavement temperature monitoring system. The sections represent the eight different regions in the Libyan desert and covering an area 1800km \*900 km. The next step was selection of the regions and locations representative of the desert area:

- 1.Nalut (Ghadames)
- 2.Wadi al Shatii (Brak)
- 3.Jufra(Wuddan)
- 4.Al Wahat(Awjila)
- 5.Ghat (Ghat)
- 6.Wadi al Hayaa (Ubari)
- 7.Murzuq (Qatrun)
- 8.Kufra (Kufra )

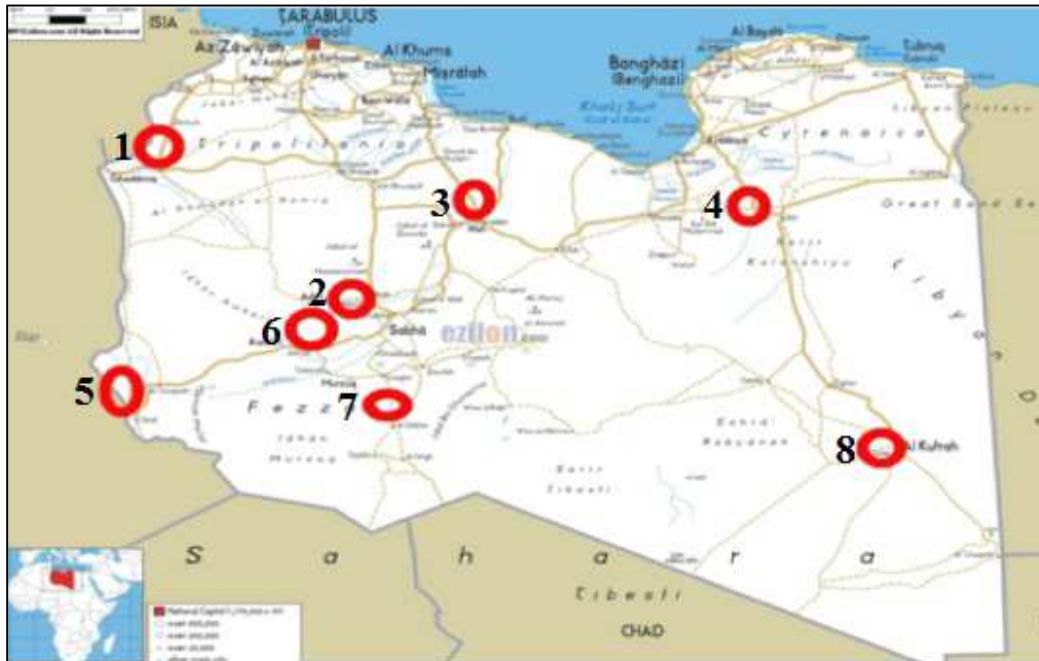


Figure 3.13 Location of the study area station (Source Ezilion maps).

Table 3.1 Latitude and longitude of the locations of the selected station for the study

Locations	Latitude	Longitude
Ghat	24°59'N	10°11'E
Ghudamis	30°11'N	09°29'E
Waddan	29°02'N	16°00'E
Al Kufrah	24°17'N	23°15'E
Al Qatron	24°56'N	15°03'E
Awbari	26°46'N	12°57'E
Awjilah	29°08'N	21°07'E
Brak	27°31'N	14°20'E

### 3.8.3 Description of study area

#### 3.8.3.1 Ghadames station

The city of Ghadames is part of Libya and is famous due to its calm atmosphere. The streets of this city are white, which gives them the refreshing look that you might not get in many other cities in the world. Ghadames is actually an oasis town, located in the western region of Libya. It is situated around 550 kilometers away from the southwestern region of Tripoli. The borders of Tunisia and Algeria are located in its proximity.

The city of Ghadames is situated around 360 meters (which is around 1170 feet) above sea level. The city hardly experiences rain or snow, and this is the major reason for the hot temperatures

throughout the year. The maximum temperature touches 48°C in June and July, which is the hottest month. The climate for Ghadames is similar to the rest of Libya, that is, very hot at times.

### **3.8.3.2 Kufra Station**

Kufra's location in Libya's southeast places it on the country's border with Egypt, Sudan (unlike any other Libyan district), and Chad. Besides the main Oasis group of the Kufra Basin, four more oases, lying northwest of Kufra Basin, belong to the region including: Rebiana, Buzema, Wadi Zighen and Tazirbu. The oasis-valleys of Jabal Arkanu and Jebel Uweinat lie southeast of the basin. It is situated around 1500 km away from the southeastern region of Tripoli, and 900 km away from south of Benghazi.

#### *Kufra Climate*

The weather and climate condition of Kufra can be summarized as:

Altitude: 435 m (1427 ft). The warmest average high temperature is 48°C in June. The coolest average low temperature is -5°C in January. Kufra receives on average 1 mm (0.0 in) of precipitation annually or 0 mm (0.0 in) each month. On balance there are 0 days annually on which greater than 0.1 mm (0.004 in) of precipitation (rain, sleet, snow or hail) occurs or 0 days on average. The months with the driest weather are January to July and September to December, when on balance, 0 mm (0.0 in) of rainfall (precipitation) occurs. The month with the wettest weather is August when on balance 1 mm (0.0 in) of rain, sleet, hail or snow falls across 0 days. Mean relative humidity for an average year is recorded as 32.1% and on a monthly basis it ranges from 23% in June, July and August to 48% in December. There is an average range of hours of sunshine in Kufra of between 8.6 hours per day in December and 12.4 hours per day in July. On balance there are 3693 sunshine hours annually and approximately 10.1 sunlight hours for each day.

### **3.8.3.3 Ghat station**

Ghat, the capital of the Ghat District, is in the Fezzan region, near the western border of Libya with Algeria. The Acacus Mountains have a large variation of landscapes, from differently coloured sand dunes to arches, gorges, isolated rocks and deep ravines (wadis). Major landmarks include the arches of Afzejare and Tin Khlega. Although this area is one of the most arid of the Sahara, there is vegetation, such as the medicinal *Calotropis procera*, and there are a number of springs and wells in the mountains. Ghat is an important tourist destination due to the existence of prehistoric rock paintings and engravings in the neighboring Tadrart Acacus and Tassili N'Ajjer mountains, in addition to the beauty of the surrounding desert landscapes. A major tourist attraction in the town itself is the Fortress of Ghat, *Koukemen*.



#### ***3.8.3.4 Waddan station***

Halfway between Sebha and the coast, east of the Tripoli-Sebha Highway, are the three adjacent Al-Jufra oases of Houn, Sokna and Waddan. Waddan is the oldest city in the Jufra District located 230 km south of Sirte, and 400 km north of Sebha. The town is at the crossroads of the Sirte-Waddan Road and the Fezzan Road.

#### ***3.8.3.5 Ubari station***

Ubari is in the Targa valley, lying between the Messak Sattafat plateau and Idhan Ubari ergsand dunes and lakes. Native plants include wetland grasses at the natural spring fed lakes' shorelines, and the native Saharan Date palm. The Ubari oasis settlement is the second center for the Kel Ajjer Tuareg people, after Ghat. Neighbouring villages include Germa, and Garran.

#### ***3.8.3.6 Brak station***

Brak station is located in Wadi al Shatii and is sometimes referred to as Ash Shati. It is one of the districts of Libya in the central-west part of the country. The area is mostly desert.

#### ***3.8.3.7 Qatrun station***

Qatrun, Al Katrun, Gatrone, or Al Gatrun is a village in the Murzuq District in southern Libya on the main road to Chad and Niger. It has a filling station and a Niger consulate office is located there. When the border checkpoint 310 kilometers south at Tumu is closed, travelers crossing into Libya from Niger report in at Qatrun.

### **3.9 Temperatures monitoring at the Libya desert stations**

Eight pavement sections in different geographical locations of the Libya desert were selected for this study. A monitoring station was set-up to collect data on air temperature, solar radiation, wind speed, and pavement temperatures at various depths. Sensors were connected to (HE70X-80X series is thermocouple thermometer, developed by HUATO company) data logger housed in a protection enclosure. The data logger was operated by a solar energy battery. Chapter 4 describes the installation and sensor locations.

## **Chapter 4 DATA PRESENTATION AND ANALYSIS**

### **4.1 General**

As HMA is a viscoelastic material, its mechanical properties vary with temperature. Thus, to study the difference in strength characteristics of various pavement designs, it is imperative to know the temperature distribution within the pavement cross-section.

#### **4.1.1 Pavement Temperature Monitoring System**

The temperature within the pavement at the pavement stations is monitored using HUAT thermocouples. As opposed to thermostats, which report a temperature change, the output from the thermocouples can be directly computed as actual temperature values. A stainless steel thermal probes (similar to the LTPP design) were installed in the road pavement sections. In each station two sensors were used with two probes for each one, thus there were four probes for each station.

One probe was placed on the surface of the pavement, a second at 3 cm from the surface, a third at 8 cm from the surface (binder course asphalt layer), and the last at 15 cm from the surface (between the binder course asphalt layer and the granular base course layer), A schematic illustration of the thermal probes' location and details of the instrumentation layout and the profile of the thermal probe installed in a pavement sections shown in figure 4.1

#### **4.1.2 Climatological Monitoring System**

In addition to the pavement temperature monitoring system, climatologically data (including air temperature, wind speed, wind direction, and solar radiation) had been monitored. This data has been collected to evaluate the effects of these environmental factors on the thermal variations of the pavement.

### **4.2 Thermocouple placements**

The thermocouples were placed at the stations in the Libyan desert study area to determine the temperature at various distances from the surface of the pavement – surface (C1), 3 cm (C2), 8 cm (C3), and 15 cm (C4).

A test site incorporating eight pavement sections representing a typical road pavement structure in the Libyan desert was constructed. All pavement sections were outfitted with temperature sensors connected to a portable data logger. The pavement cross-section information is summarized in Table4.1. It is noted that flexible pavement of roads in the Libyan desert in this

study are comprised of sub grade, 20cm aggregate base course, and asphalt concrete with a 9cm binder course and 5cm wearing course on top.

Since the total thickness of pavement layers is 34cm, thermocouples were installed in the lower portion of asphalt layers and a temperature probe was used in the upper portion. In the lower portion, thermocouples were embedded at the surface (C1) of AC, and at 3 cm (C2), 8 cm (C3), and 15 cm (C4) down to the AC layer. A digital thermocouple probe was inserted in each hole for measurement. The air temperature and pavement surface temperature were obtained using an infrared temperature gun. figure 4.1 shows the schematic of the temperature measurement layout. All temperature data were recorded at 15-minute intervals within a day.

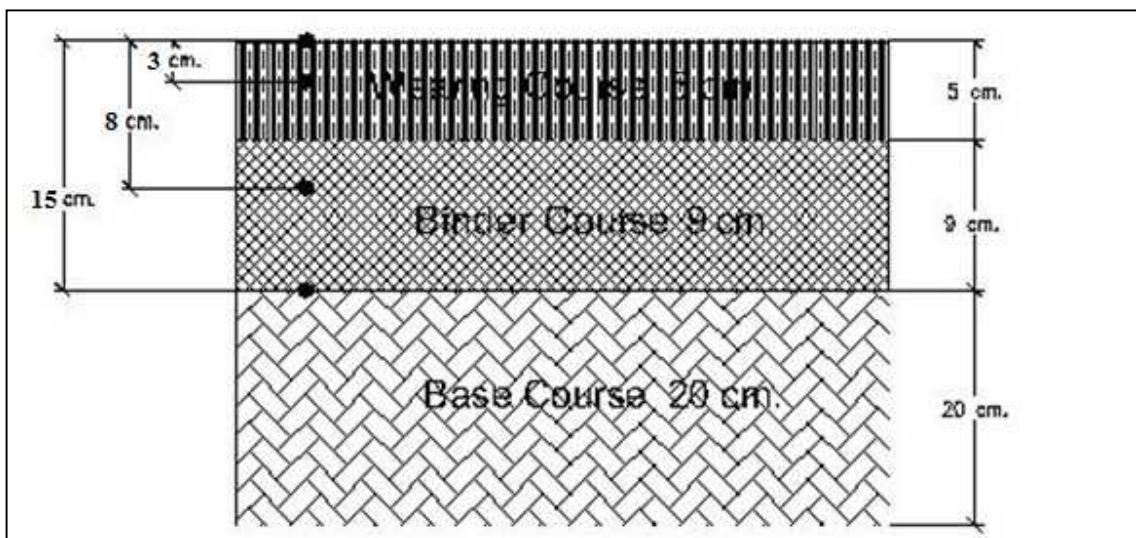


Figure 4.1 Pavement layers and thermocouples locations

Table 4.1 The typical layers of roads in roads stations

Location	Wearing course(cm)	binder course(cm)	Base course(cm)	Total thickness(cm)
Brak	5	9	20	34
Alkoufra	5	9	20	34
Awjalaha	5	9	20	34
Alkatroun	5	9	20	34
Awbarei	5	9	20	34
Gahat	5	9	20	34
Wuaddan	5	9	20	34
Ghadamess	5	9	20	34



### 4.3 Analysis of results with respect to pavement structural configuration

Prior to discussing the temperature data analysis, a brief summary of the temperature data set is presented. Figures 4.2 and 4.3 show an example of the distributions of maximal and minimal daily air and pavement temperature for four layers at the Brak station during the study period (1.3.2012.- 4.3.2013.). Appendix A presents figures of the distributions of maximal and minimal daily air and pavement temperature for four depths for the remaining stations.

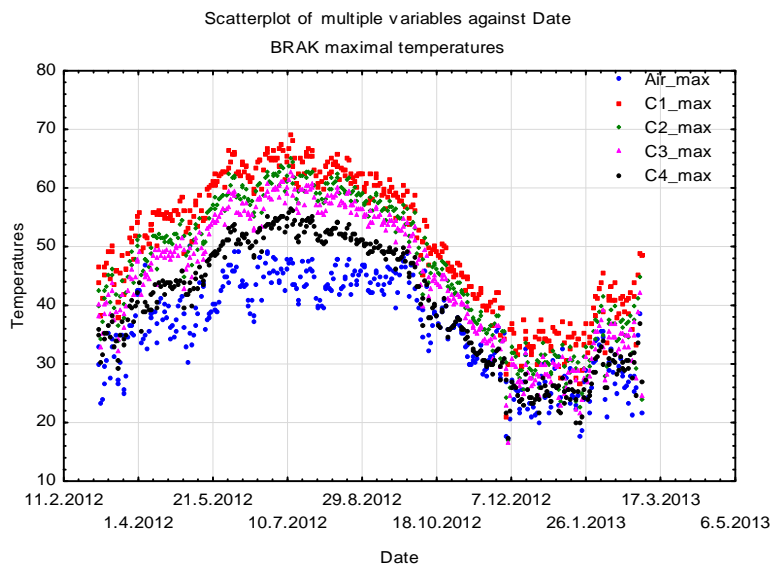


Figure 4.2 Maximal daily temperatures at Bark during the study period (1.3.2012.- 4.3.2013.)

Legend:

Air\_max – maximal daily air temperature (°C);

C1\_max – maximal daily pavement temperature at surface (°C);

C2\_max – maximal daily pavement temperature at 3 cm depth from the surface (°C);

C3\_max – maximal daily pavement temperature at 8 cm depth from the surface (°C); and

C4\_max – maximal daily pavement temperature at 15 cm depth from the surface (°C).

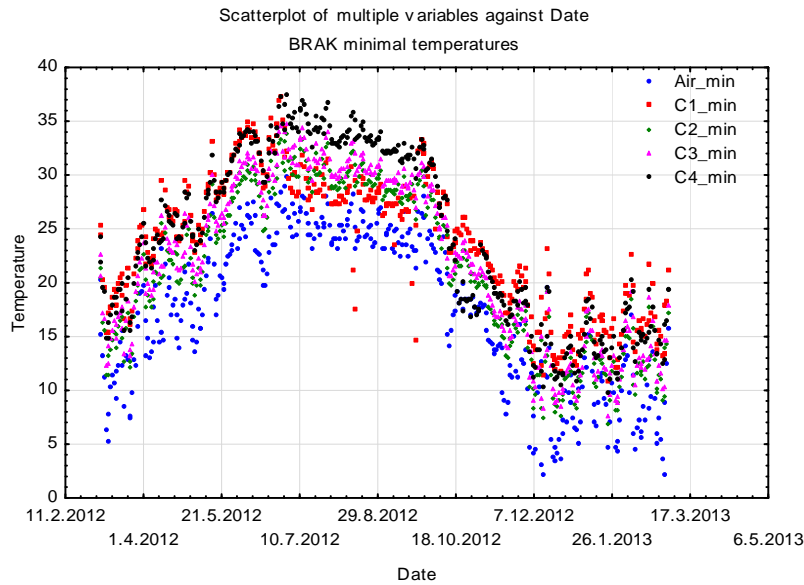


Figure 4.3 Minimal daily temperatures at Brak during the study period (1.3.2012.- 4.3.2013.)

Legend:

Air\_min – minimal daily air temperature (°C);

C1\_min – minimal daily pavement temperature at surface; (°C);

C2\_min – minimal daily pavement temperature at 3 cm depth from the surface (°C);

C3\_min – minimal daily pavement temperature at 8 cm depth from the surface (°C); and

C4\_min – minimal daily pavement temperature at 15 cm depth from the surface (°C);.

To compare the effect of pavement structural configuration on the pavement temperature at given distances from the surface, the temperatures were divided into daily maximum and daily minimum values. The daily temperatures were analyzed from the beginning of March 2012 until the beginning of May 2013.

In tables 4.2 and 4.3 the descriptive statistics for maximal and minimal daily temperatures for station Al-Jufroh are given, including the mean, 95% confidence interval, minimum, maximum standard deviation and standard error, while in Appendix B the tables of descriptive statistics for maximal and minimal temperatures for the remaining stations are given. Figure 4.4 presents the box plot of maximal daily temperatures at Al Jufroh for different layers. Figure 4.5 presents the box plot of minimal daily temperatures at Al Jufroh, Appendix B presents similar box plots for the remaining stations.

Table 4.2 The descriptive statistics for maximal daily temperatures for station Al-Jufroh

Variable	Al-Jufroh Maximal daily temperatures Descriptive Statistics							
	Valid N	Mean	Confidence -95,000%	Confidence 95,000%	Min	Max	Std.Dev.	Standard Error
Air_max	365	36,01189	35,21528	36,80850	17,290	50,330	7,73921	0,405089
C1_max	365	50,09195	48,86147	51,32242	21,650	70,080	11,95429	0,625716
C2_max	365	45,46497	44,33811	46,59183	19,440	66,880	10,94765	0,573026
C3_max	365	42,66090	41,61106	43,71075	18,930	62,045	10,19944	0,533863
C4_max	365	41,41027	40,39167	42,42888	18,545	57,930	9,89594	0,517977

Legend:

Air\_max – maximal daily air temperature (°C);

C1\_max – maximal daily pavement temperature at surface (°C);

C2\_max – maximal daily pavement temperature at 3 cm depth from the surface (°C);

C3\_max – maximal daily pavement temperature at 8 cm depth from the surface (°C); and

C4\_max – maximal daily pavement temperature at 15 cm depth from the surface (°C).

Table 4.3 The descriptive statistics for minimal daily temperatures for station Al-Jufroh

Variable	Al-Jufroh Minimal daily temperatures Descriptive Statistics							
	Valid N	Mean	Confidence -95,000%	Confidence 95,000%	Min	Max	Std.Dev.	Standard Error
Air_min	365	13,77288	13,08801	14,45775	-0,950	25,880	6,653635	0,348267
C1_min	365	17,16121	16,43312	17,88929	3,320	30,090	7,073499	0,370244
C2_min	365	17,80827	17,06790	18,54865	4,120	31,220	7,192892	0,376493
C3_min	365	19,69514	18,95914	20,43114	6,380	31,910	7,150406	0,374269
C4_min	365	20,79249	20,08777	21,49722	7,780	38,110	6,846527	0,358364

Legend:

Air\_min – minimal daily air temperature; (°C);

C1\_min - minimal daily pavement temperature at surface (°C);

C2\_min - minimal daily pavement temperature at 3 cm depth from the surface (°C);

C3\_min - minimal daily pavement temperature at 8 cm depth from the surface (°C) and

C4\_min - minimal daily pavement temperature at 15 cm depth from the surface (°C).

Mean values of maximal daily temperatures are higher for pavement temperatures than air temperatures. Mean value of maximal daily surface temperature is the highest for four layers. Mean values of maximal daily temperatures for four layers decrease with distance from the surface. Same is for maximums of maximal daily air and pavement temperatures. Minimums of maximal daily air and pavement temperatures decrease with distance from the surface. Standard

deviation of maximal air temperature is the lowest. Standard deviation of maximal surface temperature is the highest of four layers. Standard deviations of maximal daily temperatures for four layers decrease with distance from the surface, indicating less variation in deeper layers.

Mean values of minimal daily temperatures are higher for pavement temperatures than air temperatures. Mean value of minimal daily surface temperature is the lowest for four layers. Mean values of minimal daily temperatures for four layers increase with distance from the surface. Same is for maximums of minimal daily air and pavement temperatures. Minimums of minimal daily air and pavement temperatures increase with distance from the surface. Standard deviation of minimal air temperature is the lowest. Standard deviation of minimal C3 layer temperature is the highest of four layers. Standard deviations of minimal daily temperatures for C4 layer is the lowest of four layers, indicating less variation in deeper layers.

Standard deviations of maximal daily air and pavement temperatures are higher than standard deviations of maximal daily air and pavement temperatures indicating less variation in minimal than maximal temperatures.

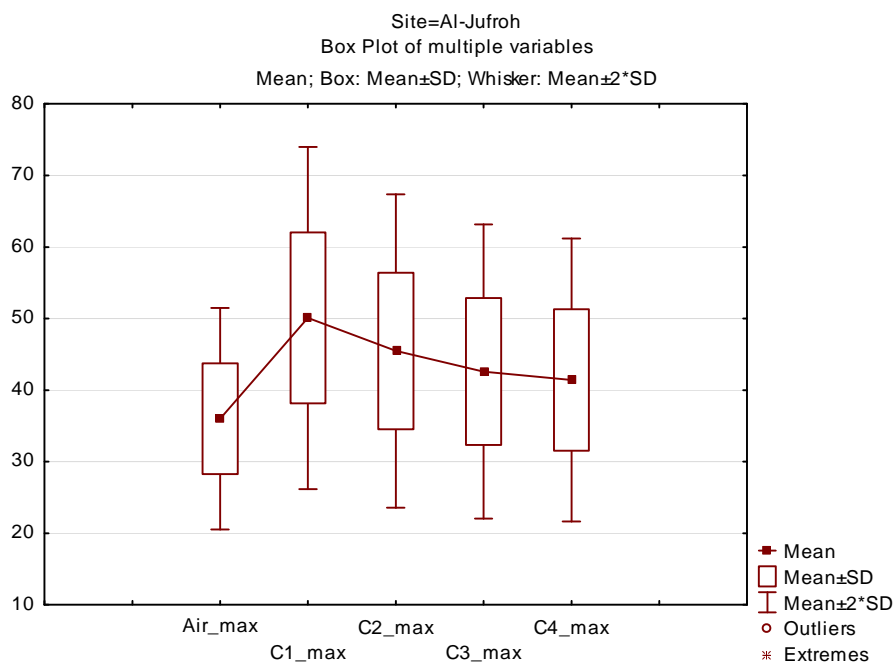


Figure 4.4 Box plot of maximal daily temperatures the Al-Jufroh location

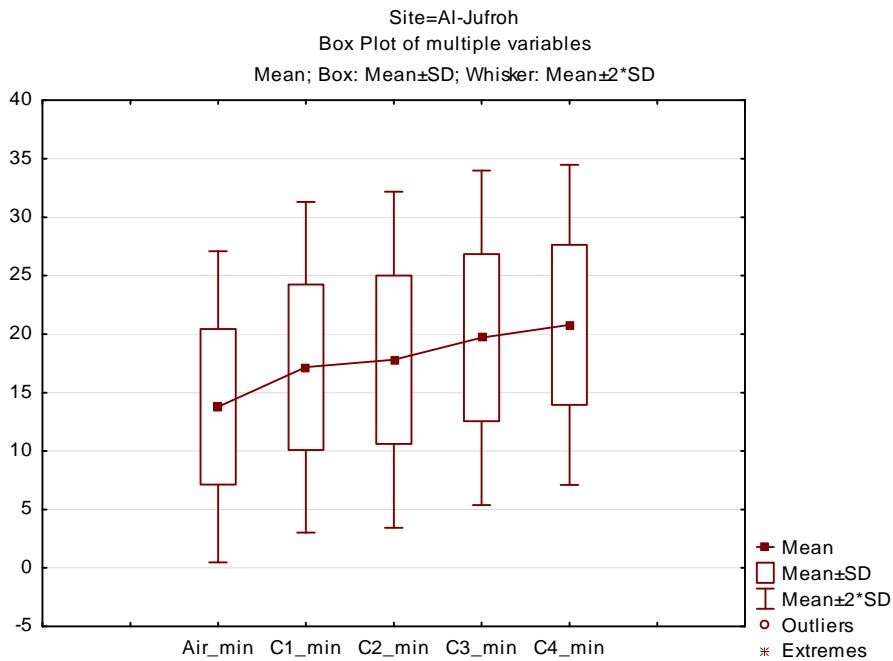


Figure 4.5 Box plot of minimal daily temperatures at the Al-Jufroh location

The development of temperature prediction models using data from the eight locations began by finding maximum and minimal daily temperatures within each layer and maximum and minimal daily air temperature. The maximal daily temperatures occurred between 14:00 and 17:00 at each layer and the minimal daily temperature occurred between 3:00 and 8:00 within each layer. For most days, the minimal daily temperature at the surface occurred just before sunrise and the maximal daily temperature at the surface occurred between 14:00 and 16:00, with the respective minimum or maximal daily temperatures in each layer occurring with a time lag that increased with increasing distance.

Figures 4.6 and 4.7 presents the temperatures for June, 30 2012 and December 30, 2012 at the Brak station. Appendix C presents similar figures for the remaining stations.

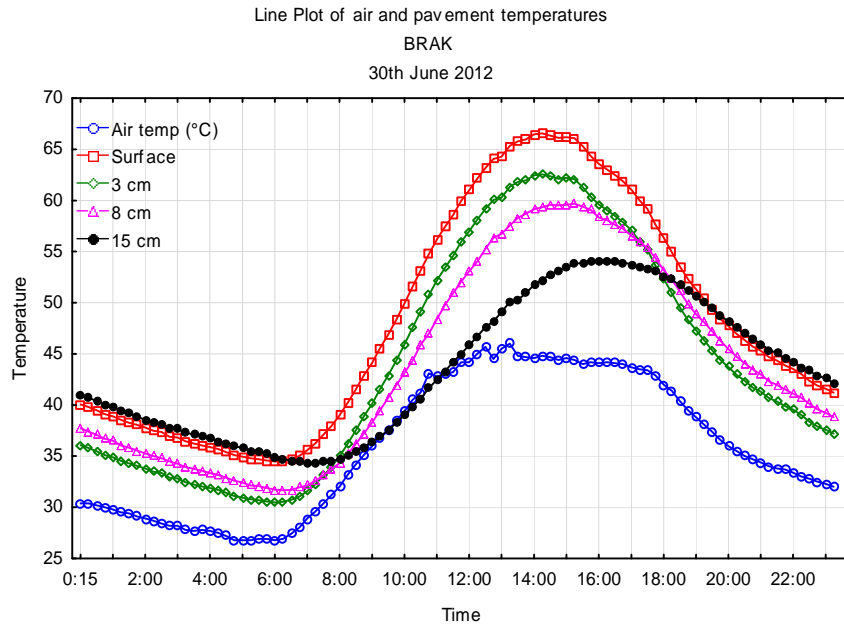


Figure 4.6 Air and pavement temperatures at four depths at the Brak location for June 30, 2012.

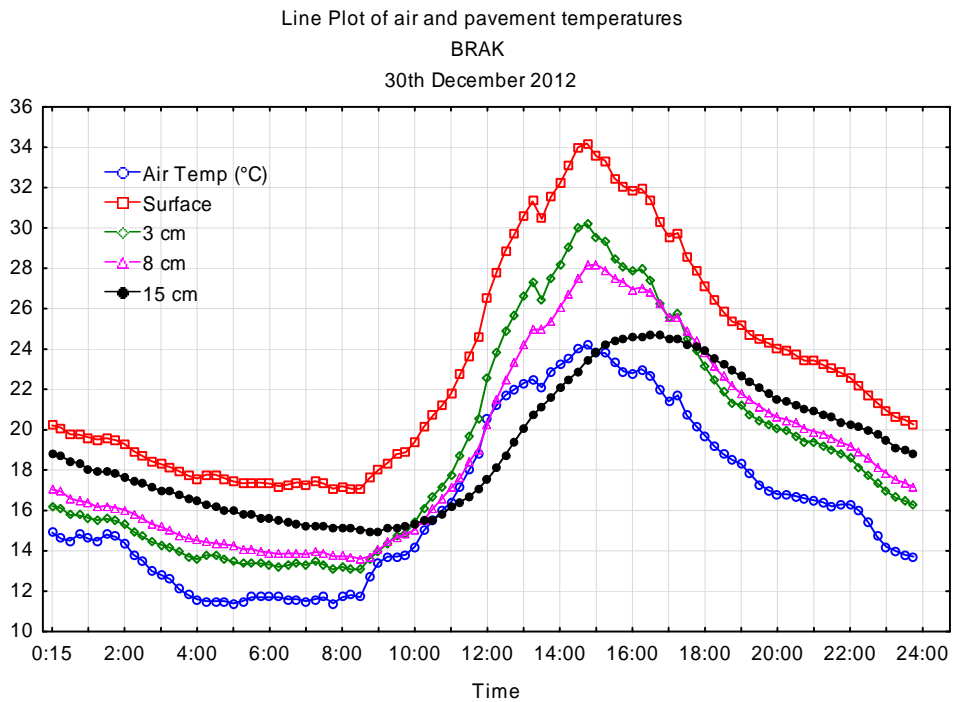


Figure 4.7 Air and pavement temperatures at four depths at Brak location for December 30, 2012.

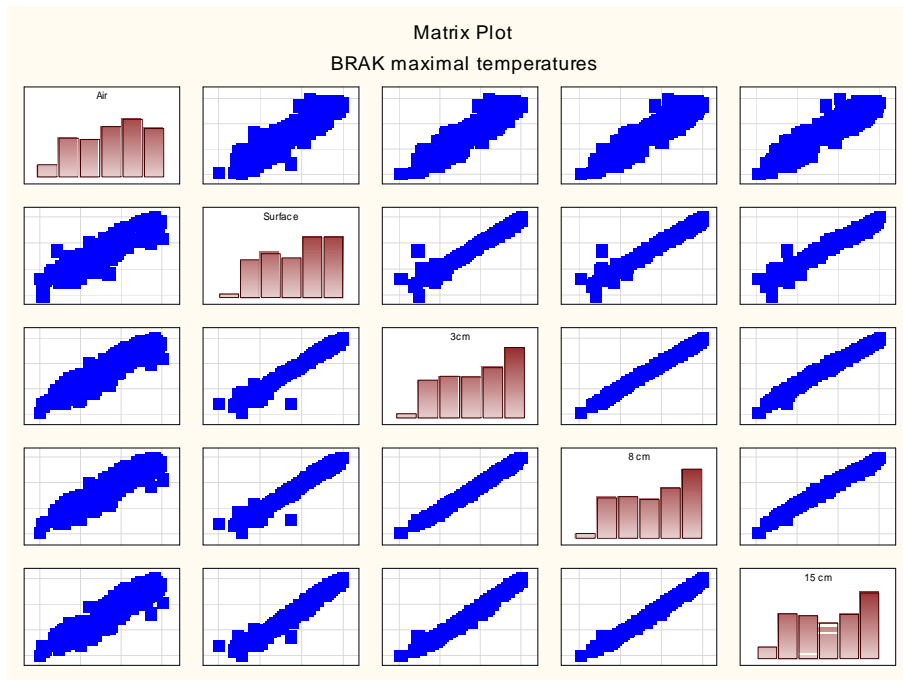


Figure 4.8 Relationship between maximal daily air (abscise) and pavement temperatures (ordinate) at the Brak location

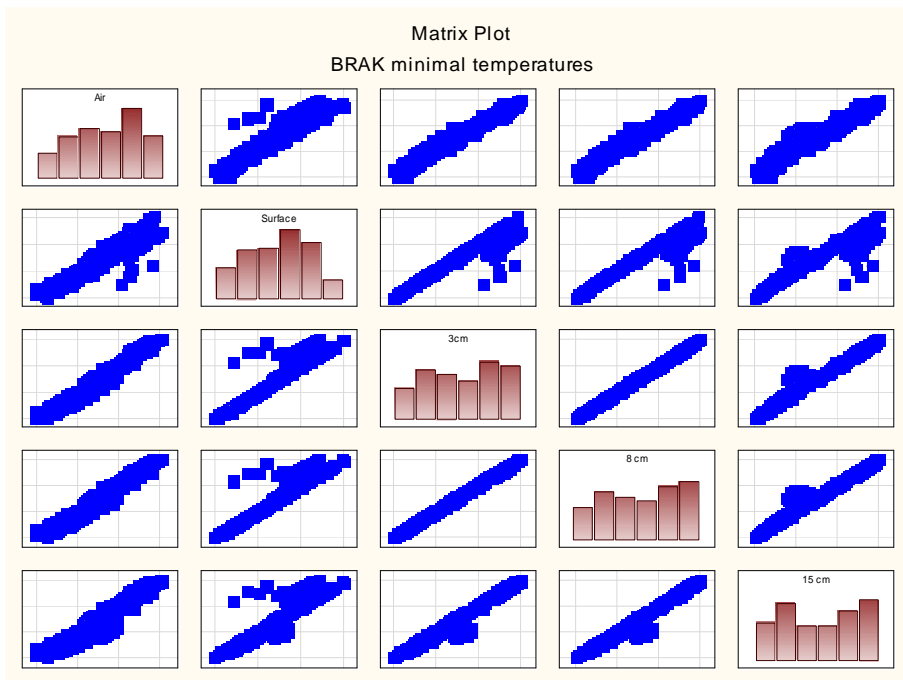


Figure 4.9 Relationship between minimal daily air (abscise) and pavement temperatures (ordinate) at the Brak location

In figures 4.8 and 4.9 the relationships between maximal and minimal daily temperatures at four different layers and maximal and minimal daily air temperatures are presented in a matrix plot. In each matrix, the histograms of the temperatures are presented on the diagonal. In the rows are the scatter plots presenting the relationships between air temperature and pavement temperatures.

These graphs show there exists a linear relation between maximal (minimal) daily air and pavement temperatures. The maximal (minimal) daily pavement temperatures depend linearly on maximal (minimal) daily air temperatures, and also there is a strong linear relationship between maximal (minimal) daily temperatures of the pavement at different layers. For maximal temperatures, there is more variation in the relationship between the air temperature and pavement temperatures than there is for minimal temperatures, suggesting that the model for maximal temperatures should include, besides the air temperature, some other variables. Appendix C presents similar figures for the remaining stations.

### 2.3.1 Cumulative solar radiation calculation

In figures 4.10 and 4.11 solar radiation is presented, together with maximum and minimal daily air and pavement temperatures. Solar radiation values were scaled (divided by 25) in order to be presented on the same graph. It can be seen that the cycle of the solar radiation is similar to the temperature cycle, and that the solar radiation has an effect on air and pavement temperatures.

In order to include solar radiation in the models, for each location the daily cumulative solar radiation was determined, for each day, as a sum of registered solar radiation during the day. Examples for the eight locations are given in table 4.4.

Table 4.4 Cumulative solar radiations at eight locations, at 15<sup>th</sup> of January and 15<sup>th</sup> of June

Locations	Latitude	Cumulative solar radiation W/m <sup>2</sup>	
		15 <sup>th</sup> of January	15 <sup>th</sup> of June
Al Kufrah	24°17'N	15937.3	32060.8
Al Qatrun	24°56'N	19151.9	25845.9
Ghat	24°59'N	19151.3	29097.9
Awbari	26°46'N	19151.3	29097.9
Brach(SEBHA)	27°31'N	13970.8	33031.5
Hun-joufra	29°02'N	16938.5	32293.9
Awjilah	29°08'N	10108.8	30236.8
hudamis	30°11'N	15756.2	25299.2



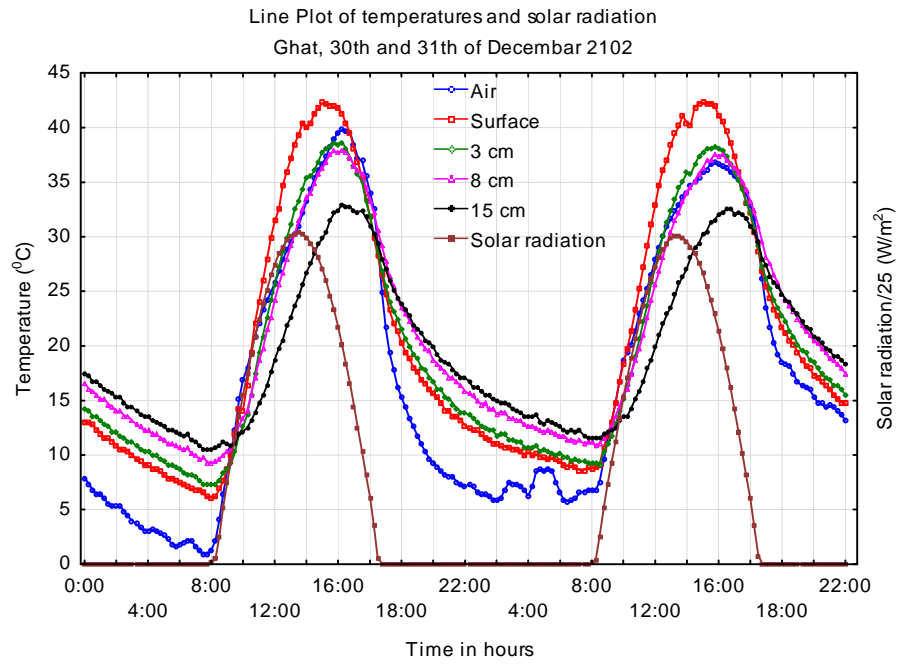


Figure 4.10 Air, pavement temperatures and solar radiation at Ghat on 30<sup>th</sup> and 31<sup>st</sup> of December 2012.

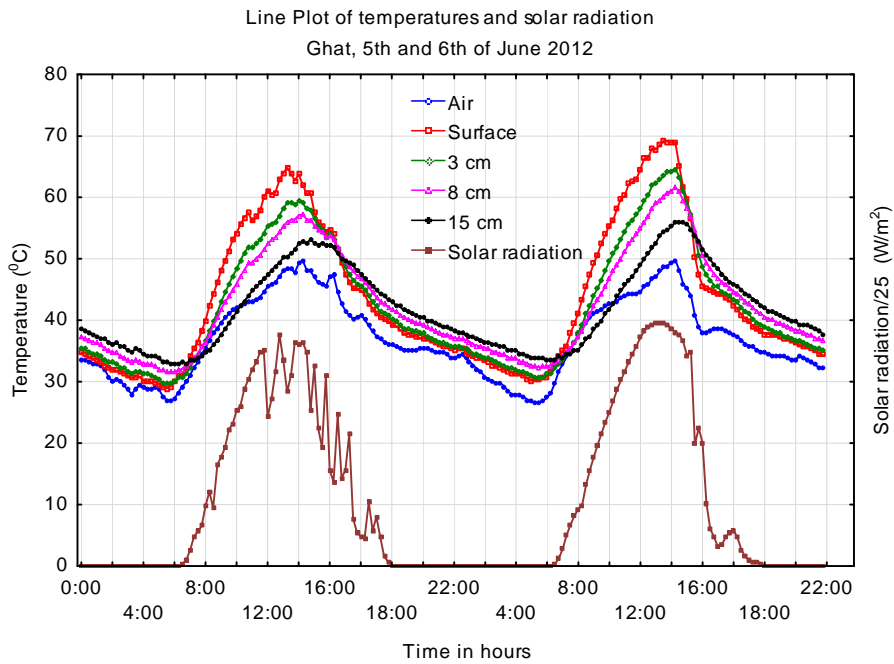


Figure 4.11 Air, pavement temperatures and solar radiation at the Ghat location 5<sup>th</sup> and 6<sup>th</sup> June 2012.

In figure 4.12, the cumulative solar radiation at the Ghat location during one year is presented.

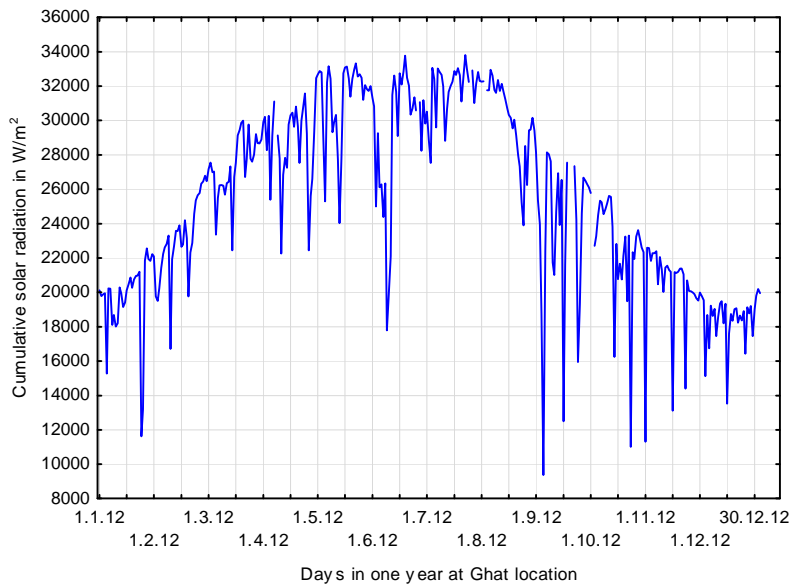


Figure 4.12 Cumulative solar radiations at the Ghat location during one year

#### 4.4 Pavement temperature prediction

Two groups of models were made for predicting maximal and minimal daily pavement temperatures at four different layers.

The first one incorporates the air temperature, day of the year, wind speed and solar radiation, as predictors, and daily pavement temperatures at four layers (surface (C1), 3 cm (C2), 8 cm (C3), and 15 cm (C4)), as response. We start with air temperature, and add other variables one by one, forming a series of models. With each combination of variables, we include the latitude in the model, using the data from all locations.

The second group of models incorporates temperature of the surface of the pavement (C1), day of the year, wind speed and solar radiation as predictors, and daily pavement temperatures at three layers: 3 cm (C2), 8 cm (C3), and 15 cm (C4), as response. We start with the temperature of the surface of the pavement (C1) and add the rest of the variables one by one, forming a series of models. With each combination of the variables, we include the latitude in the model, using the data from all locations.

As measures of the accuracy of predictions overall measure, of how well the model fits the data, we use adjusted coefficient of determination  $R^2$ , and standard error of estimate.

$R^2$  is a statistical measure of how close the data are to the fitted regression line. It is also known as the coefficient of determination, or the coefficient of multiple determination for multiple

regression. The definition of  $R^2$  is fairly straight-forward; it is the percentage of the response variable variation that is explained by a linear model.

The adjusted  $R^2$  compares the explanatory power of regression models that contain different numbers of predictors. The adjusted  $R^2$  is a modified version of  $R^2$  that has been adjusted for the number of predictors in the model. The adjusted  $R^2$  increases only if the new term improves the model more than would be expected by chance and it can also decrease with poor quality predictors.. It decreases when a predictor improves the model by less than expected by chance. The adjusted  $R^2$  can be negative, but it's usually not. It is always lower than the  $R^2$ .

Standard error of estimate represents the average distance that the observed values fall from the regression line. Conveniently, it tells how wrong the regression model is on average using the units of the response variable. Smaller values are better because it indicates that the observations are closer to the fitted line.

The regression models for predicting maximum and minimal daily pavement temperatures were developed using statistical package Statistica 12 (StatSoft Inc., Tulsa, OK, USA), university license for Novi Sad University.

## **4.5 Linear modeling for daily pavement temperature prediction incorporating air temperature**

### **4.5.1 Relationship with the air temperature**

The first model to predict daily maximal or minimal daily pavement temperatures is a simple linear regression relationship between the maximal or minimal daily air temperature and the maximal or minimal daily pavement temperature at different distances (depths) from the surface. The model is of the following form:

$$y = A * Air + B$$

where

$y$ = predicted daily pavement temperature ( $^{\circ}\text{C}$ ) (maximum or minimum);

$A$  = air temperature coefficient ;

$Air$ = daily air temperature ( $^{\circ}\text{C}$ ) (maximum or minimum); and

$B$  = intercept coefficient.

Table 4.5 presents the coefficients for the linear prediction models developed for four depths from the surface at the Al-Jufroh station. Included with the model coefficients and their standard errors are the standard errors of estimate and the adjusted coefficient of determination  $R^2$ . The coefficients statistically different from zero are denoted in red. Tables of coefficients for the pavement temperature for the remaining stations are presented in Appendix D.

Table 4.5 Parameters of the model for predicting daily pavement temperature from daily air temperature at the Al-Jufroh location

<b>Al-Jufroh</b>	<b>Maximal daily temperatures <math>y = A * Air_{max} + B</math></b>					
<b>depth</b>	B	Std.Err. of B	A	Std.Err. of A	Adjusted R <sup>2</sup>	Std.Error of estimate
C1	-1,28107	1,145059	1,42656	0,031089	0,85254646	4,5904
C2	-1,84082	1,014539	1,31362	0,027545	0,86197995	4,0672
C3	-0.704899	1.035144	1.204208	0.028105	0.83446278	4.1497
C4	-1,20210	0,936827	1,18329	0,025435	0,85597026	3,7556
	<b>Minimal daily temperatures <math>y = A * Air_{min} + B</math></b>					
C1	2.993632	0.215441	1.028658	0.014089	0.936072602	1.78845
C2	3.262923	0.185374	1.056087	0.012122	0.954229212	1.53885
C3	5.675779	0.276623	1.017896	0.018090	0.896863528	2.29634
C4	7.108064	0.214801	0.993578	0.014047	0.932168703	1.78313

Standard error of estimate for maximal daily temperature for C1 layer, equal to 4.59, indicates that the average distance of the data points from the fitted line is about 4.59 °C. Standard error of estimate for minimal daily temperature for C1 layer, equal to 1.788, indicates that the average distance of the data points from the fitted line is about 1.788 °C.

Standard errors of estimate for maximal daily temperature for four layers are higher than standard errors of estimate for minimal temperatures, indicating less variation. Standard errors of estimate for maximal daily temperature are smaller for deeper layers, indicating less variation. Such pattern does not exist for minimal daily pavement temperatures.

Adjusted R<sup>2</sup> are higher for minimal temperatures than for maximal temperatures, indicating better fit to the data.

A graphical example of the linear relationship developed for the Al-Jufroh station is shown in figures 4.13 to 4.16 where the relationship between the maximal daily temperature at different layers is shown versus the maximal daily air temperature. In figures 4.17 to 4.20, the relationship between the minimal daily temperature at different layers is shown versus the minimal daily air temperature. Figures showing those relations for the remaining locations are presented in Appendix D.

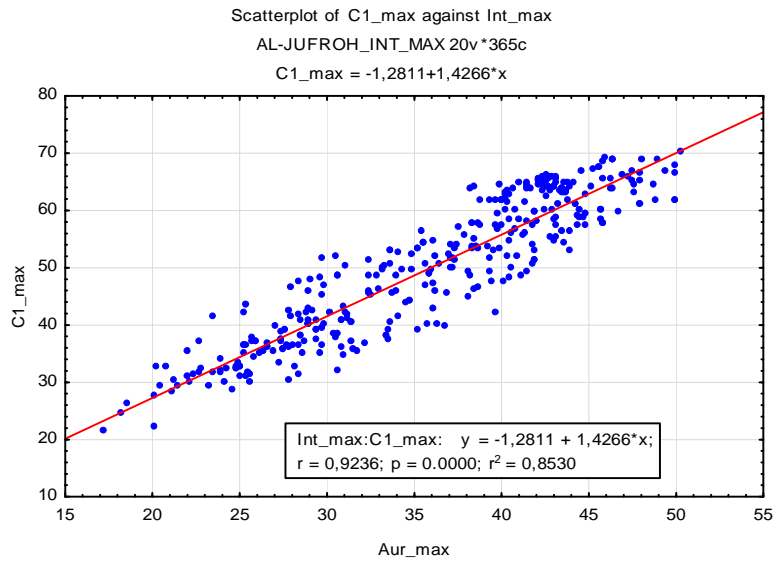


Figure 4.13 Maximal daily temperature at layer C1 versus the maximal daily air temperature at the Al-Jufroh location

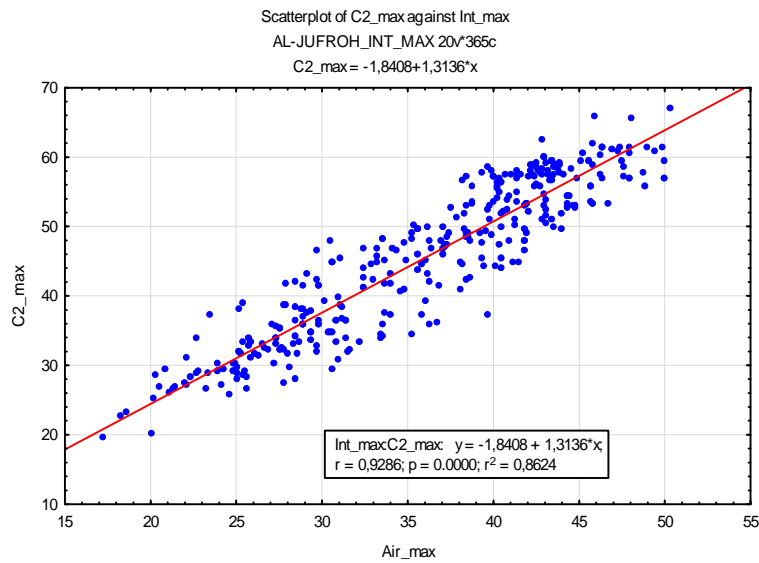


Figure 4.14 Maximal daily temperature at layer C2 versus the maximal daily air temperature at the Al-Jufroh location

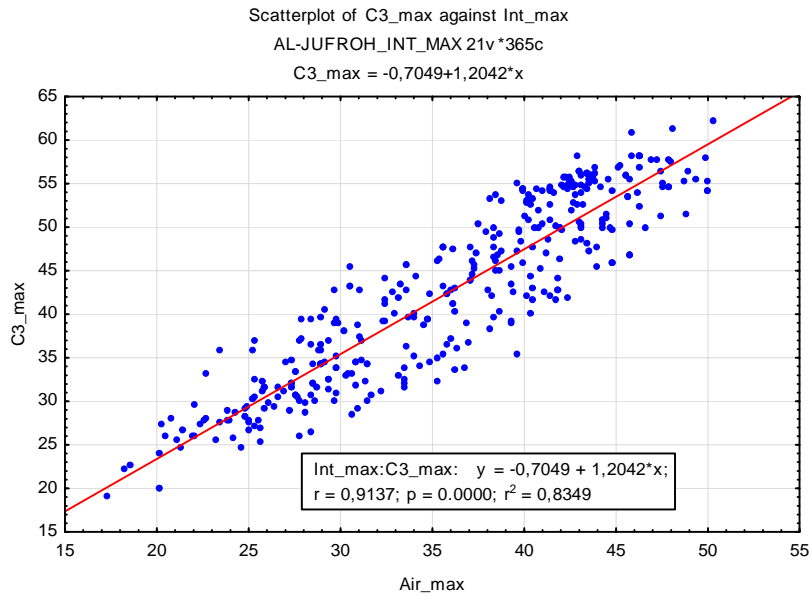


Figure 4.15 Maximal daily temperature at layer C3 versus the maximal daily air temperature at the Al-Jufroh location

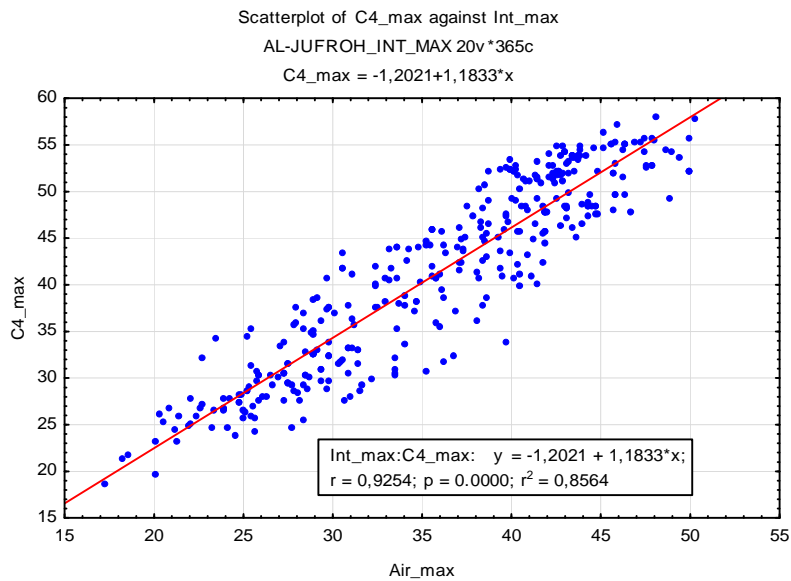


Figure 4.16 Maximal daily temperature at layer C4 versus the maximal daily air temperature at the Al-Jufroh location

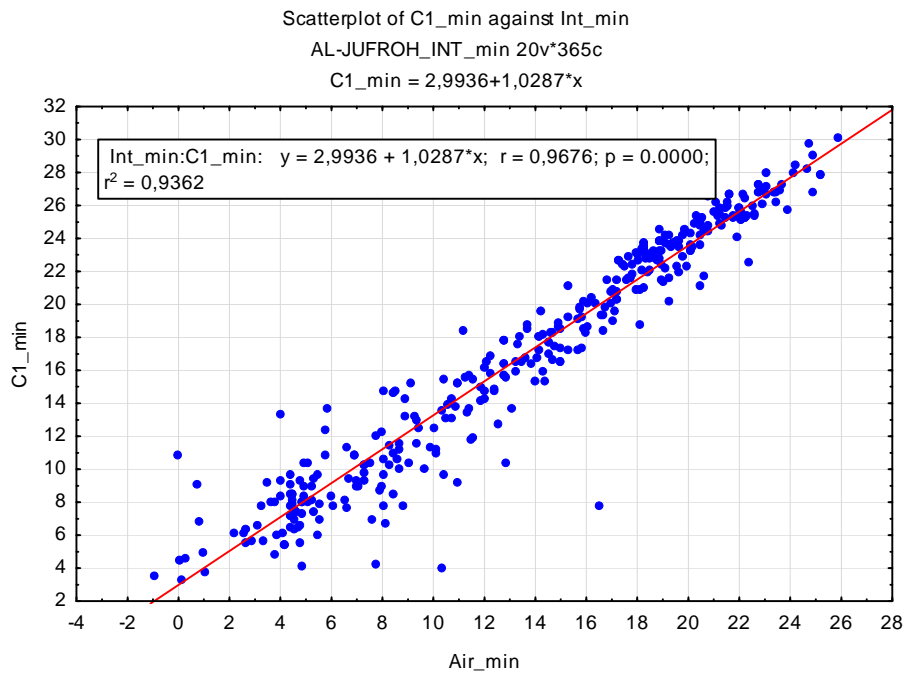


Figure 4.17 Minimal daily temperature at layer C1 versus the minimal daily air temperature at the Al-Jufroh location

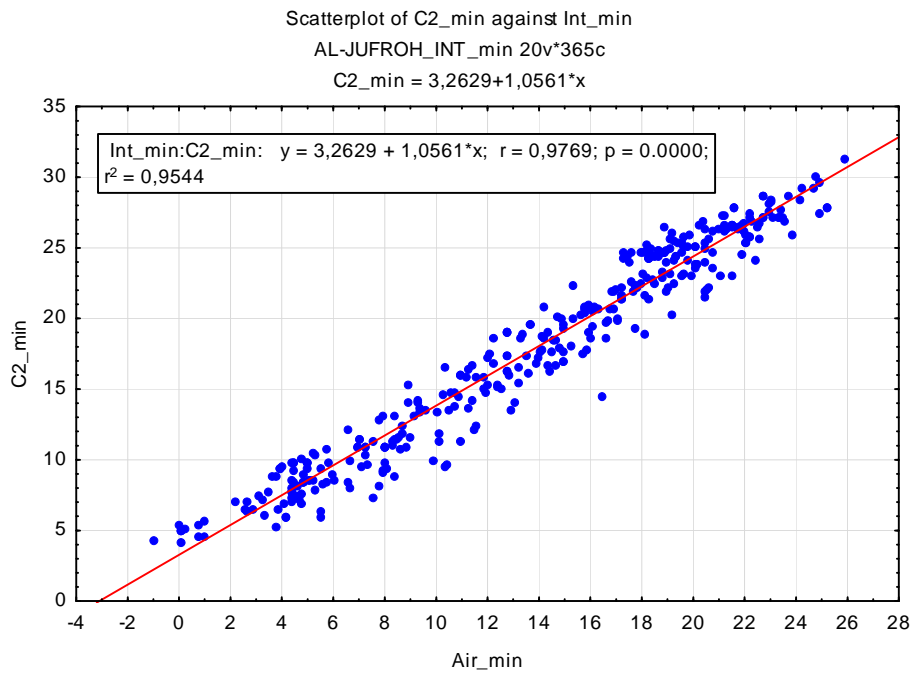


Figure 4.18 Minimal daily temperature at layer C2 versus the minimal daily air temperature at the Al-Jufroh location

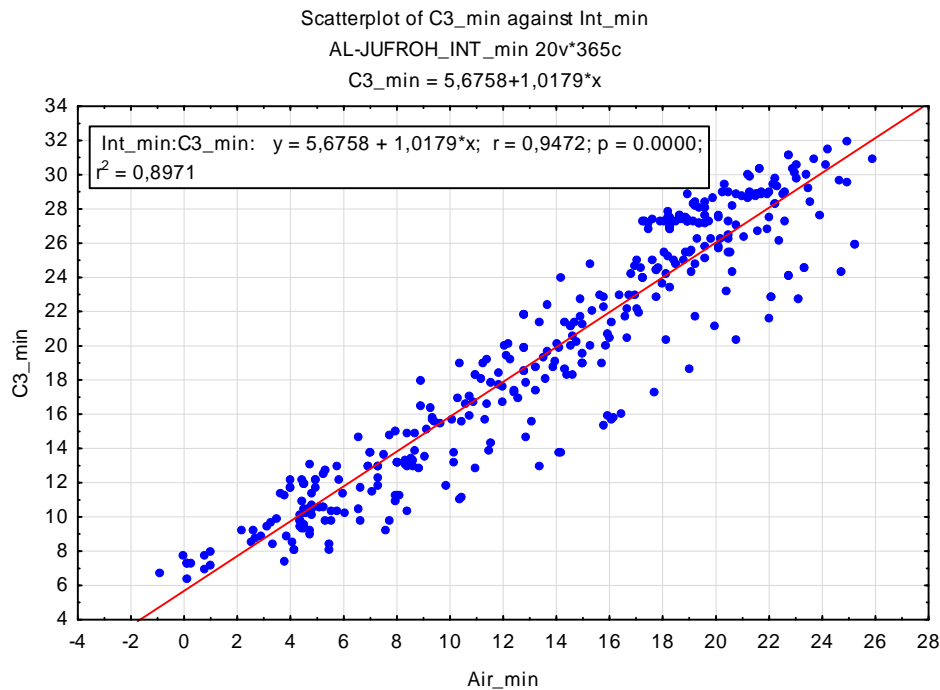


Figure 4.19 Minimal daily temperature at layer C3 versus the minimal daily air temperature at the Al-Jufroh location

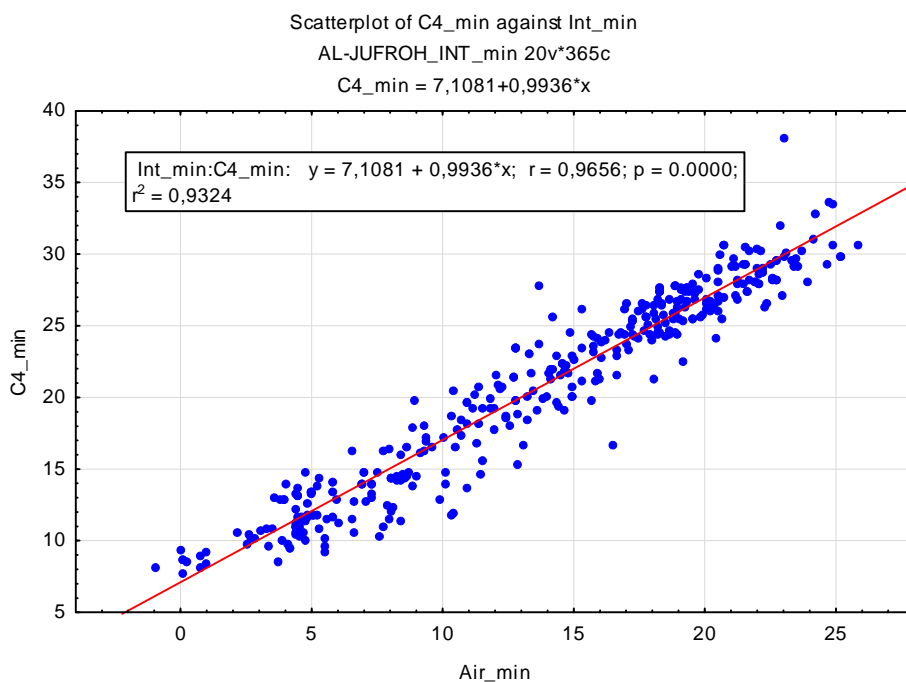


Figure 4.20 Minimal daily temperature at layer C4 versus the minimal daily air temperature at the Al-Jufroh location

The table 4.5, figures 4.13 to 4.20, and tables and figures in Appendix D show that the agreement between the maximal (minimal) daily pavement temperature and maximal (minimal) daily air



temperature in terms of a linear relationship increases with increasing distance from the surface since the standard error of estimate is smaller for deeper layer of pavement. As distance from the surface increases, the slope of the line describing the relationship between the maximal (minimal) daily air temperature and maximal (minimal) daily pavement temperature decreases. It is also noted that the relationship between the measured values is generally better for the minimal daily temperatures than the maximal daily temperatures. This can be seen from the values of adjusted  $R^2$  which are higher for minimal temperatures than for maximal temperatures, as well as from standard errors of estimates, which are lower for minimal temperatures than for maximal temperatures

Standard error of estimate for maximal daily temperatures decrease with the distance from the surface, indicating that there is less variability in the maximal daily temperatures for deeper layers.

Considering maximal daily air temperature coefficient  $A$  in table 4.5, it can be seen the maximal daily pavement temperature at all four layers is higher than maxima daily air temperatures. Considering minimal daily air temperature coefficient  $A$  in table 4.5, it can be seen the minimal daily pavement temperature at all four layers is approximately same as minimal daily air temperatures.

#### ***4.5.1.1 Relationship with the air temperature and latitude***

The next model predicts maximal (minimal) daily pavement temperatures at four different layers from maximal (minimal) daily air temperatures and includes the latitude of the locations. It was build using data from all locations. The model is of the following form:

$$y = A * Air + B * Lat + C$$

where

$y$ = predicted daily pavement temperature ( $^{\circ}\text{C}$ ) (maximal or minimal);

$A$  = air temperature coefficient;

$Air$ = daily air temperature ( $^{\circ}\text{C}$ ) (maximal or minimal);

$B$  = latitude coefficient;

$Lat$  = latitude of the station (degrees); and

$C$  = intercept coefficient.

Table 4.6 Parameters of the model for predicting pavement temperatures when including air temperature and latitude

<b>All locations</b>	<b>Maximal daily temperatures</b> $y = A * Air_{max} + B * Lat + C$					
<b>depth</b>	C	B	A		Adjusted R <sup>2</sup>	Std.Error of estimate
C1	6.726644	-0.170940	1.317137		0.803477712	5.12777219
C2	-1.18177	0.01534	1.29681		0.845510632	4.33718244
C3	4.222745	-0.208648	1.237555		0.84010897	4.25591268
C4	-1.52011	-0.04626	1.16772		0.812725747	4.39406426
	<b>Minimal daily temperatures</b> $y = A * Air_{min} + B * Lat + C$					
C1	1.670400	0.087764	0.953374		0.89188359	2.51980491
C2	9.812420	-0.205259	0.979869		0.963631337	1.45078374
C3	13.77512	-0.28955	0.97823		0.921314305	2.184078
C4	14.59235	-0.25946	0.96863		0.90469115	2.3997062

Standard errors of estimates for these models are higher than corresponding standard error of estimate for models without the latitude. This can be explained by the fact that the data from all eight stations are included, and therefore there is more variability in data - the observations are less close to regression line.

Table 4.7 Latitudes and longitudes of the stations

<b>Locations</b>	<b>Latitude</b>		<b>Longitude</b>
Al Kufrah	24°17'N	24,28333	23°15'E
Al Qatrun	24°56'N	24,93333	15°03'E
Ghat	24°59'N	24,98333	10°11'E
Awbari	26°46'N	26,76667	12°57'E
Brach(SEBHA)	27°31'N	27,51667	14°20'E
Hun-joufra	29°02'N	29,03333	16°00'E
Awjilah	29°08'N	29,13333	21°07'E
Ghadamis	30°11'N	30,18333	09°29'E

A graphical example of the linear relationship developed is shown in figure 4.21 where the relationship between the surface daily maximal temperature is shown versus different distances from the surface and the daily maximal air temperature. In figure 4.22 the relationship between the surface daily minimal temperatures are shown versus different layers and the daily minimal air temperature.

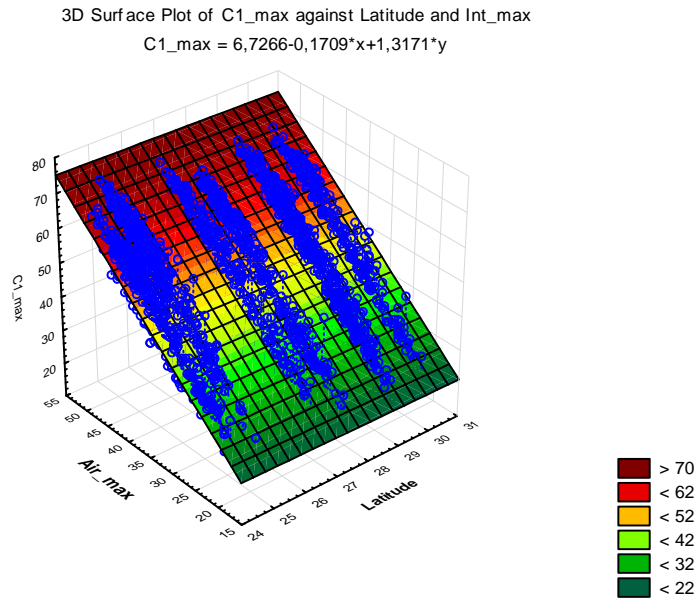


Figure 4.21 Maximal daily C1 temperatures for all locations as a function of maximum daily air temperature and latitude

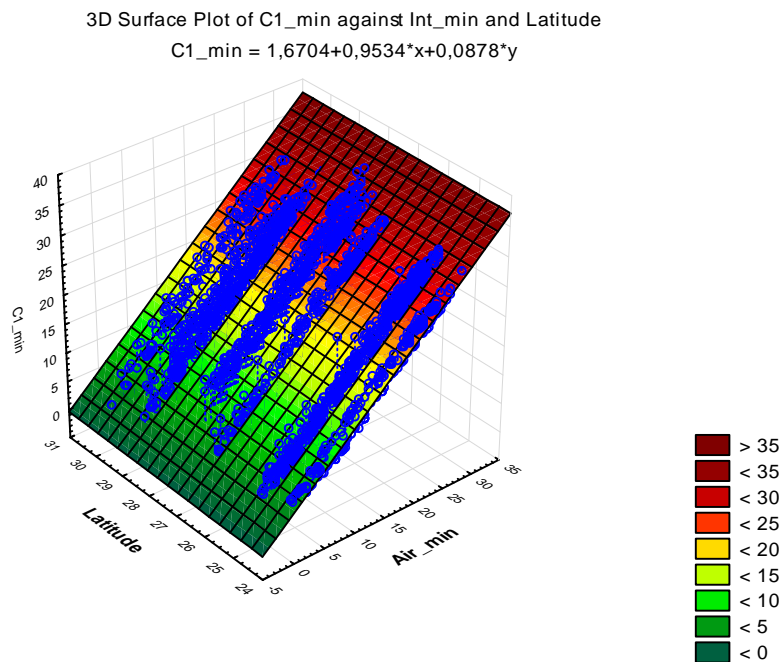


Figure 4.22 Minimal daily C1 temperatures for all locations as a function of maximum daily air temperature and latitude

In Appendix D the figures for the remaining layers are presented. The tables and figures for this model show that the agreement between maximal (minimal) pavement temperatures at all four

layers and maximal (minimal) air temperature in terms of a linear relationship. It is also noted that the relationship between the measured values is generally better for the minimal daily temperatures than the maximal daily temperatures. This can be seen from the values of adjusted  $R^2$  and standard errors of estimates, which are higher for minimal daily temperatures than maximal daily temperatures.

Furthermore, since the most of the coefficients of the latitude are negative, maximal (minimal) daily pavement temperatures decrease, as latitude increases,

#### 4.5.2 Relationship with air temperature and day of the year

The next model for predicting maximal (minimal) daily pavement temperatures at different distances includes maximal (minimal) daily air temperatures and the day of the year. The days of the year are coded from 0, for the first of January, to 365, for December 31st. (leap year) As it is presented in figures 4.23 and 4.24, there exists a nonlinear relation between maximal (minimal) daily temperatures with the day of the year, the square of the day of the year will be included in the model.

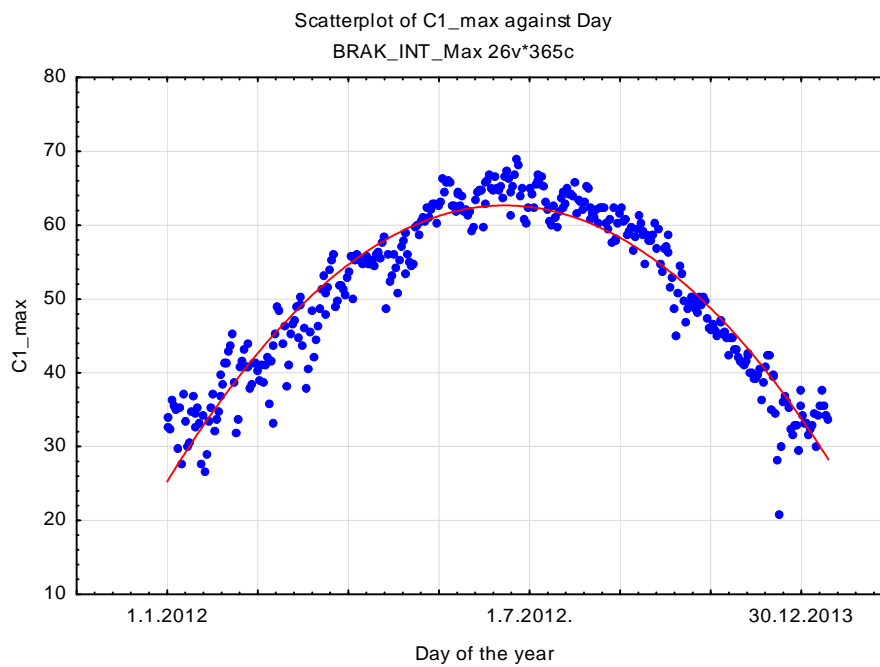


Figure 4.23 C1 maximal daily temperature as a function of the day of the year for the Brak station

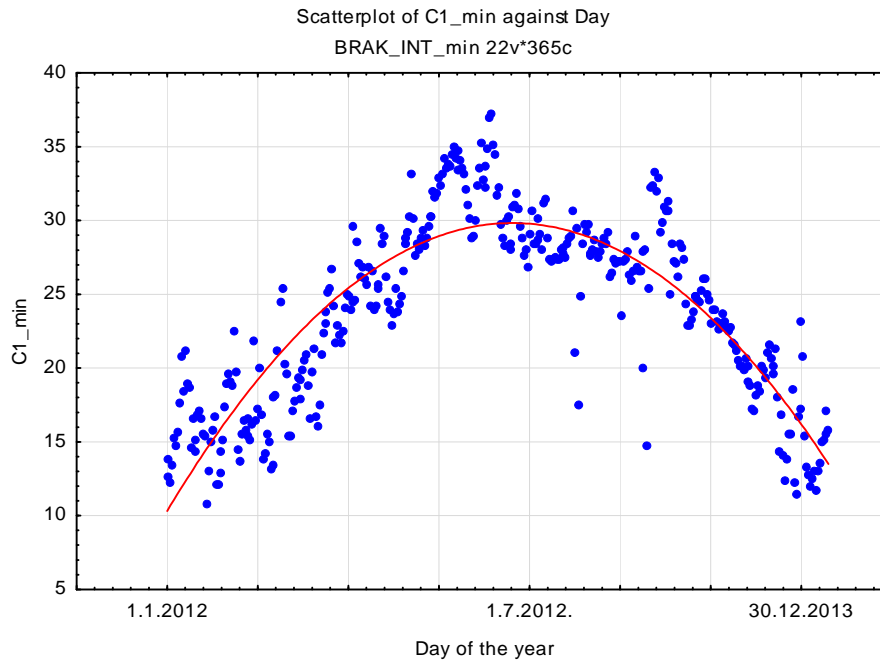


Figure 4.24 C1 minimal daily temperature as a function of the day of the year for the Brak station

Tables 4.8 to 4.11 give the characteristics of the models for maximal daily pavement temperatures for four layers at the Brak location, where the model is of the form:

$$y_{max} = A * Air_{max} + B * Day + C * Day^2 + D$$

where

$y_{max}$  = predicted maximal daily temperature for four depths of the pavement (°C);

$A$  = air temperature coefficient;

$Air_{max}$  = maximal daily air temperature (°C);

$B$  = coefficient for the day of the year;

$Day$  = day of the year;

$C$  = coefficient for the square of the day of the year;

$D$  = intercept coefficient.

In table 4.8, in the column denoted by b the regression coefficients of the model are given. So, intercept is equal to  $D=3.40893$ . The air temperature coefficient is  $A= 0.62822$ . The coefficient for the day of the year is  $B=0.23666$ . The coefficient for the square of the day of the year is  $C = -0.00065$ .

Table 4.8 Coefficients of the model for predicting maximal daily C1 temperature from maximal daily air temperature and day of the year at the Brak location.

Brak C1_max	Regression Summary for Dependent Variable: C1_max (BRAK_C1_max) R= .97744464 R <sup>2</sup> = .95539803 Adjusted R <sup>2</sup> = .95502738 F(3,361)=2577.6 p<0.0000 Std.Error of estimate: 2.4156					
	b*	Std.Err. of b*	b	Std.Err. of b	t(361)	p-value
Intercept			13.40893	0.686521	19.5317	0.00
Air_max	0.44810	0.021658	0.62822	0.030364	20.6899	0.00
Day	2.19731	0.086222	0.23666	0.009287	25.4842	0.00
Day <sup>2</sup>	-2.27299	0.084986	-0.00065	0.000024	-26.7456	0.00

$$y_{max} = 0.62822 * Air_{max} + 0.23666 * Day - 0.00065 * Day^2 + 13.40893$$

Legend:

b\* - standardized regression coefficient;

Std.Err.of b\* - Standard error of b\*;

b - regression coefficient;

Std.Err. of b - Standard error of b;

t(361) – value of test statistics for regression coefficient;

p-value - the probability of obtaining a value of test statistic at least as extreme as the one that was actually observed, assuming that the null hypothesis that regression coefficient is zero is true.

In the tables are presented standardized coefficients b\* and their standard errors. It means that first all variables were standardized so to have mean value zero and standard deviation 1, after that regression coefficients b\* were determined. One can use standardized coefficients in the equation to compare the effect of independent variables to the dependent variable.

Table 4.9 Characteristics of the model for predicting maximal daily C2 temperature from maximal daily air temperature and day of the year at the Brak location

Brak C2_max	Regression Summary for Dependent Variable: C2_max (BRAK_C1_max) R= .98036557 R <sup>2</sup> = .96111665 Adjusted R <sup>2</sup> = .96079352 F(3,361)=2974.4 p<0.0000 Std.Error of estimate: 2.3112					
	b*	Std.Err. of b*	b	Std.Err. of b	t(361)	p-value
Intercept			7.188584	0.656843	10.9441	0.000000
Air_max	0.49468	0.020222	0.710666	0.029051	24.4627	0.000000
Day	2.04180	0.080505	0.225349	0.008885	25.3623	0.000000
Day <sup>2</sup>	-2.09579	0.079351	-0.000613	0.000023	-26.4118	0.000000

$$y_{max} = 0.710666 * Air_{max} + 0.225349 * Day - 0.000613 * Day^2 + 7.188584$$

Table 4.10 Characteristics of the model for predicting maximal daily C3 temperature from maximal daily air temperature and day of the year at the Brak location

Brak C3_max	Regression Summary for Dependent Variable: C3_max (BRAK_C1_max) R= .98120351 R <sup>2</sup> = .96276034 Adjusted R <sup>2</sup> = .96245087 F(3,361)=3111.0 p<0.0000 Std.Error of estimate: 2.2046					
	b*	Std.Err. of b*	b	Std.Err. of b	t(361)	p-value
Intercept			6.005975	0.626556	9.5857	0.000000
Air_max	0.49029	0.019790	0.686538	0.027711	24.7745	0.000000
Day	2.06739	0.078786	0.222403	0.008476	26.2407	0.000000
Day <sup>2</sup>	-2.11272	0.077655	-0.000603	0.000022	-27.2063	0.000000

$$y_{max} = 0.686538 * Air_{max} + 0.222403 * Day - 0.000603 * Day^2 + 6.005975$$

Table 4.11 Characteristics of the model for predicting maximal daily C4 temperature from maximal daily air temperature and day of the year at the Brak location

Brak C4_max	Regression Summary for Dependent Variable: C4_max (BRAK_C1_max) R= .98054216 R <sup>2</sup> = .96146292 Adjusted R <sup>2</sup> = .96114267 F(3,361)=3002.2 p<0.0000 Std.Error of estimate: 2.0673					
	b*	Std.Err. of b*	b	Std.Err. of b	t(361)	p-value
Intercept			4.639623	0.587529	7.8968	0.000000
Air_max	0.47196	0.020132	0.609187	0.025985	23.4435	0.000000
Day	2.14345	0.080146	0.212552	0.007948	26.7442	0.000000
Day <sup>2</sup>	-2.17524	0.078997	-0.000572	0.000021	-27.5359	0.000000

$$y_{max} = 0.609187 * Air_{max} + 0.212552 * Day - 0.000572 * Day^2 + 4.639623$$

In figure 4.25 the relationship between the surface daily maximal temperatures are shown versus day of the year and the daily maximal air temperature.

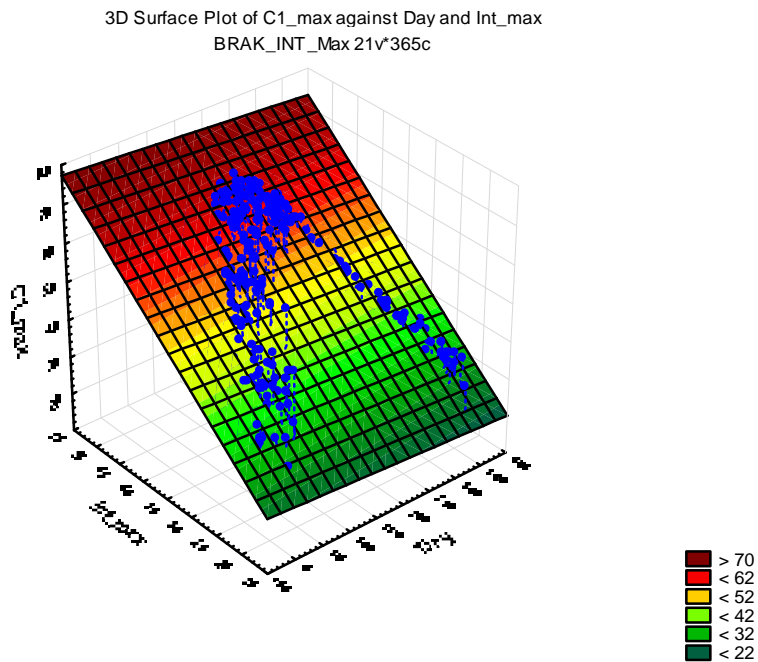


Figure 4.25 Maximal daily C1 temperature as a function of maximal daily air temperature and the day of the year for the Brak station

Tables 4.12 to 4.15 give the characteristics of the models for daily minimum temperatures at the Brak location, where the model is of the form:

$$y_{min} = A * Air_{min} + B * Day + C * Day^2 + D$$

where

$y_{min}$  = predicted minimal daily temperature for four depths of the pavement (°C);

$A$  = air temperature coefficient;

$Air_{min}$  = minimal daily air temperature (°C);

$B$  = coefficient for the day of the year;

$Day$  = day of the year;

$C$  = coefficient for the square of the day of the year;

$D$  = intercept coefficient.



Table 4.12 Characteristics of the model for predicting minimal daily C1 temperature from minimal daily air temperature and day of the year at the Brak location

<b>Brak C1_min</b>	Regression Summary for Dependent Variable: C1_min (BRAK_Air_min) R= .94704362 R <sup>2</sup> = .89689161 Adjusted R <sup>2</sup> = .89603475 F(3,361)=1046.7 p<0.0000 Std.Error of estimate: 2.0201					
	b*	Std.Err. of b*	b	Std.Err. of b	t(361)	p-value
Intercept			9.216318	0.319654	28.83215	0.000000
Air_min	0.71332	0.032338	0.627141	0.028431	22.05836	0.000000
Day	1.03322	0.128854	0.061208	0.007633	8.01851	0.000000
Day <sup>2</sup>	-1.07996	0.125654	-0.000170	0.000020	-8.59470	0.000000

$$y_{min} = 0.627141 * Air_{min} + 0.061208 * Day - 0.000170 * Day^2 + 9.216318$$

Table 4.13 Characteristics of the model for predicting minimal daily C2 temperature from minimal daily air temperature and day of the year at the Brak location

<b>Brak C2_min</b>	Regression Summary for Dependent Variable: C2_min (BRAK_Air_min) R= .99126313 R <sup>2</sup> = .98260259 Adjusted R <sup>2</sup> = .98245802 F(3,361)=6796.4 p<0.0000 Std.Error of estimate: .99175					
	b*	Std.Err. of b*	b	Std.Err. of b	t(361)	p-value
Intercept			2.544214	0.156933	16.2121	0.00
Air_min	0.776403	0.013283	0.815841	0.013958	58.4495	0.00
Day	0.965883	0.052929	0.068388	0.003748	18.2487	0.00
Day <sup>2</sup>	-0.955165	0.051614	-0.000179	0.000010	-18.5058	0.00

$$y_{min} = 0.815841 * Air_{min} + 0.068388 * Day - 0.000179 * Day^2 + 2.544214$$

Table 4.14 Characteristics of the model for predicting minimal daily C3 temperature from minimal daily air temperature and day of the year at the Brak location

<b>Brak C3_min</b>	Regression Summary for Dependent Variable: C3_min (BRAK_Air_min) R= .99079541 R <sup>2</sup> = .98167554 Adjusted R <sup>2</sup> = .98152326 F(3,361)=6446.5 p<0.0000 Std.Error of estimate: 1.0362					
	b*	Std.Err. of b*	b	Std.Err. of b	t(361)	p-value
Intercept			3.116924	0.163964	19.0098	0.00
Air_min	0.75142	0.013633	0.803832	0.014583	55.1195	0.00
Day	1.07127	0.054321	0.077218	0.003915	19.7211	0.00
Day <sup>2</sup>	-1.06163	0.052972	-0.000203	0.000010	-20.0415	0.00

$$y_{min} = 0.803832 * Air_{min} + 0.077218 * Day - 0.000203 * Day^2 + 3.116924$$

Table 4.15 Characteristics of the model for predicting minimal daily C4 temperature from minimal daily air temperature and day of the year at the Brak location

Brak C4_min	Regression Summary for Dependent Variable: C4_min (BRAK_Air_min) R= .97526875 R <sup>2</sup> = .95114913 Adjusted R <sup>2</sup> = .95074317 F(3,361)=2342.9 p<0.0000 Std.Error of estimate: 1.7882					
	b*	Std.Err. of b*	b	Std.Err. of b	t(361)	p-value
Intercept			4.682006	0.282968	16.5461	0.00
Air_min	0.67299	0.022259	0.760949	0.025168	30.2348	0.00
Day	1.33007	0.088692	0.101335	0.006757	14.9964	0.00
Day <sup>2</sup>	-1.35471	0.086490	-0.000274	0.000017	-15.6632	0.00

$$y_{min} = 0.760949 * Air_{min} + 0.101335 * Day - 0.000274 * Day^2 + 4.682006$$

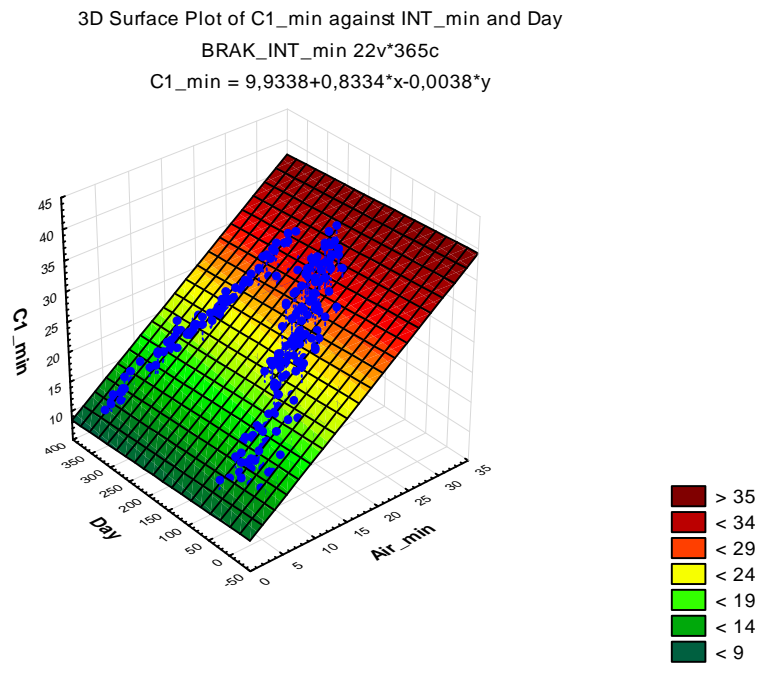


Figure 4.26 Minimal daily C1 temperature as a function of minimal daily air temperature and the day of the year for the Brak station

Appendix E presents the tables and figures of the models for predicting maximal (minimal) daily pavement temperatures at different depths depending on maximal (minimal) daily air temperatures and the day of the year for the remaining locations.

From the tables in Appendix E for the models for predicting maximal (minimal) daily pavement temperatures at different depths depending on maximal (minimal) daily air temperatures, and the day of the year, it can be seen that the air temperature coefficients are lower compared to the coefficients in the models which did not include the day of the year. This means that the day of the year has an effect on the temperatures of the pavement. Also, adjusted  $R^2$  are higher for the models, which include the day of the year, especially for maximal daily temperatures. The standard errors of the models both for maximal and minimal daily temperatures are lower compared to the models which did not include the day of the year. This means that the models with the day of the year better explain maximal and minimal daily temperatures of the pavement at all four layers than the models including only the air temperature.

Standard error of estimate for maximal daily temperatures decrease with the distance from the surface, indicating that there is less variability in the maximal daily temperatures for deeper layers.

#### ***4.5.2.1 Relationship with air temperature, day of the year and latitude***

The next model for predicting maximal (minimal) daily pavement temperatures at different distance from maximal (minimal) daily air temperatures and the day of the year was built using data from all stations and included the latitude of the locations.

The model for daily maximal temperatures is of the following form:

$$y_{max} = A * Air_{max} + B * Day + C * Day^2 + D * Lat + E$$

where

$y_{max}$  = predicted maximal daily temperature for four depths of the pavement (°C);

$A$  = air temperature coefficient;

$Air_{max}$  = maximal daily air temperature (°C);

$B$  = coefficient for the day of the year;

$Day$  = day of the year;

$C$  = coefficient for the square of the day of the year;

$D$  = latitude coefficient;

$Lat$  = latitude of the location (degrees); and

$E$  = intercept coefficient.

Tables 4.16 to 4.19 give the characteristics of the models for maximal daily pavement temperatures for four layers for all locations.

Table 4.16 Characteristics of the model for predicting maximal daily C1 temperature from maximal daily air temperature and day of the year for all locations

All locations C1_max	Regression Summary for Dependent Variable: C1_max (Max_all_locations) R= .95874772 R <sup>2</sup> = .91919720 Adjusted R <sup>2</sup> = .91908613 F(4,2910)=8275.9 p<0.0000 Std.Error of estimate: 3.2892					
	b*	Std.Err. of b*	b	Std.Err. of b	t(2911)	p-value
Intercept			24.89776	0.932980	26.6863	0.00
Air_max	0.47839	0.008475	0.70665	0.012519	56.4458	0.00
Day	2.01658	0.033218	0.22056	0.003633	60.7084	0.00
Day <sup>2</sup>	-2.11827	0.033397	-0.00061	0.000010	-63.4272	0.00
Latitude	-0.08727	0.005394	-0.48402	0.029918	-16.1781	0.00

$$y_{max} = 0.70665 * Air_{max} + 0.22056 * Day - 0.00061 * Day^2 - 0.48402 * Lat + 24.89776$$

Table 4.17 Characteristics of the model for predicting maximal daily C2 temperature from maximal daily air temperature and day of the year for all locations

All locations C2_max	Regression Summary for Dependent Variable: C2_max (Max_all_locations) R= .97400806 R <sup>2</sup> = .94869169 Adjusted R <sup>2</sup> = .94862117 F(4,2910)=13451. p<0.0000 Std.Error of estimate: 2.5012					
	b*	Std.Err. of b*	b	Std.Err. of b	t(2911)	p-value
Intercept			15.09352	0.709476	21.2742	0.000000
Air_max	0.52563	0.006754	0.74095	0.009520	77.8302	0.000000
Day	1.93441	0.026470	0.20191	0.002763	73.0805	0.000000
Day <sup>2</sup>	-2.01524	0.026613	-0.00056	0.000007	-75.7252	0.000000
Latitude	-0.05096	0.004298	-0.26971	0.022751	-11.8550	0.000000

$$y_{max} = 0.74095 * Air_{max} + 0.20191 * Day - 0.00056 * Day^2 - 0.2697 * Lat + 15.09352$$

Table 4.18 Characteristics of the model for predicting maximal daily C3 temperature from maximal daily air temperature and day of the year for all locations

All locations C3_max	Regression Summary for Dependent Variable: C3_max (Max_all_locations) R= .96476177 R <sup>2</sup> = .93076527 Adjusted R <sup>2</sup> = .93067007 F(4,2909)=9776.9 p<0.0000 Std.Error of estimate: 2.8025					
	b*	Std.Err. of b*	b	Std.Err. of b	t(2910)	p-value
Intercept			18.94276	0.795015	23.8269	0.00
Air_max	0.54074	0.007845	0.73521	0.010667	68.9251	0.00
Day	1.81295	0.030756	0.18249	0.003096	58.9464	0.00
Day <sup>2</sup>	-1.88885	0.030922	-0.00050	0.000008	-61.0841	0.00
Latitude	-0.09140	0.004994	-0.46665	0.025496	-18.3028	0.00

$$y_{max} = 0.73521 * Air_{max} + 0.18249 * Day - 0.00050 * Day^2 - 0.46665 * Lat + 18.94276$$

Table 4.19 Characteristics of the model for predicting maximal daily C3 temperature from maximal daily air temperature and day of the year for all locations.

All locations C4_max	Regression Summary for Dependent Variable: C4_max (Max_all_locations) R= .95348649 R <sup>2</sup> = .90913648 Adjusted R <sup>2</sup> = .90901159 F(4,2910)=7279.0 p<0.0000 Std.Error of estimate: 3.0628					
	b*	Std.Err. of b*	b	Std.Err. of b	t(2911)	p-value
Intercept			12.66080	0.868776	14.5732	0.000000
Air_max	0.51326	0.008987	0.66576	0.011658	57.1090	0.000000
Day	1.91986	0.035225	0.18439	0.003383	54.5031	0.000000
Day <sup>2</sup>	-1.96552	0.035415	-0.00050	0.000009	-55.4996	0.000000
Latitude	-0.06235	0.005720	-0.30365	0.027860	-10.8994	0.000000

$$y_{max} = 0.66576 * Air_{max} + 0.18439 * Day - 0.00050 * Day^2 - 0.30365 * Lat + 12.66080$$

The model for minimal daily temperatures is of the following form:

$$y_{min} = A * Air_{min} + B * Day + C * Day^2 + D * Lat + E$$

where

$y_{min}$ = predicted minimal daily temperature for four depths of the pavement (°C);

$A$  = air temperature coefficient;

$Air_{min}$  = minimal daily air temperature (°C);

$B$  = coefficient for the day of the year;

$Day$  = day of the year;

$C$  = coefficient for the square of the day of the year;

$Day^2$  = square of the day of the year;  
*D* = latitude coefficient;  
*Lat* = latitude of the location (degrees); and  
*E* = intercept coefficient.

Tables 4.20 to 4.23 give the characteristics of the models for minimal daily pavement temperatures for four layers for all locations.

Table 4.20 Characteristics of the model for predicting minimal daily C1 temperature from minimal daily air temperature and day of the year for all locations

All locations C1_min	Regression Summary for Dependent Variable: C1_min (Min_all_locations) R= .94769674 R <sup>2</sup> = .89812911 Adjusted R <sup>2</sup> = .89798912 F(4,2911)=6416.1 p<0.0000 Std.Error of estimate: 2.4476					
	b*	Std.Err. of b*	b	Std.Err. of b	t(2911)	p-value
Intercept			1.525863	0.605489	2.5201	0.011787
Air_min	0.833175	0.010731	0.840662	0.010827	77.6451	0.000000
Day	0.520239	0.042613	0.037716	0.003089	12.2085	0.000000
Day <sup>2</sup>	-0.543774	0.042417	-0.000105	0.000008	-12.8196	0.000000
Latitude	0.020274	0.005926	0.074524	0.021782	3.4214	0.000632

$$y_{min} = 0.840662 * Air_{min} + 0.037716 * Day - 0.000105 * Day^2 + 0.074524 * Lat + 1.525863$$

Table 4.21 Characteristics of the model for predicting minimal daily C2 temperature from minimal daily air temperature and day of the year for all locations

All locations C2_min	Regression Summary for Dependent Variable: C2_min (Min_all_locations) R= .98756678 R <sup>2</sup> = .97528814 Adjusted R <sup>2</sup> = .97525418 F(4,2911)=28722. p<0.0000 Std.Error of estimate: 1.1967					
	b*	Std.Err. of b*	b	Std.Err. of b	t(2911)	p-value
Intercept			9.203415	0.296041	31.0883	0.00
Air_min	0.815107	0.005285	0.816427	0.005294	154.2286	0.00
Day	0.775277	0.020988	0.055795	0.001510	36.9393	0.00
Day <sup>2</sup>	-0.771101	0.020892	-0.000147	0.000004	-36.9096	0.00
Latitude	-0.061513	0.002919	-0.224462	0.010650	-21.0769	0.00

$$y_{min} = 0.816427 * Air_{min} + 0.055795 * Day - 0.000147 * Day^2 - 0.224462 * Lat + 9.203415$$

Table 4.22 Characteristics of the model for predicting minimal daily C3 temperature from minimal daily air temperature and day of the year for all locations

All locations C3_min	Regression Summary for Dependent Variable: C3_min (Min_all_locations) R= .97156229 R <sup>2</sup> = .94393329 Adjusted R <sup>2</sup> = .94385625 F(4,2911)=12252. p<0.0000 Std.Error of estimate: 1.8449					
	b*	Std.Err. of b*	b	Std.Err. of b	t(2911)	p-value
Intercept			13.08012	0.456386	28.6602	0.00
Air_min	0.72841	0.007961	0.74673	0.008161	91.5016	0.00
Day	1.06663	0.031613	0.07857	0.002329	33.7401	0.00
Day <sup>2</sup>	-1.07666	0.031468	-0.00021	0.000006	-34.2143	0.00
Latitude	-0.08549	0.004396	-0.31927	0.016418	-19.4467	0.00

$$y_{min} = 0.74673 * Air_{min} + 0.07857 * Day - 0.00021 * Day^2 - 0.31927 * Lat + 13.08012$$

Table 4.23 Characteristics of the model for predicting minimal daily C4 temperature from minimal daily air temperature and day of the year for all locations

All locations C4_min	Regression Summary for Dependent Variable: C4_min (Min_all_locations) R= .96461979 R <sup>2</sup> = .93049135 Adjusted R <sup>2</sup> = .93039583 F(4,2911)=9742.2 p<0.0000 Std.Error of estimate: 2.0507					
	b*	Std.Err. of b*	b	Std.Err. of b	t(2911)	p-value
Intercept			13.73368	0.507307	27.0717	0.00
Air_min	0.70401	0.008864	0.72050	0.009071	79.4254	0.00
Day	1.14945	0.035199	0.08452	0.002588	32.6553	0.00
Day <sup>2</sup>	-1.14947	0.035038	-0.00022	0.000007	-32.8064	0.00
Latitude	-0.07741	0.004895	-0.28861	0.018250	-15.8146	0.00

$$y_{min} = 0.72050 * Air_{min} + 0.08452 * Day - 0.00022 * Day^2 - 0.28861 * Lat + 13.73368$$

Most of the coefficients of the latitude are negative, indicating that as latitude increases, pavement temperatures decreases. Compared with the models including only maximal daily air temperature and latitude, the models including the maximal daily air temperature, the day of the year and latitude have higher adjusted R<sup>2</sup> and standard error of estimate, indicating better fit to the data.

### 4.5.3 Relationship with air temperature and wind speed

The next model for predicting maximal (minimal) daily pavement temperatures at different depths included maximal (minimal) daily air temperatures and wind speed.

Tables 4.24 to 4.27 give the characteristics of the models for maximal daily pavement temperatures for four layers at the Awbari location, where the model is of the form:

$$y_{max} = A * Air_{max} + B * WS + C$$

where

$y_{max}$ = predicted maximal daily pavement temperature (°C);

$A$  = air temperature coefficient;

$Air_{max}$ = maximal daily air temperature (°C);

$B$  = coefficient for the wind speed;

$WS$  = wind speed(m/s); and

$C$  = intercept coefficient.

Table 4.24 Characteristics of the model for predicting maximal daily C1 temperature from maximal daily air temperature and the wind speed for the Awbari location

Awbari C1_max	Regression Summary for Dependent Variable: C1_max (AWBARI_C1_max) R= .86686882 R <sup>2</sup> = .75146156 Adjusted R <sup>2</sup> = .75008461 F(2,361)=545.75 p<0.0000 Std.Error of estimate: 5.5627					
	b*	Std.Err. of b*	b	Std.Err. of b	t(361)	p-value
Intercept			5.691504	1.498995	3.79688	0.000172
Air_max	0.870801	0.026570	1.189832	0.036304	32.77425	0.000000
Wind Speed, (m/s)	0.027745	0.026570	0.000987	0.000946	1.04423	0.297080

$$y_{max} = 1.189832 * Air_{max} + 0.000987 * WS + 5.691504$$

Table 4.25 Characteristics of the model for predicting maximal daily C2 temperature from maximal daily air temperature and the wind speed for the Awbari location

Awbari C2_max	Regression Summary for Dependent Variable: C2_max (AWBARI_C1_max) R= .90932612 R <sup>2</sup> = .82687400 Adjusted R <sup>2</sup> = .82591485 F(2,361)=862.09 p<0.0000 Std.Error of estimate: 4.3934					
	b*	Std.Err. of b*	b	Std.Err. of b	t(361)	p-value
Intercept			3.347029	1.183891	2.82714	0.004958
Air_max	0.908650	0.022175	1.174872	0.028672	40.97568	0.000000
Wind Speed, (m/s)	-0.004237	0.022175	-0.000143	0.000747	-0.19106	0.848588

$$y_{max} = 1.174872 * Air_{max} - 0.000143 * WS + 3.347029$$



Table 4.26 Characteristics of the model for predicting maximal daily C3 temperature from maximal daily air temperature and the wind speed for the Awbari location

Awbari C3_max	Regression Summary for Dependent Variable: C3_max (AWBARI_C1_max) R= .91098301 R <sup>2</sup> = .82989005 Adjusted R <sup>2</sup> = .82894761 F(2,361)=880.58 p<0.0000 Std.Error of estimate: 4.3025					
	b*	Std.Err. of b*	b	Std.Err. of b	t(361)	p-value
Intercept			2.342969	1.159398	2.02085	0.044033
Air_max	0.909843	0.021981	1.162244	0.028079	41.39159	0.000000
Wind Speed, (m/s)	-0.007078	0.021981	-0.000235	0.000731	-0.32200	0.747637

$$y_{max} = 1.162244 * Air_{max} - 0.000235 * WS + 2.342969$$

Table 4.27 Characteristics of the model for predicting maximal daily C4 temperature from maximal daily air temperature and the wind speed for the Awbari location

Awbari C4_max	Regression Summary for Dependent Variable: C1_max (AWBARI_C1_max) R= .91166155 R <sup>2</sup> = .83112679 Adjusted R <sup>2</sup> = .83019120 F(2,361)=888.35 p<0.0000 Std.Error of estimate: 3.9029					
	b*	Std.Err. of b*	b	Std.Err. of b	t(361)	p-value
Intercept			-0.851159	1.051738	-0.80929	0.418882
Air_max	0.909075	0.021901	1.057280	0.025472	41.50782	0.000000
Wind Speed, (m/s)	-0.015613	0.021901	-0.000473	0.000663	-0.71289	0.476374

$$y_{max} = 1.057280 * Air_{max} - 0.000473 * WS - 0.851159$$

Tables 4.28 to 4.31 give the characteristics of the models for minimal daily pavement temperatures for four layers at the Awbari location.

The model for minimum temperatures is of the following form:

$$y_{min} = A * Air_{min} + B * WS + C$$

where

$y_{min}$  = predicted minimal daily pavement temperature (°C);

$A$  = air temperature coefficient;

$Air_{min}$  = minimal daily air temperature (°C);

$B$  = coefficient for the wind speed;

$WS$  = wind speed(m/s); and

$C$  = intercept coefficient.

Table 4.28 Characteristics of the model for predicting minimal daily C1 temperature from minimal daily air temperature and wind speed for Awbari location

Awbari C1_min	Regression Summary for Dependent Variable: C1_min (AWBARI_Air_min) R= .97008280 R <sup>2</sup> = .94106065 Adjusted R <sup>2</sup> = .94073411 F(2,361)=2882.0 p<0.0000 Std.Error of estimate: 1.8870					
	b*	Std.Err. of b*	b	Std.Err. of b	t(361)	p-value
Intercept			2.624441	0.231399	11.34164	0.000000
Air_min	0.964115	0.013192	0.997554	0.013650	73.08242	0.000000
Wind Speed, (m/s)	0.022967	0.013192	0.001674	0.000962	1.74092	0.082549

$$y_{min} = 0.997554 * Air_{min} + 0.001674 * WS + 2.624441$$

Table 4.29 Characteristics of the model for predicting minimal daily C2 temperature from minimal daily air temperature and wind speed for the Awbari location

Awbari C2_min	Regression Summary for Dependent Variable: C2_min (AWBARI_Air_min) R= .97879550 R <sup>2</sup> = .95804063 Adjusted R <sup>2</sup> = .95780817 F(2,361)=4121.3 p<0.0000 Std.Error of estimate: 1.5282					
	b*	Std.Err. of b*	b	Std.Err. of b	t(361)	p-value
Intercept			4.685447	0.187394	25.00325	0.000000
Air_min	0.973207	0.011131	0.966484	0.011054	87.43335	0.000000
Wind Speed, (m/s)	0.021573	0.011131	0.001510	0.000779	1.93816	0.053384

$$y_{min} = 0.966484 * Air_{min} + 0.001510 * WS + 4.685447$$

Table 4.30 Characteristics of the model for predicting minimal daily C3 temperature from minimal daily air temperature and wind speed for the Awbari location

Awbari C3_min	Regression Summary for Dependent Variable: C3_min (AWBARI_Air_min) R= .97028617 R <sup>2</sup> = .94145525 Adjusted R <sup>2</sup> = .94113090 F(2,361)=2902.6 p<0.0000 Std.Error of estimate: 1.7667					
	b*	Std.Err. of b*	b	Std.Err. of b	t(361)	p-value
Intercept			7.702494	0.216644	35.55368	0.000000
Air_min	0.975935	0.013148	0.948578	0.012779	74.22724	0.000000
Wind Speed, (m/s)	-0.023812	0.013148	-0.001631	0.000900	-1.81110	0.070957

$$y_{min} = 0.948578 * Air_{min} - 0.001631 * WS + 7.702494$$

Table 4.31 Characteristics of the model for predicting minimal daily C4 temperature from minimal daily air temperature and wind speed for the Awbari location

Awbari C4_min	Regression Summary for Dependent Variable: C4_min (AWBARI_Air_min) R= .96400826 R <sup>2</sup> = .92931193 Adjusted R <sup>2</sup> = .92892031 F(2,361)=2373.0 p<0.0000 Std.Error of estimate: 1.9676					
	b*	Std.Err. of b*	b	Std.Err. of b	t(361)	p-value
Intercept			9.266781	0.241274	38.40766	0.000000
Air_min	0.971125	0.014447	0.956670	0.014232	67.21845	0.000000
Wind Speed, (m/s)	-0.030423	0.014447	-0.002112	0.001003	-2.10578	0.035914

$$y_{min} = 0.956670 * Air_{min} - 0.002112 * WS + 9.266781$$

Appendix F presents the tables and figures of the models for predicting maximal (minimal) daily pavement temperatures at different depths depending on maximal (minimal) daily air temperatures, and wind speed for the remaining stations.

From tables 4.24 to 4.31 and the tables in Appendix F for the models for predicting maximal (minimal) daily pavement temperatures at different depths depending on maximal (minimal) daily air temperatures and wind speed, it can be seen the wind speed coefficients are negative, so as wind speed increases, the pavement temperature decreases. However, these coefficients are small, especially for deeper layers and are usually not statistically significant. Also, it can be seen that the air temperature coefficients are similar to the coefficients in the models which did not include the wind speed. This means that the wind speed has little effect on the temperatures of the pavement. Furthermore, adjusted R<sup>2</sup> are lower for the models which include the wind speed. The standard errors of the models both for maximal and minimal temperatures are similar to the standard errors of the models which did not include wind speed. This means that the models with the wind speed do not better explain maximal and minimal daily temperatures of the pavement than the models including only maximal and minimal daily air temperature.

#### 4.5.3.1 Relationship with air temperature, wind speed, and latitude

The next model for predicting maximal (minimal) daily pavement temperatures at four different layers from maximal (minimal) daily air temperatures and the wind speed was built using data from all locations and included the latitude of the locations.

The model for maximum temperatures is of the following form:

$$y_{max} = A * Air_{max} + B * WS + C * Lat + D$$

where

$y_{max}$  = predicted maximal daily pavement temperature (°C);

$A$  = air temperature coefficient;

$Air_{max}$  = maximal daily air temperature (°C);

$B$  = coefficient for the wind speed (m/s);

$WS$  = wind speed;

$C$  = latitude coefficient;

$Lat$  = latitude of the location (degrees);

$D$  = intercept coefficient.

Tables 4.32 to 4.35 give the characteristics of the models for maximal daily pavement temperatures for four layers.

Table 4.32 Characteristics of the model for predicting maximal daily C1 temperature from maximal daily air temperature and wind speed for all locations

All locations C1_max	Regression Summary for Dependent Variable: C1_max (Max_all_locations) R= .89654196 R <sup>2</sup> = .80378749 Adjusted R <sup>2</sup> = .80358527 F(3,2911)=3975.0 p<0.0000 Std.Error of estimate: 5.1246					
	b*	Std.Err. of b*	b	Std.Err. of b	t(2911)	p-value
Intercept			6.895916	1.387568	4.9698	0.000001
Air_max	0.891351	0.008288	1.316651	0.012242	107.5525	0.000000
Wind Speed, (m/s)	-0.017612	0.008215	-0.001277	0.000596	-2.1438	0.032133
Latitude	-0.031411	0.008291	-0.174221	0.045984	-3.7887	0.000154

$$y_{max} = 1.316651 * Air_{max} - 0.001277 * WS - 0.174221 * Lat + 6.895916$$

Table 4.33 Characteristics of the model for predicting maximal daily C2 temperature from maximal daily air temperature and wind speed for all locations

All locations C2_max	Regression Summary for Dependent Variable: C2_max (Max_all_sites) R= .91973352 R <sup>2</sup> = .84590975 Adjusted R <sup>2</sup> = .84575095 F(3,2911)=5326.8 p<0.0000 Std.Error of estimate: 4.3338					
	b*	Std.Err. of b*	b	Std.Err. of b	t(2911)	p-value
Intercept			-1.02465	1.173446	-0.8732	0.382628
Air_max	0.919642	0.007344	1.29636	0.010353	125.2180	0.000000
Wind Speed, (m/s)	-0.017131	0.007280	-0.00119	0.000504	-2.3531	0.018686
Latitude	0.002323	0.007347	0.01230	0.038888	0.3162	0.751850

$$y_{max} = 1.29636 * Air_{max} - 0.00119 * WS + 0.01230 * Lat - 1.02465$$

Table 4.34 Characteristics of the model for predicting maximal daily C3 temperature from maximal daily air temperature and wind speed for all locations

All locations C3_max	Regression Summary for Dependent Variable: C3_max (Max_all_sites) R= .91676381 R <sup>2</sup> = .84045588 Adjusted R <sup>2</sup> = .84029140 F(3,2910)=5109.8 p<0.0000 Std.Error of estimate: 4.2535					
	b*	Std.Err. of b*	b	Std.Err. of b	t(2910)	p-value
Intercept			4.086301	1.151777	3.5478	0.000395
Air_max	0.910508	0.007474	1.237945	0.010162	121.8208	0.000000
Wind Speed, (m/s)	0.015409	0.007409	0.001028	0.000494	2.0797	0.037641
Latitude	-0.040350	0.007477	-0.205999	0.038173	-5.3965	0.000000

$$y_{max} = 1.237945 * Air_{max} + 0.001028 * WS - 0.205999 * Lat + 4.086301$$

Table 4.35 Characteristics of the model for predicting maximal daily C4 temperature from maximal daily air temperature and wind speed for all locations

All locations C4_max	Regression Summary for Dependent Variable: C4_max (Max_all_sites) R= .90412211 R <sup>2</sup> = .81743679 Adjusted R <sup>2</sup> = .81724865 F(3,2911)=4344.7 p<0.0000 Std.Error of estimate: 4.3407					
	b*	Std.Err. of b*	b	Std.Err. of b	t(2911)	p-value
Intercept			-0.948412	1.175306	-0.8069	0.419762
Air_max	0.898986	0.007994	1.166081	0.010369	112.4558	0.000000
Wind Speed, (m/s)	-0.067739	0.007924	-0.004312	0.000504	-8.5480	0.000000
Latitude	-0.011773	0.007997	-0.057340	0.038950	-1.4721	0.141089

$$y_{max} = 1.166081 * Air_{max} - 0.004312 * WS - 0.057340 * Lat - 0.948412$$

The model for minimum temperatures is of the following form:

$$y_{min} = A * Air_{min} + B * WS + C * Lat + D$$

where

$y_{min}$  = predicted minimal daily pavement temperature (°C);

$A$  = air temperature coefficient;

$Air_{min}$  = minimal daily air temperature (°C);

$B$  = coefficient for the wind speed;

$WS$  = wind speed (m/s);

$C$  = latitude coefficient;

$Lat$  = latitude of the location (degrees); and

$D$  = intercept coefficient.

Tables 4.36 to 4.39 give the characteristics of the models for minimal daily pavement temperatures for four layers.

Table 4.36 Characteristics of the model for predicting minimal daily C1 temperature from minimal daily air temperature and wind speed for all locations

<b>All locations C1_min</b>	Regression Summary for Dependent Variable: C1_min (Min_all_locations) R= .94435930 R <sup>2</sup> = .89181449 Adjusted R <sup>2</sup> = .89170296 F(3,2910)=7996.1 p<0.0000 Std.Error of estimate: 2.5207					
	b*	Std.Err. of b*	b	Std.Err. of b	t(2910)	p-value
Intercept			1.664344	0.619445	2.6868	0.007254
Air_min	0.944903	0.006128	0.953313	0.006183	154.1821	0.000000
Wind Speed, (m/s)	-0.001238	0.006127	-0.000221	0.001095	-0.2021	0.839839
Latitude	0.023991	0.006101	0.088140	0.022415	3.9323	0.000086

$$y_{min} = 0.953313 * Air_{min} - 0.000221 * WS + 0.088140 * Lat + 1.664344$$

Table 4.37 Characteristics of the model for predicting minimal daily C2 temperature from minimal daily air temperature and wind speed for all locations

<b>All locations C2_min</b>	Regression Summary for Dependent Variable: C2_min (Min_all_locations) R= .98168449 R <sup>2</sup> = .96370444 Adjusted R <sup>2</sup> = .96366702 F(3,2910)=25755. p<0.0000 Std.Error of estimate: 1.4494					
	b*	Std.Err. of b*	b	Std.Err. of b	t(2910)	p-value
Intercept			9.792971	0.356196	27.4932	0.000000
Air_min	0.977323	0.003550	0.978881	0.003555	275.3230	0.000000
Wind Speed, (m/s)	0.010242	0.003549	0.001817	0.000630	2.8862	0.003928
Latitude	-0.056108	0.003534	-0.204646	0.012889	-15.8777	0.000000

$$y_{min} = 0.978881 * Air_{min} + 0.001817 * WS - 0.204646 * Lat + 9.792971$$

Table 4.38 Characteristics of the model for predicting minimal daily C3 temperature from minimal daily air temperature and wind speed for all locations

All locations C3_min	Regression Summary for Dependent Variable: C3_min (Min_all_locations) R= .95997377 R <sup>2</sup> = .92154964 Adjusted R <sup>2</sup> = .92146876 F(3,2910)=11395. p<0.0000 Std.Error of estimate: 2.1813					
	b*	Std.Err. of b*	b	Std.Err. of b	t(2910)	p-value
Intercept			13.74768	0.536037	25.6469	0.000000
Air_min	0.952653	0.005219	0.97670	0.005350	182.5444	0.000000
Wind Speed, (m/s)	0.016652	0.005217	0.00302	0.000947	3.1916	0.001430
Latitude	-0.078030	0.005195	-0.29132	0.019396	-15.0194	0.000000

$$y_{min} = 0.97670 * Air_{min} + 0.00302 * WS - 0.29132 * Lat + 13.74768$$

Table 4.39 Characteristics of the model for predicting minimal daily C4 temperature from minimal daily air temperature and wind speed for all locations

All locations C4_min	Regression Summary for Dependent Variable: C4_min (Min_all_locations) R= .95129068 R <sup>2</sup> = .90495397 Adjusted R <sup>2</sup> = .90485598 F(3,2910)=9235.6 p<0.0000 Std.Error of estimate: 2.3964					
	b*	Std.Err. of b*	b	Std.Err. of b	t(2910)	p-value
Intercept			14.55120	0.588906	24.7089	0.000000
Air_min	0.944641	0.005744	0.96666	0.005878	164.4490	0.000000
Wind Speed, (m/s)	0.018792	0.005743	0.00341	0.001041	3.2723	0.001079
Latitude	-0.069249	0.005718	-0.25805	0.021309	-12.1097	0.000000

$$y_{min} = 0.96666 * Air_{min} + 0.00341 * WS - 0.25805 * Lat + 14.55120$$

Most of the coefficients of the latitude are negative, indicating that as latitude increases, minimal daily pavement temperatures decreases. Compared with the models including only minimal daily air temperature and latitude, the models including the minimal daily air temperature, the wind speed, and latitude have very similar adjusted R<sup>2</sup> and standard error of estimate, indicating similar fit to the data.

#### 4.5.4 Relationship with air temperature, and cumulative solar radiation

For each location the daily cumulative solar radiation was determined as a sum of registered solar radiations during the day. Examples of daily cumulative solar radiation for two days - January 15<sup>th</sup> and June 15<sup>th</sup> for the eight locations are given in table 4.40.

Table 4.40 Cumulative solar radiations at eight locations for January 15<sup>th</sup> and June 15<sup>th</sup>

Locations	Latitude	Solar radiation W/m <sup>2</sup>	
		15 <sup>th</sup> of January 2012	15 <sup>th</sup> of June 2012
Al Kufrah	24°17'N	15937.3	32060.8
Al Qatrun	24°56'N	19151.9	25845.9
Ghat	24°59'N	19151.3	29097.9
Awbari	26°46'N	19151.3	29097.9
Brach(SEBHA)	27°31'N	13970.8	33031.5
Hun-joufra	29°02'N	16938.5	32293.9
Awjilah	29°08'N	10108.8	30236.8
hudamis	30°11'N	15756.2	25299.2

The next model for predicting maximal (minimal) daily pavement temperatures at four different layers included maximal (minimal) daily air temperatures and cumulative solar radiation.

Tables 4.41 to 4.44 give the characteristics of the models for daily maximal daily pavement temperatures for four layers at the Awjilah location, where the model is of the form:

$$y_{max} = A * Air_{max} + B * Cum\_SR + C$$

where

$y_{max}$  = predicted maximal daily pavement temperature (°C);

$A$  = air temperature coefficient;

$Air_{max}$  = maximal daily air temperature (°C);

$B$  = coefficient for the cumulative solar radiation;

$Cum\_SR$  = cumulative solar radiation (W/m<sup>2</sup>); and

$C$  = intercept coefficient.

Table 4.41 Characteristics of the model for predicting maximal daily C1 temperature from maximal daily air temperature and cumulative solar radiation for the Awjilah location

Awjilah C1_max	Regression Summary for Dependent Variable: C1_max (AWJILAH_C1_max) R= .95801599 R <sup>2</sup> = .91779463 Adjusted R <sup>2</sup> = .91733793 F(2,360)=2009.6 p<0.0000 Std.Error of estimate: 3.2508					
	b*	Std.Err. of b*	b	Std.Err. of b	t(360)	p-value
Intercept			1.669272	0.780947	2.13750	0.033231
Air_max	0.810979	0.018883	1.138747	0.026515	42.94718	0.000000
Cum_SR	0.218388	0.018883	0.000325	0.000028	11.56524	0.000000

$$y_{max} = 1.138747 * Air_{max} + 0.000325 * Cum\_SR + 1.669272$$



Table 4.42 Characteristics of the model for predicting maximal daily C2 temperature from maximal daily air temperature and cumulative solar radiation for the Awjilah location

Awjilah C2_max	Regression Summary for Dependent Variable: C2_max (AWJILAH_C1_max) R= .95922141 R <sup>2</sup> = .92010572 Adjusted R <sup>2</sup> = .91966186 F(2,360)=2073.0 p<0.0000 Std.Error of estimate: 3.3159					
	b*	Std.Err. of b*	b	Std.Err. of b	t(360)	p-value
Intercept			-3.28738	0.796590	-4.12682	0.000046
Air_max	0.800360	0.018616	1.16281	0.027046	42.99348	0.000000
Cum_SR	0.234109	0.018616	0.00036	0.000029	12.57579	0.000000

$$y_{max} = 1.16281 * Air_{max} + 0.00036 * Cum_{SR} - 3.28738$$

Table 4.43 Characteristics of the model for predicting maximal daily C3 temperature from maximal daily air temperature and cumulative solar radiation for the Awjilah location

Awjilah C3_max	Regression Summary for Dependent Variable: C3_max (AWJILAH_C1_max) R= .95230364 R <sup>2</sup> = .90688222 Adjusted R <sup>2</sup> = .90636490 F(2,360)=1753.0 p<0.0000 Std.Error of estimate: 3.1942					
	b*	Std.Err. of b*	b	Std.Err. of b	t(360)	p-value
Intercept			-0.982305	0.767348	-1.28013	0.201324
Air_max	0.786105	0.020097	1.019067	0.026053	39.11462	0.000000
Cum_SR	0.243539	0.020097	0.000334	0.000028	12.11788	0.000000

$$y_{max} = 1.019067 * Air_{max} + 0.000334 * Cum_{SR} - 0.982305$$

Table 4.44 Characteristics of the model for predicting maximal daily C4 temperature from maximal daily air temperature and cumulative solar radiation for the Awjilah location

Awjilah C4_max	Regression Summary for Dependent Variable: C4_max (AWJILAH_C1_max) R= .95648216 R <sup>2</sup> = .91485813 Adjusted R <sup>2</sup> = .91438512 F(2,360)=1934.1 p<0.0000 Std.Error of estimate: 2.9207					
	b*	Std.Err. of b*	b	Std.Err. of b	t(360)	p-value
Intercept			-1.39134	0.701660	-1.98293	0.048135
Air_max	0.828040	0.019217	1.02649	0.023823	43.08783	0.000000
Cum_SR	0.193210	0.019217	0.00025	0.000025	10.05389	0.000000

$$y_{max} = 1.02649 * Air_{max} + 0.00025 * Cum_{SR} - 1.39134$$

Tables 4.45 to 4.48 give the characteristics of the models for minimal daily pavement temperatures for four layers at the Awjilah location where the model is of the form:

$$y_{min} = A * Air_{min} + B * Cum_{SR} + C$$

where

$y_{min}$  = predicted minimal daily pavement temperature (°C);

$A$  = air temperature coefficient;

$Air_{min}$  = minimal daily air temperature (°C);

$B$  = coefficient for the cumulative solar radiation;

$Cum_{SR}$  = cumulative solar radiation( $W/m^2$ ); and

$C$  = intercept coefficient.

Table 4.45 Characteristics of the model for predicting minimal daily C1 temperature from minimal daily air temperature and cumulative solar radiation for the Awjilah location

Awjilah C1_min	Regression Summary for Dependent Variable: C1_min (AWJILAH_Air_min) R= .91279489 R <sup>2</sup> = .83319452 Adjusted R <sup>2</sup> = .83226782 F(2,360)=899.10 p<0.0000 Std.Error of estimate: 2.7053					
	b*	Std.Err. of b*	b	Std.Err. of b	t(360)	p-value
Intercept			5.232376	0.427273	12.24598	0.000000
Air_min	0.772668	0.027762	0.691628	0.024850	27.83166	0.000000
Cum_SR	0.200722	0.027762	0.000174	0.000024	7.23005	0.000000

$$y_{min} = 0.691628 * Air_{min} + 0.000174 * Cum_{SR} + 5.232376$$

Table 4.46 Characteristics of the model for predicting minimal daily C2 temperature from minimal daily air temperature and cumulative solar radiation for the Awjilah location.

Awjilah C2_min	Regression Summary for Dependent Variable: C2_min (AWJILAH_Air_min) R= .98435714 R <sup>2</sup> = .96895897 Adjusted R <sup>2</sup> = .96878652 F(2,360)=5618.8 p<0.0000 Std.Error of estimate: 1.2687					
	b*	Std.Err. of b*	b	Std.Err. of b	t(360)	p-value
Intercept			3.202931	0.200377	15.98454	0.000000
Air_min	0.930087	0.011976	0.905069	0.011654	77.66163	0.000000
Cum_SR	0.082631	0.011976	0.000078	0.000011	6.89959	0.000000

$$y_{min} = 0.905069 * Air_{min} + 0.000078 * Cum_{SR} + 3.202931$$

Table 4.47 Characteristics of the model for predicting minimal daily C3 temperature from minimal daily air temperature and cumulative solar radiation for the Awjilah location

Awjilah C3_min	Regression Summary for Dependent Variable: C3_min (AWJILAH_Air_min) R= .97031262 R <sup>2</sup> = .94150658 Adjusted R <sup>2</sup> = .94118161 F(2,360)=2897.3 p<0.0000 Std.Error of estimate: 1.7245					
	b*	Std.Err. of b*	b	Std.Err. of b	t(360)	p-value
Intercept			4.597323	0.272358	16.87973	0.000000
Air_min	0.910736	0.016440	0.877521	0.015840	55.39748	0.000000
Cum_SR	0.090330	0.016440	0.000084	0.000015	5.49454	0.000000

$$y_{min} = 0.877521 * Air_{min} + 0.000084 * Cum_{SR} + 4.597323$$

Table 4.48 Characteristics of the model for predicting minimal daily C4 temperature from minimal daily air temperature and cumulative solar radiation for the Awjilah location

Awjilah C4_min	Regression Summary for Dependent Variable: C4_min (AWJILAH_Air_min) R= .97270518 R <sup>2</sup> = .94615536 Adjusted R <sup>2</sup> = .94585623 F(2,360)=3163.0 p<0.0000 Std.Error of estimate: 1.6629					
	b*	Std.Err. of b*	b	Std.Err. of b	t(360)	p-value
Intercept			4.693005	0.262626	17.86957	0.000000
Air_min	0.913831	0.015773	0.884934	0.015274	57.93563	0.000000
Cum_SR	0.089317	0.015773	0.000084	0.000015	5.66257	0.000000

$$y_{min} = 0.884934 * Air_{min} + 0.000084 * Cum_{SR} + 4.693005$$

Appendix F presents the tables of the models for predicting maximal (minimal) daily pavement temperatures at different depending on maximal (minimal) daily air temperatures and the cumulative solar radiation for the remaining stations.

From the tables in Appendix F for the models for predicting maximal (minimal) daily pavement temperatures at different depths depending on maximal (minimal) daily air temperatures, and the cumulative solar radiation, it can be seen that the air temperature coefficients are lower compared to the coefficients in the models which did not include the cumulative solar radiation. This means that cumulative solar radiation has an effect on the temperatures of the pavement. Also, adjusted R<sup>2</sup> are higher for the models which include cumulative solar radiation, especially for maximum temperatures. The standard errors of the models both for maximal (minimal) daily pavement temperatures are lower compared to the models which did not include cumulative solar radiation. This means that the models with the cumulative solar radiation explain better maximal and minimal daily temperatures of the pavement.

#### 4.5.4.1 Relationship with air temperature, cumulative solar radiation, and latitude

The next model for predicting maximal (minimal) daily pavement temperatures at different depths from maximal (minimal) daily air temperatures, and the cumulative solar radiation was built using data from all stations and included the latitude of the locations.

The model for maximal daily temperatures is of the following form:

$$y_{max} = A * Air_{max} + B * Cum\_SR + C * Lat + D$$

where

$y_{max}$  = predicted maximal daily pavement temperature (°C);

$A$  = air temperature coefficient;

$Air_{max}$  = maximal daily air temperature (°C);

$B$  = coefficient for the cumulative solar radiation;

$Cum\_SR$  = cumulative solar radiation(W/m<sup>2</sup>);

$C$  =latitude coefficient;

$Lat$  = latitude of the location (degrees); and

$D$  = intercept coefficient.

Tables 4.49 to 4.52 give the characteristics of the models for maximal daily pavement temperatures for four layers.

Table 4.49 Characteristics of the model for predicting maximal daily C1 temperature from maximal daily air temperature and cumulative solar radiation for all locations

All locations C1_max	Regression Summary for Dependent Variable: C1_max (Max_all_locations) R= .91250894 R <sup>2</sup> = .83267256 Adjusted R <sup>2</sup> = .83249928 F(3,2897)=4805.5 p<0.0000 Std.Error of estimate: 4.7282					
	b*	Std.Err. of b*	b	Std.Err. of b	t(2897)	p-value
Intercept			5.705999	1.280502	4.45606	0.000009
Air_max	0.796426	0.008737	1.176934	0.012911	91.16075	0.000000
Cum_SR	0.196719	0.008669	0.000289	0.000013	22.69304	0.000000
Latitude	-0.034286	0.007669	-0.189953	0.042489	-4.47065	0.000008

$$y_{max} = 1.176934 * Air_{max} + 0.000289 * Cum\_SR - 0.189953 * Lat + 5.705999$$

Table 4.50 Characteristics of the model for predicting maximal daily C2 temperature from maximal daily air temperature and cumulative solar radiation for all locations

All locations C2_max	Regression Summary for Dependent Variable: C2_max (Max_all_locations) R= .93354624 R <sup>2</sup> = .87150858 Adjusted R <sup>2</sup> = .87137552 F(3,2897)=6549.8 p<0.0000 Std.Error of estimate: 3.9545					
	b*	Std.Err. of b*	b	Std.Err. of b	t(2897)	p-value
Intercept			-2.13711	1.070961	-1.9955	0.046081
Air_max	0.830451	0.007656	1.17128	0.010798	108.4734	0.000000
Cum_SR	0.184922	0.007596	0.00026	0.000011	24.3433	0.000000
Latitude	-0.000080	0.006721	-0.00042	0.035536	-0.0119	0.990539

$$y_{max} = 1.17128 * Air_{max} + 0.00026 * Cum_{SR} - 0.00042 * Lat - 2.13711$$

Table 4.51 Characteristics of the model for predicting maximal daily C3 temperature from maximal daily air temperature and cumulative solar radiation for all locations

All locations C3_max	Regression Summary for Dependent Variable: C3_max (Max_all_locations) R= .92543614 R <sup>2</sup> = .85643204 Adjusted R <sup>2</sup> = .85628332 F(3,2896)=5758.5 p<0.0000 Std.Error of estimate: 4.0303					
	b*	Std.Err. of b*	b	Std.Err. of b	t(2896)	p-value
Intercept			3.478156	1.091566	3.1864	0.001456
Air_max	0.839021	0.008093	1.140951	0.011005	103.6745	0.000000
Cum_SR	0.147258	0.008030	0.000199	0.000011	18.3381	0.000000
Latitude	-0.043187	0.007105	-0.220179	0.036223	-6.0784	0.000000

$$y_{max} = 1.140951 * Air_{max} + 0.000199 * Cum_{SR} - 0.220179 * Lat + 3.478156$$

Table 4.52 Characteristics of the model for predicting maximal daily C4 temperature from maximal daily air temperature and cumulative solar radiation for all locations

All locations C4_max	Regression Summary for Dependent Variable: C4_max (Max_all_locations) R= .91760567 R <sup>2</sup> = .84200016 Adjusted R <sup>2</sup> = .84183654 F(3,2897)=5146.2 p<0.0000 Std.Error of estimate: 4.0334					
	b*	Std.Err. of b*	b	Std.Err. of b	t(2897)	p-value
Intercept			-2.39620	1.092323	-2.19368	0.028338
Air_max	0.805176	0.008490	1.04454	0.011013	94.84374	0.000000
Cum_SR	0.196313	0.008424	0.00025	0.000011	23.30510	0.000000
Latitude	-0.012995	0.007452	-0.06320	0.036245	-1.74372	0.081315

$$y_{max} = 1.04454 * Air_{max} + 0.00025 * Cum\_SR - 0.06320 * Lat - 2.39620$$

The model for minimal daily temperatures is of the following form:

$$y_{min} = A * Air_{min} + B * Cum\_SR + C * Lat + D$$

where

$y_{min}$ = predicted daily minimal daily pavement temperature (°C);

$A$  = air temperature coefficient;

$Air_{min}$ = minimal daily air temperature (°C);

$B$  = coefficient for cumulative solar radiation;

$Cum\_SR$  = cumulative solar radiation(W/m<sup>2</sup>);

$C$  =latitude coefficient;

$Lat$  = latitude of the location (degrees); and

$D$  = intercept coefficient.

Tables 4.53 to 4.56 give the characteristics of the models for daily minimum pavement temperatures for four layers.

Table 4.53 Characteristics of the model for predicting minimal daily C1 temperature from minimal daily air temperature and cumulative solar radiation for all locations

All locations C1_min	Regression Summary for Dependent Variable: C1_min (Min_all_locations) R= .94599942 R <sup>2</sup> = .89491490 Adjusted R <sup>2</sup> = .89480596 F(3,2894)=8215.2 p<0.0000 Std.Error of estimate: 2.4886					
	b*	Std.Err. of b*	b	Std.Err. of b	t(2534)	p-value
Intercept			0.440099	0.627523	0.7013	0.483155
Air_min	0.915134	0.006855	0.923500	0.006918	133.5001	0.000000
Cum_SR	0.062436	0.006861	0.000061	0.000007	9.0998	0.000000
Latitude	0.026402	0.006034	0.097200	0.022216	4.3753	0.000013

$$y_{min} = 0.923500 * Air_{min} + 0.000061 * Cum\_SR + 0.097200 * Lat + 0.440099$$

Table 4.54 Characteristics of the model for predicting minimal daily C2 temperature from minimal daily air temperature and cumulative solar radiation for all locations

All locations C2_min	Regression Summary for Dependent Variable: C2_min (Min_all_locations) R= .98320604 R <sup>2</sup> = .96669412 Adjusted R <sup>2</sup> = .96665960 F(3,2894)=27999. p<0.0000 Std.Error of estimate: 1.3903					
	b*	Std.Err. of b*	b	Std.Err. of b	t(2534)	p-value
Intercept			8.615312	0.350578	24.5746	0.00
Air_min	0.950826	0.003859	0.952180	0.003865	246.3815	0.00
Cum_SR	0.058471	0.003863	0.000057	0.000004	15.1372	0.00
Latitude	-0.053244	0.003397	-0.194524	0.012411	-15.6731	0.00

$$y_{min} = 0.952180 * Air_{min} + 0.000057 * Cum\_SR - 0.194524 * Lat + 8.615312$$

Table 4.55 Characteristics of the model for predicting minimal daily C3 temperature from minimal daily air temperature and the cumulative solar radiation for all locations

All locations C3_min	Regression Summary for Dependent Variable: C3_min (Min_all_locations) R= .96167393 R <sup>2</sup> = .92481676 Adjusted R <sup>2</sup> = .92473882 F(3,2894)=11866. p<0.0000 Std.Error of estimate: 2.1375					
	b*	Std.Err. of b*	b	Std.Err. of b	t(2534)	p-value
Intercept			12.44787	0.538984	23.0951	0.000000
Air_min	0.925350	0.005798	0.94823	0.005942	159.5926	0.000000
Cum_SR	0.061786	0.005804	0.00006	0.000006	10.6463	0.000000
Latitude	-0.074720	0.005104	-0.27934	0.019081	-14.6394	0.000000

$$y_{min} = 0.94823 * Air_{min} + 0.00006 * Cum\_SR - 0.27934 * Lat + 12.44787$$

Table 4.56 Characteristics of the model for predicting minimal daily C4 temperature from minimal daily air temperature and cumulative solar radiation for all locations

All locations C4_min	Regression Summary for Dependent Variable: C4_min (Min_all_locations) R= .95344555 R <sup>2</sup> = .90905841 Adjusted R <sup>2</sup> = .90896414 F(3,2894)=9642.9 p<0.0000 Std.Error of estimate: 2.3474					
	b*	Std.Err. of b*	b	Std.Err. of b	t(2534)	p-value
Intercept			13.06372	0.591919	22.0701	0.000000
Air_min	0.912596	0.006377	0.93380	0.006525	143.1082	0.000000
Cum_SR	0.071999	0.006383	0.00007	0.000006	11.2801	0.000000
Latitude	-0.065642	0.005614	-0.24504	0.020955	-11.6936	0.000000

$$y_{min} = 0.93380 * Air_{min} + 0.00007 * Cum\_SR - 0.24504 * Lat + 13.06372$$

All of the coefficients of the latitude are negative, indicating that as latitude increases, maximal (minimal) daily pavement temperatures decreases. Compared with the models including only air temperature and latitude, the models including air temperature, cumulative solar radiation and latitude have very similar, but higher adjusted  $R^2$  and standard error of estimate, indicating better fit to the data.

#### 4.5.5 Relationship with air temperature, day of the year, and cumulative solar radiation

The next model for predicting maximal (minimal) daily pavement temperatures at different depth includes maximal (minimal) daily air temperatures, the day of the year and the cumulative solar radiation.

The model for maximal daily pavement temperatures for different locations is of the form:

$$y_{max} = A * Air_{max} + B * Day + C * Day^2 + D * Cum\_SR + E$$

where

$y_{max}$  = predicted maximal daily pavement temperature ( $^{\circ}C$ );

$A$  = air temperature coefficient;

$Air_{max}$  = maximal daily air temperature ( $^{\circ}C$ );

$B$  = coefficient of a day of the year;

$Day$  = day of the year;

$C$  = coefficient of the square of the day;

$Day^2$  = square of the day of the year;

$D$  = coefficient of cumulative solar radiation;

$Cum\_SR$  = cumulative solar radiation ( $W/m^2$ ); and

$E$  = intercept.

Tables 4.57 to 4.60 present the coefficients for the linear prediction models developed for four layers at station Al Qatrun. Included with the model coefficients and their standard errors are the standard errors of estimate and the adjusted  $R^2$ . The coefficients statistically different from zero are denoted in red. Tables of coefficients for the maximal daily pavement temperature for the remaining stations are presented in Appendix G.



Table 4.57 Characteristics of the model for predicting maximal daily C1 temperature from maximal daily air temperature, the day of the year, and cumulative solar radiation for the Al Qatrun location

Al-Qatrun C1_max	Regression Summary for Dependent Variable: C1_max (AL-QATRUN_INT_MAX) R= ,97312855 R <sup>2</sup> = ,94697917 Adjusted R <sup>2</sup> = ,94638841 F(4,359)=1603,0 p<0,0000 Std.Error of estimate: 2,7514					
	b*	Std.Err. of b*	b	Std.Err. of b	t(359)	p-value
Intercept			4,020631	1,387296	2,8982	0,003984
Air_max	0,35606	0,018625	0,610327	0,031926	19,1168	0,000000
Day	2,06818	0,108379	0,231862	0,012150	19,0827	0,000000
Day <sup>2</sup>	-2,11946	0,116652	-0,000631	0,000035	-18,1691	0,000000
Cum_SR (W/m <sup>2</sup> )	0,16708	0,025802	0,000363	0,000056	6,4754	0,000000

$$y_{max} = 0,610327 * Air_{max} + 0,231862 * Day - 0,000631 * Day^2 + 0,000363 * Cum\_SR + 4,020631$$

Table 4.58 Characteristics of the model for predicting maximal daily C2 temperature from maximal daily air temperature, the day of the year and cumulative solar radiation for the Al Qatrun location.

Al-Qatrun C2_max	Regression Summary for Dependent Variable: C2_max (AL-QATRUN_INT_MAX) R= ,98234336 R <sup>2</sup> = ,96499847 Adjusted R <sup>2</sup> = ,96460848 F(4,359)=2474,4 p<0,0000 Std.Error of estimate: 2,0133					
	b*	Std.Err. of b*	b	Std.Err. of b	t(359)	p-value
Intercept			3,653849	1,015134	3,5994	0,000364
Air_max	0,42238	0,015133	0,652049	0,023362	27,9112	0,000000
Day	1,99333	0,088058	0,201259	0,008891	22,6367	0,000000
Day <sup>2</sup>	-2,02330	0,094779	-0,000542	0,000025	-21,3475	0,000000
Cum_SR (W/m <sup>2</sup> )	0,13585	0,020964	0,000266	0,000041	6,4803	0,000000

$$y_{max} = 0,652049 * Air_{max} + 0,201259 * Day - 0,000542 * Day^2 + 0,000266 * Cum\_SR + 3,653849$$

Table 4.59 Characteristics of the model for predicting maximal daily C3 temperature from maximal daily air temperature, the day of the year, and wind speed for the Al Qatrun location

Al-Qatrun C3_max	Regression Summary for Dependent Variable: C3_max (AL-QATRUN_INT_MAX) R= ,97859744 R <sup>2</sup> = ,95765296 Adjusted R <sup>2</sup> = ,95718112 F(4,359)=2029,6 p<0,0000 Std.Error of estimate: 2,1554					
	b*	Std.Err. of b*	b	Std.Err. of b	t(359)	p-value
Intercept			3,549284	1,086781	3,2659	0,001196
Air_max	0,42150	0,016645	0,633320	0,025010	25,3223	0,000000
Day	2,05727	0,096858	0,202170	0,009518	21,2400	0,000000
Day <sup>2</sup>	-2,10980	0,104251	-0,000550	0,000027	-20,2377	0,000000
Cum_SR (W/m <sup>2</sup> )	0,10700	0,023059	0,000204	0,000044	4,6403	0,000005

$$y_{max} = 0,633320 * Air_{max} + 0,202170 * Day - 0,000550 * Day^2 + 0,000204 * Cum\_SR + 3,549284$$

Table 4.60 Characteristics of the model for predicting maximal daily C4 temperature from maximal daily air temperature, the day of the year, and cumulative solar radiation for the Al Qatrun location

Al-Qatrun C4_max	Regression Summary for Dependent Variable: C4_max (AL-QATRUN_INT_MAX) R= ,98307922 R <sup>2</sup> = ,96644476 Adjusted R <sup>2</sup> = ,96607089 F(4,359)=2584,9 p<0,0000 Std.Error of estimate: 1,7502					
	b*	Std.Err. of b*	b	Std.Err. of b	t(359)	p-value
Intercept			4,981980	0,882474	5,6455	0,000000
Air_max	0,44696	0,014817	0,612607	0,020309	30,1649	0,000000
Day	1,99559	0,086219	0,178891	0,007729	23,1455	0,000000
Day <sup>2</sup>	-2,02093	0,092800	-0,000481	0,000022	-21,7772	0,000000
Cum_SR (W/m <sup>2</sup> )	0,11061	0,020526	0,000192	0,000036	5,3889	0,000000

$$y_{max} = 0,612607 * Air_{max} + 0,178891 * Day - 0,000481 * Day^2 + 0,000192 * Cum\_SR + 4,981980$$

From these tables it can be seen that the cumulative solar radiation coefficients are statistically significant and positive, which means that as cumulative solar radiation increases, temperatures increases. Compared with the model including daily minimal air temperature and the day of the year, we see that adjusted R<sup>2</sup> coefficients are higher, and standard error of estimate are lower, indicating better fit to the data.

The model for minimal daily pavement temperatures for different locations is of the form:

$$y_{min} = A * Air_{min} + B * Day + C * Day^2 + D * Cum\_SR + E$$

where

$y_{min}$  = predicted minimal daily pavement temperature (°C);

$A$  = air temperature coefficient;

$Air_{min}$  = minimal daily air temperature (°C);

$B$  = coefficient of a day of the year;

$Day$  = day of the year;

$C$  = coefficient of the square of the day of the year;

$Day^2$  = square of the day of the year;

$D$  = coefficient of cumulative solar radiation;

$Cum\_SR$  = cumulative solar radiation (W/m<sup>2</sup>); and

$E$  = intercept.

Tables 4.61 to 4.64 present the coefficients for the linear prediction models developed for each layer at station Al Qatrun. Included with the model coefficients and their standard errors are the standard errors of estimate and the adjusted R<sup>2</sup>. The coefficients statistically different from zero are denoted in red. Tables of coefficients for the pavement temperature for the remaining stations are presented in Appendix G.

Table 4.61 Characteristics of the model for predicting minimal daily C1 temperature from minimal daily air temperature, the day of the year, and cumulative solar radiation for the Al Qatrun location

Al Qatrun C1_min	Regression Summary for Dependent Variable: C1_min (AL-QATRUN_INT_Min) R= ,98500322 R <sup>2</sup> = ,97023134 Adjusted R <sup>2</sup> = ,96990057 F(4,360)=2933,3 p<0,0000 Std.Error of estimate: 1,2724					
	b*	Std.Err. of b*	b	Std.Err. of b	t(360)	p-value
Intercept			3,370473	0,482636	6,98347	0,000000
Air_min	0,829142	0,019161	0,796853	0,018415	43,27146	0,000000
Day	0,751824	0,100536	0,052070	0,006963	7,47814	0,000000
Day <sup>2</sup>	-0,764532	0,105204	-0,000140	0,000019	-7,26711	0,000000
Cum_SR (W/m <sup>2</sup> )	-0,023301	0,019311	-0,000031	0,000026	-1,20662	0,228373

$$y_{min} = 0,796853 * Air_{min} + 0,052070 * Day - 0,000140 * Day^2 - 0,000031 * Cum\_SR + 3,370473$$

Table 4.62 Characteristics of the model for predicting minimal daily C2 temperature from minimal daily air temperature, the day of the year, and cumulative solar radiation for the Al Qatrun location

Al Qatrun C2_min	Regression Summary for Dependent Variable: C2_min (AL-QATRUN_INT_Min) R= ,99041456 R <sup>2</sup> = ,98092099 Adjusted R <sup>2</sup> = ,98070900 F(4,360)=4627,2 p<0,0000 Std.Error of estimate: 1,0385					
	b*	Std.Err. of b*	b	Std.Err. of b	t(360)	p-value
Intercept			3,494134	0,393922	8,87011	0,000000
Air_min	0,839143	0,015340	0,822201	0,015030	54,70290	0,000000
Day	0,614170	0,080486	0,043366	0,005683	7,63076	0,000000
Day <sup>2</sup>	-0,606594	0,084223	-0,000114	0,000016	-7,20222	0,000000
Cum_SR (W/m <sup>2</sup> )	0,018350	0,015460	0,000025	0,000021	1,18698	0,236019

$$y_{min} = 0,822201 * Air_{min} + 0,043366 * Day - 0,000114 * Day^2 + 0,000025 * Cum\_SR + 3,494134$$

Table 4.63 Characteristics of the model for predicting minimal daily C3 temperature from minimal daily air temperature, the day of the year, and cumulative solar radiation for the Al Qatrun location.

Al Qatrun C3_min	Regression Summary for Dependent Variable: C3_min (AL-QATRUN_INT_Min) R= ,98548342 R <sup>2</sup> = ,97117757 Adjusted R <sup>2</sup> = ,97085732 F(4,360)=3032,6 p<0,0000 Std.Error of estimate: 1,3795					
	b*	Std.Err. of b*	b	Std.Err. of b	t(360)	p-value
Intercept			0,272264	0,523270	0,5203	0,603166
Air_min	0,67584	0,018854	0,715672	0,019966	35,8451	0,000000
Day	1,04238	0,098926	0,079546	0,007549	10,5370	0,000000
Day <sup>2</sup>	-1,06476	0,103519	-0,000216	0,000021	-10,2856	0,000000
Cum_SR (W/m <sup>2</sup> )	0,08808	0,019001	0,000130	0,000028	4,6355	0,000005

$$y_{min} = 0,715672 * Air_{min} + 0,079546 * Day - 0,000216 * Day^2 + 0,000130 * Cum\_SR + 0,272264$$

Table 4.64 Characteristics of the model for predicting minimal daily C4 temperature from minimal daily air temperature, the day of the year, and cumulative solar radiation for the Al Qatrun location.

Al Qatrun C4_min	Regression Summary for Dependent Variable: C4_min (AL-QATRUN_INT_Min) R= ,98520199 R <sup>2</sup> = ,97062297 Adjusted R <sup>2</sup> = ,97029656 F(4,360)=2973,6 p<0,0000 Std.Error of estimate: 1,3678					
	b*	Std.Err. of b*	b	Std.Err. of b	t(360)	p-value
Intercept			2,197511	0,518835	4,23547	0,000029
Air_min	0,706848	0,019035	0,735125	0,019796	37,13423	0,000000
Day	0,882451	0,099873	0,066137	0,007485	8,83575	0,000000
Day <sup>2</sup>	-0,886899	0,104510	-0,000176	0,000021	-8,48626	0,000000
Cum_SR (W/m <sup>2</sup> )	0,101209	0,019183	0,000147	0,000028	5,27590	0,000000

$$y_{min} = 0,735125 * Air_{min} + 0,066137 * Day - 0,000176 * Day^2 + 0,000147 * Cum\_SR + 2,197511$$

From these tables it can be seen that the cumulative solar radiation coefficients are statistically significant and positive, which means that as cumulative solar radiation increases, temperatures increases. Compared with the model including daily minimal air temperature and the day of the year, we see that adjusted R<sup>2</sup> coefficients are slightly higher, and standard error of estimate are slightly lower, indicating similar fit to the data.

#### 4.5.5.1 Relationship with air temperature, day of the year, cumulative solar radiation and latitude

The next model for predicting maximal daily pavement temperatures at four different layers, based on the maximal daily air temperatures, the day of the year and the cumulative solar radiation was built using data from all stations, and includes the latitude of the locations. The model is of the form

$$y_{max} = A * Air_{max} + B * Day + C * Day^2 + D * Lat + E * Cum\_SR + F$$

where

$y_{max}$  = predicted maximal daily pavement temperature (°C);

$A$  = air temperature coefficient;

$Air_{max}$  = maximal daily air temperature (°C);

$B$  = coefficient of a day of the year;

$Day$  = day of the year;

$C$  = coefficient of square of the day;

$Day^2$  = square of the day of the year;

$D$  = coefficient of latitude;

$Lat$  = latitude (degrees);

$E$  = coefficient of cumulative solar radiation;  
 $Cum\_SR$  = cumulative solar radiation( $W/m^2$ ); and  
 $F$  = intercept.

Tables 4.65 to 4.68 give the characteristics of the models for maximal daily pavement temperatures for four layers.

Table 4.65 Characteristics of the model for predicting maximal daily C1 temperature from maximal daily air temperature, the day of the year and cumulative solar radiation for all locations.

All locations C1_max	Regression Summary for Dependent Variable: C1_max (Max_all_locations) R= ,95900914 R <sup>2</sup> = ,91969853 Adjusted R <sup>2</sup> = ,91955984 F(5,2895)=6631,3 p<0,0000 Std.Error of estimate: 3,2766					
	b*	Std.Err. of b*	b	Std.Err. of b	t(2909)	p-value
Intercept			24,14976	0,947652	25,4838	0,000000
Air_max	0,47617	0,008471	0,70367	0,012518	56,2105	0,000000
Day	1,96000	0,036223	0,21415	0,003958	54,1090	0,000000
Day <sup>2</sup>	-2,05579	0,036937	-0,00060	0,000011	-55,6565	0,000000
Cum_SR ( $W/m^2$ )	0,03019	0,006744	0,00004	0,000010	4,4763	0,000008
Latitude	-0,08632	0,005398	-0,47821	0,029907	-15,9898	0,000000

$$y_{max} = 0,70367 * Air_{max} + 0,21415 * Day - 0,00060 * Day^2 - 0,47821 * Lat + 0,00004 * Cum\_SR + 24,14976$$

Table 4.66 Characteristics of the model for predicting maximal daily C2 temperature from maximal daily air temperature, the day of the year, and cumulative solar radiation for all locations.

All locations C2_max	Regression Summary for Dependent Variable: C2_max (Max_all_locations) R= ,97427306 R <sup>2</sup> = ,94920799 Adjusted R <sup>2</sup> = ,94912026 F(5,2895)=10820, p<0,0000 Std.Error of estimate: 2,4871					
	b*	Std.Err. of b*	b	Std.Err. of b	t(2909)	p-value
Intercept			14,33569	0,719325	19,9294	0,000000
Air_max	0,52367	0,006737	0,73859	0,009502	77,7281	0,000000
Day	1,87709	0,028809	0,19575	0,003004	65,1573	0,000000
Day <sup>2</sup>	-1,95186	0,029376	-0,00054	0,000008	-66,4430	0,000000
Cum_SR ( $W/m^2$ )	0,03005	0,005364	0,00004	0,000008	5,6025	0,000000
Latitude	-0,04970	0,004293	-0,26281	0,022702	-11,5769	0,000000

$$y_{max} = 0,73859 * Air_{max} + 0,19575 * Day - 0,00054 * Day^2 - 0,26281 * Lat + 0,00004 * Cum\_SR + 14,33569$$

Table 4.67 Characteristics of the model for predicting maximal daily C3 temperature from maximal daily air temperature, the day of the year, and cumulative solar radiation for all locations.

All locations C3_max	Regression Summary for Dependent Variable: C3_max (Max_all_locations) R= ,96472889 R <sup>2</sup> = ,93070184 Adjusted R <sup>2</sup> = ,93058211 F(5,2894)=7773,5 p<0,0000 Std.Error of estimate: 2,8011					
	b*	Std.Err. of b*	b	Std.Err. of b	t(2908)	p-value
Intercept			19,04707	0,810177	23,5098	0,000000
Air_max	0,54000	0,007870	0,73432	0,010702	68,6178	0,000000
Day	1,83005	0,033657	0,18398	0,003384	54,3741	0,000000
Day <sup>2</sup>	-1,90676	0,034320	-0,00051	0,000009	-55,5582	0,000000
Cum_SR (W/m <sup>2</sup> )	-0,00470	0,006265	-0,00001	0,000008	-0,7502	0,453169
Latitude	-0,09164	0,005016	-0,46720	0,025571	-18,2707	0,000000

$$y_{max} = 0,73432 * Air_{max} + 0,18398 * Day - 0,00051 * Day^2 - 0,46720 * Lat - 0,00001 * Cum\_SR + 19,04707$$

Table 4.68 Characteristics of the model for predicting maximal daily C4 temperature from maximal daily air temperature, the day of the year, and cumulative solar radiation for all locations.

All locations C4_max	Regression Summary for Dependent Variable: C4_max (Max_all_locations) R= ,95450058 R <sup>2</sup> = ,91107136 Adjusted R <sup>2</sup> = ,91091777 F(5,2895)=5931,8 p<0,0000 Std.Error of estimate: 3,0270					
	b*	Std.Err. of b*	b	Std.Err. of b	t(2909)	p-value
Intercept			11,37024	0,875456	12,9878	0,000000
Air_max	0,51030	0,008915	0,66200	0,011565	57,2427	0,000000
Day	1,80328	0,038119	0,17297	0,003656	47,3063	0,000000
Day <sup>2</sup>	-1,83736	0,038871	-0,00047	0,000010	-47,2685	0,000000
Cum_SR (W/m <sup>2</sup> )	0,05780	0,007097	0,00007	0,000009	8,1437	0,000000
Latitude	-0,06021	0,005681	-0,29282	0,027629	-10,5982	0,000000

$$y_{max} = 0,66200 * Air_{max} + 0,17297 * Day - 0,00047 * Day^2 - 0,29282 * Lat + 0,00007 * Cum\_SR + 11,37024$$

All of the coefficients of the latitude are negative, indicating that as latitude increases, pavement temperature decreases. Compared with the models including only maximal daily air temperature, the day of the year, and latitude, the models including the maximal daily air temperature, the day of the year, the cumulative solar radiation and latitude have very higher adjusted R<sup>2</sup> and lower standard error of estimate, indicating better fit to the data.

The next model for predicting minimal daily pavement temperatures at four different layers, based on minimal daily air temperatures, the day of the year, and cumulative solar radiation was built using data from all stations and includes the latitude of the locations. The model is of the form

$$y_{min} = A * Air_{min} + B * Day + C * Day^2 + D * Lat + E * Cum\_SR + F$$

where

$y_{min}$  = predicted minimal daily pavement temperature (°C);

$A$  = air temperature coefficient;

$Air_{min}$  = minimal daily air temperature (°C);

$B$  = coefficient of a day of the year;

$Day$  = day of the year;

$C$  = coefficient of square of the day of the year;

$Day^2$  = square of the day of the year;

$D$  = coefficient of Latitude;

$Lat$  = latitude (degrees);

$E$  = coefficient of cumulative solar radiation;

$Cum\_SR$  = cumulative solar radiation( $W/m^2$ ); and

$F$  = intercept.

Tables 4.69 to 4.72 give the characteristics of the models for daily minimal pavement temperatures for four layers.

Table 4.69 Characteristics of the model for predicting minimal daily C1 temperature from minimal daily air temperature, the day of the year, and cumulative solar radiation for all locations.

All locations C1_min	Regression Summary for Dependent Variable: C1_min (Min_all_locations) R= ,94797464 R <sup>2</sup> = ,89865592 Adjusted R <sup>2</sup> = ,89848070 F(5,2892)=5128,9 p<0,0000 Std.Error of estimate: 2,4447					
	b*	Std.Err. of b*	b	Std.Err. of b	t(2908)	p-value
Intercept			1,013228	0,625111	1,6209	0,105153
Air_min	0,832853	0,010775	0,840467	0,010873	77,2977	0,000000
Day	0,464054	0,046772	0,033665	0,003393	9,9216	0,000000
Day <sup>2</sup>	-0,482437	0,047237	-0,000093	0,000009	-10,2132	0,000000
Cum_SR ( $W/m^2$ )	0,026424	0,007647	0,000026	0,000008	3,4556	0,000557
Latitude	0,021501	0,005947	0,079158	0,021895	3,6154	0,000305

$$y_{min} = 0,840467 * Air_{min} + 0,033665 * Day - 0,000093 * Day^2 + 0,079158 * Lat + E0,000026 * Cum\_SR + 1,013228$$



Table 4.70 Characteristics of the model for predicting minimal daily C2 temperature from minimal daily air temperature, the day of the year, and cumulative solar radiation for all locations.

All locations C2_min	Regression Summary for Dependent Variable: C2_min (Min_all_locations) R= ,98771434 R <sup>2</sup> = ,97557961 Adjusted R <sup>2</sup> = ,97553739 F(5,2892)=23107, p<0,0000 Std.Error of estimate: 1,1909					
	b*	Std.Err. of b*	b	Std.Err. of b	t(2908)	p-value
Intercept			8,947653	0,304509	29,3839	0,000000
Air_min	0,816966	0,005289	0,818129	0,005297	154,4632	0,000000
Day	0,742537	0,022960	0,053455	0,001653	32,3410	0,000000
Day <sup>2</sup>	-0,735875	0,023188	-0,000141	0,000004	-31,7357	0,000000
Cum_SR (W/m <sup>2</sup> )	0,011839	0,003754	0,000012	0,000004	3,1540	0,001627
Latitude	-0,060532	0,002919	-0,221149	0,010665	-20,7351	0,000000

$$y_{min} = 0,818129 * Air_{min} + 0,053455 * Day - 0,000141 * Day^2 - 0,221149 * Lat + 0,000012 * Cum\_SR + 8,947653$$

Table 4.71 Characteristics of the model for predicting minimal daily C3 temperature from minimal daily air temperature, the day of the year, and cumulative solar radiation for all locations.

All locations C3_min	Regression Summary for Dependent Variable: C3_min (Min_all_locations) R= ,97167991 R <sup>2</sup> = ,94416184 Adjusted R <sup>2</sup> = ,94406530 F(5,2892)=9780,1 p<0,0000 Std.Error of estimate: 1,8427					
	b*	Std.Err. of b*	b	Std.Err. of b	t(2908)	p-value
Intercept			13,31895	0,471173	28,2677	0,000000
Air_min	0,72922	0,007998	0,74725	0,008196	91,1779	0,000000
Day	1,09559	0,034718	0,08071	0,002557	31,5569	0,000000
Day <sup>2</sup>	-1,10830	0,035063	-0,00022	0,000007	-31,6091	0,000000
Cum_SR (W/m <sup>2</sup> )	-0,01388	0,005676	-0,00001	0,000006	-2,4462	0,014495
Latitude	-0,08582	0,004414	-0,32083	0,016503	-19,4410	0,000000

$$y_{min} = 0,74725 * Air_{min} + 0,08071 * Day - 0,00022 * Day^2 - 0,32083 * Lat - 0,00001 * Cum\_SR + 13,31895$$

Table 4.72 Characteristics of the model for predicting minimal daily C4 temperature from minimal daily air temperature, the day of the year, and cumulative solar radiation for all locations.

All locations C4_min	Regression Summary for Dependent Variable: C4_min (Min_all_locations) R= ,96458927 R <sup>2</sup> = ,93043245 Adjusted R <sup>2</sup> = ,93031218 F(5,2892)=7735,8 p<0,0000 Std.Error of estimate: 2,0538					
	b*	Std.Err. of b*	b	Std.Err. of b	t(2908)	p-value
Intercept			13,77346	0,525150	26,2277	0,000000
Air_min	0,70504	0,008927	0,72141	0,009134	78,9777	0,000000
Day	1,15512	0,038752	0,08497	0,002850	29,8081	0,000000
Day <sup>2</sup>	-1,15584	0,039137	-0,00023	0,000008	-29,5336	0,000000
Cum_SR (W/m <sup>2</sup> )	-0,00392	0,006335	-0,00000	0,000006	-0,6192	0,535858
Latitude	-0,07715	0,004927	-0,28800	0,018393	-15,6578	0,000000

$$y_{min} = 0,72141 * Air_{min} + 0,08497 * Day - 0,00023 * Day^2 - 0,28800 * Lat - 0,00000 * Cum\_SR + 13,77346$$

All of the coefficients of the latitude are negative, indicating that as latitude increases, pavement temperature decreases. Compared with the models including only minimal daily air temperature, the day of the year, and latitude, the models including the minimal daily air temperature, the day of the year, cumulative solar radiation and latitude have very similar adjusted R<sup>2</sup> and standard error of estimate, indicating similar fit to the data.

#### 4.5.6 Relationship with air temperature, cumulative solar radiation and wind speed

The model for predicting maximal (minimal) daily pavement temperatures at different depths including maximal (minimal) daily air temperatures, cumulative solar radiation and wind speed was built. However, the model is similar to the model that included only air temperature, solar radiation, and wind speed due to having similar adjusted R<sup>2</sup> and standard errors of estimate. This indicates a similar fit to the data; therefore, the results are not presented here.

#### 4.5.7 Evaluation of the models with air temperature

As can be seen from the fit of the models which included only the maximal/minimal daily air temperature, those models could be improved (especially models for maximal daily pavement temperatures) by adding new variables, such as day of the year, wind speed and cumulative solar radiation. However, wind speed did not improve the models significantly, as can be seen from the values of adjusted R<sup>2</sup> and standard errors of estimate. In table 4.73 values of adjusted R<sup>2</sup> and standard errors are presented for all considered models based on data from all eight locations.

The best values of adjusted  $R^2$  and standard error of estimate were obtained when the model included maximal/minimal daily air temperature, day of the year, latitude and cumulative solar radiation.

Table 4.73 Adjusted  $R^2$  and standard errors for different models which are based on the data from all locations.

<b>Models for maximal daily temperatures</b>										
The model including latitude and:										
	Air temp		Air temp, wind speed		Air temp, cum. solar radiation		Air temp, day of the year		Air temp, day of the year, cum. solar radiation	
Layer	Adj. $R^2$	Std.Err of est.	Adj. $R^2$	Std.Err of est.	Adj. $R^2$	Std.Err of est.	Adj. $R^2$	Std.Err of est.	Adj. $R^2$	Std.Err of est.
C1	.80347	5.12777	.80358	5.1246	.83249	4.7282	.91908	3.2892	.91955	3.2766
C2	.84551	4.33718	.84575	4.3338	.87137	3.9545	.94862	2.5012	.94912	2.4871
C3	.84010	4.25591	.84029	4.2535	.85628	4.0303	.93067	2.8025	.93058	2.8011
C4	.81272	4.39406	.81724	4.3407	.84183	4.0334	.90901	3.0628	.91092	3.0270

<b>Models for minimal daily temperatures</b>										
The model including latitude and:										
	Air temp		Air temp, wind speed		Air temp, cum. solar radiation		Air temp, day of the year		Air temp, day of the year, cum. solar radiation	
Layer	Adj. $R^2$	Std.Err of est.	Adj. $R^2$	Std.Err of est.	Adj. $R^2$	Std.Err of est.	Adj. $R^2$	Std.Err of est.	Adj. $R^2$	Std.Err of est.
C1	.89188	2.51980	.89170	2.5207	.88989	2.5492	.89798	2.4476	.89848	2.4447
C2	.96363	1.45078	.96366	1.4494	.96657	1.4003	.97525	1.1967	.97553	1.1909
C3	.92131	2.18407	.92146	2.1813	.92255	2.1767	.94385	1.8449	.94407	1.8427
C4	.90469	2.39970	.90485	2.3964	.91220	2.3134	.93039	2.0507	.93031	2.0538

Therefore, we conclude that the best model for predicting the maximal/minimal daily pavement temperatures is linear regression with maximal/minimal daily air temperature, day of the year, and cumulative solar radiation.

The best models for maximal daily pavement temperatures are:

Surface (C1):

$$T_{pav,surf}^{max} = 24,14976 + 0,70367T_{air}^{max} + 0,21415Day - 0.00060Day^2 + 0,00004Cum\_SR - 0,47821Lat$$

3 cm (C2):

$$T_{pav,3cm}^{max} = 14,33569 + 0,73859T_{air}^{max} + 0,19575Day - 0,00054Day^2 + 0,00004Cum\_SR - 0,26281Lat$$

8 cm (C3):

$$T_{pav,8cm}^{max} = 19,04707 + 0,73432T_{air}^{max} + 0,18398Day - 0,00051Day^2 - 0,00001Cum\_SR - 0,46720Lat$$

15 cm(C4):

$$T_{pav,15cm}^{max} = 11,37024 + 0,66200T_{air}^{max} + 0,17297Day - 0,00047Day^2 + 0,00007Cum\_SR - 0,29282Lat$$

where

$T_{pav,*}^{max}$  =maximal daily pavement temperature at certain depth, (°C);

$T_{air}^{max}$  = maximal daily air temperature, (°C);

$Day$  = day of the year;

$Day^2$  = square of the day of the year;

$Cum\_SR$  = cumulative solar radiation (W/m<sup>2</sup>)and

$Lat$ = latitude of the section, (degrees).

The best models for minimal daily pavement temperatures are:

Surface (C1):

$$T_{pav,surf}^{min} = 1,013228 + 0,840467T_{air}^{min} + 0,033665Day - 0,000093Day^2 + 0,000026Cum\_SR + 0,079158Lat$$

3 cm (C2):

$$T_{pav,3cm}^{min} = 8,947653 + 0,818129T_{air}^{min} + 0,053455Day - 0,000141Day^2 + 0,000012Cum\_SR - 0,221149Lat$$

8 cm (C3):

$$T_{pav,8cm}^{min} = 13,31895 + 0,74725T_{air}^{min} + 0,08071Day - 0,00022Day^2 - 0,00001Cum\_SR - 0,32083Lat$$

15 cm(C4):

$$T_{pav,15cm}^{min} = 13,77346 + 0,72141T_{air}^{min} + 0,08497Day - 0,00023Day^2 - 0,00000Cum\_SR - 0,28800Lat$$

where

$T_{pav,*}^{min}$  =minimal daily pavement temperature at certain depth, (°C);

$T_{air}^{min}$  = minimal daily air temperature, (°C);

$Day$  = day of the year;

$Day^2$  = square of the day of the year;

$Cum\_SR$  = cumulative solar radiation (W/m<sup>2</sup>) and

*Lat*= latitude of the section, (degrees).

In the case when data on cumulative solar radiation are not available, the next best model for predicting the maximal/minimal daily pavement temperatures is linear regression with maximal/minimal daily air temperature, and day of the year, obtained in section 4.5.2.

Figures 4.27 to 4.34 present actual maximal and minimal daily pavement temperatures at four layers together with predicted values from the model including the air temperature, cumulative solar radiation and the day of the year at the Al-Jufroh location. In Appendix H, similar figures for other locations are given.

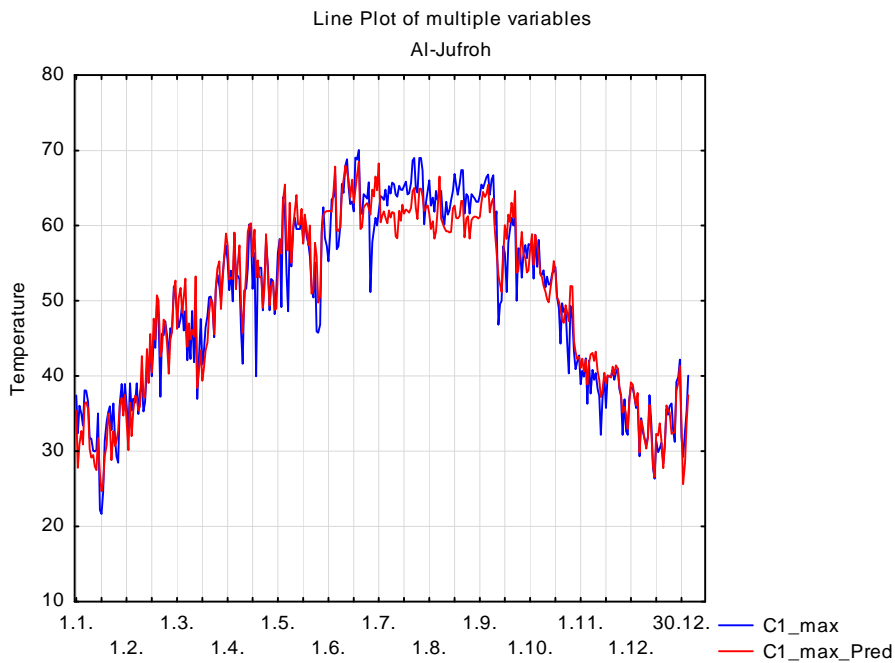


Figure 4.27 Actual maximal daily pavement temperature at C1 depth versus predictions from the model including maximal daily air temperature, latitude, the day of the year, and cumulative solar radiation at the Al Jufroh location.

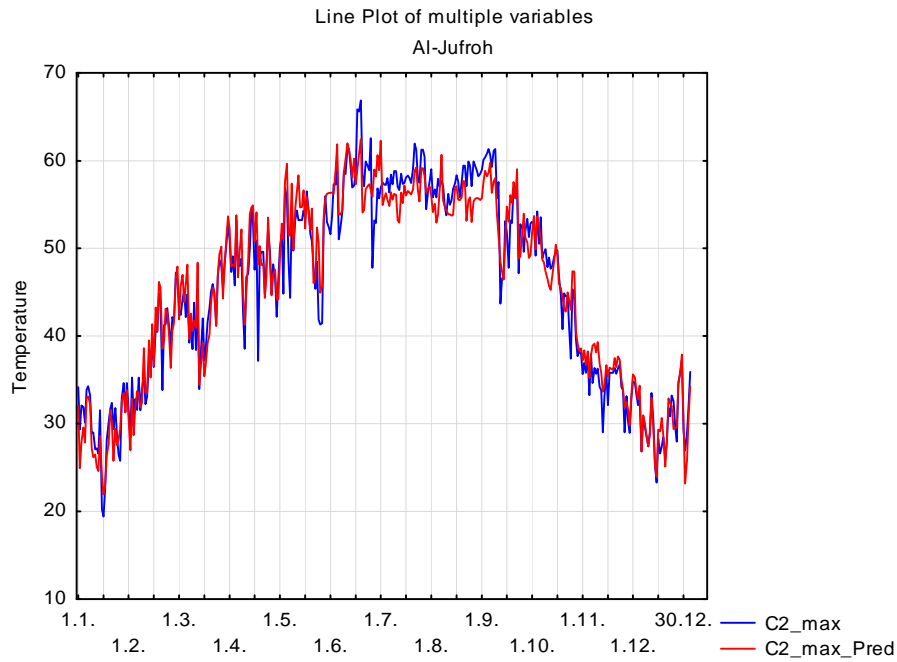


Figure 4.28 Actual maximal daily pavement temperature at C2 depth versus predictions from the model including maximal daily air temperature, latitude, the day of the year, and cumulative solar radiation at the Al Jufroh location.

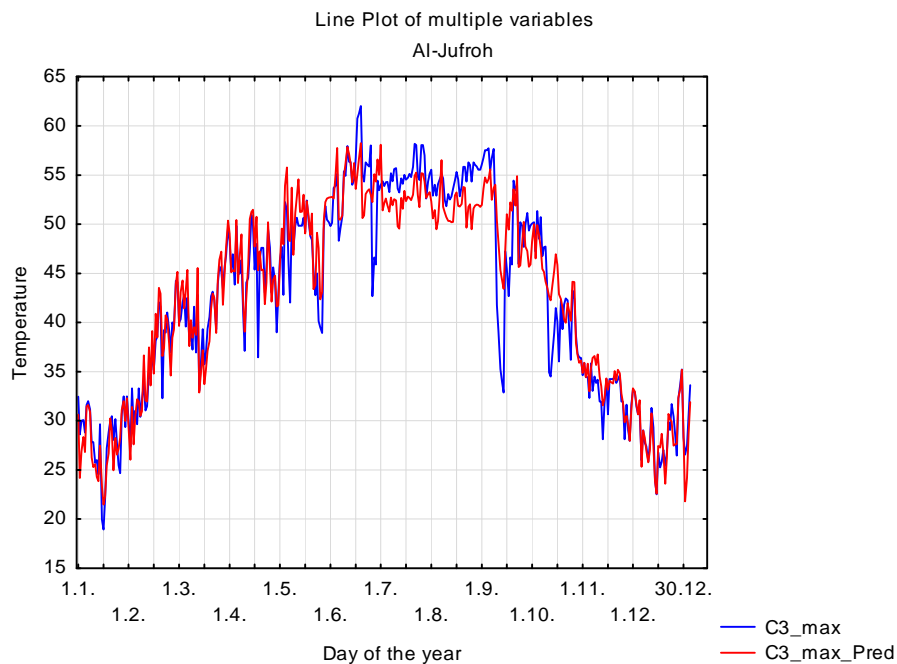


Figure 4.29 Actual maximal daily pavement temperature at C3 depth versus predictions from the model including maximal daily air temperature, latitude, the day of the year, and cumulative solar radiation at the Al Jufroh location.

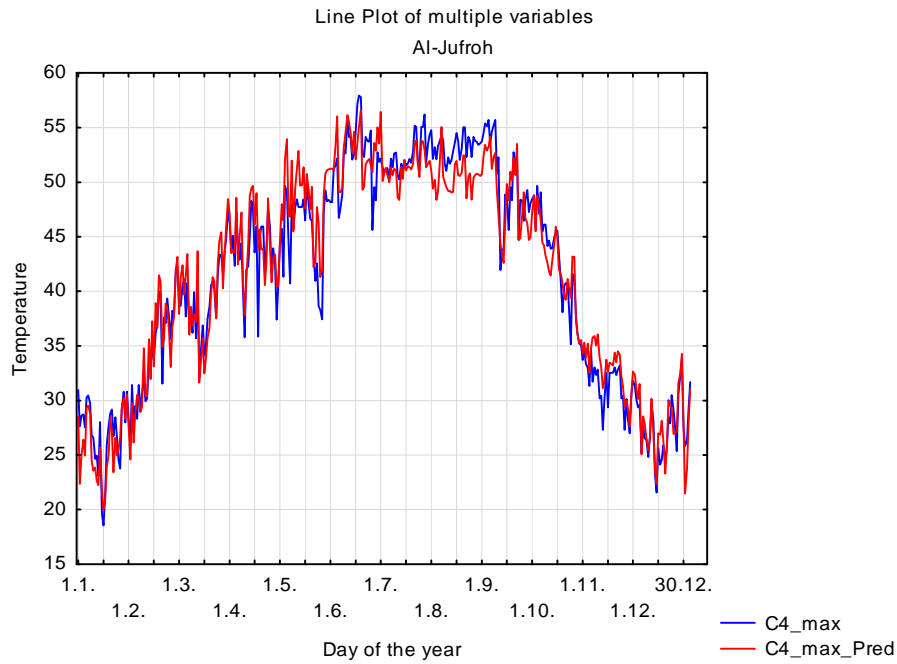


Figure 4.30 Actual maximal daily pavement temperature at C4 depth versus predictions from the model including maximal daily air temperature, latitude, the day of the year, and cumulative solar radiation at the Al Jufroh location.

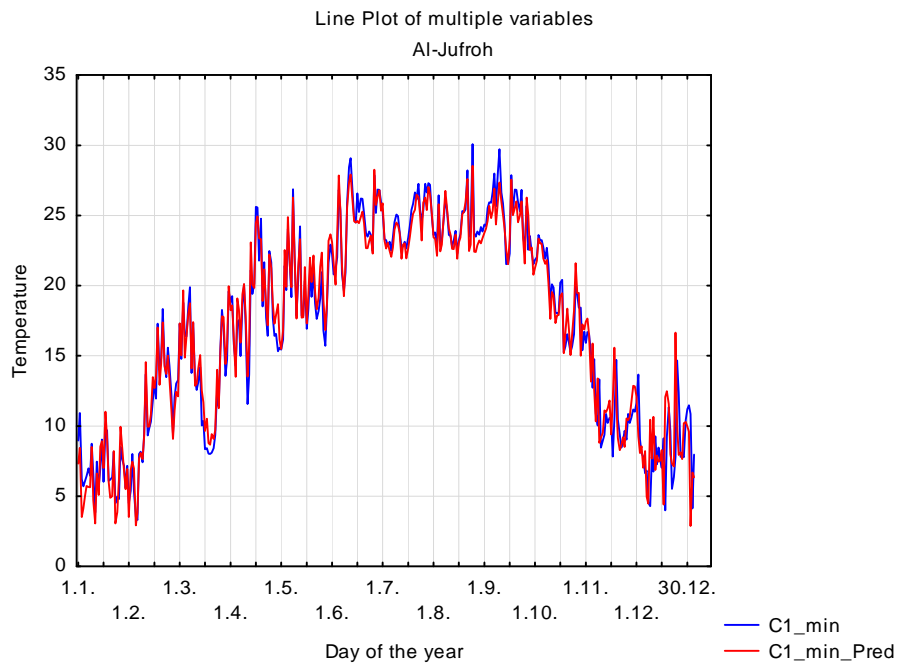


Figure 4.31 Actual minimal daily pavement temperature at C1 depth versus predictions from the model including minimal daily air temperature, latitude, the day of the year, and cumulative solar radiation at the Al Jufroh location.

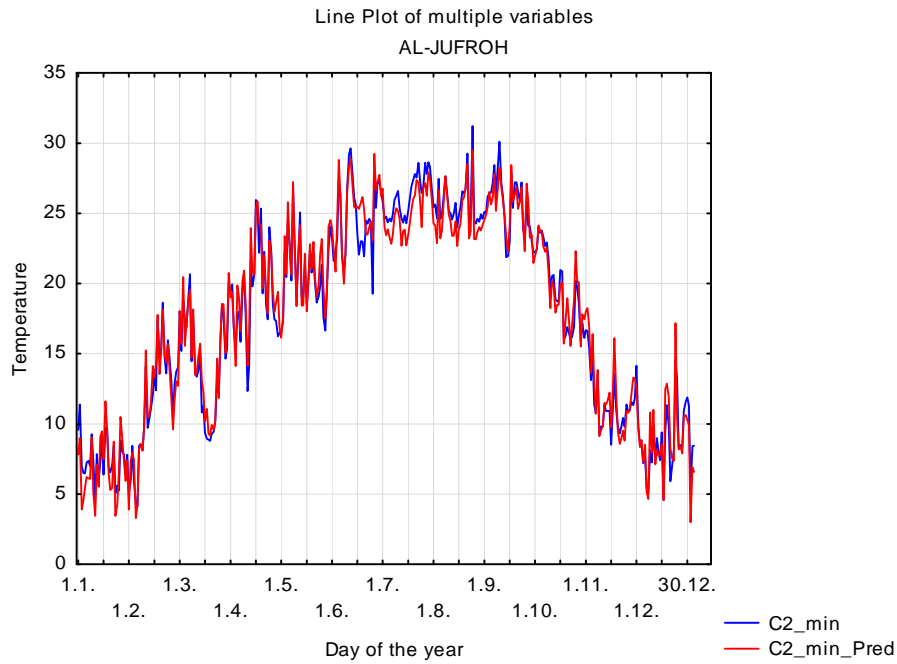


Figure 4.32 Actual minimal daily pavement temperature at C2 depth versus predictions from the model including minimal daily air temperature, latitude, the day of the year, and cumulative solar radiation at the Al Jufroh location.

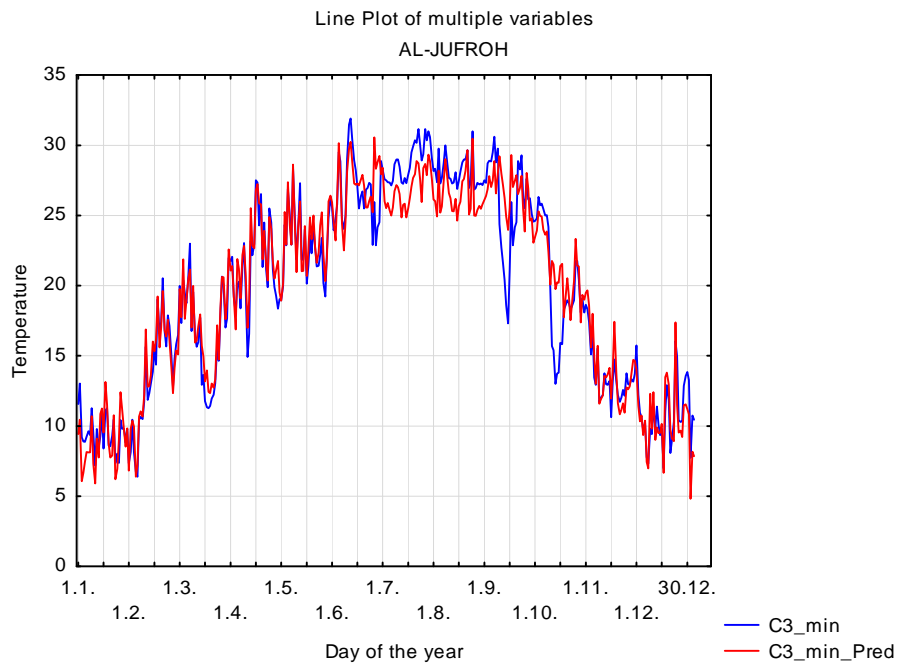


Figure 4.33 Actual minimal daily pavement temperature at C3 depth versus predictions from the model including minimal daily air temperature, latitude, the day of the year, and cumulative solar radiation at the Al Jufroh location.



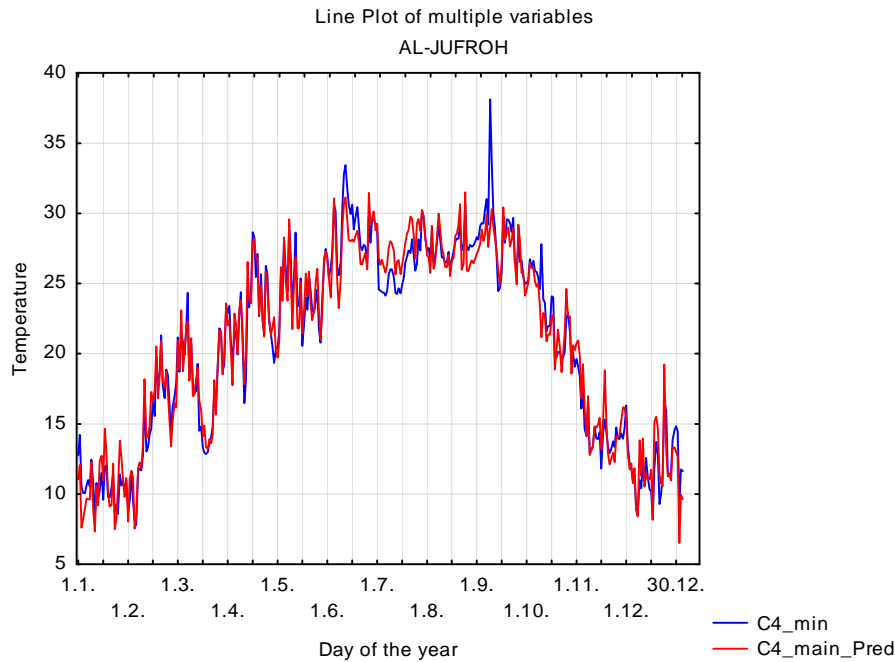


Figure 4.34 Actual minimal daily pavement temperature at C4 depth versus predictions from the model including minimal daily air temperature, latitude, the day of the year, and cumulative solar radiation at the Al Jufroh location.

## 4.6 Pavement temperature prediction models incorporating air temperature and the distance from the surface (depth)

### 4.6.1 Relationship with air temperature and the distance from the surface (depth)

The next models describe the relationship between daily maximal/minimal pavement temperatures, daily maximal/minimal air temperatures and distance from the surface.

The model for maximal daily temperatures of the pavement including maximal daily air temperature and distance from the surface is of the following form:

$$y_{max} = A * Air_{max} + B * Depth + C$$

where

$y_{max}$  = predicted maximal daily pavement temperature (°C);

$A$  = coefficient of air temperature;

$Air_{max}$  = maximal daily air temperature (°C);

$B$  = coefficient of the depth;

$Depth$  = depth from the surface (cm); and

$C$  = intercept.

Tables 4.74 and 4.75 present the coefficients for the linear prediction models developed for location Al Jufroh. Included with the model coefficients and their standard errors are the standard errors of estimate and the adjusted R<sup>2</sup>. The coefficients statistically different from zero are denoted in red. Tables of coefficients for the pavement temperature for the remaining stations are represented in Appendix I.

Table 4.74 Characteristics of the model for predicting maximal daily pavement temperatures from maximal daily air temperature and depth from the surface at the Al Jufroh location.

Al Jufroh max	Regression Summary for Dependent Variable: Temperature_max (Temp_depth_C1_max_Novo) R= .91932677 R <sup>2</sup> = .84516170 Adjusted R <sup>2</sup> = .84494916 F(2,1457)=3976.4 p<0.0000 Std.Error of estimate: 4.4386 Include condition: Site=102					
	b*	Std.Err. of b*	b	Std.Err. of b	t(1457)	p-value
Intercept			2.206741	0.569341	3.8760	0.000111
Air_max	0.879221	0.010309	1.281917	0.015030	85.2882	0.000000
Depth	-0.268573	0.010309	-0.532918	0.020455	-26.0527	0.000000

$$y_{max} = 1.281917 * Air_{max} - 0.532918 * Depth + 2.206741$$

The model for minimal temperatures of the pavement including maximal daily air temperature and depth from the surface is of the following form:

$$y_{min} = A * Air_{min} + B * Depth + C$$

where

$y_{min}$  = predicted minimal daily pavement temperature (°C);

$A$  = coefficient of minimal daily air temperature;

$Air_{min}$  = minimal daily air temperature (°C);

$B$  = coefficient of the depth;

$Depth$  = distance from the surface (cm); and

$C$  = intercept.

Table 4.75 Characteristics of the model for predicting minimal daily pavement temperatures from minimal daily air temperature and depth from the surface at the Al Jufroh location.

Al Jufroh min	Regression Summary for Dependent Variable: Temperature_min (Temp_depth_Air_min_Novo) R= .96491149 R <sup>2</sup> = .93105419 Adjusted R <sup>2</sup> = .93095955 F(2,1457)=9837.8 p<0.0000 Std.Error of estimate: 1.8938 Include condition: Site=102					
	b*	Std.Err. of b*	b	Std.Err. of b	t(1457)	p-value
Intercept			3.127436	0.127395	24.5491	0.00
Depth	0.197975	0.006879	0.251179	0.008728	28.7797	0.00
Air_min	0.944383	0.006879	1.024055	0.007459	137.2853	0.00

$$y_{min} = 1.024055 * Air_{min} + 0.251179 * Depth + 3.127436$$

#### 4.6.1.1 Relationship with air temperature, depth from the surface, and latitude

The next models describe the relationship between maximal/minimal daily pavement temperatures and maximal/minimal daily air temperatures, depth from the surface and latitude.

The model for maximal daily temperatures of the pavement including maximal daily air temperature and depth from the surface is of the following form:

$$y_{max} = A * Air_{max} + B * Depth + C * Lat + D$$

where

$y_{max}$  = predicted maximal daily pavement temperature (°C);

$A$  = coefficient of air temperature;

$Air_{max}$  = maximal daily air temperature (°C);

$B$  = coefficient of the distance from the surface;

$Depth$  = distance from the surface (cm);

$C$  = coefficient of the latitude;

$Lat$  = latitude (degrees); and

$D$  = intercept.

Tables 4.76 and 4.77 present the coefficients for the linear prediction models developed for all locations. Included with the model coefficients and their standard errors are the standard errors of estimate and the adjusted R<sup>2</sup>. The coefficients statistically different from zero are denoted in red.

Table 4.76 Characteristics of the model for predicting maximal daily pavement temperatures from maximal daily air temperature, depth from the surface, and latitude

All locations max	Regression Summary for Dependent Variable: Temperature_max (Temp_depth_C1_max_Novo) R= .91629732 R <sup>2</sup> = .83960079 Adjusted R <sup>2</sup> = .83955950 F(3,11655)=20336. p<0.0000 Std.Error of estimate: 4.6105					
	b*	Std.Err. of b*	b	Std.Err. of b	t(11655)	p-value
Intercept			6.368723	0.625088	10.1885	0.000000
Depth	-0.326919	0.003710	-0.662561	0.007518	-88.1241	0.000000
Air_max	0.853275	0.003744	1.254808	0.005506	227.8961	0.000000
Latitude	-0.018587	0.003744	-0.102636	0.020675	-4.9643	0.000001

$$y_{max} = 1.254808 * Air_{max} - 0.662561 * Depth - 0.102636 * Lat + 6.368723$$

Maximal daily temperature of pavement at different layers depends mostly on maximal daily air temperatures. Maximal daily pavement temperatures decrease with distance from the surface because its coefficient is negative and decreases with latitude because its coefficient is negative .

The model for minimal daily temperatures of the pavement including minimal daily air temperature and depth from the surface is of the following form:

$$y_{min} = A * Air_{min} + B * Depth + C * Lat + D$$

where

$y_{min}$  = predicted minimal daily pavement temperature (°C);

$A$  = coefficient of air temperature;

$Air_{min}$  = minimal daily air temperature (°C);

$B$  = coefficient of the distance from the surface;

$Depth$  = distance from the surface (cm);

$C$  = coefficient of the latitude;

$Lat$  = latitude; and

$D$  = intercept.

Table 4.77 Characteristics of the model for predicting minimal daily pavement temperatures from minimal daily air temperature, depth from the surface and latitude.

All locations min	Regression Summary for Dependent Variable: Temperature_min (Temp_depth_Air_min_Novo)					
	R= .95968313 R <sup>2</sup> = .92099171 Adjusted R <sup>2</sup> = .92097138 F(3,11660)=45306. p<0.0000 Std.Error of estimate: 2.2049					
	b*	Std.Err. of b*	b	Std.Err. of b	t(11660)	p-value
Intercept			8.300106	0.271852	30.5317	0.00
Depth	0.185191	0.002603	0.255764	0.003595	71.1430	0.00
Air_min	0.939202	0.002604	0.970025	0.002690	360.6271	0.00
Latitude	-0.044452	0.002604	-0.167257	0.009799	-17.0682	0.00

$$y_{min} = 0.970025 * Air_{min} + 0.255764 * Depth - 0.167257 * Lat + 8.300106$$

Minimal daily temperature of pavement at different layers depends mostly on minimal daily air temperatures. Minimal daily pavement temperatures, increase with distance from the surface because its coefficient is positive and decreases with latitude because its coefficient is negative.

#### 4.6.2 Relationship with daily air temperature, distance from the surface, and day of the year

The next models describe the relationship between maximal/minimal daily pavement temperatures and maximal/minimal daily air temperatures, distance from the surface and the day of the year.

The model for maximal daily temperatures of the pavement including the maximal daily air temperature, distance from the surface and the day of the year is of the following form:

$$y_{max} = A * Air_{max} + B * Depth + C * Day + D * Day^2 + E$$

Where:

$y_{max}$  = predicted maximal daily pavement temperature (°C);

$A$  = coefficient of air temperature;

$Air_{max}$  = maximal daily air temperature (°C);

$B$  = coefficient of the distance from the surface;

$Depth$  = distance from the surface (cm);

$C$  = coefficient for the day of the year;

$Day$  = day of the year;

$D$  = coefficient for the square of the day of the year;

$E$  = intercept.

Tables 4.78 and 4.79 present the coefficients for the linear prediction models developed for location Al Jufroh. Included with the model coefficients and their standard errors are the standard errors of estimate and the adjusted R<sup>2</sup>. The coefficients statistically different from zero are denoted in red. Tables of coefficients for the pavement temperature for the remaining stations are presented in Appendix I.

Table 4.78 Characteristics of the model for predicting maximal daily pavement temperatures from maximal daily air temperature, the day of the year, and depth from the surface at the Al Jufroh location.

Al Jufroh max	Regression Summary for Dependent Variable: Temperature_max (Temp_depth_C1_max_Novo) R= .96210316 R <sup>2</sup> = .92564250 Adjusted R <sup>2</sup> = .92543808 F(4,1455)=4528.2 p<0.0000 Std.Error of estimate: 3.0780 Include condition: Site=102					
	b*	Std.Err. of b*	b	Std.Err. of b	t(1455)	p-value
Intercept			9.698754	0.451588	21.4770	0.00
Depth	-0.26857	0.007149	-0.532918	0.014185	-37.5692	0.00
Air_max	0.51907	0.011585	0.756818	0.016891	44.8063	0.00
Day	1.77022	0.045675	0.188626	0.004867	38.7566	0.00
Day <sup>2</sup>	-1.82921	0.046175	-0.000517	0.000013	-39.6142	0.00

$$y_{max} = 0.756818 * Air_{max} - 0.532918 * Depth + 0.188626 * Day - 0.000517 * Day^2 + 9.698754$$

Model for maximal daily temperature of pavement at different layers including maximal daily air temperatures, distance from the surface and day of the year improve the model without day of the year, since it has higher R<sup>2</sup> and lower standard error of estimate. Maximal daily temperature of pavement decreases with distance from the surface for maximal temperatures.

The model for minimal daily temperatures of the pavement including the minimal daily air temperature, depth from the surface, and the day of the year is of the following form:

$$y_{min} = A * Air_{min} + B * Depth + C * Day + D * Day^2 + E$$

where

$y_{min}$  = predicted minimal daily pavement temperature (°C);

$A$  = coefficient of air temperature;

$Air_{min}$  = minimal daily air temperature (°C);

$B$  = coefficient of the distance from the surface ;

$Depth$  = distance from the surface (cm);

$C$  = coefficient for the day of the year;

$Day$  = day of the year;

$D$  = coefficient for the square of the day of the year;

$E$  = intercept.

Table 4.79 Characteristics of the model for predicting minimal daily pavement temperatures from minimal daily air temperature, the day of the year, and depth from the surface at the Al Jufroh location

Al Jufroh min	Regression Summary for Dependent Variable: Temperature_min (Temp_depth_Air_min_Novo) R= .97707320 R <sup>2</sup> = .95467203 Adjusted R <sup>2</sup> = .95454742 F(4,1455)=7661.1 p<0.0000 Std.Error of estimate: 1.5366 Include condition: Site=102					
	b*	Std.Err. of b*	b	Std.Err. of b	t(1451)	p-value
Intercept			1.809737	0.128372	14.0976	0.00
Depth	0.19798	0.005582	0.251179	0.007081	35.4698	0.00
Air_min	0.71109	0.010175	0.771079	0.011033	69.8873	0.00
Day	1.10287	0.040466	0.075141	0.002757	27.2544	0.00
Day <sup>2</sup>	-1.10814	0.040246	-0.000200	0.000007	-27.5338	0.00

$$y_{min} = 0.771079 * Air_{min} + 0.251179 * Depth + 0.075141 * Day - 0.000200 * Day^2 + 1.809737$$

Model for minimal daily temperature of pavement at different layers including minimal daily air temperatures, distance from the surface and day of the year improve the model without day of the year, since it has higher R<sup>2</sup> and lower standard error of estimate. Minimal daily temperature of pavement increases with distance from the surface for maximal temperatures, since its coefficient is positive.

#### 4.6.2.1 Relationship with daily air temperature, the distance from the surface, day of the year, and the latitude

The next models describe the relationship between maximal/minimal daily pavement temperatures and maximal/minimal daily air temperatures, the day of the year, distance from the surface, and latitude.

The model for maximal daily temperatures is of the following form:

$$y_{max} = A * Air_{max} + B * Depth + C * Lat + D * Day + E * Day^2 + F$$

where

$y_{max}$  = predicted maximal daily pavement temperature (°C);

$A$  = coefficient of air temperature;

$Air_{max}$  = maximal daily air temperature (°C);

$B$  = coefficient of the distance from the surface;  
 $Depth$  = distance from the surface (cm);  
 $C$  = coefficient of the latitude  
 $Lat$  = latitude (degrees);  
 $D$  = coefficient of the day of the year;  
 $Day$  = day of the year;  
 $E$  = coefficient of the square of the day of the year;  
 $Day^2$  = square of the day of the year; and  
 $F$  = intercept.

Table 4.80 Characteristics of the model for predicting maximal daily pavement temperatures from maximal daily air temperature, distance from the surface, the day of the year and latitude.

All locations max	Regression Summary for Dependent Variable: Temperature_max (Temp_depth_C1_max_Novo) R= .96411733 R <sup>2</sup> = .92952222 Adjusted R <sup>2</sup> = .92949198 F(5,11653)=30738. p<0.0000 Std.Error of estimate: 3.0564					
	b*	Std.Err. of b*	b	Std.Err. of b	t(11657)	p-value
Intercept			22.20576	0.434694	51.084	0.00
Depth	0.48426	0.003955	0.71214	0.005817	122.433	0.00
Air_max	1.81237	0.015503	0.19734	0.001688	116.904	0.00
Day	-1.88488	0.015587	-0.00054	0.000005	-120.928	0.00
Day <sup>2</sup>	-0.06900	0.002517	-0.38103	0.013901	-27.410	0.00
Latitude	-0.32691	0.002459	-0.66255	0.004984	-132.931	0.00

$$y_{max} = 0.19734 * Air_{max} + 0.71214 * Depth - 0.66255 * Lat - 0.00054 * Day - 0.38103 * Day^2 + 22.20576$$

Model for maximal daily temperature of pavement at different layers including maximal daily air temperatures, distance from the surface and day of the year and latitude improves the model without day of the year, since it has higher R<sup>2</sup> and lower standard error of estimate. Maximal daily temperature of pavement decreases with distance from the surface for maximal temperatures, and decreases with latitude.

The model for minimal daily temperatures is of the following form:

$$y_{min} = A * Air_{min} + B * Depth + C * Lat + D * Day + E * Day^2 + F$$

where

$y_{min}$  = predicted minimal daily pavement temperature (°C);

$A$  = coefficient of air temperature;

$Air_{min}$  = minimum air temperature (°C);



$B$  = coefficient of the distance from the surface ;  
 $Depth$  = distance from the surface (cm);  
 $C$  = coefficient of the latitude;  
 $Lat$  = latitude (degrees);  
 $D$ = coefficient of the day of the year;  
 $Day$ = day of the year;  
 $E$ = coefficient of the square of the day of the year;  
 $F$  = intercept.

Table 4.81 Characteristics of the model for predicting minimal daily pavement temperatures from minimal daily air temperature, distance from the surface, the day of the year, and latitude

All locations min	Regression Summary for Dependent Variable: Temperature_min (Temp_depth_Air_min_Novo) R= .96735568 R <sup>2</sup> = .93577702 Adjusted R <sup>2</sup> = .93574948 F(5,11658)=33973. p<0.0000 Std.Error of estimate: 1.9881					
	b*	Std.Err. of b*	b	Std.Err. of b	t(11658)	p-value
Intercept			7.723302	0.246810	31.2925	0.00
Depth	0.185191	0.002347	0.255764	0.003242	78.9017	0.00
Air_min	0.756259	0.004257	0.781078	0.004397	177.6313	0.00
Day	0.864448	0.016907	0.064150	0.001255	51.1292	0.00
Day <sup>2</sup>	-0.871677	0.016830	-0.000172	0.000003	-51.7943	0.00
Latitude	-0.050351	0.002351	-0.189455	0.008846	-21.4165	0.00

$$y_{min} = 0.781078 * Air_{min} + 0.255764 * Depth - 0.189455 * Lat + 0.064150 * Day - 0.000172 * Day^2 + 7.723302$$

Model for minimal daily temperature of pavement at different layers including minimal daily air temperatures, distance from the surface and day of the year improves the model without day of the year, since it has higher R<sup>2</sup> and lower standard error of estimate. Minimal daily temperature of pavement increases with distance from the surface for maximal temperatures, since its coefficient is positive and decrease with latitude, since its coefficient is negative.

#### 4.6.3 Relationship with air temperature, the depth from the surface and cumulative solar radiation

The next models describe the relationship between maximal/minimal daily pavement temperatures and maximal/minimal daily air temperatures, distance from the surface, and cumulative solar radiation.

The model for maximal daily temperatures of the pavement including the maximal daily air temperature, distance from the surface and cumulative solar radiation is of the following form:

$$y_{max} = A * Air_{max} + B * Depth + C * Cum\_SR + D$$

where

$y_{max}$  = predicted maximal daily pavement temperature (°C);

$A$  = coefficient of air temperature;

$Air_{max}$  = maximal daily air temperature (°C);

$B$  = coefficient of the distance from the surface;

$Depth$  = distance from the surface (cm);

$C$  = coefficient for the cumulative solar radiation;

$Cum\_SR$  = the solar radiation (W/m<sup>2</sup>); and

$D$  = intercept

Tables 4.82 and 4.83 present the coefficients for the linear prediction models developed for location Al Kufrah. Included with the model coefficients and their standard errors are the standard errors of estimate and the adjusted R<sup>2</sup>. The coefficients statistically different from zero are denoted in red. Tables of coefficients for the pavement temperature for the remaining stations are presented in Appendix I.

Table 4.82 Characteristics of the model for predicting maximal daily pavement temperatures from maximal daily air temperature, cumulative solar radiation, and distance from the surface at the Al Jufroh location.

Al Jufroh max	Regression Summary for Dependent Variable: Temperature_max (Temp_depth_C1_max_Novo) R= .95879770 R <sup>2</sup> = .91929303 Adjusted R <sup>2</sup> = .91912489 F(3,1440)=5467.4 p<0.0000 Std.Error of estimate: 3.2067 Include condition: Site=102					
	b*	Std.Err. of b*	b	Std.Err. of b	t(1440)	p-value
Intercept			1.762678	0.412291	4.2753	0.000020
Depth	-0.268224	0.007486	-0.532401	0.014860	-35.8281	0.000000
Air_max	0.561909	0.011598	0.817344	0.016870	48.4503	0.000000
Cum_SR	0.416882	0.011598	0.000702	0.000020	35.9455	0.000000

$$y_{max} = 0.817344 * Air_{max} - 0.532401 * Depth + 0.000702 * Cum\_SR + 1.762678$$

Model for maximal daily temperature of pavement at different layers including maximal daily air temperatures, distance from the surface and cumulative solar radiation improves the model without cumulative solar radiation, since it has higher R<sup>2</sup> and lower standard error of estimate. Maximal daily temperature of pavement decreases with distance from the surface for maximal temperatures and increases with cumulative solar radiation.

The model for minimal daily temperatures of the pavement including the minimal daily air temperature, distance from the surface and cumulative solar radiation is of the following form:

$$y_{min} = A * Air_{min} + B * Depth + C * Cum\_SR + D$$

where

$y_{min}$  = predicted minimal daily pavement temperature (°C);

$A$  = coefficient of air temperature;

$Air_{min}$  = minimal daily air temperature (°C);

$B$  = coefficient of the distance from the surface;

$Depth$  = distance from the surface (cm);

$C$  = coefficient for the solar radiation;

$Cum\_SR$  = the solar radiation (W/m<sup>2</sup>); and

$D$  = intercept.

Table 4.83 Characteristics of the model for predicting minimal daily pavement temperatures from minimal daily air temperature, cumulative solar radiation and distance from the surface at the Al Jufroh location

Al Jufroh min	Regression Summary for Dependent Variable: Temperature_min (Temp_depth_Air_min_Novo) R= .97442993 R <sup>2</sup> = .94951369 Adjusted R <sup>2</sup> = .94940851 F(3,1440)=9027.5 p<0.0000 Std.Error of estimate: 1.6205 Include condition: Site=102					
	b*	Std.Err. of b*	b	Std.Err. of b	t(1440)	p-value
Intercept			-0.003224	0.174256	-0.01850	0.985240
Depth	0.197893	0.005921	0.250968	0.007509	33.42144	0.000000
Air_min	0.787752	0.008994	0.853639	0.009746	87.59018	0.000000
Cum_SR	0.207921	0.008994	0.000224	0.000010	23.11877	0.000000

$$y_{min} = 0.853639 * Air_{min} + 0.250968 * Depth + 0.000224 * Cum\_SR - 0.003224$$

Model for minimal daily temperature of pavement at different layers including minimal daily air temperatures, distance from the surface and cumulative solar radiation improves the model without cumulative solar radiation, since it has higher R<sup>2</sup> and lower standard error of estimate. Minimal daily temperature of pavement increases with distance from the surface for maximal temperatures and increases with cumulative solar radiation.

#### 4.6.3.1 Relationship with air temperature, the depth from the surface, cumulative solar radiation and latitude

The next models describe the relationship between maximal/minimal daily pavement temperatures and maximal/minimal daily air temperatures, cumulative solar radiation, distance from the surface and latitude.

The model for maximal daily temperatures is of the following form:

$$y_{max} = A * Air_{max} + B * Depth + C * Lat + D * Cum\_SR + E$$

where

$y_{max}$  = predicted maximal daily pavement temperature (°C);

$A$  = coefficient of air temperature;

$Air_{max}$  = maximal daily air temperature (°C);

$B$  = coefficient of the distance from the surface;

$Depth$  = distance from the surface (cm);

$C$  = coefficient of the latitude;

$Lat$  = latitude (degrees);

$D$  = coefficient of the cumulative solar radiation;

$Cum\_SR$  = cumulative solar radiation (W/m<sup>2</sup>); and

$E$  = intercept.

Table 4.84 Characteristics of the model for predicting maximal daily pavement temperatures from maximal daily air temperature, distance from the surface, cumulative solar radiation and latitude

All locations max	Regression Summary for Dependent Variable: Temperature_max (Temp_depth_Air_max_Novo) R= .92840003 R <sup>2</sup> = .86192661 Adjusted R <sup>2</sup> = .86187898 F(4,11594)=18094. p<0.0000 Std.Error of estimate: 4.2745					
	b*	Std.Err. of b*	b	Std.Err. of b	t(11657)	p-value
Intercept			5.400752	0.580828	9.2984	0.000000
Depth	-0.327079	0.003451	-0.662318	0.006988	-94.7796	0.000000
Air_max	0.769974	0.003969	1.132778	0.005839	194.0158	0.000000
Cum_SR	0.171804	0.003938	0.000252	0.000006	43.6260	0.000000
Latitude	-0.021115	0.003482	-0.116494	0.019212	-6.0635	0.000000

$$y_{max} = 1.132778 * Air_{max} - 0.662318 * Depth - 0.116494 * Lat + 0.000252 * Cum\_SR + 5.400752$$

The model for minimal daily temperatures is of the following form:

$$y_{min} = A * Air_{min} + B * Depth + C * Lat + D * Cum\_SR + E$$

where

$y_{min}$  = predicted minimal daily pavement temperature (°C);

*A* = coefficient of air temperature;  
*Air\_min* = minimal daily air temperature (°C);  
*B* = coefficient of the depth;  
*Depth* = depth from the surface (cm);  
*C* = coefficient of the latitude;  
*Lat* = latitude (degrees);  
*D*= coefficient of the cumulative solar radiation;  
*Cum\_SR*= cumulative solar radiation (W/m<sup>2</sup>); and  
*E*= intercept.

Table 4.85 Characteristics of the model for predicting minimal daily pavement temperatures from minimal daily air temperature, depth from the surface, cumulative solar radiation and latitude.

All locations min	Regression Summary for Dependent Variable: Temperature_min (Temp_depth_Air_min_Novo) R= .96141723 R <sup>2</sup> = .92432309 Adjusted R <sup>2</sup> = .92429697 F(4,11587)=35381. p<0.0000 Std.Error of estimate: 2.1599					
	b*	Std.Err. of b*	b	Std.Err. of b	t(11587)	p-value
Intercept			6.979389	0.273293	25.5381	0.00
Depth	0.185016	0.002556	0.255748	0.003533	72.3957	0.00
Air_min	0.909756	0.002907	0.939427	0.003002	312.9298	0.00
Cum_SR	0.062595	0.002910	0.000063	0.000003	21.5111	0.00
Latitude	-0.041257	0.002559	-0.155426	0.009641	-16.1214	0.00

$$y_{min} = 0.939427 * Air_{min} + 0.255748 * Depth - 0.155426 * Lat + 0.000063 * Cum_{SR} + 6.979389$$

Maximum temperature of pavement at different depths depends mostly on maximum air temperatures but decreases with depth and depends on the day of the year. It decreases with latitude and increases with cumulative solar radiation.

Minimum temperature of pavement at different depths depends mostly on minimum air temperature and the day of the year. It increases with depth and cumulative solar radiation and decreases with latitude.

#### 4.6.4 Relationship with air temperature, the distance from the surface, day of the year and cumulative solar radiation and latitude

The next models describe the relationship between maximal/minimal daily pavement temperatures and maximal/minimal daily air temperatures, day of the year cumulative solar radiation, distance from the surface and latitude.

The model for maximal daily temperatures is of the following form:

$$y_{max} = A * Air_{max} + B * Depth + C * Day + D * Day^2 + E * Lat + F * Cum\_SR + G$$

where

$y_{max}$  = predicted maximal daily pavement temperature (°C);

$A$  = coefficient of air temperature;

$Air_{max}$  = maximal daily air temperature (°C);

$B$  = coefficient of the distance from the surface;

$Depth$  = distance from the surface (cm);

$C$  = coefficient of the day of the year;

$Day$  = day of the year;

$D$  = coefficient of square of the day of the year;

$E$  = coefficient of the latitude;

$Lat$  = latitude (degrees);

$F$  = coefficient of the cumulative solar radiation;

$Cum\_SR$  = cumulative solar radiation (W/m<sup>2</sup>); and

$G$  = intercept.

Table 4.86 Characteristics of the model for predicting maximal daily pavement temperatures from maximal daily air temperature, distance from the surface, day of the year, cumulative solar radiation and latitude.

All locations max	Regression Summary for Dependent Variable: Temperature_max (Temp_depth_Air_max_Novo) R= ,96431664 R <sup>2</sup> = ,92990659 Adjusted R <sup>2</sup> = ,92987031 F(6,11592)=25631, p<0,0000 Std.Error of estimate: 3,0459					
	b*	Std.Err. of b*	b	Std.Err. of b	t(11657)	p-value
Intercept			21,53130	0,442136	48,698	0,000000
Depth	-0,32724	0,002459	-0,66265	0,004979	-133,080	0,000000
Air_max	0,48241	0,003956	0,70972	0,005819	121,956	0,000000
Day	1,76231	0,016934	0,19170	0,001842	104,069	0,000000
Day <sup>2</sup>	-1,82946	0,017271	-0,00053	0,000005	-105,927	0,000000
Cum_SR	0,02639	0,003155	0,00004	0,000005	8,366	0,000000
Latitude	-0,06802	0,002521	-0,37526	0,013909	-26,980	0,000000

$$y_{max} = 0,70972 * Air_{max} - 0,66265 * Depth + 0,19170 * Day - 0,00053 * Day^2 - 0,37526 * Lat + 0,00004 * Cum\_SR + 21,53130$$

The model for minimal daily temperatures is of the following form:

$$y_{min} = A * Air_{min} + B * Depth + C * Day + D * Day^2 + E * Lat + F * Cum\_SR + G$$

where

$y_{min}$  = predicted minimal daily pavement temperature (°C);

$A$  = coefficient of air temperature;

$Air_{min}$  = minimal daily air temperature (°C);

$B$  = coefficient of the depth;

$Depth$  = distance from the surface (cm);

$C$  = coefficient of the day of the year;

$Day$  = day of the year;

$D$  = coefficient of square of the day of the year;

$E$  = coefficient of the latitude;

$Lat$  = latitude (degrees);

$F$  = coefficient of the cumulative solar radiation;

$Cum\_SR$  = cumulative solar radiation (W/m<sup>2</sup>); and

$G$  = intercept.

Table 4.87 Characteristics of the model for predicting minimal daily pavement temperatures from minimal daily air temperature, depth from the surface, day of the year, cumulative solar radiation and latitude.

All locations min	Regression Summary for Dependent Variable: Temperature_min (Temp_depth_Air_min_Novo) R= ,96744913 R <sup>2</sup> = ,93595782 Adjusted R <sup>2</sup> = ,93592465 F(6,11585)=28219, p<0,0000 Std.Error of estimate: 1,9872					
	b*	Std.Err. of b*	b	Std.Err. of b	t(11587)	p-value
Intercept			7,600962	0,254932	29,8156	0,000000
Depth	0,185016	0,002351	0,255748	0,003250	78,6908	0,000000
Air_min	0,757123	0,004279	0,781816	0,004419	176,9209	0,000000
Day	0,851365	0,018577	0,063198	0,001379	45,8293	0,000000
Day <sup>2</sup>	-0,857574	0,018761	-0,000169	0,000004	-45,7096	0,000000
Cum_SR	0,004910	0,003037	0,000005	0,000003	1,6166	0,105992
Latitude	-0,049826	0,002362	-0,187706	0,008898	-21,0946	0,000000

$$y_{min} = 0,781816 * Air_{min} + 0,255748 * Depth + 0,063198 * Day - 0,000169 * Day^2 - 0,187706 * Lat + 0,000005 * Cum\_SR + 7,600962$$

Maximal daily temperature of pavement at different depths depends mostly on daily maximal air temperatures but decreases with depth and depends on the day of the year. It decreases with latitude and increases with cumulative solar radiation.

Minimal daily temperature of pavement at different depths depends mostly on daily minimal air temperature and the day of the year. It increases with depth and cumulative solar radiation and decreases with latitude.

#### 4.6.5 Evaluation of the models including air temperature and the distance from the surface

As can be seen from the fit of the models which included only the maximal/minimal daily air temperature, those models could be improved (especially models for maximal temperatures) by adding new variables, such as day of the year, wind speed and cumulative solar radiation. However, the wind speed did not improve the models significantly, as can be seen from the values of adjusted  $R^2$  and standard errors in table 4.88. Higher values of adjusted  $R^2$  and lower standard errors were obtained when the model included day of the year and the solar radiation. The best values of adjusted  $R^2$  and standard error were obtained when the model included day of the year, cumulative solar radiation:

Table 4.88 Adjusted  $R^2$  and standard errors for different models which are based on the data from all locations.

<b>Models for maximal daily temperatures</b>									
The model including latitude, distance from the surface and									
Air temp		Air temp, wind speed		Air temp, day of the year		Air temp, cum. solar radiation		Air temp, day of the year, cum. solar radiation	
Adj. $R^2$	Std.Err of est.	Adj. $R^2$	Std.Err of est.	Adj. $R^2$	Std.Err of est.	Adj. $R^2$	Std.Err of est.	Adj. $R^2$	Std.Err of est.
.83955	4.6105	-	-	.92818	3.0865	.86165	4.2775	.92987	3.0459
<b>Models for minimal daily temperatures</b>									
The model including latitude, distance from the surface and									
Air temp		Air temp, wind speed		Air temp, day of the year		Air temp, cum. solar radiation		Air temp, day of the year, cum. solar radiation	
Adj. $R^2$	Std.Err of est.	Adj. $R^2$	Std.Err of est.	Adj. $R^2$	Std.Err of est.	Adj. $R^2$	Std.Err of est.	Adj. $R^2$	Std.Err of est.
.92097	2.2049	-	-	.93574948	1.9881	.92429	2.1599	.93592	1.9872

Therefore, we conclude that the best model for predicting the pavement temperatures is linear regression including the air temperature, distance from the surface and day of the year and cumulative solar radiation.



The best model for maximal daily pavement temperatures are:

$$T_{pav,d}^{max} = 24,14976 + 0,70972T_{air}^{max} - 0,66265d + 0,19170Day - 0,00053Day^2 + 0,00004Cum\_SR - 0,37526Lat$$

where

$T_{pav,d}^{max}$  = maximal daily pavement temperature at distance  $d$  from the surface, (°C);

$T_{air}^{max}$  = maximal daily air temperature, (°C);

$d$  = distance from the surface (cm);

$Day$  = day of the year;

$Cum\_SR$  = cumulative solar radiation (W/m<sup>2</sup>)and

$Lat$  = latitude of the section, (degrees).

The best model for minimal daily pavement temperatures are:

$$T_{pav,d}^{min} = 7,600962 + 0,781816T_{air}^{min} + 0,255748d + 0,063198Day - 0,000169Day^2 + 0,000005Cum\_SR - 0,187706Lat$$

where

$T_{pav,d}^{min}$  = minimal daily pavement temperature at distance  $d$  from the surface, (°C);

$T_{air}^{min}$  = minimal daily air temperature, (°C);

$Day$  = day of the year;

$d$  = distance from the surface (cm);

$Cum\_SR$  = cumulative solar radiation (W/m<sup>2</sup>)and

$Lat$  = latitude of the section, (degrees).

Figures 4.35 and 4.36 present actual maximal and minimal daily pavement temperature versus predictions from the model including air temperature, depth from the surface, and day of the year at the Al-Jufroh location. In Appendix J, similar figures for other locations are given.

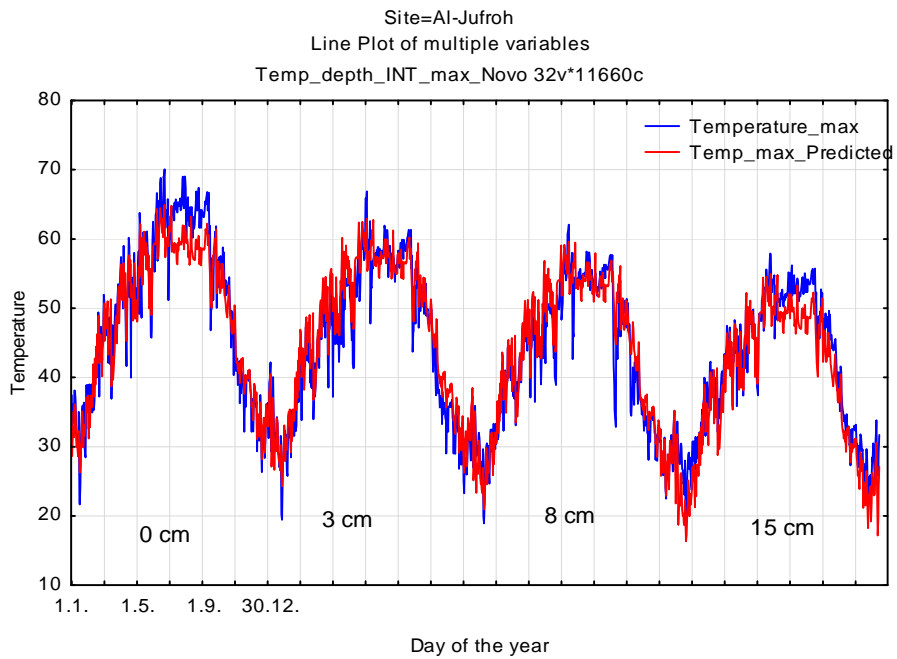


Figure 4.35 Actual maximal daily pavement temperature and predicted maximal daily pavement temperatures from the model including maximal daily air temperature, distance from the surface, and day of the year at the Al-Jufroh location.

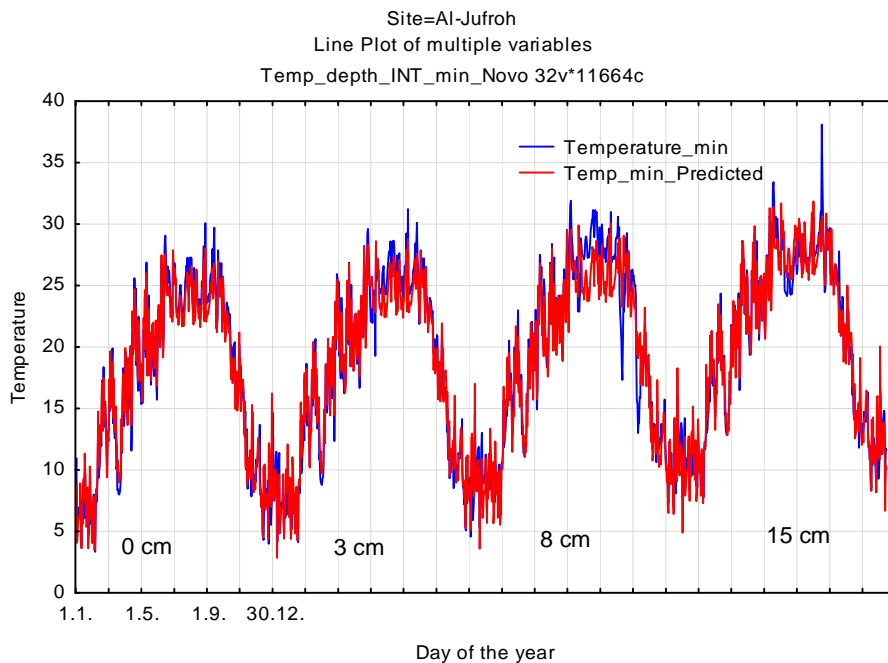


Figure 4.36 Actual minimal daily pavement temperature and predicted minimal daily pavement temperatures from the model including minimal daily air temperature, distance from the surface and day of the year at the Al Jufroh location.

## 4.7 Linear modeling for daily pavement temperature prediction incorporating surface (C1) temperature

### 4.7.1 Relationship with the surface temperature

The next models are built for modeling the relationship between maximal and minimal daily temperatures of surface temperature C1 and maximal and minimal daily temperatures of layers C2, C3, C4.

The first model type to predict maximal and minimal daily pavement temperatures is a single linear regression relationship between the surface temperature and the pavement temperature at three different distances from the surface: 3 cm, 8 cm and 15 cm (C2, C3, C4). The model is of the following form:

$$y = A * C1 + B$$

where

$y$  = predicted daily pavement temperature (°C) (maximum or minimum);

$A$  = surface temperature coefficient;

$C1$  = surface daily temperature (°C) (maximum or minimum); and

$B$  = intercept coefficient.

Table 4.89 presents the coefficients for the linear prediction models developed for three depths at station Al-Jufroh. Included with the model coefficients and their standard errors are the standard errors of estimate and the adjusted  $R^2$ . The coefficients statistically different from zero are denoted in red. Tables of coefficients for the pavement temperature for the remaining stations are presented in Appendix K.

Table 4.89 Parameters of the model for predicting daily maximal and minimal pavement temperature from daily maximal and minimal surface temperature at the Al-Jufroh location.

AL-Jufroh	Daily maximal temperatures $y = A * C1_{max} + B$					
layer	B	Std.Err. of B	A	Std.Err. of A	Adjusted $R^2$	Std.Error of estimate
C2	-0.268022	0.193819	0.912981	0.003764	0.993851433	0.85843603
C3	0.711501	0.441118	0.837448	0.008566	0.963307467	1.95373301
C4	0.277176	0.283299	0.821152	0.005502	0.983923239	1.25474684
	Daily minimal temperatures $y = A * C1_{min} + B$					
C2	0.606090	0.166621	1.002388	0.008978	0.971623943	1.21165662
C3	3.014627	0.270463	0.971989	0.014574	0.924341803	1.96679306
C4	4.524688	0.190533	0.947941	0.010267	0.959045582	1.38554525

A graphical example of this linear relationship developed for the Al-Jufroh station is shown in figures 4.37 to 4.39 where the relationship between the maximal daily temperature at three different layers are shown versus the maximal daily surface temperature. In figures 4.40 to

4.42 the relationship between the minimal daily temperature at different layers is shown versus the minimal daily surface temperature. Graphs showing those relations for the remaining locations are presented in Appendix K.

Graphs of the maximal daily pavement temperatures against the maximal daily surface temperature are presented in figures 4.37 to 4.39.

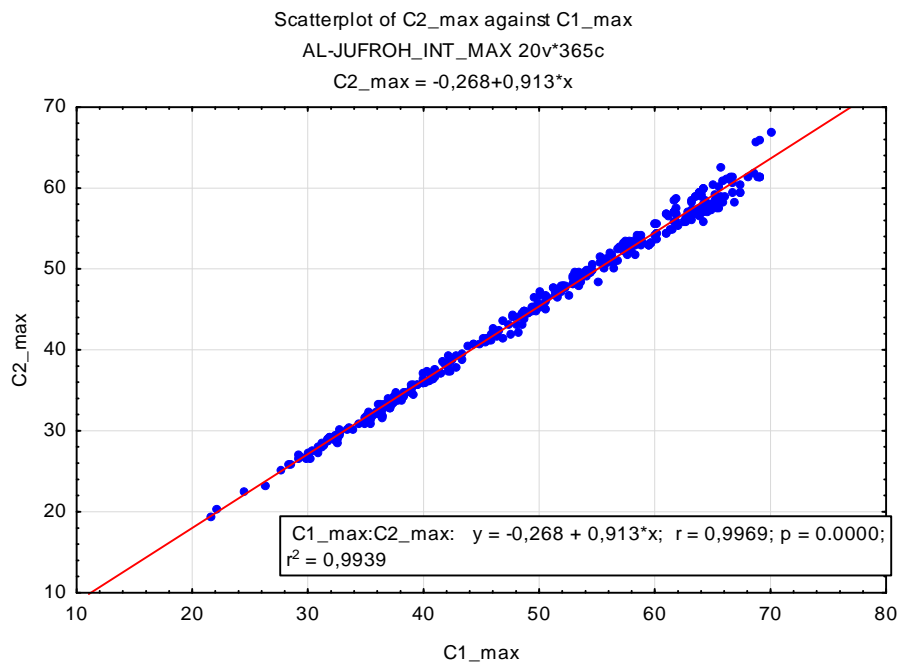


Figure 4.37 Maximal daily temperature at layer C2 versus the maximal daily surface temperature at the Al-Jufroh location.

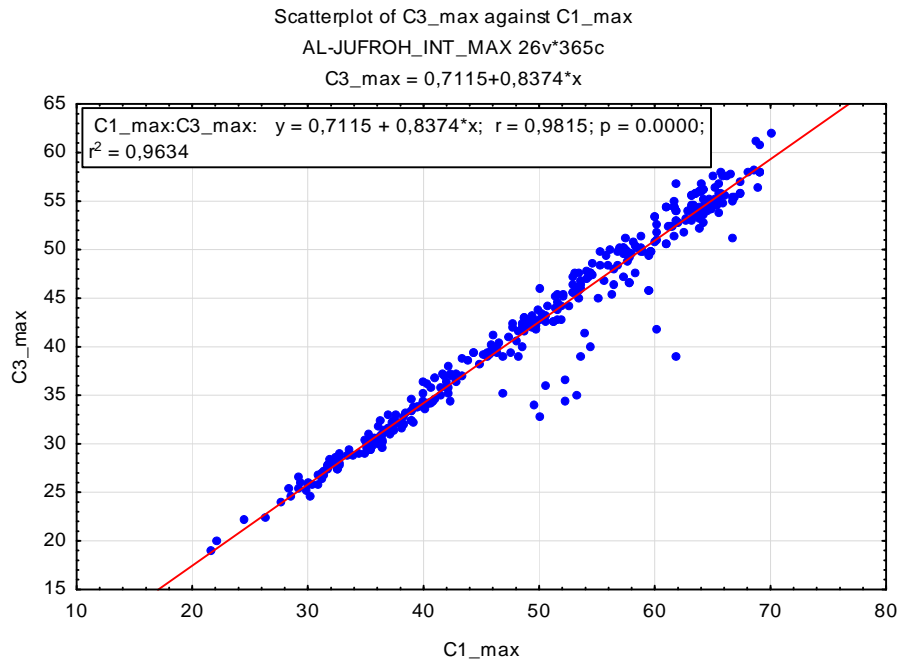


Figure 4.38 Maximal daily temperature at layer C3 versus the maximal daily surface temperature at the Al-Jufroh location.

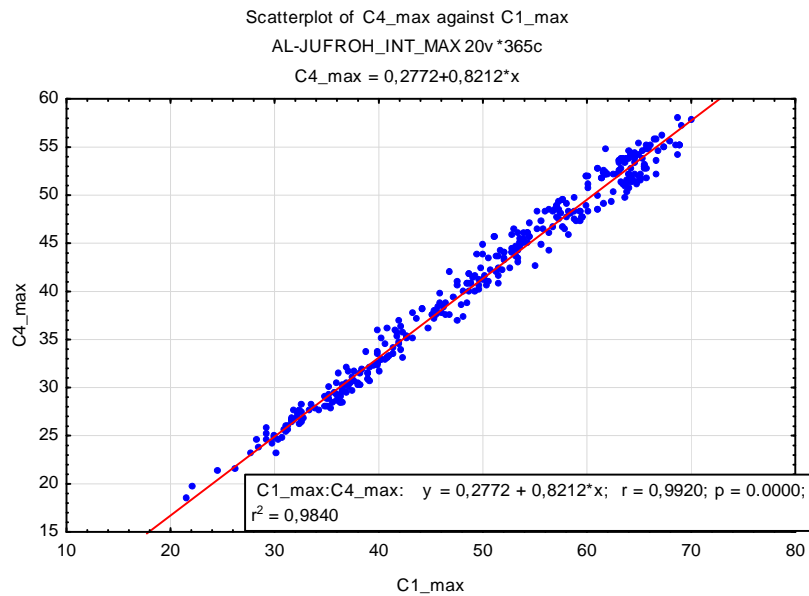


Figure 4.39 Maximal daily temperature at layer C4 versus the maximal daily surface temperature at the Al-Jufroh location.

Graphs of minimal daily temperatures against minimal daily surface temperature are presented in figures 4.40 to 4.42.

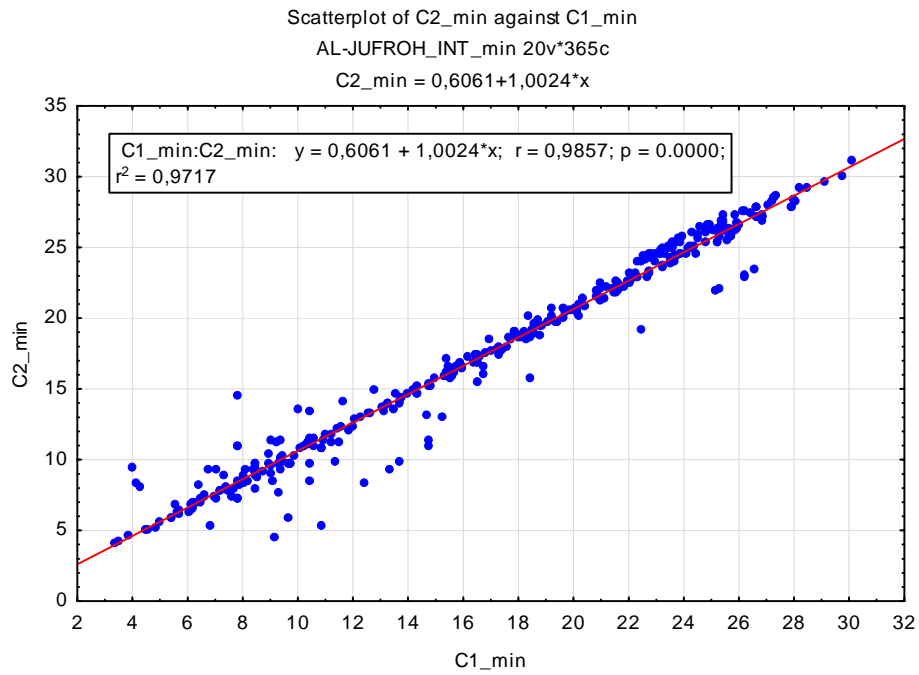


Figure 4.40 Minimal daily temperature at layer C2 versus the minimal daily surface temperature at the Al-Jufroh location.

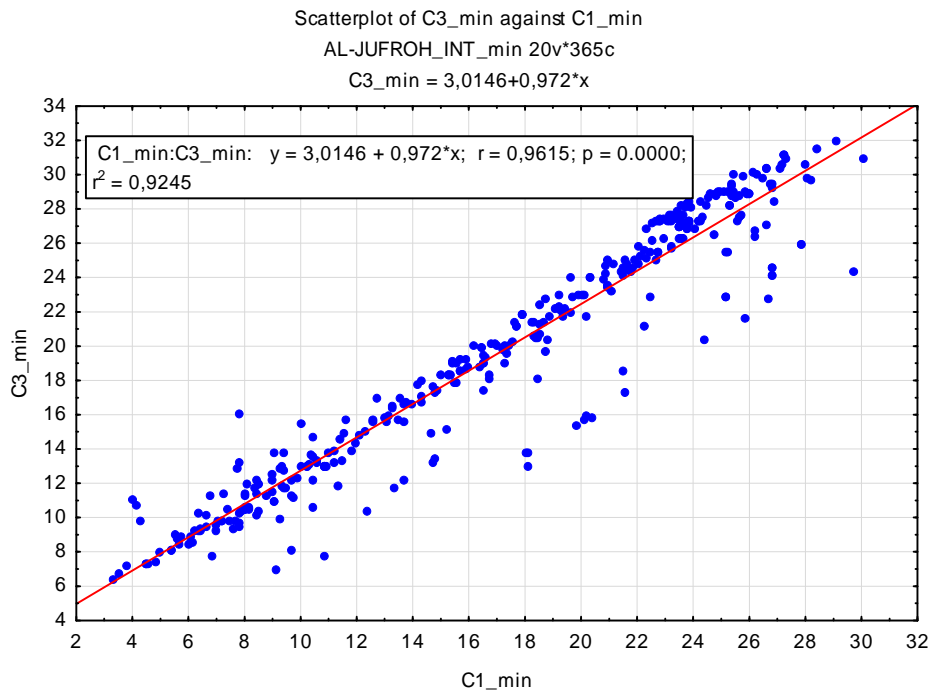


Figure 4.41 Minimal daily temperature at layer C3 versus the minimal daily surface temperature at the Al-Jufroh location.

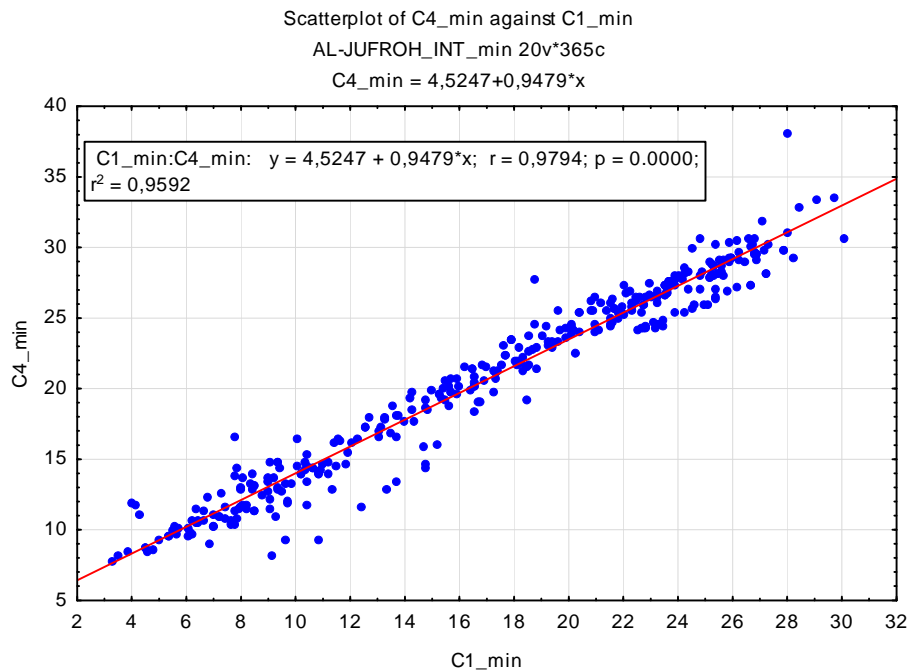


Figure 4.42 Minimal daily temperature at layer C4 versus the minimal daily surface temperature at the Al-Jufroh location.

#### 4.7.1.1 Relationship with surface temperature and latitude

The next model for predicting maximal/minimal daily pavement temperatures at depths C2, C3, C4 from maximal/minimal daily surface temperature C1, was built using data from all stations and includes the latitude of the locations. The model is of the following form:

$$y = A * C1 + B * Lat + C$$

where

$y$  = predicted daily pavement temperature (°C) (maximum or minimum);

$A$  = surface temperature coefficient;

$C1$  = surface daily temperature (°C) (maximum or minimum);

$B$  = latitude coefficient;

$Lat$  = latitude of the location (degrees); and

$C$  = intercept coefficient.

Table 4.90 presents the coefficients for the linear prediction models developed for each depth for all locations. Included with the model coefficients and their standard errors are the standard errors of estimate and the adjusted  $R^2$ . The coefficients statistically different from zero are denoted in red.

Table 4.90 Parameters of the model for predicting pavement temperature from the surface temperature at the Al-Jufroh location.

All locations	Maximal daily temperatures $y = A * C1\_max + B * Lat + C$				
depth	C	B	A	Adjusted R <sup>2</sup>	Std.Error of estimate
C2	-4.37177	0.14449	0.93795	0.958619301	2.24469482
C3	1.207663	-0.086149	0.894940	0.950342756	2.37176669
C4	-3.98304	0.06536	0.83902	0.909167326	3.06019018
	Minimal daily temperatures $y = A * C1\_min + B * Lat + C$				
C2	9.615039	-0.297134	0.948882	0.921141385	2.13630661
C3	13.65339	-0.38388	0.94338	0.873718286	2.76688102
C4	14.52431	-0.35042	0.93140	0.8529213	2.98103002

3D Surface Plot of C2\_max against C1\_max and Latitude  
 $C2\_max = -4,3718+0,938*x+0,1445*y$

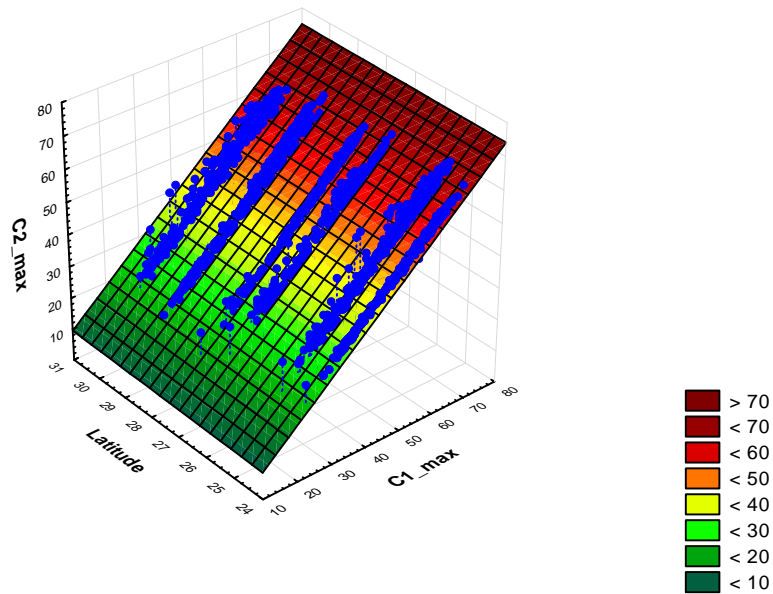


Figure 4.43 Maximal daily C2 temperatures for all locations as a function of the maximal daily surface temperature and latitude.



3D Surface Plot of C3\_max against C1\_max and Latitude  
 $C3\_max = 1,2077+0,8949*x-0,0861*y$

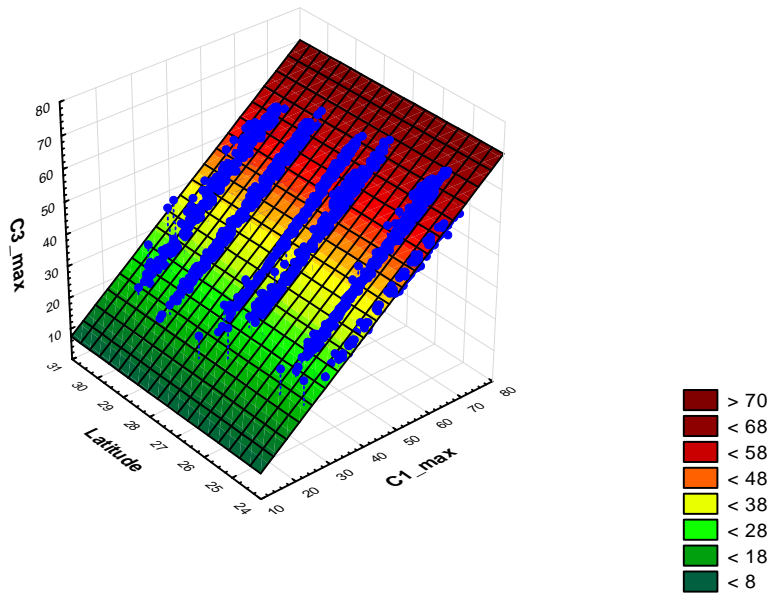


Figure 4.44 Maximal daily C3 temperatures for all locations as a function of the maximal daily surface temperature and latitude.

3D Surface Plot of C4\_max against C1\_max and Latitude  
 $C4\_max = -3,983+0,839*x+0,0654*y$

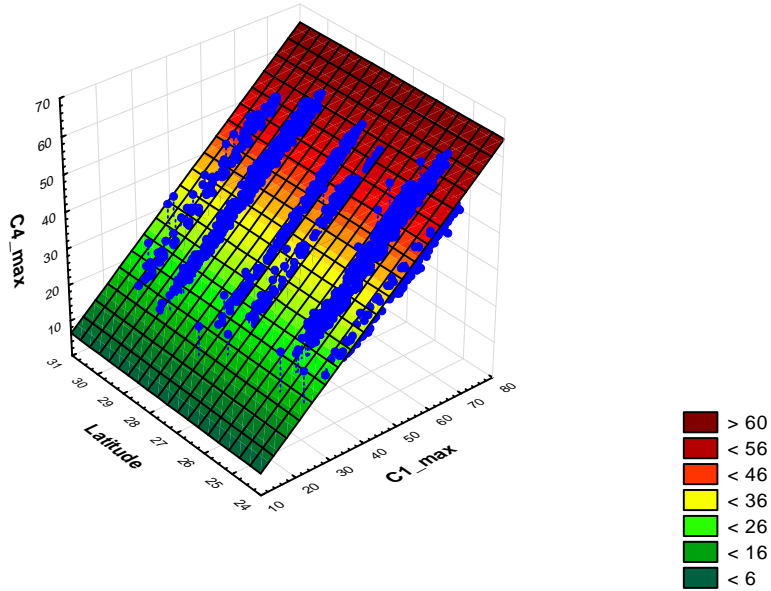


Figure 4.45 Maximal daily C4 temperatures for all locations as a function of the maximal daily surface temperature and latitude.

3D Surface Plot of C2\_min against Latitude and C1\_min  
 $C2_{min} = 9,615 - 0,2971 * x + 0,9489 * y$

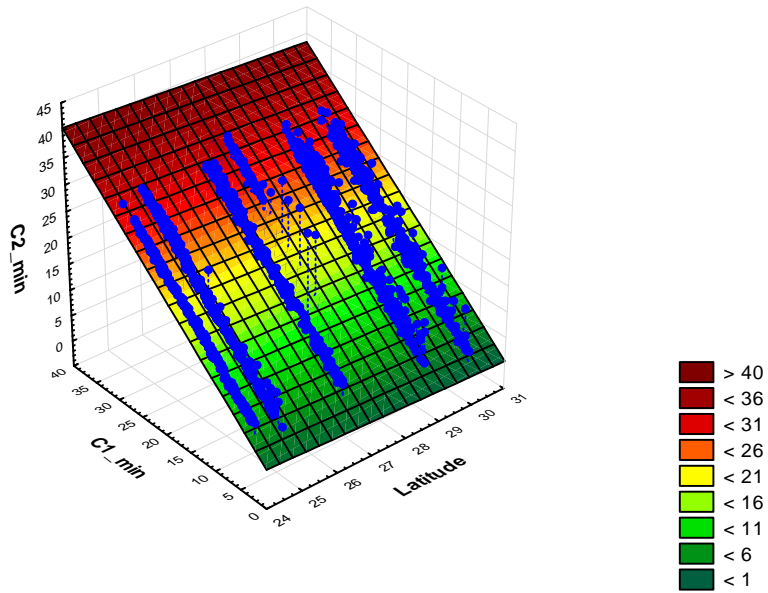


Figure 4.46 Minimal daily C2 temperatures for all locations as a function of the minimal daily surface temperature and latitude.

3D Surface Plot of C3\_min against Latitude and C1\_min  
 $C3_{min} = 13,6534 - 0,3839 * x + 0,9434 * y$

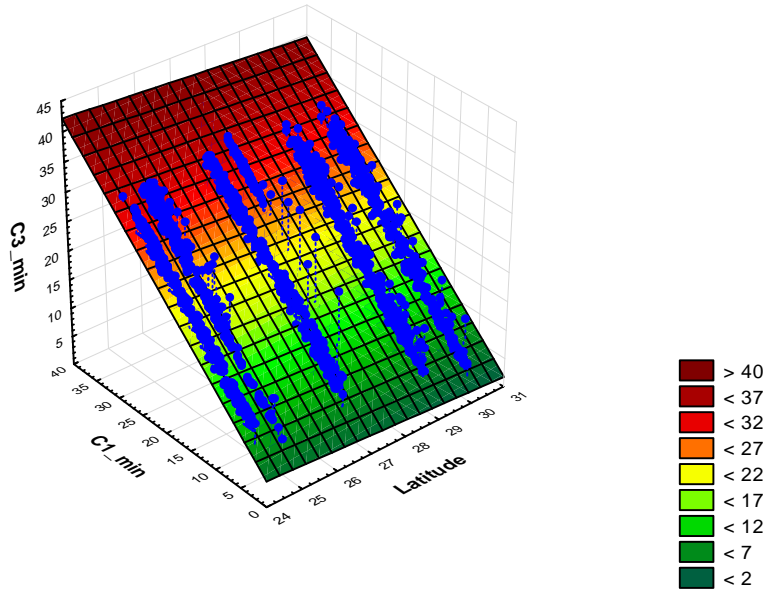


Figure 4.47 Minimal daily C3 temperatures for all locations as a function of the minimal daily surface temperature and latitude.

3D Surface Plot of C4\_min against Latitude and C1\_min  
 $C4\_min = 14,5243-0,3504*x+0,9314*y$

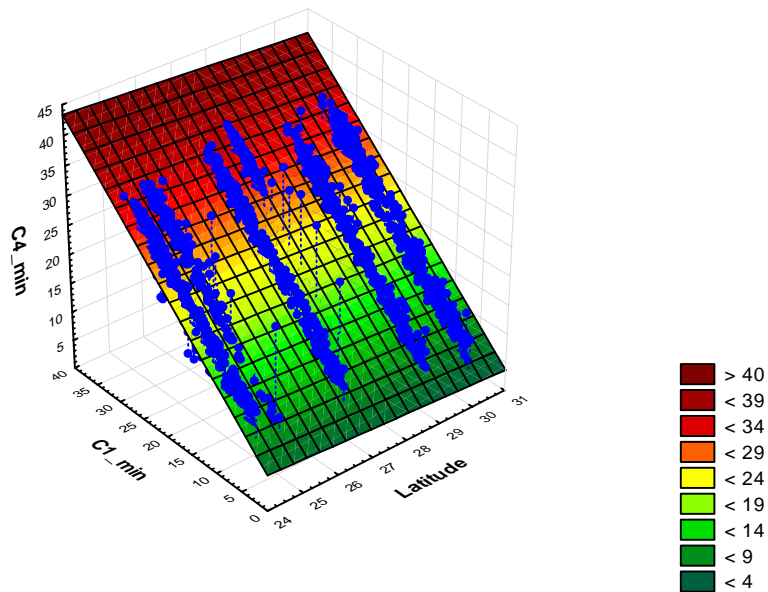


Figure 4.48 Minimal daily C4 temperatures for all locations as a function of the minimal daily surface temperature and latitude.

#### 4.7.2 Relationship with the surface temperature and day of the year

The next model for predicting maximal (minimal) daily pavement temperatures at three different layers includes maximal (minimal) daily surface temperatures and the day of the year. The days of the year are coded from 0, for first of January, to 365 for December 31<sup>st</sup>. As there exists a nonlinear relation between maximal (minimal) daily temperatures with the day of the year, the square of the day of the year is included in the model.

Tables 4.91 to 4.93 give the characteristics of the models for daily minimal pavement temperatures for three layers at the Brak location, where the model is of the form:

$$y_{max} = A * C1_{max} + B * Day + C * Day^2 + D$$

where

$y_{max}$  = predicted maximal daily pavement temperature (°C);

A = surface temperature coefficient;

$C1_{max}$  = maximal daily surface temperature (°C);

B = coefficient for the day of the year;

Day = day of the year;

C = coefficient for the square of the day of the year;

D = intercept coefficient.

Table 4.91 Characteristics of the model for predicting maximal daily C2 temperature from maximal daily surface temperature and day of the year at the Brak location.

Brak C2_max	Regression Summary for Dependent Variable: C2_max (BRAK_C1_Max) R= .99075740 R <sup>2</sup> = .98160023 Adjusted R <sup>2</sup> = .98144732 F(3,361)=6419.6 p<0.0000 Std.Error of estimate: 1.5899					
	b*	Std.Err. of b*	b	Std.Err. of b	t(361)	p-value
Intercept			-3.56358	0.642157	-5.54939	0.000000
C1_max	0.933414	0.022865	0.95648	0.023430	40.82280	0.000000
Day	0.251828	0.089860	0.02779	0.009918	2.80245	0.005345
Day <sup>2</sup>	-0.230074	0.090854	-0.00007	0.000027	-2.53236	0.011753

$$y_{max} = 0.95648 * C1_{max} + 0.02779 * Day - 0.00007 * Day^2 - 3.56358$$

Table 4.92 Characteristics of the model for predicting maximal daily C3 temperature from maximal daily surface temperature and day of the year at the Brak location.

Brak C3_max	Regression Summary for Dependent Variable: C3_max (BRAK_C1_Max) R= .99129707 R <sup>2</sup> = .98266989 Adjusted R <sup>2</sup> = .98252587 F(3,361)=6823.3 p<0.0000 Std.Error of estimate: 1.5040					
	b*	Std.Err. of b*	b	Std.Err. of b	t(361)	p-value
Intercept			-4.35153	0.607452	-7.16357	0.000000
C1_max	0.923944	0.022190	0.92284	0.022164	41.63702	0.000000
Day	0.297699	0.087209	0.03203	0.009382	3.41363	0.000714
Day <sup>2</sup>	-0.268013	0.088173	-0.00008	0.000025	-3.03962	0.002542

$$y_{max} = 0.92284 * C1_{max} + 0.03203 * Day - 0.00008 * Day^2 - 4.35153$$

Table 4.93 Characteristics of the model for predicting maximal daily C4 temperature from maximal daily surface temperature and day of the year at the Brak location.

Brak C4_max	Regression Summary for Dependent Variable: C4_max (BRAK_C1_Max) R= .99028015 R <sup>2</sup> = .98065477 Adjusted R <sup>2</sup> = .98049401 F(3,361)=6100.0 p<0.0000 Std.Error of estimate: 1.4647					
	b*	Std.Err. of b*	b	Std.Err. of b	t(361)	p-value
Intercept			-4.65039	0.591605	-7.86063	0.000000
C1_max	0.893677	0.023445	0.82280	0.021586	38.11786	0.000000
Day	0.423983	0.092140	0.04204	0.009137	4.60152	0.000006
Day <sup>2</sup>	-0.383368	0.093158	-0.00010	0.000024	-4.11522	0.000048

$$y_{max} = 0.82280 * C1_{max} + 0.04204 * Day - 0.00010 * Day^2 - 4.65039$$

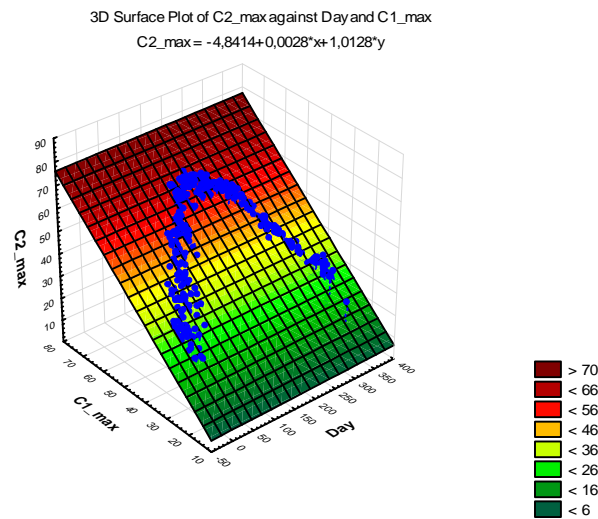


Figure 4.49 Maximal daily C2 temperature as a function of maximal daily surface temperature and the day of the year for the Brak station.

Figures 4.91 to 4.96 give the characteristics of the models for minimal daily temperatures at the Brak location, where the model is of the form:

$$y_{min} = A * C1_{min} + B * Day + C * Day^2 + D$$

where

$y_{min}$  = predicted minimal daily pavement temperature (°C);

$A$  = surface temperature coefficient;

$C1_{min}$  = minimal daily surface temperature (°C);

$B$  = coefficient for the day of the year;

$Day$  = day of the year;

$C$  = coefficient for square of the day of the year;

$D$  = intercept coefficient.

Table 4.94 Characteristics of the model for predicting minimal daily C2 temperature from minimal daily surface temperature and day of the year at the Brak location

Brak C2_min	Regression Summary for Dependent Variable: C2_min (BRAK_C1_min)					
	b*	Std.Err. of b*	b	Std.Err. of b	t(361)	p-value
Intercept			-3.95149	0.505779	-7.8127	0.000000
C1_min	0.64300	0.030623	0.76851	0.036600	20.9975	0.000000
Day	1.38093	0.121687	0.09778	0.008616	11.3482	0.000000
Day <sup>2</sup>	-1.30310	0.120717	-0.00024	0.000023	-10.7946	0.000000

$$y_{min} = 0.76851 * C1_{min} + 0.09778 * Day - 0.00024 * Day^2 - 3.95149$$

Table 4.95 Characteristics of the model for predicting minimal daily C3 temperature from minimal daily surface temperature and day of the year at the Brak location.

<b>Brak C3_min</b>	Regression Summary for Dependent Variable: C3_min (BRAK_C1_min) R= .96033328 R <sup>2</sup> = .92224001 Adjusted R <sup>2</sup> = .92159381 F(3,361)=1427.2 p<0.0000 Std.Error of estimate: 2.1345					
	b*	Std.Err. of b*	b	Std.Err. of b	t(361)	p-value
Intercept			-3.32601	0.501561	-6.6313	0.000000
C1_min	0.62572	0.029829	0.76135	0.036295	20.9768	0.000000
Day	1.46116	0.118535	0.10532	0.008544	12.3269	0.000000
Day <sup>2</sup>	-1.38670	0.117590	-0.00027	0.000022	-11.7927	0.000000

$$y_{min} = 0.76135 * C1_{min} + 0.10532 * Day - 0.00027 * Day^2 - 3.32601$$

Table 4.96 Characteristics of the model for predicting minimal daily C4 temperature from minimal daily surface temperature and day of the year at the Brak location.

<b>Brak C4_min</b>	Regression Summary for Dependent Variable: C4_min (BRAK_C1_min) R= .94699007 R <sup>2</sup> = .89679020 Adjusted R <sup>2</sup> = .89593250 F(3,361)=1045.6 p<0.0000 Std.Error of estimate: 2.5992					
	b*	Std.Err. of b*	b	Std.Err. of b	t(361)	p-value
Intercept			-1.08277	0.610765	-1.7728	0.077104
C1_min	0.53521	0.034366	0.68832	0.044197	15.5739	0.000000
Day	1.76637	0.136562	0.13458	0.010404	12.9346	0.000000
Day <sup>2</sup>	-1.73203	0.135473	-0.00035	0.000027	-12.7850	0.000000

$$y_{min} = 0.68832 * C1_{min} + 0.13458 * Day - 0.00035 * Day^2 - 1.08277$$

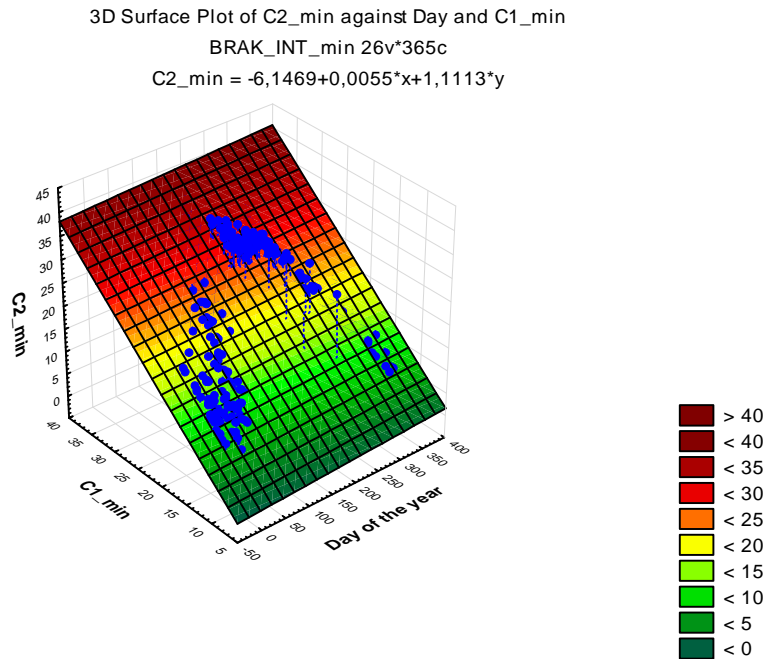


Figure 4.50 Minimal daily C2 temperature as a function of minimal daily surface temperature and the day of the year for the Brak station.

Appendix L presents the tables and figures of the models for predicting maximal (minimal) daily pavement temperatures at three different depths depending on maximal (minimal) daily surface temperatures and the day of the year for the remaining locations.

From the tables in Appendix L for the models for predicting maximal (minimal) daily pavement temperatures at three different layers depending on maximal (minimal) daily surface temperatures and the day of the year, it can be seen that the surface temperature coefficients are lower compared to the coefficients in the models that did not include the day of the year. This means that the day of the year has an effect on the temperature of the pavement. Also, adjusted  $R^2$  are higher for the models which include the day of the year, especially for maximal daily temperatures. The standard errors of the models both for maximal and minimal daily temperatures are lower compared to the models which did not include the day of the year. This means that the models with the surface temperature and the day of the year better explain maximal and minimal daily temperatures of the pavement than the models including only maximal and minimal daily surface temperature.

#### ***4.7.2.1 Relationship with surface temperature, day of the year, and latitude***

The next model for predicting maximal (minimal) daily pavement temperatures at different depths from maximal (minimal) daily surface temperatures and the day of the year was built using data from all stations and includes the latitude of the locations.

The model for maximal daily temperatures is of the following form:

$$y_{max} = A * C1_{max} + B * Day + C * Day^2 + D * Lat + E$$

where

$y_{max}$  = predicted maximal daily pavement temperature (°C);

$A$  = surface temperature coefficient;

$C1_{max}$  = maximal daily surface temperature (°C);

$B$  = coefficient for the day of the year;

$Day$  = day of the year;

$C$  = coefficient for the square of the day of the year;

$Day^2$  = square of the day of the year;

$D$  = latitude coefficient;

$Lat$  = latitude of the location (degrees); and

$E$  = intercept coefficient.

Table 4.97 Characteristics of the model for predicting maximal daily C2 temperature from maximal daily surface temperature and day of the year for all locations.

All locations C2_max	Regression Summary for Dependent Variable: C2_max (Max_all_locations) R= .98129485 R <sup>2</sup> = .96293959 Adjusted R <sup>2</sup> = .96288865 F(4,2910)=18903. p<0.0000 Std.Error of estimate: 2.1257					
	b*	Std.Err. of b*	b	Std.Err. of b	t(2911)	p-value
Intercept			1.248690	0.672633	1.8564	0.063494
C1_max	0.845656	0.008674	0.807009	0.008278	97.4942	0.000000
Day	0.596634	0.033283	0.062274	0.003474	17.9258	0.000000
Day <sup>2</sup>	-0.594768	0.034186	-0.000165	0.000009	-17.3981	0.000000
Latitude	0.006368	0.003806	0.033706	0.020142	1.6734	0.094359

$$y_{max} = 0.807009 * C1_{max} + 0.062274 * Day - 0.000165 * Day^2 + 0.033706 * Lat + 1.248690$$

Table 4.98 Characteristics of the model for predicting maximal daily C3 temperature from maximal daily surface temperature and day of the year for all locations.

All locations C3_max	Regression Summary for Dependent Variable: C3_max (Max_all_locations) R= .97582817 R <sup>2</sup> = .95224062 Adjusted R <sup>2</sup> = .95217495 F(4,2909)=14500. p<0.0000 Std.Error of estimate: 2.3276					
	b*	Std.Err. of b*	b	Std.Err. of b	t(2910)	p-value
Intercept			4.209074	0.736533	5.71471	0.000000
C1_max	0.891308	0.009846	0.820492	0.009064	90.52562	0.000000
Day	0.362333	0.037790	0.036472	0.003804	9.58807	0.000000
Day <sup>2</sup>	-0.350674	0.038815	-0.000094	0.000010	-9.03458	0.000000
Latitude	-0.029214	0.004321	-0.149149	0.022058	-6.76170	0.000000

$$y_{max} = 0.820492 * C1_{max} + 0.036472 * Day - 0.000094 * Day^2 - 0.149149 * Lat + 4.209074$$



Table 4.99 Characteristics of the model for predicting maximal daily C3 temperature from maximal daily surface temperature and day of the year for all locations.

All locations C4_max	Regression Summary for Dependent Variable: C4_max (Max_all_locations) R= .95748951 R <sup>2</sup> = .91678616 Adjusted R <sup>2</sup> = .91667178 F(4,2910)=8015.0 p<0.0000 Std.Error of estimate: 2.9311					
	b*	Std.Err. of b*	b	Std.Err. of b	t(2911)	p-value
Intercept			1.179969	0.927448	1.2723	0.203377
C1_max	0.804243	0.012997	0.706221	0.011413	61.8770	0.000000
Day	0.688187	0.049874	0.066096	0.004790	13.7986	0.000000
Day <sup>2</sup>	-0.655568	0.051226	-0.000167	0.000013	-12.7976	0.000000
Latitude	-0.009647	0.005702	-0.046986	0.027773	-1.6918	0.090796

$$y_{max} = 0.706221 * C1_{max} + 0.066096 * Day - 0.000167 * Day^2 - 0.046986 * Lat + 1.179969$$

The model for minimum temperatures is of the following form:

$$y_{min} = A * C1_{min} + B * Day + C * Day^2 + D * Lat + E$$

where

$y_{min}$  = predicted minimal daily pavement temperature (°C);

$A$  = surface temperature coefficient;

$C1_{min}$  = minimal daily surface temperature (°C);

$B$  = coefficient for the day of the year;

$Day$  = day of the year;

$C$  = coefficient for the square of the day of the year;

$Day^2$  = square of the day of the year;

$D$  = latitude coefficient;

$Lat$  = latitude of the location (degrees); and

$E$  = intercept coefficient.

Table 4.100 Characteristics of the model for predicting minimal daily C2 temperature from minimal daily surface temperature and day of the year for all locations.

All locations C2_min	Regression Summary for Dependent Variable: C2_min (Min_all_locations) R= .97139820 R <sup>2</sup> = .94361446 Adjusted R <sup>2</sup> = .94353698 F(4,2911)=12179. p<0.0000 Std.Error of estimate: 1.8077					
	b*	Std.Err. of b*	b	Std.Err. of b	t(2911)	p-value
Intercept			8.683694	0.447654	19.3982	0.00
C1_min	0.73770	0.007869	0.732315	0.007811	93.7528	0.00
Day	1.05453	0.031182	0.075892	0.002244	33.8182	0.00
Day <sup>2</sup>	-1.02861	0.031217	-0.000196	0.000006	-32.9503	0.00
Latitude	-0.08288	0.004401	-0.302433	0.016061	-18.8306	0.00

$$y_{min} = 0.732315 * C1_{min} + 0.075892 * Day - 0.000196 * Day^2 - 0.302433 * Lat + 8.683694$$

Table 4.101 Characteristics of the model for predicting minimal C3 temperature from minimal daily surface temperature and day of the year for all locations.

All locations C3_min	Regression Summary for Dependent Variable: C3_min (Min_all_locations) R= .95468991 R <sup>2</sup> = .91143283 Adjusted R <sup>2</sup> = .91131113 F(4,2911)=7489.2 p<0.0000 Std.Error of estimate: 2.3188					
	b*	Std.Err. of b*	b	Std.Err. of b	t(2911)	p-value
Intercept			12.67724	0.574217	22.0774	0.00
C1_min	0.64153	0.009862	0.65181	0.010020	65.0535	0.00
Day	1.37419	0.039081	0.10122	0.002879	35.1630	0.00
Day <sup>2</sup>	-1.36488	0.039124	-0.00027	0.000008	-34.8861	0.00
Latitude	-0.10470	0.005516	-0.39101	0.020602	-18.9796	0.00

$$y_{min} = 0.65181 * C1_{min} + 0.10122 * Day - 0.00027 * Day^2 - 0.39101 * Lat + 12.67724$$

Table 4.102 Characteristics of the model for predicting minimal daily C4 temperature from minimal daily surface temperature and day of the year for all locations.

All locations C4_min	Regression Summary for Dependent Variable: C4_min (Min_all_locations) R= .94685214 R <sup>2</sup> = .89652897 Adjusted R <sup>2</sup> = .89638679 F(4,2911)=6305.6 p<0.0000 Std.Error of estimate: 2.5021					
	b*	Std.Err. of b*	b	Std.Err. of b	t(2911)	p-value
Intercept			13.38319	0.619612	21.5993	0.00
C1_min	0.61068	0.010659	0.61941	0.010812	57.2914	0.00
Day	1.47736	0.042241	0.10864	0.003106	34.9745	0.00
Day <sup>2</sup>	-1.45873	0.042288	-0.00028	0.000008	-34.4954	0.00
Latitude	-0.09603	0.005962	-0.35805	0.022230	-16.1064	0.00

$$y_{min} = 0.61941 * C1_{min} + 0.10864 * Day - 0.00028 * Day^2 - 0.35805 * Lat + 13.38319$$

Most of the coefficients of the latitude are negative, indicating that as latitude increases, pavement temperatures decreases. Compared with the models including only surface temperature and latitude, the models including the surface temperature, the day of the year and latitude have similar adjusted R<sup>2</sup> and standard error of estimate, indicating similar fit to the data.

### 4.7.3 Relationship with surface temperature and wind speed

The next model for predicting maximal (minimal) daily pavement temperatures at three different layers includes maximal (minimal) daily surface temperatures and wind speed.

Tables 4.103 to 4.105 give the characteristics of the models for daily maximal daily pavement temperatures for four layers at the Awbari location, where the model is of the form:

$$y_{max} = A * C1_{max} + B * WS + C$$

where

$y_{max}$  = predicted maximal daily pavement temperature (°C);

$A$  = surface temperature coefficient;

$C1_{max}$  = maximal daily surface temperature (°C);

$B$  = coefficient for the wind speed;

$WS$  = wind speed(m/s); and

$C$  = intercept coefficient.

Table 4.103 Characteristics of the model for predicting maximal daily C2 temperature from maximal daily surface temperature and the wind speed for the Awbari location.

Awbari C2_max	Regression Summary for Dependent Variable: C2_max (AWBARI_C1_max) R= .98201422 R <sup>2</sup> = .96435193 Adjusted R <sup>2</sup> = .96415444 F(2,361)=4882.9 p<0.0000 Std.Error of estimate: 1.9936					
	b*	Std.Err. of b*	b	Std.Err. of b	t(361)	p-value
Intercept			1.053706	0.522408	2.01702	0.044434
C1_max	0.976767	0.009997	0.924311	0.009460	97.70546	0.000000
Wind Speed, (m/s)	-0.040475	0.009997	-0.001363	0.000337	-4.04867	0.000063

$$y_{max} = 0.924311 * C1_{max} - 0.001363 * WS + 1.053706$$

Table 4.104 Characteristics of the model for predicting maximal daily C3 temperature from maximal daily surface temperature and wind speed for the Awbari location.

Awbari C3_max	Regression Summary for Dependent Variable: C3_max (AWBARI_C1_max) R= .97651939 R <sup>2</sup> = .95359012 Adjusted R <sup>2</sup> = .95333300 F(2,361)=3708.8 p<0.0000 Std.Error of estimate: 2.2473					
	b*	Std.Err. of b*	b	Std.Err. of b	t(361)	p-value
Intercept			0.436131	0.588890	0.74060	0.459419
C1_max	0.970706	0.011407	0.907511	0.010664	85.09977	0.000000
Wind Speed, (m/s)	-0.044166	0.011407	-0.001469	0.000379	-3.87194	0.000128

$$y_{max} = 0.907511 * C1_{max} - 0.001469 * WS + 0.436131$$

Table 4.105 Characteristics of the model for predicting maximal daily C4 temperature from maximal daily surface temperature and wind speed for the Awbari location.

Awbari C4_max	Regression Summary for Dependent Variable: C4_max (AWBARI_C1_max) R= .96271533 R <sup>2</sup> = .92682080 Adjusted R <sup>2</sup> = .92641538 F(2,361)=2286.0 p<0.0000 Std.Error of estimate: 2.5692					
	b*	Std.Err. of b*	b	Std.Err. of b	t(361)	p-value
Intercept			-1.93018	0.673259	-2.86692	0.004388
C1_max	0.955274	0.014323	0.81311	0.012192	66.69292	0.000000
Wind Speed, (m/s)	-0.054267	0.014323	-0.00164	0.000434	-3.78865	0.000177

$$y_{max} = 0.81311 * C1_{max} - 0.00164 * WS - 1.93018$$

The model for minimal daily temperatures is of the following form:

$$y_{min} = A * C1_{min} + B * WS + C$$

where

$y_{min}$ = predicted minimal daily pavement temperature (°C);

$A$  = surface temperature coefficient;

$C1_{min}$ = minimal daily surface temperature (°C);

$B$  = coefficient for the wind speed;

$WS$  = wind speed (m/s); and

$C$  = intercept coefficient.

Table 4.106 Characteristics of the model for predicting minimal daily C2 temperature from minimal daily surface temperature and the wind speed for the Awbari location.

Awbari C2_min	Regression Summary for Dependent Variable: C2_min (AWBARI_C1_min) R= .98061768 R <sup>2</sup> = .96161104 Adjusted R <sup>2</sup> = .96139836 F(2,361)=4521.4 p<0.0000 Std.Error of estimate: 1.4617					
	b*	Std.Err. of b*	b	Std.Err. of b	t(361)	p-value
Intercept			2.648648	0.198539	13.34071	0.000000
C1_min	0.978914	0.010688	0.939564	0.010258	91.59236	0.000000
Wind Speed, (m/s)	0.006409	0.010688	0.000448	0.000748	0.59962	0.549133

$$y_{min} = 0.939564 * C1_{min} + 0.000448 * WS + 2.648648$$

Table 4.107 Characteristics of the model for predicting minimal daily C3 temperature from minimal daily surface temperature and wind speed for the Awbari location.

Awbari C3_min	Regression Summary for Dependent Variable: C3_min (AWBARI_C1_min) R= .97275829 R <sup>2</sup> = .94625868 Adjusted R <sup>2</sup> = .94596095 F(2,361)=3178.2 p<0.0000 Std.Error of estimate: 1.6927					
	b*	Std.Err. of b*	b	Std.Err. of b	t(361)	p-value
Intercept			5.692666	0.229911	24.76035	0.000000
C1_min	0.982322	0.012646	0.922780	0.011879	77.68146	0.000000
Wind Speed, (m/s)	-0.039194	0.012646	-0.002684	0.000866	-3.09942	0.002091

$$y_{min} = 0.922780 * C1_{min} - 0.002684 * WS + 5.692666$$

Table 4.108 Characteristics of the model for predicting minimal daily C4 temperature from minimal daily surface temperature and wind speed for the Awbari location.

Awbari C4_min	Regression Summary for Dependent Variable: C4_min (AWBARI_C1_min) R= .97674881 R <sup>2</sup> = .95403824 Adjusted R <sup>2</sup> = .95378361 F(2,361)=3746.7 p<0.0000 Std.Error of estimate: 1.5866					
	b*	Std.Err. of b*	b	Std.Err. of b	t(361)	p-value
Intercept			7.060357	0.215496	32.76335	0.000000
C1_min	0.988392	0.011694	0.941042	0.011134	84.51791	0.000000
Wind Speed, (m/s)	-0.048596	0.011694	-0.003373	0.000812	-4.15545	0.000041

$$y_{min} = 0.941042 * C1_{min} - 0.003373 * WS + 7.060357$$

Appendix M presents the tables of the characteristics of the models for predicting maximal (minimal) daily pavement temperatures at different depths depending on maximal (minimal) daily surface temperatures and wind speed for the remaining locations.

From tables 4.100 to 4.105 and the tables in Appendix M for the models for predicting maximal (minimal) daily pavement temperatures at different depths depending on maximal (minimal) daily surface temperatures and wind speed, it can be seen the wind speed coefficients are negative, so as wind speed increases, the pavement temperature decreases. However, these coefficients are small, especially for deeper layers, and are usually not statistically significant. Also, it can be seen that the surface temperature coefficients are similar to the coefficients in the models that did not include wind speed, meaning wind speed has little effect on the temperature of pavement. Furthermore, adjusted R<sup>2</sup> are similar for the models that include wind speed. The standard errors of the models both for maximal (minimal) daily temperatures are similar to the standard errors of the models that did not include the wind speed. This means that the models with surface temperature and the wind speed do not better explain maximal (minimal) daily temperatures of the pavement than the models including only the surface temperature.

#### 4.7.3.1 Relationship with surface temperature, wind speed, and latitude

The next model for predicting maximal (minimal) daily pavement temperatures at three different layers from maximal (minimal) daily surface temperatures and the wind speed was built using data from all stations and included the latitude of the locations.

The model for maximal daily pavement temperatures is of the following form:

$$y_{max} = A * C1_{max} + B * WS + C * Lat + D$$

where

$y_{max}$ = predicted maximal daily pavement temperature (°C);

$A$  = surface temperature coefficient;

$C1_{max}$ =maximal daily surface temperature (°C);

$B$  = coefficient for the wind speed;

$WS$  = wind speed (m/s);

$C$  =latitude coefficient;

$Lat$  = latitude of the location (degrees); and

$D$  = intercept coefficient.

Table 4.109 Characteristics of the model for predicting maximal daily C2 temperature from maximal daily surface temperature and wind speed for all locations.

All locations C2_max	Regression Summary for Dependent Variable: C2_max (Max_all_locations) R= .97910576 R <sup>2</sup> = .95864809 Adjusted R <sup>2</sup> = .95860547 F(3,2911)=22495. p<0.0000 Std.Error of estimate: 2.2451					
	b*	Std.Err. of b*	b	Std.Err. of b	t(2911)	p-value
Intercept			-4.36539	0.606157	-7.2017	0.000000
C1_max	0.982846	0.003815	0.93793	0.003641	257.6106	0.000000
Wind Speed, (m/s)	-0.000621	0.003773	-0.00004	0.000261	-0.1645	0.869369
Latitude	0.027275	0.003815	0.14437	0.020195	7.1486	0.000000

$$y_{max} = 0.93793 * C1_{max} - 0.00004 * WS + 0.14437C * Lat - 4.36539$$

Table 4.110 Characteristics of the model for predicting maximal daily C3 temperature from maximal daily surface temperature and wind speed for all locations.

All locations C3_max	Regression Summary for Dependent Variable: C3_max (Max_all_locations) R= .97538798 R <sup>2</sup> = .95138171 Adjusted R <sup>2</sup> = .95133158 F(3,2910)=18981. p<0.0000 Std.Error of estimate: 2.3480					
	b*	Std.Err. of b*	b	Std.Err. of b	t(2910)	p-value
Intercept			0.892980	0.633985	1.4085	0.159084
C1_max	0.973279	0.004137	0.895951	0.003809	235.2421	0.000000
Wind Speed, (m/s)	0.031733	0.004092	0.002117	0.000273	7.7553	0.000000
Latitude	-0.015719	0.004138	-0.080253	0.021124	-3.7992	0.000148

$$y_{max} = 0.895951 * C1_{max} + 0.002117 * WS - 0.080253 * Lat + 0.892980$$

Table 4.111 Characteristics of the model for predicting maximal daily C4 temperature from maximal daily surface temperature and wind speed for all locations.

All locations C4_max	Regression Summary for Dependent Variable: C4_max (Max_all_locations) R= .95494046 R <sup>2</sup> = .91191129 Adjusted R <sup>2</sup> = .91182050 F(3,2911)=10045. p<0.0000 Std.Error of estimate: 3.0152					
	b*	Std.Err. of b*	b	Std.Err. of b	t(2911)	p-value
Intercept			-3.49288	0.814079	-4.2906	0.000018
C1_max	0.953675	0.005568	0.83744	0.004890	171.2641	0.000000
Wind Speed, (m/s)	-0.051840	0.005507	-0.00330	0.000351	-9.4137	0.000000
Latitude	0.011536	0.005569	0.05619	0.027122	2.0716	0.038394

$$y_{max} = 0.83744 * C1_{max} - 0.00330 * WS + 0.05619 * Lat - 3.49288$$

The model for minimal daily pavement temperatures is of the following form:

$$y_{min} = A * C1_{min} + B * WS + C * Lat + D$$

where

$y_{min}$ = predicted minimal daily pavement temperature (°C);

$A$  = surface temperature coefficient;

$C1_{min}$ = minimal daily surface temperature (°C);

$B$  = coefficient for the wind speed;

$WS$  = wind speed (m/s);

$C$  =latitude coefficient;

$Lat$  = latitude of the location; and

$D$  = intercept coefficient.

Table 4.112 Characteristics of the model for predicting minimal daily C2 temperature from minimal daily surface temperature and wind speed for all locations.

All locations C2_min	Regression Summary for Dependent Variable: C2_min (Min_all_locations) R= .95991105 R <sup>2</sup> = .92142922 Adjusted R <sup>2</sup> = .92134822 F(3,2910)=11376. p<0.0000 Std.Error of estimate: 2.1326					
	b*	Std.Err. of b*	b	Std.Err. of b	t(2910)	p-value
Intercept			9.581599	0.524684	18.2617	0.000000
C1_min	0.954204	0.005217	0.947295	0.005179	182.8966	0.000000
Wind Speed, (m/s)	0.018695	0.005218	0.003316	0.000926	3.5828	0.000346
Latitude	-0.081164	0.005197	-0.296034	0.018956	-15.6170	0.000000

$$y_{min} = 0.947295 * C1_{min} + 0.003316 * WS - 0.296034 * Lat + 9.581599$$

Table 4.113 Characteristics of the model for predicting minimal C3 temperature from minimal surface temperature and wind speed for all locations.

All locations C3_min	Regression Summary for Dependent Variable: C3_min (Min_all_locations) R= .93503753 R <sup>2</sup> = .87429518 Adjusted R <sup>2</sup> = .87416559 F(3,2910)=6746.5 p<0.0000 Std.Error of estimate: 2.7611					
	b*	Std.Err. of b*	b	Std.Err. of b	t(2910)	p-value
Intercept			13.61043	0.679326	20.0352	0.000000
C1_min	0.926270	0.006599	0.94127	0.006706	140.3641	0.000000
Wind Speed, (m/s)	0.025235	0.006600	0.00458	0.001198	3.8235	0.000134
Latitude	-0.102465	0.006574	-0.38255	0.024543	-15.5871	0.000000

$$y_{min} = 0.94127 * C1_{min} + 0.00458 * WS - 0.38255 * Lat + 13.61043$$

Table 4.114 Characteristics of the model for predicting minimal daily C4 temperature from minimal daily surface temperature and wind speed for all locations.

All locations C4_min	Regression Summary for Dependent Variable: C4_min (Min_all_locations) R= .92386568 R <sup>2</sup> = .85352780 Adjusted R <sup>2</sup> = .85337679 F(3,2910)=5652.4 p<0.0000 Std.Error of estimate: 2.9749					
	b*	Std.Err. of b*	b	Std.Err. of b	t(2910)	p-value
Intercept			14.46745	0.731917	19.7665	0.000000
C1_min	0.915752	0.007123	0.92883	0.007225	128.5568	0.000000
Wind Speed, (m/s)	0.027548	0.007125	0.00499	0.001291	3.8666	0.000113
Latitude	-0.093486	0.007096	-0.34837	0.026443	-13.1746	0.000000

$$y_{min} = 0.92883 * C1_{min} + 0.00499 * WS - 0.34837 * Lat + 14.46745$$

Most of the coefficients of the latitude are negative, indicating that as latitude increases, pavement temperatures decreases. Compared with the models including only surface temperature and latitude, the models including surface temperature, wind speed and latitude have very similar adjusted R<sup>2</sup> and standard error of estimate, indicating similar fit to the data.

#### 4.7.4 Relationship with surface temperature, and cumulative solar radiation

For each location the daily cumulative solar radiation was determined as a sum of registered solar radiations during the day. Examples for the eight locations on 15<sup>th</sup> of January and 15<sup>th</sup> of June are given in Table 4.115.



Table 4.115 Cumulative solar radiations at eight locations, on 15<sup>th</sup> of January and 15<sup>th</sup> of June

Locations	Latitude	Solar radiation	
		15 <sup>th</sup> of January	15 <sup>th</sup> of June
Al Kufrah	24°17'N	15937.3	32060.8
Al Qatrun	24°56'N	19151.9	25845.9
Ghat	24°59'N	19151.3	29097.9
Awbari	26°46'N	19151.3	29097.9
Brach(SEBHA)	27°31'N	13970.8	33031.5
Hun-joufra	29°02'N	16938.5	32293.9
Awjilah	29°08'N	10108.8	30236.8
hudamis	30°11'N	15756.2	25299.2

The next model for predicting maximal (minimal) daily pavement temperatures at different depths includes maximal (minimal) daily surface temperatures and cumulative solar radiation.

Tables 4.116 to 4.118 give the characteristics of the models for daily maximal daily pavement temperatures for four layers at the Awjilah location, where the model is of the form:

$$y_{max} = A * C1_{max} + B * Cum_{SR} + C$$

where

$y_{max}$  = predicted maximal daily pavement temperature (°C);

$A$  = surface temperature coefficient;

$C1_{max}$  = maximal daily surface temperature (°C);

$B$  = coefficient for the cumulative solar radiation;

$Cum_{SR}$  = cumulative solar radiation (W/m<sup>2</sup>); and

$C$  = intercept coefficient.

Table 4.116 Characteristics of the model for predicting maximal daily C2 temperature from maximal daily surface temperature and cumulative solar radiation for the Awjilah location.

Awjilah C2_max	Regression Summary for Dependent Variable: C2_max (AWJILAH_C1_max) R= .99726217 R <sup>2</sup> = .99453183 Adjusted R <sup>2</sup> = .99450145 F(2,360)=32738. p<0.0000 Std.Error of estimate: .86748					
	b*	Std.Err. of b*	b	Std.Err. of b	t(360)	p-value
Intercept			-4.83180	0.205349	-23.5297	0.000000
C1_max	0.981212	0.005493	1.01524	0.005684	178.6254	0.000000
Cum_SR	0.022592	0.005493	0.00003	0.000008	4.1128	0.000048

$$y_{max} = 1.01524 * C1_{max} + 0.00003 * Cum_{SR} - 4.83180$$

Table 4.117 Characteristics of the model for predicting maximal daily C3 temperature from maximal daily surface temperature and cumulative solar radiation for the Awjilah location.

Awjilah C3_max	Regression Summary for Dependent Variable: C3_max (AWJILAH_C1_max) R= .98250228 R <sup>2</sup> = .96531072 Adjusted R <sup>2</sup> = .96511801 F(2,360)=5008.9 p<0.0000 Std.Error of estimate: 1.9496					
	b*	Std.Err. of b*	b	Std.Err. of b	t(360)	p-value
Intercept			-1.98748	0.461495	-4.30662	0.000021
C1_max	0.949856	0.013836	0.87693	0.012773	68.65330	0.000000
Cum_SR	0.045571	0.013836	0.00006	0.000019	3.29374	0.001087

$$y_{max} = 0.87693A * C1_{max} + 0.00006 * Cum_{SR} - 1.98748$$

Table 4.118 Characteristics of the model for predicting maximal daily C4 temperature from maximal daily surface temperature and cumulative solar radiation for the Awjilah location.

Awjilah C4_max	Regression Summary for Dependent Variable: C4_max (AWJILAH_C1_max) R= .99402629 R <sup>2</sup> = .98808826 Adjusted R <sup>2</sup> = .98802208 F(2,360)=14931. p<0.0000 Std.Error of estimate: 1.0925					
	b*	Std.Err. of b*	b	Std.Err. of b	t(360)	p-value
Intercept			-1.39134	0.701660	-1.98293	0.048135
C1_max	0.828040	0.019217	1.02649	0.023823	43.08783	0.000000
Cum_SR	0.193210	0.019217	0.00025	0.000025	10.05389	0.000000

$$y_{max} = 1.02649 * C1_{max} + 0.00025 * Cum_{SR} - 1.39134$$

Tables 4.119 to 4.121 give the characteristics of the models for daily minimal pavement temperatures for four layers at the Awjilah location, where the model is of the form:

$$y_{min} = A * C1_{min} + B * Cum_{SR} + C$$

where

$y_{min}$ = predicted minimal daily pavement temperature (°C);

$A$  = surface temperature coefficient;

$C1_{min}$ = minimal daily surface temperature (°C);

$B$  = coefficient for the cumulative solar radiation;

$Cum_{SR}$  = cumulative solar radiation (W/m<sup>2</sup>); and

$C$  = intercept coefficient.

Table 4.119 Characteristics of the model for predicting minimal daily C2 temperature from minimal daily surface temperature and cumulative solar radiation for the Awjilah location.

Awjilah C2_min	Regression Summary for Dependent Variable: C2_min (AWJILAH_C1_min) R= .98435714 R <sup>2</sup> = .96895897 Adjusted R <sup>2</sup> = .96878652 F(2,360)=5618.8 p<0.0000 Std.Error of estimate: 1.2687					
	b*	Std.Err. of b*	b	Std.Err. of b	t(360)	p-value
Intercept			3.202931	0.200377	15.98454	0.000000
C1_min	0.930087	0.011976	0.905069	0.011654	77.66163	0.000000
Cum_SR	0.082631	0.011976	0.000078	0.000011	6.89959	0.000000

$$y_{min} = 0.905069 * C1_{min} + 0.000078 * Cum_{SR} + 3.202931$$

Table 4.120 Characteristics of the model for predicting minimal daily C3 temperature from minimal daily surface temperature and cumulative solar radiation for the Awjilah location.

Awjilah C3_min	Regression Summary for Dependent Variable: C3_min (AWJILAH_C1_min) R= .97031262 R <sup>2</sup> = .94150658 Adjusted R <sup>2</sup> = .94118161 F(2,360)=2897.3 p<0.0000 Std.Error of estimate: 1.7245					
	b*	Std.Err. of b*	b	Std.Err. of b	t(360)	p-value
Intercept			4.597323	0.272358	16.87973	0.000000
C1_min	0.910736	0.016440	0.877521	0.015840	55.39748	0.000000
Cum_SR	0.090330	0.016440	0.000084	0.000015	5.49454	0.000000

$$y_{min} = 0.877521 * C1_{min} + 0.000084 * Cum_{SR} + 4.597323$$

Table 4.121 Characteristics of the model for predicting minimal C4 temperature from minimal daily surface temperature and cumulative solar radiation for the Awjilah location.

Awjilah C4_min	Regression Summary for Dependent Variable: C4_min (AWJILAH_C1_min) R= .97270518 R <sup>2</sup> = .94615536 Adjusted R <sup>2</sup> = .94585623 F(2,360)=3163.0 p<0.0000 Std.Error of estimate: 1.6629					
	b*	Std.Err. of b*	b	Std.Err. of b	t(360)	p-value
Intercept			4.693005	0.262626	17.86957	0.000000
C1_min	0.913831	0.015773	0.884934	0.015274	57.93563	0.000000
Cum_SR	0.089317	0.015773	0.000084	0.000015	5.66257	0.000000

$$y_{min} = 0.884934 * C1_{min} + 0.000084 * Cum_{SR} + 4.693005$$

Appendix M presents the tables of the models for predicting maximal (minimal) daily pavement temperatures at different depths depending on maximal (minimal) daily surface temperatures and cumulative solar radiation for the remaining locations.

From the tables in Appendix M for the models for predicting maximal (minimal) daily pavement temperatures at different depths depending on maximal (minimal) daily surface temperatures and the cumulative solar radiation, it can be seen that the surface temperature coefficients are lower compared to the coefficients in the models which did not include the cumulative solar radiation. This means that cumulative solar radiation has an effect on the temperature of the pavement. Also, adjusted  $R^2$  are higher for the models which include the cumulative solar radiation, especially for maximal daily temperatures. The standard errors of the models both for maximal (minimal) daily temperatures are lower compared to the models that did not include the day of the year. This means that the models with the cumulative solar radiation better explain maximal (minimal) daily temperatures of the pavement than the models including only surface temperature.

#### 4.7.4.1 Relationship with surface temperature, cumulative solar radiation, and latitude

The next model for predicting maximal (minimal) daily pavement temperatures at different depths from maximal (minimal) daily surface temperatures and cumulative solar radiation was built using data from all stations and includes the latitude of the locations.

The model for maximal temperatures is of the following form:

$$y_{max} = A * C1_{max} + B * Cum_{SR} + C * Lat + D$$

where

$y_{max}$  = predicted maximal daily pavement temperature ( $^{\circ}C$ );

$A$  = surface temperature coefficient;

$C1_{max}$  = maximal daily surface temperature ( $^{\circ}C$ );

$B$  = coefficient for cumulative solar radiation;

$Cum_{SR}$  = cumulative solar radiation ( $W/m^2$ );

$C$  = latitude coefficient;

$Lat$  = latitude of the location (degrees); and

$D$  = intercept coefficient.

Table 4.122 Characteristics of the model for predicting maximal C2daily temperature from maximal daily surface temperature and cumulative solar radiation for all locations.

All locations C2_max	Regression Summary for Dependent Variable: C2_max (Max_all_locations) R= .97917824 R <sup>2</sup> = .95879003 Adjusted R <sup>2</sup> = .95874736 F(3,2897)=22467. p<0.0000 Std.Error of estimate: 2.2395					
	b*	Std.Err. of b*	b	Std.Err. of b	t(2897)	p-value
Intercept			-4.38136	0.604246	-7.2509	0.000000
C1_max	0.970080	0.004688	0.92586	0.004474	206.9379	0.000000
Cum_SR	0.021601	0.004640	0.00003	0.000007	4.6551	0.000003
Latitude	0.026788	0.003819	0.14165	0.020194	7.0145	0.000000

$$y_{max} = 0.92586 * C1_{max} + 0.00003 * Cum_{SR} + 0.14165 * Lat - 4.38136$$

Table 4.123 Characteristics of the model for predicting maximal daily C3 temperature from maximal daily surface temperature and cumulative solar radiation for all locations.

All locations C3_max	Regression Summary for Dependent Variable: C3_max (Max_all_locations) R= .97486237 R <sup>2</sup> = .95035664 Adjusted R <sup>2</sup> = .95030522 F(3,2896)=18480. p<0.0000 Std.Error of estimate: 2.3700					
	b*	Std.Err. of b*	b	Std.Err. of b	t(2896)	p-value
Intercept			1.126503	0.639470	1.7616	0.078239
C1_max	0.983794	0.005145	0.905406	0.004735	191.2158	0.000000
Cum_SR	-0.019846	0.005093	-0.000027	0.000007	-3.8966	0.000100
Latitude	-0.015651	0.004192	-0.079796	0.021373	-3.7335	0.000192

$$y_{max} = 0.905406 * C1_{max} - 0.000027 * Cum_{SR} - 0.079796 * Lat + 1.126503$$

Table 4.124 Characteristics of the model for predicting maximal daily C4 temperature from maximal daily surface temperature and cumulative solar radiation for all locations.

All locations C4_max	Regression Summary for Dependent Variable: C4_max (Max_all_locations) R= .95392536 R <sup>2</sup> = .90997360 Adjusted R <sup>2</sup> = .90988037 F(3,2897)=9760.8 p<0.0000 Std.Error of estimate: 3.0446					
	b*	Std.Err. of b*	b	Std.Err. of b	t(2897)	p-value
Intercept			-3.89181	0.821455	-4.7377	0.000002
C1_max	0.928923	0.006929	0.81547	0.006082	134.0690	0.000000
Cum_SR	0.044657	0.006859	0.00006	0.000009	6.5111	0.000000
Latitude	0.011633	0.005645	0.05658	0.027453	2.0609	0.039402

$$y_{max} = 0.81547 * C1_{max} + 0.00006 * Cum_{SR} + 0.05658 * Lat - 3.89181$$

The model for minimal temperatures is of the following form:

$$y_{min} = A * C1_{min} + B * Cum_{SR} + C * Lat + D$$

where

$y_{min}$ = predicted minimal daily pavement temperature (°C);

$A$  = surface temperature coefficient;

$C1_{min}$ = minimal daily surface temperature (°C);

$B$  = coefficient for cumulative solar radiation;

$Cum_{SR}$  = cumulative solar radiation (W/m<sup>2</sup>);

$C$  =latitude coefficient;

$Lat$  = latitude of the location (degrees); and

$D$  = intercept coefficient.

Table 4.125 Characteristics of the model for predicting minimal daily C2 temperature from minimal daily surface temperature and cumulative solar radiation for all locations.

All locations C2_min	Regression Summary for Dependent Variable: C2_min (Min_all_locations) R= .96069454 R <sup>2</sup> = .92293400 Adjusted R <sup>2</sup> = .92285411 F(3,2894)=11553. p<0.0000 Std.Error of estimate: 2.1148					
	b*	Std.Err. of b*	b	Std.Err. of b	t(2534)	p-value
Intercept			8.698897	0.533306	16.3113	0.000000
C1_min	0.933030	0.005950	0.925894	0.005904	156.8161	0.000000
Cum_SR	0.046418	0.005958	0.000045	0.000006	7.7910	0.000000
Latitude	-0.078372	0.005169	-0.286328	0.018885	-15.1616	0.000000

$$y_{min} = 0.925894 * C1_{min} + 0.000045 * Cum_{SR} - 0.286328 * Lat + 8.698897$$

Table 4.126 Characteristics of the model for predicting minimal daily C3 temperature from minimal daily surface temperature and cumulative solar radiation for all locations.

All locations C3_min	Regression Summary for Dependent Variable: C3_min (Min_all_locations) R= .93606840 R <sup>2</sup> = .87622405 Adjusted R <sup>2</sup> = .87609574 F(3,2894)=6829.0 p<0.0000 Std.Error of estimate: 2.7426					
	b*	Std.Err. of b*	b	Std.Err. of b	t(2534)	p-value
Intercept			12.55833	0.691598	18.1584	0.000000
C1_min	0.902784	0.007540	0.91673	0.007657	119.7270	0.000000
Cum_SR	0.052671	0.007551	0.00005	0.000008	6.9757	0.000000
Latitude	-0.099061	0.006551	-0.37034	0.024490	-15.1217	0.000000

$$y_{min} = 0.91673 * C1_{min} + 0.00005 * Cum_{SR} - 0.37034 * Lat + 12.55833$$

Table 4.127 Characteristics of the model for predicting minimal daily C4 temperature from minimal daily surface temperature and cumulative solar radiation for all locations.

All locations C4_min	Regression Summary for Dependent Variable: C4_min (Min_all_locations) R= .92546182 R <sup>2</sup> = .85647958 Adjusted R <sup>2</sup> = .85633080 F(3,2894)=5756.8 p<0.0000 Std.Error of estimate: 2.9489					
	b*	Std.Err. of b*	b	Std.Err. of b	t(2534)	p-value
Intercept			13.19311	0.743632	17.7415	0.000000
C1_min	0.886363	0.008120	0.89874	0.008233	109.1645	0.000000
Cum_SR	0.064992	0.008131	0.00006	0.000008	7.9936	0.000000
Latitude	-0.089561	0.007054	-0.33433	0.026333	-12.6964	0.000000

$$y_{min} = 0.89874 * C1_{min} + 0.00006 * Cum_{SR} - 0.33433 * Lat + 13.19311$$

All of the coefficients of the latitude are negative, indicating that as latitude increases, pavement temperatures decreases. Compared with the models including only surface temperature and latitude, the models including the surface temperature, cumulative solar radiation and latitude have very similar adjusted  $R^2$  and standard error of estimate, indicating similar fit to the data.

#### **4.7.5 Relationship with surface temperature, day of the year, and cumulative solar radiation**

The next model for predicting maximal (minimal) daily pavement temperatures at different depths includes maximal (minimal) daily surface of the pavement temperatures, the day of the year and the cumulative solar radiation.

The model for maximal daily surface of the pavement temperatures for different locations is of the form:

$$y_{max} = A * CI_{max} + B * Day + C * Day^2 + D * Cum_{SR} + E * Lat + F$$

where

$y_{max}$  = predicted maximal daily pavement temperature (°C);

$A$  = surface of the pavement temperature coefficient;

$CI_{max}$  = maximal daily surface of the pavement temperature (°C);

$B$  = coefficient of a day of the year;

$Day$  = day of the year;

$C$  = coefficient of the square of the day;

$Day^2$  = square of the day of the year;

$D$  = coefficient of cumulative solar radiation;

$Cum_{SR}$  = cumulative solar radiation ( $W/m^2$ ); and

$E$  = coefficient of latitude;

$Lat$  = latitude (degrees); and

$F$  = intercept.

Tables 4.128 to 4.130 give the characteristics of the models for maximal daily pavement temperatures for four layers.

Table 4.128 Characteristics of the model for predicting maximal daily C2 temperature from maximal daily surface of the pavement temperature, the day of the year, and cumulative solar radiation and latitude.

All locations C2_max	Regression Summary for Dependent Variable: C2_max (Max_all_locations) R= ,98123973 R <sup>2</sup> = ,96283141 Adjusted R <sup>2</sup> = ,96276722 F(5,2895)=14999, p<0,0000 Std.Error of estimate: 2,1276					
	b*	Std.Err. of b*	b	Std.Err. of b	t(2909)	p-value
Intercept			1,082944	0,680826	1,5906	0,111802
C1_max	0,843968	0,008743	0,805500	0,008345	96,5257	0,000000
Day	0,587187	0,034434	0,061233	0,003591	17,0524	0,000000
Day <sup>2</sup>	-0,583982	0,035517	-0,000162	0,000010	-16,4424	0,000000
Cum_SR (W/m <sup>2</sup> )	0,007267	0,004600	0,000010	0,000006	1,5798	0,114270
Latitude	0,006784	0,003823	0,035870	0,020215	1,7744	0,076098

$$y_{max} = 0,805500 * C1_{max} + 0,061233 * Day - 0,000162 * Day^2 + 0,000010 * Cum_{SR} + 0,035870 * Lat + 1,082944$$

Table 4.129 Characteristics of the model for predicting maximal daily C3 temperature from maximal daily surface of the pavement temperature, the day of the year, and cumulative solar radiation and latitude.

All locations C3_max	Regression Summary for Dependent Variable: C3_max (Max_all_locations) R= ,97596220 R <sup>2</sup> = ,95250221 Adjusted R <sup>2</sup> = ,95242015 F(5,2894)=11607, p<0,0000 Std.Error of estimate: 2,3190					
	b*	Std.Err. of b*	b	Std.Err. of b	t(2908)	p-value
Intercept			4,751260	0,742088	6,4026	0,000000
C1_max	0,894835	0,009883	0,823534	0,009096	90,5413	0,000000
Day	0,416405	0,038933	0,041861	0,003914	10,6956	0,000000
Day <sup>2</sup>	-0,410040	0,040157	-0,000109	0,000011	-10,2110	0,000000
Cum_SR (W/m <sup>2</sup> )	-0,029160	0,005200	-0,000039	0,000007	-5,6074	0,000000
Latitude	-0,029731	0,004322	-0,151577	0,022036	-6,8786	0,000000

$$y_{max} = 0,823534 * C1_{max} + 0,041861 * Day - 0,000109 * Day^2 - 0,000039 * Cum_{SR} - 0,151577 * Lat + 4,751260$$



Table 4.130 Characteristics of the model for predicting maximal daily C4 temperature from maximal daily surface of the pavement temperature, the day of the year, and cumulative solar radiation and latitude.

All locations C4_max	Regression Summary for Dependent Variable: C4_max (Max_all_locations) R= ,95766649 R <sup>2</sup> = ,91712511 Adjusted R <sup>2</sup> = ,91698197 F(5,2895)=6407,4 p<0,0000 Std.Error of estimate: 2,9221					
	b*	Std.Err. of b*	b	Std.Err. of b	t(2909)	p-value
Intercept			0,592487	0,935073	0,6336	0,526375
C1_max	0,797110	0,013056	0,699752	0,011461	61,0537	0,000000
Day	0,631958	0,051418	0,060615	0,004932	12,2906	0,000000
Day <sup>2</sup>	-0,592758	0,053034	-0,000151	0,000013	-11,1769	0,000000
Cum_SR (W/m <sup>2</sup> )	0,036626	0,006869	0,000047	0,000009	5,3320	0,000000
Latitude	-0,008966	0,005709	-0,043606	0,027764	-1,5706	0,116390

$$y_{max} = 0,699752 * C1_{max} + 0,060615 * Day - 0,000151 * Day^2 + 0,000047 * Cum_{SR} - 0,043606 * Lat + 0,592487$$

All of the coefficients of the latitude are negative, indicating that as latitude increases, pavement temperature decreases. Compared with the models including only maximal daily surface of the pavement temperature, the day of the year, and latitude, the models including the maximal daily surface of the pavement temperature, the day of the year, the cumulative solar radiation and latitude have higher adjusted R<sup>2</sup> and lower standard error of estimate, indicating better fit to the data.

The next model for predicting minimal daily pavement temperatures at four different layers, based on minimal daily surface of the pavement temperatures, the day of the year, and cumulative solar radiation was built using data from all stations and includes the latitude of the locations. The model is of the form

$$y_{min} = A * C1_{min} + B * Day + C * Day^2 + D * Lat + E * Cum_{SR} + F$$

where

$y_{min}$  = predicted minimal daily pavement temperature (°C);

$A$  = surface of the pavement temperature coefficient;

$C1_{min}$  = minimal daily surface of the pavement temperature (°C);

$B$  = coefficient of a day of the year;

$Day$  = day of the year;

$C$  = coefficient of square of the day of the year;

$Day^2$  = square of the day of the year;

$D$  = coefficient of Latitude;

$Lat$  = latitude (degrees);

$E$  = coefficient of cumulative solar radiation;

$Cum\_SR$  = cumulative solar radiation( $W/m^2$ ); and  
 $F$ = intercept.

Tables 4.131 to 4.133 give the characteristics of the models for daily minimal pavement temperatures for three layers.

Table 4.131 Characteristics of the model for predicting minimal daily C2 temperature from minimal daily surface of the pavement temperature, the day of the year, and cumulative solar radiation and latitude.

All locations C2_min	Regression Summary for Dependent Variable: C2_min (Min_all_locations) R= ,97136969 R <sup>2</sup> = ,94355907 Adjusted R <sup>2</sup> = ,94346148 F(5,2892)=9669,5 p<0,0000 Std.Error of estimate: 1,8105					
	b*	Std.Err. of b*	b	Std.Err. of b	t(2908)	p-value
Intercept			8,958163	0,463111	19,3434	0,000000
C1_min	0,73846	0,007925	0,732817	0,007865	93,1791	0,000000
Day	1,08345	0,033979	0,077997	0,002446	31,8859	0,000000
Day <sup>2</sup>	-1,06005	0,034466	-0,000202	0,000007	-30,7562	0,000000
Cum_SR ( $W/m^2$ )	-0,01393	0,005701	-0,000014	0,000006	-2,4436	0,014601
Latitude	-0,08357	0,004429	-0,305306	0,016183	-18,8664	0,000000

$$y_{min} = 0,732817 * C1_{min} + 0,077997 * Day - 0,000202 * Day^2 - 0,305306 * Lat - 0,000014 * Cum\_SR + 8,958163$$

Table 4.132 Characteristics of the model for predicting minimal daily C3 temperature from minimal daily surface of the pavement temperature, the day of the year, and cumulative solar radiation and latitude.

All locations C3_min	Regression Summary for Dependent Variable: C3_min (Min_all_locations) R= ,95500275 R <sup>2</sup> = ,91203025 Adjusted R <sup>2</sup> = ,91187816 F(5,2892)=5996,6 p<0,0000 Std.Error of estimate: 2,3129					
	b*	Std.Err. of b*	b	Std.Err. of b	t(2908)	p-value
Intercept			13,39739	0,591624	22,6451	0,000000
C1_min	0,64278	0,009894	0,65271	0,010047	64,9658	0,000000
Day	1,45362	0,042421	0,10708	0,003125	34,2667	0,000000
Day <sup>2</sup>	-1,45148	0,043029	-0,00028	0,000008	-33,7323	0,000000
Cum_SR ( $W/m^2$ )	-0,03688	0,007117	-0,00004	0,000007	-5,1812	0,000000
Latitude	-0,10651	0,005530	-0,39819	0,020673	-19,2611	0,000000

$$y_{min} = 0,65271 * C1_{min} + 0,10708 * Day - 0,00028 * Day^2 - 0,39819 * Lat - 0,00004 * Cum_{SR} + 13,39739$$

Table 4.133 Characteristics of the model for predicting minimal daily C4 temperature from minimal daily surface of the pavement temperature, the day of the year, and cumulative solar radiation and latitude.

All locations C4_min	Regression Summary for Dependent Variable: C4_min (Min_all_locations) R= ,94691879 R <sup>2</sup> = ,89665519 Adjusted R <sup>2</sup> = ,89647652 F(5,2892)=5018,4 p<0,0000 Std.Error of estimate: 2,5032					
	b*	Std.Err. of b*	b	Std.Err. of b	t(2908)	p-value
Intercept			13,89021	0,640308	21,6930	0,000000
C1_min	0,61170	0,010724	0,62024	0,010874	57,0403	0,000000
Day	1,53333	0,045979	0,11279	0,003382	33,3488	0,000000
Day <sup>2</sup>	-1,51976	0,046638	-0,00030	0,000009	-32,5861	0,000000
Cum_SR (W/m <sup>2</sup> )	-0,02615	0,007714	-0,00003	0,000008	-3,3893	0,000710
Latitude	-0,09723	0,005994	-0,36297	0,022374	-16,2228	0,000000

$$y_{min} = 0,62024 * C1_{min} + 0,11279 * Day - 0,00030 * Day^2 - 0,36297 * Lat - 0,00003 * Cum\_SR + 13,89021$$

All of the coefficients of the latitude are negative, indicating that as latitude increases, pavement temperature decreases. Compared with the models including only minimal daily surface of the pavement temperature, the day of the year, and latitude, the models including the minimal daily surface of the pavement temperature, the day of the year, cumulative solar radiation and latitude have very similar adjusted R<sup>2</sup> and standard error of estimate, indicating similar fit to the data.

#### 4.7.6 Evaluation of the models with surface temperature

As can be seen from the fit of the models which included only the (maximal/minimal daily surface of the pavement temperature, those models could be improved (especially models for maximal daily pavement temperatures) by adding new variables, such as day of the year, wind speed and cumulative solar radiation. However, wind speed did not improve the models significantly, as can be seen from the values of adjusted R<sup>2</sup> and standard errors of estimate. In table 4.134 values of adjusted R<sup>2</sup> and standard errors are presented for all considered models based on data from all eight locations. The best values of adjusted R<sup>2</sup> and standard error of estimate were obtained when the model included maximal/minimal daily surface of the pavement temperature, day of the year, and cumulative solar radiation.

Table 4.134 Adjusted R<sup>2</sup> and standard errors for different models based on the data from all locations.

<b>Models for maximal daily temperatures</b>										
The model including latitude and										
	Surface temp		Surface temp, wind speed		Surface temp, cum. solar radiation		Surface temp, day of the year		Surface temp, day of the year, cum. solar radiation	
Layer	Adj. R <sup>2</sup>	Std.Err of est.	Adj. R <sup>2</sup>	Std.Err of est.	Adj. R <sup>2</sup>	Std.Err of est.	Adj. R <sup>2</sup>	Std.Err of est.	Adj. R <sup>2</sup>	Std.Err of est.
C2	.95861	2.2446	.958605	2.2451	.95874	2.2395	.96288	2.1257	.96276	2,1276
C3	.95034	2.3717	.95133	2.3480	.950305	2.3700	.95217	2.3276	.95242	2,3190
C4	.90916	3.0601	.91182	3.0152	.909880	3.0446	.91667	2.9311	.91698	2,9221

<b>Models for minimal daily temperatures</b>										
The model including latitude and										
	Surface temp		Surface temp, wind speed		Surface temp, cum. solar radiation		Surface temp, day of the year		Surface temp, day of the year, cum. solar radiation	
Layer	Adj. R <sup>2</sup>	Std.Err of est.	Adj. R <sup>2</sup>	Std.Err of est.	Adj. R <sup>2</sup>	Std.Err of est.	Adj. R <sup>2</sup>	Std.Err of est.	Adj. R <sup>2</sup>	Std.Err of est.
C2	0.92114	2.1363	.92134	2.1326	.92285	2.1148	.94353	1.8077	.94346	1,8105
C3	0.87371	2.7668	.87416	2.7611	.87609	2.7426	.91131	2.3188	.91187	2,3129
C4	0.85292	2.9810	.85337	2.9749	.85633	2.9489	.89638	2.5021	.89647	2,5032

Therefore, we conclude that the best model for predicting the maximal/minimal daily pavement temperatures is linear regression with maximal/minimal daily surface temperature, day of the year, and cumulative solar radiation.

The best models for maximal daily pavement temperatures are:

3 cm (C2):

$$T_{pav,3cm}^{max} = 1,082944 + 0,805500T_{surf}^{max} + 0,061233Day - 0,000162Day^2 + 0,000010Cum\_SR + 0,035870Lat$$

8 cm (C3):

$$T_{pav,8cm}^{max} = 4,751260 + 0,823534T_{surf}^{max} + 0,041861Day - 0,000109Day^2 - 0,000039Cum\_SR - 0,151577Lat$$

15 cm(C4):

$$T_{pav,15cm}^{max} = 0,592487 + 0,699752T_{surf}^{max} + 0,060615Day - 0,000151Day^2 + 0,000047Cum\_SR - 0,043606Lat$$

where

$T_{pav,*}^{max}$  =maximal daily pavement temperature at certain depth, (°C);

$T_{surf}^{max}$ = maximal daily surface of the pavement temperature, (°C);

$Day$  = day of the year;

$Day^2$  = square of the day of the year;

$Cum\_SR$  = cumulative solar radiation (W/m<sup>2</sup>)and

$Lat$ = latitude of the section, (degrees).

The best models for minimal daily pavement temperatures are:

3 cm (C2):

$$T_{pav,3cm}^{min} = 8,958163 + 0,732817T_{surf}^{min} + 0,077997Day - 0,000202Day^2 - 0,000014Cum\_SR - 0,305306Lat$$

8 cm (C3):

$$T_{pav,8cm}^{min} = 13,39739 + 0,65271T_{surf}^{min} + 0,10708Day - 0,00028Day^2 - 0,00004Cum\_SR - 0,39819Lat$$

15 cm(C4):

$$T_{pav,15cm}^{min} = 13,89021 + 0,62024T_{surf}^{min} + 0,11279Day - 0,00030Day^2 - 0,00003Cum\_SR - 0,36297Lat$$

where

$T_{pav,*}^{min}$  =minimal daily pavement temperature at certain depth, (°C);

$T_{surf}^{min}$ = minimal daily surface of the pavement temperature, (°C);

$Day$  = day of the year;

$Day^2$  = square of the day of the year;

$Cum\_SR$  = cumulative solar radiation (W/m<sup>2</sup>)and

$Lat$ = latitude of the section, (degrees).

In the case when data on cumulative solar radiation are not available, the next best model for predicting the maximal/minimal daily pavement temperatures is linear regression with maximal/minimal daily surface of the pavement temperature, and day of the year, developed in section 4.7.2.

Figures 4.51 and 4.56 present actual maximal and minimal daily pavement temperature at the three layers together with predicted values from the model including the surface temperature,

cumulative solar radiation and the day of the year at the Al-Jufroh location. In Appendix N, similar figures for other locations are given.

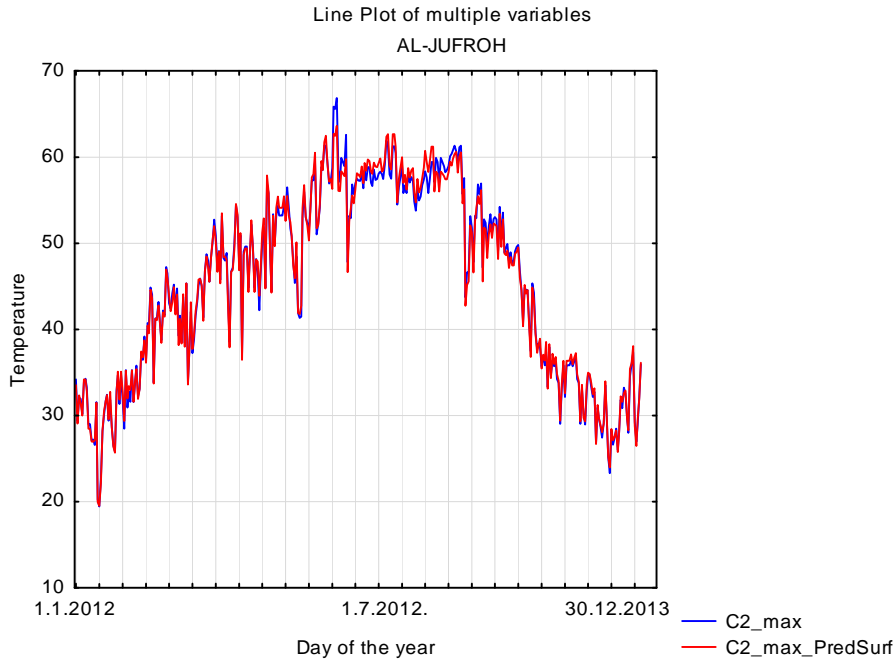


Figure 4.51 Actual maximal daily pavement temperature at C2 layer and predictions from the model including the maximal daily surface temperature, cumulative solar radiation and the day of the year at the Al-Jufroh location.

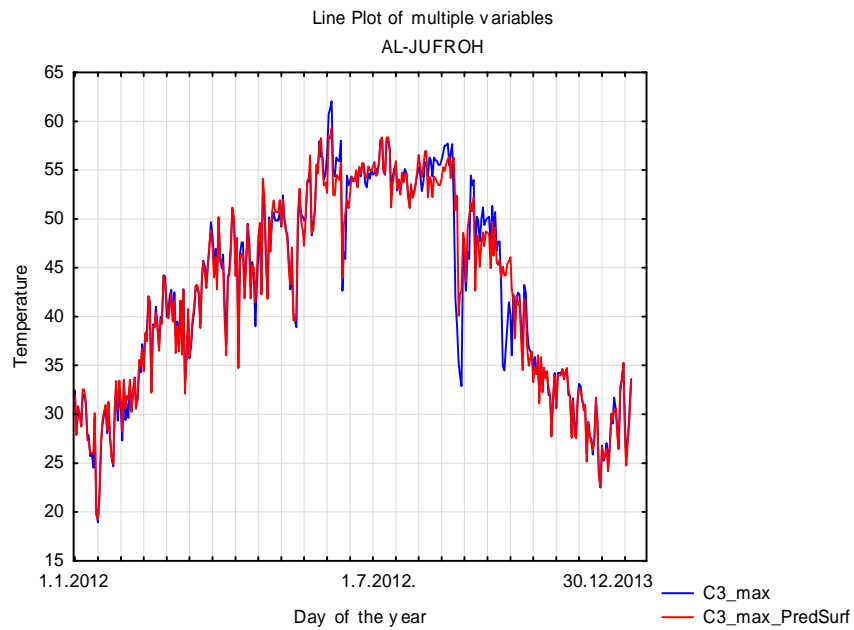


Figure 4.52 Actual maximal daily pavement temperature at C3 depth versus predictions from the model including maximal daily surface temperature, cumulative solar radiation and the day of the year at the Al-Jufroh location.

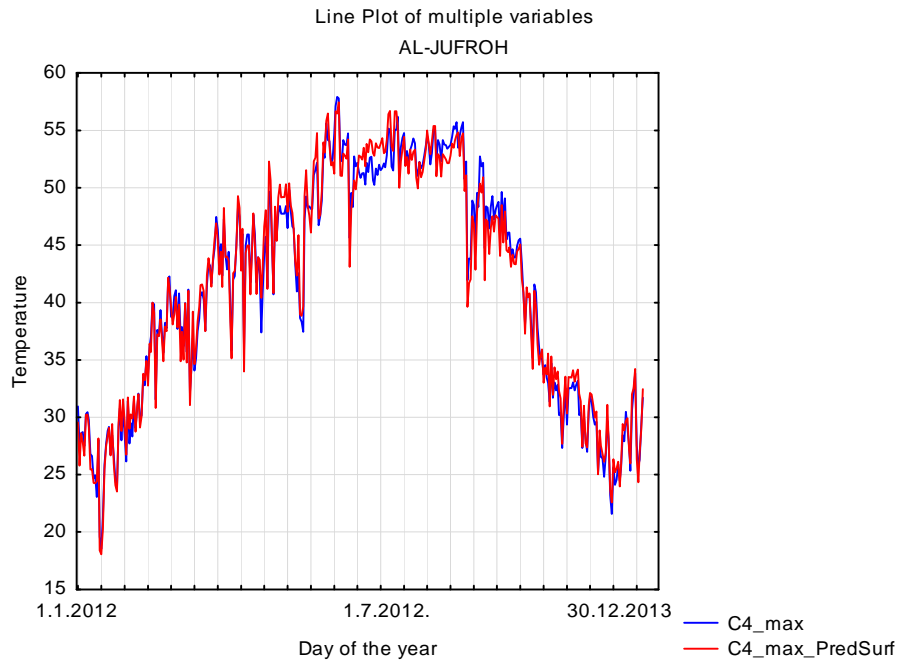


Figure 4.53 Actual maximal daily pavement temperature at C4 depth versus predictions from the model including maximal daily surface temperature, cumulative solar radiation and the day of the year at the Al-Jufroh location.

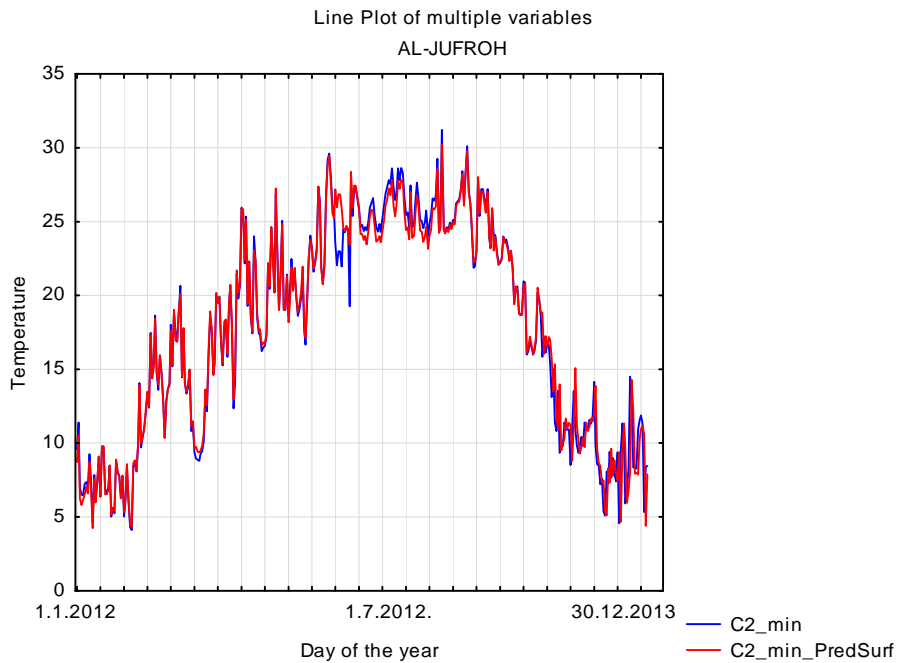


Figure 4.54 Actual minimal daily pavement temperature at C2 depth versus predictions from the model including minimal daily surface temperature and the day of the year at the Al Jufroh location.

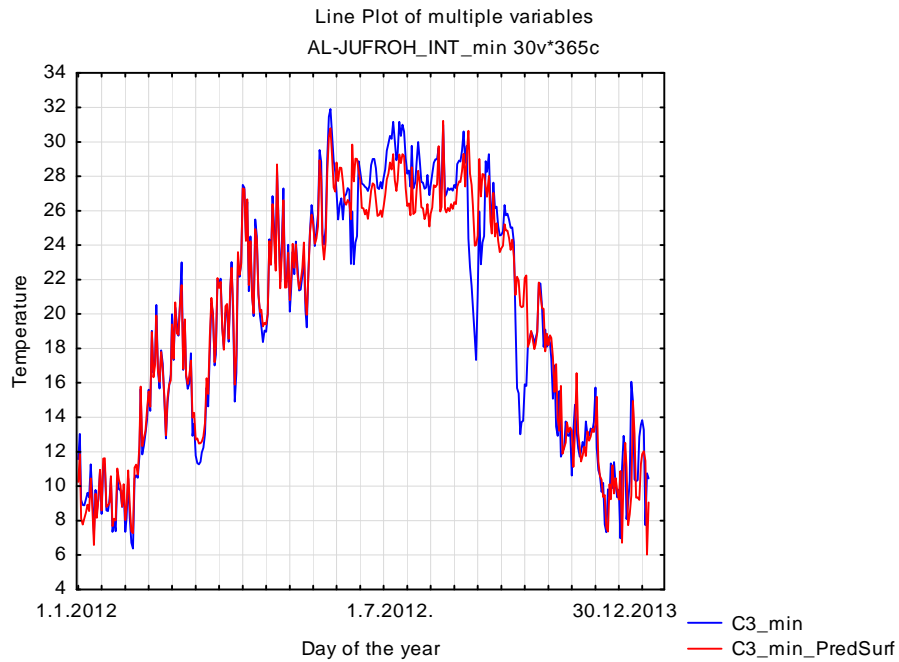


Figure 4.55 Actual minimal daily pavement temperature at C3 depth versus predictions from the model including minimal daily surface temperature, cumulative solar radiation and the day of the year at the Al Jufroh location.

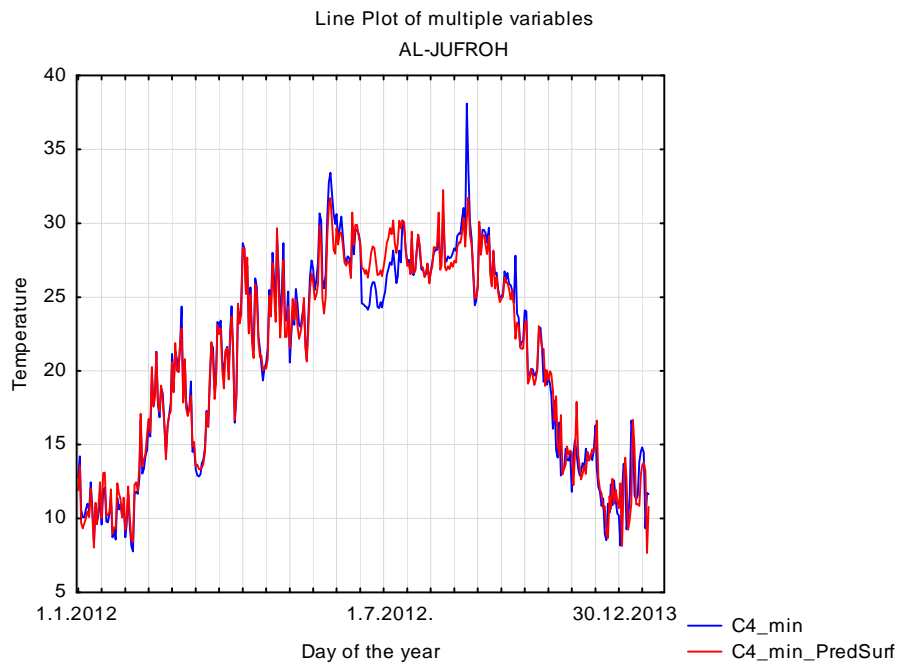


Figure 4.56 Actual minimal daily pavement temperature at C4 depth versus predictions from the model including minimal daily surface temperature, cumulative solar radiation and the day of the year at the Al Jufroh location.



## 4.8 Pavement temperature prediction models incorporating surface (C1) temperature and the distance from the surface (depth)

### 4.8.1 Relationship with surface temperature and the distance from the surface (depth)

The next models describe the relationship between maximal/minimal daily pavement temperatures at three different layers (C2, C3, C4) and surface temperature C1 for different locations.

The model for maximal daily temperatures of the pavement including maximal daily surface temperature of the pavement C1 temperature and distance from the surface is of the following form:

$$y_{max} = A * C1_{max} + B * Depth + C$$

where

$y_{max}$  = predicted maximal daily pavement temperature (°C);

$A$  = coefficient of surface temperature C1;

$C1_{max}$  = maximal daily surface temperature (°C);

$B$  = coefficient of the depth;

$Depth$  = distance from the surface (cm); and

$C$  = intercept.

Table 4.135 presents the coefficients for the linear prediction models developed for location Al-Jufroh. Included with the model coefficients and their standard errors are the standard errors of estimate and the adjusted  $R^2$ . The coefficients statistically different from zero are denoted in red. Tables of coefficients for the pavement temperature for the remaining stations are presented in Appendix O.

It can be seen that the coefficients of distance from the surface (depth) are negative as the temperature of the pavement layers decreases with depth.

Table 4.135 Characteristics of the model for predicting maximal daily pavement temperatures from maximal daily surface temperature and depth from the surface at the Al Jufroh location.

Al Jufroh max	Regression Summary for Dependent Variable: Temperature_max (Temp_depth_C1_max_Novo) R= .98840239 R <sup>2</sup> = .97693929 Adjusted R <sup>2</sup> = .97689705 F(2,1092)=23131. p<0.0000 Std.Error of estimate: 1.5938 Include condition: Site=102					
	b*	Std.Err. of b*	b	Std.Err. of b	t(1457)	p-value
Intercept			3.079988	0.224405	13.7251	0.00
Depth	-0.153864	0.004595	-0.327666	0.009786	-33.4821	0.00
C1_max	0.976353	0.004595	0.857194	0.004035	212.4623	0.00

$$y_{max} = 0.857194 * C1_{max} - 0.327666 * Depth + 3.079988$$

The model for minimal temperatures is of the following form

$$y_{min} = A * C1_{min} + B * Depth + C$$

where

$y_{min}$  = predicted minimum pavement temperature (°C);

$A$  = coefficient of surface temperature  $C1$ ;

$C1_{min}$  = minimum surface temperature (°C);

$B$  = coefficient of the depth;

$Depth$  = depth from the surface (cm); and

$C$  = intercept.

Table 4.136 presents the coefficients for the linear prediction models developed for station Al-Jufroh. Included with the model coefficients and their standard errors are the standard errors of estimate and the adjusted  $R^2$ . The coefficients statistically different from zero are denoted in red. Tables of coefficients for the pavement temperature for the remaining locations are presented in Appendix O.

It can be seen that the coefficients of distance from the surface (depth) are positive as the minimal temperatures of the pavement layers increase with depth.

Table 4.136 Characteristics of the model for predicting minimal daily pavement temperatures from minimal daily surface temperature and depth from the surface at the Al Jufroh location.

Al Jufroh min	Regression Summary for Dependent Variable: Temperature_min (Temp_depth_C1_min_Novo) R= .97511347 R <sup>2</sup> = .95084629 Adjusted R <sup>2</sup> = .95075626 F(2,1092)=10562. p<0.0000 Std.Error of estimate: 1.5901 Include condition: Site=102					
	b*	Std.Err. of b*	b	Std.Err. of b	t(1457)	p-value
Intercept			0.611026	0.151977	4.0205	0.000062
Depth	0.166833	0.006709	0.242782	0.009763	24.8665	0.000000
C1_min	0.960736	0.006709	0.974106	0.006803	143.1980	0.000000

$$y_{min} = 0.974106 * C1_{min} + 0.242782 * Depth + 0.611026$$

#### 4.8.1.1 Relationship with surface temperature, depth from the surface, and latitude

The next models describe the relationship between and maximal/minimal daily pavement temperatures and maximal/minimal daily surface temperatures, depth from the surface, and latitude.

The model for maximal daily temperatures of the pavement including maximal daily air temperature and depth from the surface is of the following form:

$$y_{max} = A * C1_{max} + B * Depth + C * Lat + D$$

where

$y_{max}$  = predicted maximal daily pavement temperature (°C);

$A$  = coefficient of surface temperature  $C1$ ;

$C1_{max}$  = maximal daily surface temperature (°C);

$B$  = coefficient of the depth;

$Depth$  = distance from the surface (cm);

$C$  = coefficient of latitude;

$Lat$  = latitude of the location (degrees); and

$D$  = intercept.

Table 4.137 Characteristics of the model for predicting maximal daily pavement temperatures from maximal daily surface temperature and depth from the surface for all locations.

All locations max	Regression Summary for Dependent Variable: Temperature_max (Temp_depth_C1_max_Novo) R= .97083688 R <sup>2</sup> = .94252424 Adjusted R <sup>2</sup> = .94250451 F(3,8740)=47775. p<0.0000 Std.Error of estimate: 2.6314					
	b*	Std.Err. of b*	b	Std.Err. of b	t(8744)	p-value
Intercept			2.517653	0.412345	6.1057	0.000000
C1_min	0.938287	0.002594	0.890634	0.002463	361.6749	0.000000
Depth	-0.253602	0.002564	-0.565418	0.005717	-98.8929	0.000000
Latitude	0.007834	0.002594	0.041245	0.013658	3.0199	0.002536

$$y_{max} = 0.890634 * C1_{max} - 0.565418 * Depth + 0.041245 * Lat + D2.517653$$

Maximal daily temperature of pavement at different layers depends mostly on maximal daily surface temperature temperatures. Maximal daily pavement temperatures decrease with distance from the surface because its coefficient is.

The model for minimal daily temperatures of the pavement including minimal daily surface temperature and depth from the surface is of the following form:

$$y_{min} = A * C1_{min} + B * Depth + C * Lat + D$$

where

$y_{min}$  = predicted minimum pavement temperature (°C);

$A$  = coefficient of surface temperature  $C1$ ;

$C1_{min}$  = minimum surface temperature (°C);

$B$  = coefficient of the depth;

$Depth$  = distance from the surface (cm);

$C$  = coefficient of latitude;

$Lat$  = latitude of the location (degrees); and

$D$  = intercept.

Table 4.138 Characteristics of the model for predicting minimal daily pavement temperatures from minimal daily surface temperature and depth from the surface for all locations.

All locations min	Regression Summary for Dependent Variable: Temperature_min (Temp_depth_C1_min_Novo) R= .94066899 R <sup>2</sup> = .88485815 Adjusted R <sup>2</sup> = .88481864 F(3,8744)=22399. p<0.0000 Std.Error of estimate: 2.6565					
	b*	Std.Err. of b*	b	Std.Err. of b	t(8743)	p-value
Intercept			10.35300	0.380531	27.2067	0.00
C1_max	0.921401	0.003629	0.94122	0.003707	253.9101	0.00
Depth	0.162855	0.003629	0.25899	0.005771	44.8787	0.00
Latitude	-0.091563	0.003629	-0.34381	0.013626	-25.2320	0.00

$$y_{min} = 0.94122 * C1_{min} + 0.25899 * Depth - 0.34381 * Lat + 10.35300$$

Temperature of pavement at different depths depends mostly on surface temperatures. It decreases with depth for maximal daily temperatures, increases for minimal daily temperatures. It increases with latitude for maximal daily temperatures, and decreases for minimal daily temperatures.

#### 4.8.2 Relationship with surface temperature, depth from the surface, and day of the year

The next models describe the relationship between maximal/minimal daily pavement temperatures and maximal/minimal daily surface temperature temperatures, distance from the surface and the day of the year.

The model for maximal daily temperatures of the pavement including the maximal daily surface temperature temperature, distance from the surface and the day of the year is of the following form:

$$y_{max} = A * C1_{max} + B * Depth + C * Day + D * Day^2 + E$$

where

$y_{max}$ = predicted maximal daily pavement temperature (°C);

$A$  = coefficient of surface temperature;

$C1_{max}$ = maximal daily surface temperature (°C);

$B$  = coefficient of the depth;

$Depth$  = distance from the surface (cm);

$C$  = coefficient for the day of the year;

$Day$  = day of the year;

$D$  = coefficient for the square of the day of the year;

$E$  = intercept.

Tables 4.139 and 4.140 present the coefficients for the linear prediction models developed for location Al Jufroh. Included with the model coefficients and their standard errors are the standard errors of estimate and the adjusted R<sup>2</sup>. The coefficients statistically different from zero are denoted in red. Tables of coefficients for the pavement temperature for the remaining stations are presented in Appendix O.

Table 4.139 Characteristics of the model for predicting maximal daily pavement temperatures from maximal daily surface temperature, the day of the year, and depth from the surface at the Al Jufroh location.

Al Jufroh max	Regression Summary for Dependent Variable: Temperature_max (Temp_depth_C1_max_Novo) R= .98856847 R <sup>2</sup> = .97726761 Adjusted R <sup>2</sup> = .97718419 F(4,1090)=11715. p<0.0000 Std.Error of estimate: 1.5839 Include condition: Site=102					
	b*	Std.Err. of b*	b	Std.Err. of b	t(1455)	p-value
Intercept			3.717944	0.298704	12.4469	0.000000
Depth	-0.153864	0.004567	-0.327666	0.009725	-33.6922	0.000000
C1_max	0.937313	0.011054	0.822918	0.009705	84.7943	0.000000
Day	0.170018	0.043142	0.016850	0.004276	3.9409	0.000086
Day <sup>2</sup>	-0.170647	0.044094	-0.000045	0.000012	-3.8700	0.000115

$$y_{max} = 0.822918 * C1_{max} - 0.327666 * Depth + 0.016850 * Day - 0.000045 * Day^2 + 3.717944$$

The model for minimal daily temperatures of the pavement including the minimal daily surface temperature, depth from the surface, and day of the year is of the following form:

$$y_{min} = A * C1_{min} + B * Depth + C * Day + D * Day^2 + E$$

where

$y_{min}$ = predicted minimum pavement temperature (°C);

$A$  = coefficient of surface temperature;

$C1_{min}$ = minimum surface temperature (°C);

$B$  = coefficient of the depth;

$Depth$  = distance from the surface (cm);

$C$  = coefficient for the day of the year;

Day = day of the year;

$D$  = coefficient for the square of the day of the year;

$E$  = intercept.

Table 4.140 Characteristics of the model for predicting minimal daily pavement temperatures from minimal daily surface temperature, the day of the year, and depth from the surface at the Al Jufroh location.

Al Jufroh min	Regression Summary for Dependent Variable: Temperature_min (Temp_depth_C1_min_Novo) R= .97781001 R <sup>2</sup> = .95611242 Adjusted R <sup>2</sup> = .95595136 F(4,1090)=5936.5 p<0.0000 Std.Error of estimate: 1.5039 Include condition: Site=102					
	b*	Std.Err. of b*	b	Std.Err. of b	t(1451)	p-value
Intercept			0.584464	0.159082	3.6740	0.000250
Depth	0.166833	0.006345	0.242782	0.009234	26.2921	0.000000
C1_min	0.836221	0.013617	0.847858	0.013806	61.4118	0.000000
Day	0.548897	0.054174	0.037174	0.003669	10.1321	0.000000
Day <sup>2</sup>	-0.574319	0.053730	-0.000103	0.000010	-10.6889	0.000000

$$y_{min} = 0.847858A * C1_{min} + 0.242782 * Depth + 0.037174 * Day - 0.000103 * Day^2 + 0.584464$$

#### 4.8.2.1 Relationship with surface temperature, the depth from the surface, day of the year, and the latitude

The next models describe the relationship between maximal/minimal daily pavement temperatures at three layers and surface temperatures, the day of the year, depth from the surface, and latitude.

The model for maximal daily temperatures is of the following form:

$$y_{max} = A * C1_{max} + B * Depth + C * Lat + D * Day + E * Day^2 + F$$

where

$y_{max}$ = predicted maximal daily pavement temperature (°C);

$A$  = coefficient of surface temperature;

$C1_{max}$ = maximal daily surface temperature (°C);

$B$  = coefficient of the depth;

$Depth$  = distance from the surface (cm);

$C$  = coefficient of the latitude;

$Lat$  = latitude (degrees);

$D$ = coefficient of the day of the year;

$Day$ = day of the year;

$E$ = coefficient of the square of the day of the year;

$F$  = intercept.

Table 4.141 Characteristics of the model for predicting maximal daily pavement temperatures from maximal daily surface temperature, depth from the surface, day of the year, and latitude.

All locations max	Regression Summary for Dependent Variable: Temperature_max (Temp_depth_C1_max_Novo) R= .97281528 R <sup>2</sup> = .94636956 Adjusted R <sup>2</sup> = .94633888 F(5,8738)=30838. p<0.0000 Std.Error of estimate: 2.5422					
	b*	Std.Err. of b*	b	Std.Err. of b	t(11657)	p-value
Intercept			7.112629	0.466886	15.234	0.000000
Depth	-0.253602	0.002477	-0.565419	0.005524	-102.365	0.000000
C1_max	0.819528	0.006021	0.777906	0.005715	136.111	0.000000
Day	0.529299	0.023106	0.054947	0.002399	22.908	0.000000
Day <sup>2</sup>	-0.514847	0.023732	-0.000142	0.000007	-21.694	0.000000
Latitude	-0.010282	0.002642	-0.054130	0.013908	-3.892	0.000100

$$y_{max} = 0.777906 * C1_{max} - 0.565419 * Depth - 0.054130 * Lat + 0.054947 * Day - 0.000142 * Day^2 + 7.112629$$

The model for minimal daily temperatures is of the following form:

$$y_{min} = A * C1_{min} + B * Depth + C * Lat + D * Day + E * Day^2 + F$$

where

$y_{min}$ = predicted minimum pavement temperature (°C);

$A$  = coefficient of surface temperature;

$C1_{min}$ = minimum surface temperature (°C);

$B$  = coefficient of the depth;

$Depth$  = distance from the surface (cm);

$C$  = coefficient of the latitude;

$Lat$  = latitude (degrees);

$D$ = coefficient of the day of the year;

$Day$ = day of the year;

$E$ = coefficient of the square of the day of the year;

$Day^2$ = square of the day of the year; and

$F$  = intercept.



Table 4.142 Characteristics of the model for predicting minimal daily pavement temperatures from minimal daily surface temperature, depth from the surface, day of the year, and latitude.

Al locations min	Regression Summary for Dependent Variable: Temperature_min (Temp_depth_C1_min_Novo) R= .95804407 R <sup>2</sup> = .91784844 Adjusted R <sup>2</sup> = .91780145 F(5,8742)=19534. p<0.0000 Std.Error of estimate: 2.2441					
	b*	Std.Err. of b*	b	Std.Err. of b	t(11658)	p-value
Intercept			9.336789	0.323623	28.8508	0.00
Depth	0.16286	0.003066	0.258991	0.004875	53.1251	0.00
C1_min	0.65378	0.005481	0.667845	0.005599	119.2882	0.00
Day	1.28618	0.021719	0.095249	0.001608	59.2178	0.00
Day <sup>2</sup>	-1.26853	0.021743	-0.000249	0.000004	-58.3406	0.00
Latitude	-0.09334	0.003066	-0.350496	0.011511	-30.4477	0.00

$$y_{min} = 0.667845 * C1_{min} + 0.258991 * Depth - 0.350496 * Lat + 0.095249 * Day - 0.000249 * Day^2 + 9.336789$$

### 4.8.3 Relationship with surface temperature, depth from the surface and cumulative solar radiation

The next models describe the relationship between maximal/minimal daily pavement temperatures and surface temperatures, depth from the surface and cumulative solar radiation.

The model for maximal daily temperatures of the pavement including the maximal daily surface temperature, depth from the surface and cumulative solar radiation is of the following form:

$$y_{max} = A * C1_{max} + B * Depth + C * Cum\_SR + D$$

where

$y_{max}$  = predicted maximal daily pavement temperature (°C);

$A$  = coefficient of surface temperature;

$C1_{max}$  = maximal daily surface temperature (°C);

$B$  = coefficient of the depth;

$Depth$  = depth from the surface (cm);

$C$  = coefficient for the cumulative solar radiation;

$Cum\_SR$  = the solar radiation (W/m<sup>2</sup>); and

$D$  = intercept.

Tables 4.143 and 4.144 present the coefficients for the linear prediction models developed for location Al Jufroh. Included with the model coefficients and their standard errors are the standard errors of estimate and the adjusted R<sup>2</sup>. The coefficients statistically different from zero are denoted in red. Tables of coefficients for the pavement temperature for the remaining stations are presented in Appendix O.

Table 4.143 Characteristics of the model for predicting maximal daily pavement temperatures from maximal daily surface temperature, cumulative solar radiation and depth from the surface at the Al Jufroh location.

Al Jufroh max	Regression Summary for Dependent Variable: Temperature_max (Temp_depth_C1_max_Novo) R= .98831079 R <sup>2</sup> = .97675823 Adjusted R <sup>2</sup> = .97669361 F(3,1079)=15115. p<0.0000 Std.Error of estimate: 1.6015 Include condition: Site=102					
	b*	Std.Err. of b*	b	Std.Err. of b	t(1440)	p-value
Intercept			3.093709	0.226606	13.6524	0.000000
Depth	-0.153814	0.004641	-0.327692	0.009888	-33.1416	0.000000
C1_max	0.976495	0.010375	0.857138	0.009107	94.1231	0.000000
Cum_SR	-0.000253	0.010375	-0.000000	0.000016	-0.0244	0.980529

$$y_{max} = 0.857138 * C1_{max} - 0.327692 * Depth - 0.000000 * Cum\_SR + 3.093709$$

The model for minimal daily temperatures of the pavement including the minimal daily surface temperature, depth form the surface, and cumulative solar radiation is of the following form:

$$y_{min} = A * C1_{min} + B * Depth + C * Cum\_SR + D$$

where

$y_{min}$  = predicted minimum pavement temperature (°C);

$A$  = coefficient of surface temperature;

$C1_{min}$  = minimum surface temperature (°C);

$B$  = coefficient of the depth;

$Depth$  = depth from the surface (cm);

$C$  = coefficient for solar radiation;

$Cum\_SR$  = solar radiation (W/m<sup>2</sup>); and

$D$  = intercept.

Table 4.144 Characteristics of the model for predicting minimal daily pavement temperatures from minimal daily surface temperature, cumulative solar radiation and depth from the surface at the Al Jufroh location.

Al Jufroh min	Regression Summary for Dependent Variable: Temperature_min (Temp_depth_C1_min_Novo) R= .97687919 R <sup>2</sup> = .95429296 Adjusted R <sup>2</sup> = .95416588 F(3,1079)=7509.3 p<0.0000 Std.Error of estimate: 1.5331 Include condition: Site=102					
	b*	Std.Err. of b*	b	Std.Err. of b	t(1440)	p-value
Intercept			-0.628669	0.198618	-3.16522	0.001593
Depth	0.167141	0.006508	0.243078	0.009465	25.68049	0.000000
C1_min	0.877760	0.010972	0.889057	0.011113	79.99868	0.000000
Cum_SR	0.102823	0.010972	0.000110	0.000012	9.37123	0.000000

$$y_{min} = 0.889057 * C1_{min} + 0.243078 * Depth + 0.000110 * Cum\_SR - 0.628669$$

#### 4.8.3.1 Relationship with surface temperature, the depth from the surface, cumulative solar radiation, and latitude

The next models describe the relationship between maximal/minimal daily pavement temperatures and maximal/minimal daily surface temperatures, cumulative solar radiation, depth from the surface, and latitude.

The model for maximal temperatures is of the following form:

$$y_{max} = A * C1_{max} + B * Depth + C * Lat + D * Cum\_SR + E$$

where

$y_{max}$ = predicted maximal daily pavement temperature (°C);

$A$  = coefficient of surface temperature;

$C1_{max}$  = maximal daily surface temperature (°C);

$B$  = coefficient of the depth;

$Depth$  = depth from the surface (cm);

$C$  = coefficient of the latitude;

$Lat$  = latitude (degrees);

$D$ = coefficient of the cumulative solar radiation;

$Cum\_SR$ = cumulative solar radiation (W/m<sup>2</sup>);and

$E$ = intercept.

Table 4.145 Characteristics of the model for predicting maximal daily pavement temperatures from maximal daily surface temperature, depth from the surface, cumulative solar radiation, and latitude.

All locations max	Regression Summary for Dependent Variable: Temperature_max (Temp_depth_C1_max_Novo) R= .97074322 R <sup>2</sup> = .94234240 Adjusted R <sup>2</sup> = .94231587 F(4,8693)=35519. p<0.0000 Std.Error of estimate: 2.6336					
	b*	Std.Err. of b*	b	Std.Err. of b	t(11657)	p-value
Intercept			2.522759	0.413393	6.1026	0.000000
Depth	-0.253984	0.002575	-0.565855	0.005738	-98.6191	0.000000
C1_max	0.929537	0.003206	0.882265	0.003043	289.9655	0.000000
Cum_SR	0.014533	0.003174	0.000020	0.000004	4.5791	0.000005
Latitude	0.007499	0.002607	0.039447	0.013715	2.8763	0.004034

$$y_{max} = 0.882265 * C1_{max} - 0.565855 * Depth + 0.039447 * Lat + 0.000020 * Cum\_SR + 2.522759$$

The model for minimal daily temperatures is of the following form:

$$y_{min} = A * C1_{min} + B * Depth + C * Lat + D * Cum\_SR + E$$

where

$y_{min}$ = predicted minimum pavement temperature (°C);

$A$  = coefficient of surface temperature;

$C1_{min}$  = minimum surface temperature (°C);

$B$  = coefficient of the depth;

$Depth$  = depth from the surface (cm);

$C$  = coefficient of the latitude;

$Lat$  = latitude (degrees);

$D$ = coefficient of the cumulative solar radiation;

$Cum\_SR$ = cumulative solar radiation (W/m<sup>2</sup>); and

$E$ = intercept.

Table 4.146 Characteristics of the model for predicting minimal daily pavement temperatures from minimal daily surface temperature, depth from the surface, cumulative solar radiation, and latitude.

All locations min	Regression Summary for Dependent Variable: Temperature_min (Temp_depth_C1_min_Novo) R= .94196712 R <sup>2</sup> = .88730205 Adjusted R <sup>2</sup> = .88725017 F(4,8689)=17103. p<0.0000 Std.Error of estimate: 2.6304					
	b*	Std.Err. of b*	b	Std.Err. of b	t(11587)	p-value
Intercept			9.237925	0.386171	23.9219	0.000000
Depth	0.162793	0.003601	0.259098	0.005732	45.2025	0.000000
C1_min	0.894934	0.004152	0.913787	0.004240	215.5236	0.000000
Cum_SR	0.054011	0.004158	0.000054	0.000004	12.9897	0.000000
Latitude	-0.087874	0.003607	-0.330332	0.013561	-24.3587	0.000000

$$y_{min} = 0.913787 * C1_{min} + 0.259098 * Depth - 0.330332 * Lat + 0.000054 * Cum\_SR + 9.237925$$

The maximal daily temperature of pavement at different depths depends mostly on maximal daily surface temperatures. It decreases with depth and latitude, increases with cumulative solar radiation and depends on the day of the year.

The minimal daily temperature of pavement at different depths depends mostly on minimal daily surface temperature and the day of the year. It increases with depth and cumulative solar radiation and decreases with latitude.

#### 4.8.4 Models including wind speed

The model for predicting maximal/minimal daily pavement temperatures at different depths including maximal/minimal daily surface temperatures, cumulative solar radiation and wind speed

were made. However, the models have very similar adjusted  $R^2$  and standard error of estimate compared to models including only surface temperature, cumulative solar radiation, and wind speed, indicating a similar fit to the data. Therefore, we do not present them here.

#### **4.6.5 Relationship with surface temperature, the distance from the surface, day of the year and cumulative solar radiation and latitude**

The next models describe the relationship between maximal/minimal daily pavement temperatures and maximal/minimal daily surface temperatures, day of the year cumulative solar radiation, distance from the surface and latitude.

The model for maximal daily temperatures is of the following form:

$$y_{max} = A * C1_{max} + B * Depth + C * Day + D * Day^2 + E * Lat + F * Cum\_SR + G$$

where

$y_{max}$  = predicted maximal daily pavement temperature ( $^{\circ}\text{C}$ );

$A$  = coefficient of surface temperature;

$C1_{max}$  = maximal daily surface temperature ( $^{\circ}\text{C}$ );

$B$  = coefficient of the distance from the surface;

$Depth$  = distance from the surface (cm);

$C$  = coefficient of the day of the year;

$Day$  = day of the year;

$D$  = coefficient of square of the day of the year;

$Day^2$  = square of the day of the year;

$E$  = coefficient of the latitude;

$Lat$  = latitude (degrees);

$F$  = coefficient of the cumulative solar radiation;

$Cum\_SR$  = cumulative solar radiation ( $\text{W}/\text{m}^2$ ); and

$G$  = intercept.

Table 4.147 Characteristics of the model for predicting maximal daily pavement temperatures from maximal daily surface temperature, distance from the surface, day of the year, cumulative solar radiation and latitude.

All locations max	Regression Summary for Dependent Variable: Temperature_max (Temp_depth_C1_max_Novo) R= ,97267866 R <sup>2</sup> = ,94610378 Adjusted R <sup>2</sup> = ,94636657 F(6,8691)=25427, p<0,0000 Std.Error of estimate: 2,5465					
	b*	Std.Err. of b*	b	Std.Err. of b	t(11587)	p-value
Intercept			7,059526	0,473429	14,911	0,000000
Depth	-0,254015	0,002490	-0,565925	0,005548	-102,003	0,000000
C1_min	0,817837	0,006076	0,776246	0,005767	134,606	0,000000
Day	0,526803	0,023947	0,054628	0,002483	21,998	0,000000
Day <sup>2</sup>	-0,511625	0,024702	-0,000141	0,000007	-20,712	0,000000
Cum_SR	0,004101	0,003205	0,000006	0,000004	1,280	0,200748
Latitude	-0,010152	0,002657	-0,053402	0,013978	-3,820	0,000134

$$y_{max} = 0,776246 * C1_{max} - 0,565925 * Depth + 0,054628 * Day - 0,000141 * Day^2 - 0,053402 * Lat + 0,000006 * Cum\_SR + 7,059526$$

The model for minimal daily temperatures is of the following form:

$$y_{min} = A * C1_{min} + B * Depth + C * Day + D * Day^2 + E * Lat + F * Cum\_SR + G$$

where

$y_{min}$  = predicted minimal daily pavement temperature (°C);

$A$  = coefficient of surface temperature;

$Air_{min}$  = minimal daily surface temperature (°C);

$B$  = coefficient of the depth;

$Depth$  = distance from the surface (cm);

$C$  = coefficient of the day of the year;

$Day$  = day of the year;

$D$  = coefficient of square of the day of the year;

$Day^2$  = square of the day of the year;

$E$  = coefficient of the latitude;

$Lat$  = latitude (degrees);

$F$  = coefficient of the cumulative solar radiation;

$Cum\_SR$  = cumulative solar radiation (W/m<sup>2</sup>); and

$G$  = intercept.

Table 4.148 Characteristics of the model for predicting minimal daily pavement temperatures from minimal daily surface temperature, depth from the surface, day of the year, cumulative solar radiation and latitude

All locations min	Regression Summary for Dependent Variable: Temperature_min (Temp_depth_C1_min_Novo) R= ,95814254 R <sup>2</sup> = ,91803713 Adjusted R <sup>2</sup> = ,91798052 F(6,8687)=16217, p<0,0000 Std.Error of estimate: 2,2435					
	b*	Std.Err. of b*	b	Std.Err. of b	t(11587)	p-value
Intercept			9,836403	0,334020	29,4486	0,000000
Depth	0,16279	0,003072	0,259098	0,004889	52,9983	0,000000
C1_min	0,65480	0,005510	0,668591	0,005627	118,8281	0,000000
Day	1,34042	0,023626	0,099289	0,001750	56,7356	0,000000
Day <sup>2</sup>	-1,32764	0,023965	-0,000261	0,000005	-55,3999	0,000000
Cum_SR	-0,02539	0,003964	-0,000025	0,000004	-6,4058	0,000000
Latitude	-0,09457	0,003080	-0,355490	0,011577	-30,7055	0,000000

$$y_{min} = 0,668591 * C1_{min} + 0,259098 * Depth + 0,099289 * Day - 0,000261 * Day^2 - 0,355490 * Lat - 0,000025 * Cum\_SR + 9,836403$$

Daily maximal temperature of pavement at different depths depends mostly on daily maximal surface temperatures but decreases with depth and depends on the day of the year. It decreases with latitude and increases with cumulative solar radiation.

Daily minimal temperature of pavement at different depths depends mostly on daily minimal surface temperature and the day of the year. It increases with depth and cumulative solar radiation and decreases with latitude.

#### 4.8.5 Evaluation of the models including surface temperature and depth from the surface

As can be seen from the models which included the surface temperature and depth from the surface, could be improved (especially models for maximal temperatures) by adding new variables, such as day of the year, wind speed and cumulative solar radiation. However, wind speed did not improve the models significantly, as can be seen from the values of adjusted R<sup>2</sup> and standard errors in table 4.149. Higher values of adjusted R<sup>2</sup> and lower standard errors were obtained when the model included day of the year or solar radiation. The best values of adjusted R<sup>2</sup> and standard error were obtained when the model included day of the year.

Table 4.149 Adjusted R<sup>2</sup> and standard errors for different models which are based on the data from all locations.

<b>Models for maximal daily temperatures</b>									
The model including latitude, distance from the surface and									
Surface temp		Surface temp, wind speed		Surface temp, day of the year		Surface temp, cum. solar radiation		Surface temp, day of the year, cum. solar radiation	
Adj. R <sup>2</sup>	Std.Err of est.	Adj. R <sup>2</sup>	Std.Err of est.	Adj. R <sup>2</sup>	Std.Err of est.	Adj. R <sup>2</sup>	Std.Err of est.	Adj. R <sup>2</sup>	Std.Err of est.
.94250	2.6314	.94253	2,6308	.94633	2,5422	.94231	2.6336	,94636	2,5465
<b>Models for minimal daily temperatures</b>									
The model including latitude, distance from the surface and									
Surface temp		Surface temp, wind speed		Surface temp, day of the year		Surface temp, cum. solar radiation		Surface temp, day of the year, cum. solar radiation	
Adj. R <sup>2</sup>	Std.Err of est.	Adj. R <sup>2</sup>	Std.Err of est.	Adj. R <sup>2</sup>	Std.Err of est.	Adj. R <sup>2</sup>	Std.Err of est.	Adj. R <sup>2</sup>	Std.Err of est.
.88481	2.6565	,88519	2,6510	.91780	2.2441	.88725	2.6304	,91798	2,2435

Therefore, we conclude that the best model for predicting pavement temperatures is linear regression with surface temperature, distance from the surface, cumulative solar radiation and day of the year.

The best model maximal daily pavement temperatures are:

$$T_{pav,d}^{max} = 7,059526 + 0,776246T_{surf}^{max}d + 0,054628Day - 0,000141Day^2 + 0,000006Cum\_SR - 0,053402Lat$$

where

$T_{pav,d}^{max}$  = maximal daily pavement temperature at distance  $d$  from the surface, (°C);

$T_{surf}^{max}$  = maximal daily surface temperature, (°C);

$d$  = distance from the surface (cm);

$Day$  = day of the year;

$Day^2$  = square of the day of the year;

Cum\_SR = cumulative solar radiation (W/m<sup>2</sup>)and

$Lat$  = latitude of the section, (degrees).



The best model minimal daily pavement temperatures are:

$$T_{pav,d}^{min} = 9,836403 + 0,668591T_{surf}^{min} + 0,259098d + 0,099289Day - 0,000261Day^2 - 0,000025Cum\_SR - 0,355490Lat$$

where

$T_{pav,d}^{min}$  =minimal daily pavement temperature at distance  $d$  from the surface, (°C);

$T_{surf}^{min}$ = minimal daily surface temperature, (°C);

$Day$  = day of the year;

$d$ = distance from the surface (cm);

$Day^2$  = square of the day of the year;

$Cum\_SR$  = cumulative solar radiation (W/m<sup>2</sup>)and

$Lat$ = latitude of the section, (degrees).

In the case when data on cumulative solar radiation are not available, the next best model for predicting the maximal/minimal daily pavement temperatures is linear regression with maximal/minimal daily surface temperature, and day of the year, developed in section 4.8.2.

Figures 4.57 and 4.58 present actual maximal/minimal daily pavement temperature and predicted values from the model including maximal/minimal daily surface temperature, distance from the surface and the day of the year at the Al-Jufroh location. In Appendix P, similar figures for other locations are given.

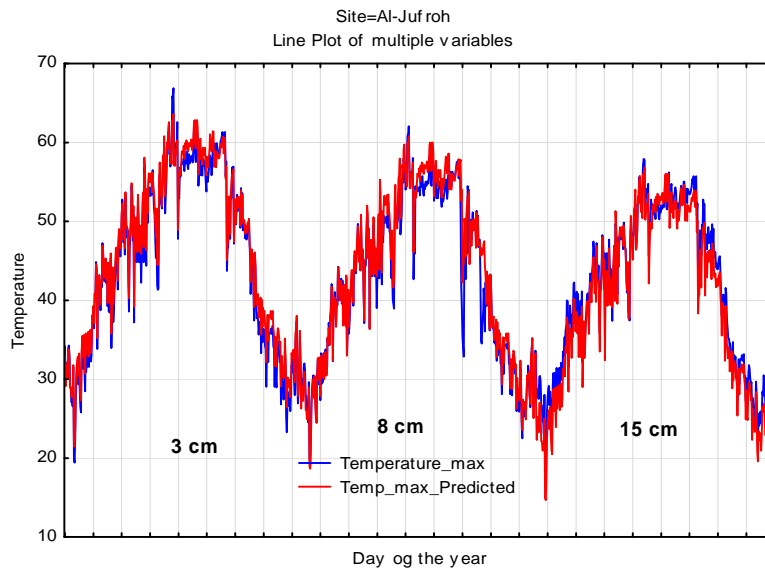


Figure 4.57 Actual maximal daily pavement temperature and predicted values from the model including maximal daily surface temperature, depth from the surface and day of the year at the Al-Jufroh location.

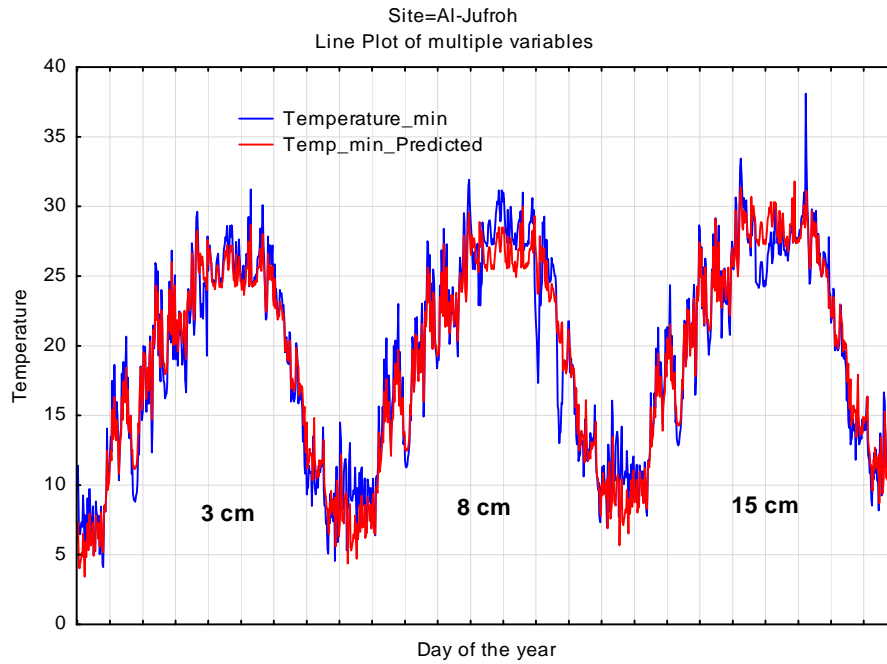


Figure 4.58 Actual minimal daily pavement temperature and predicted values from the model including maximal daily surface temperature, depth from the surface and day of the year at the Al Jufroh location.

#### 4.9 Comparison of model developed for Libyan Desert with SHRP and LTPP models

Using the models obtained in section 4.5, including air temperature, day of the year, and daily cumulative solar radiation, the predicted temperatures for pavement temperatures for four layers were calculated, and the comparison with the SHRP and LTPP models was made. In figures 4.59 and 4.60, this comparison is presented for daily maximal and minimal surface pavement temperatures at the Ghat location.

In order to compare our model and SHRP and LTPP low temperature prediction models for pavement surface temperature, we consider the SHRP model,

$$T_{surf}^{min} = 0.859 * T_{air}^{min} + 1.7 \quad (4.1)$$

and LTPP model

$$T_{surf}^{min} = -1.56 + 0.72 * T_{air}^{min} - 0.004 * Lat^2 + 6.26 \log_{10}(25) \quad (4.2)$$

where  $T_{surf}^{min}$  is the daily minimum pavement surface temperature, and  $T_{air}^{min}$  is the daily minimum air temperature in °C and  $Lat$  is latitude.

In order to compare our model and SHRP and LTPP high temperature prediction models for pavement surface temperature, we consider the SHRP model,

$$T_{surf}^{max} = (T_{air}^{max} - 0.00618 * Lat^2 + 0.2289 * Lat + 42.4) * 0.9545 - 17.78 \quad (4.3)$$

and LTPP model

$$T_{surf}^{max} = 54.32 + 0.78 * T_{air}^{max} - 0.0025 * Lat^2 - 15.14 \log_{10}(25) \quad (4.4)$$

where  $T_{surf}^{max}$  is the daily minimum pavement surface temperature, and  $T_{air}^{max}$  is the daily minimum air temperature in °C and  $Lat$  is latitude

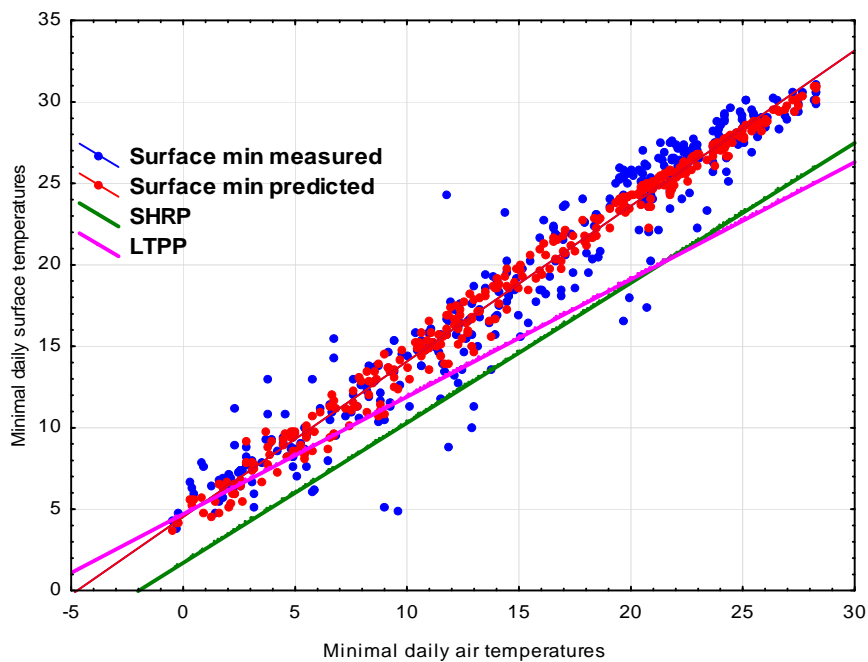


Figure 4.59 Comparison between daily minimal surface pavement temperature prediction model and SHRP and LTPP models at the Ghat location.

It can be seen that the predicted daily minimal surface pavement temperatures using the SHRP model are lower than both the measured values and the minimal surface pavement temperature predicted by the developed models. SHRP and LTPP models underestimate minimal daily surface pavement temperatures both for the measured values and for predicted temperatures by the developed models. Therefore, the developed model is more representative of Libya's climatic conditions. SHRP and LTPP models would be expected to result in a different selection of the PG binder.

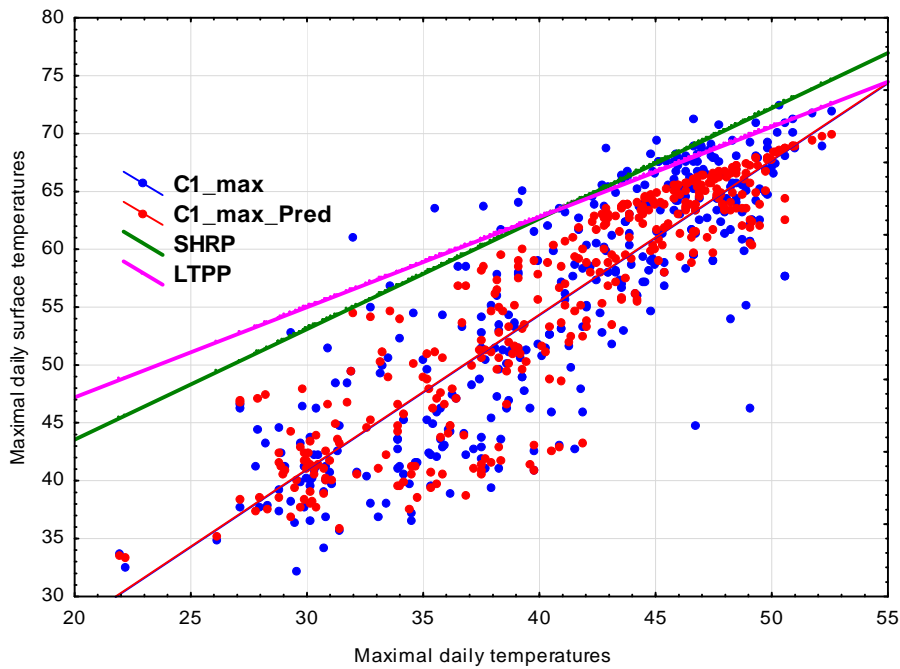


Figure 4.60 Comparison between daily maximal surface pavement temperature prediction model and SHRP and LTPP models.

It can be seen that the predicted daily maximal surface pavement temperatures by the SHRP and LTPP models are higher than both the measured values and the maximal surface pavement temperature predicted by the developed model. SHRP and LTPP model overestimates maximal daily surface pavement temperatures both for the measured values and for predicted temperatures by the developed models. Therefore, the developed model is more representative of Libya's climatic conditions. SHRP and LTPP models would be expected to result in a different selection of the PG binder.

# **Chapter 5 PERFORMANCE GRADE OF BITUMEN ON LIBYAN DESERT**

## **5.1 Introduction**

The current asphalt binder specifications in Libya are based on the Penetration Grade penetration test performed at 25°C. Penetration is an empirical measure of consistency; it is used as an empirical indicator of the rutting and fatigue susceptibility of asphalt binder and is not related to pavement performance. The new mix design methodology developed under the SHRP is called the Superpave; it is a performance-based approach. The first step in the implementation of Superpave methodology is to establish high and low pavement temperatures for a location. The temperatures define the required PG of asphalt binder.

## **5.2 Superpave performance grading (PG system)**

From October 1987 through March 1993, the SHRP conducted research to develop new ways to specify, test, and design asphalt materials. The end result of this asphalt research program was the development of the Superior Performing Asphalt Pavements (Superpave) system. One of the key aspects of the Superpave is the development of the performance based binder specifications termed as Performance Grade (PG) asphalt. Since the major objective of the SHRP program was to relate mechanical properties of asphalt binder to field performance, the new specification tests were developed to characterize asphalt binders at a broad range of temperatures and aging conditions. The three aging conditions specified are original, short term and long term. Original aging refers to virgin asphalt from the production plant; short-term aging refers to properties at the time of production and placement of asphalt mix; and long-term aging refers to properties of asphalt binder during the service life of pavements. In addition to aging conditions, Superpave characterizes the asphalt binders at the actual pavement temperatures they are likely to experience. Behind the short presentation of PG system given in Chapter 2.8 and 2.13 a brief summary of the binder grading systems for the purpose of mix design follows:

For example a binder classified as a PG 58-34 means and the low temperature physical property requirements down to -34°C. That it will meet the high temperature physical property requirements up to a temperature of 58°C

## **5.3 Binder Specifications**

The development of binder testing goes back to 1888, when H. C. Bowen invented the Bowen Penetration Machine (Strategic Highway Research Program, 1994). After several modifications of penetration equipment, by 1910 the penetration equipment became the standard for establishing the

consistency of asphalt at 25°C. In 1918 the Bureau of Public Road (USA) introduced the penetration grading system, and by 1931 the American Association of State Highway and Transportation Officials (AASHTO) published the standard specification to grade asphalt on penetration.

The next major change in asphalt grading specification came with the introduction of the viscosity grading system in the early 1960s. Both ASTM and AASHTO adopted the viscosity grading system and provided grading specification by measuring the viscosity at 60°C.

The penetration grading system, based on penetration of a standard needle under standard conditions in asphalt binder, is empirical in nature. The test provides the relative consistency of binder at specific temperatures, which can be used as an indicator of susceptibility of asphalt binder to rutting or cracking. It has performed quite satisfactorily for many decades and has provided the means for identifying the major asphalt pavement distresses: permanent deformation and cracking (fatigue and thermal). ASTM D946 specifies the five binder grades based upon penetration at 25°C. The greater the penetration, the softer the binder.

In the case of viscosity grading, viscosity at 60°C (close to maximum pavement temperature) is specified. The specifications also require a minimum viscosity to be measured at 135°C to reduce the potential of tender mix at the time of compaction. ASTM D3381 specifies six binder grades based upon the viscosity measured at 60°C. Table 5.1 provides the standard penetration and viscosity grades. The top row values in Table 5.1 represent relatively harder binders, whereas the lower rows represent the softer binder.

Table 5.1 Penetration and viscosity grading system

<b>Penetration grading</b>		<b>Viscosity Grading</b>	
<b>Grade</b>	<b>Penetration in 0.1 mm</b>	<b>Grade</b>	<b>Viscosity @ 60°C, Poise</b>
Pen 40/50	40-50	AC - 40	4000 ± 800
Pen 60/70	60-70	AC - 30	3000 ± 600
Pen 85/100	85-100	AC - 20	2000 ± 400
Pen 120/150	120-150	AC - 10	1000 ± 200
Pen 200/300	200-300	AC - 5	500 ± 100
		AC - 2.5	250 ± 50

Generally, softer binder grades are used in cold climates to resist cracking potential and harder binders are used in warmer climates to resist rutting potential. In Libya, a standard grade of Pen 60/70 is used for construction of flexible pavement. However, the refineries in Libya also produce Pen 60/70. Viscosity grading is not yet established in Libya.

The viscosity grading system based on the fundamental property, is considered a step forward in specifying the binder as compared to penetration grading. It requires binder to be tested at 60°C

and 135°C, which corresponds to typical maximum pavement temperature and temperature at the time of mix production and placement in the field, respectively. Viscosity specification at 60°C helps in minimizing rutting potential, whereas, viscosity at 135°C minimizes the potential for tender mixes during paving operation. Despite these added benefits, it fails to characterize the binder at low temperatures to minimize the potential of thermal cracking and pavement performance prediction. Figure 5.1 shows the criteria used for penetration and viscosity grading systems. Two asphalt binders A and B, which meet the penetration and viscosity specifications, may behave very differently at other temperatures.

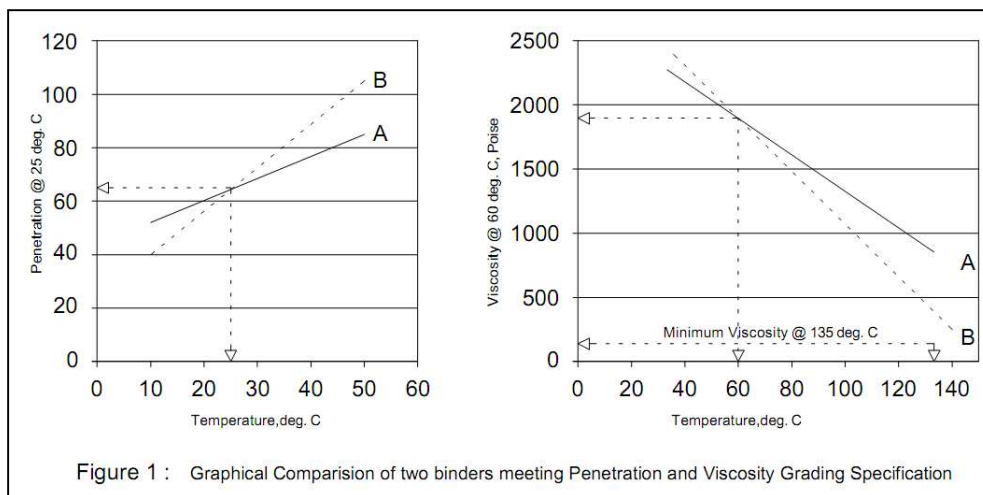


Figure 5.1 Graphical comparison of two binders meeting penetration and viscosity grading specification.

The Superpave system is unique in a sense that asphalt binder is specified on the basis of the maximum and minimum pavement temperatures in which the binder is expected to serve. While the mechanical properties requirement remain the same, the temperature at which the asphalt binders achieve the physical properties corresponds to the pavement minimum and maximum temperature. For example, a high temperature requires binder to have  $G^*/\sin$  to be at least 1.0 kPa for aged condition ( $G^*$  is the shear modulus in kPa and is the phase angle). The value of 1.0 kPa remains constant, but the temperature at which this value has to be achieved depends upon the maximum pavement temperature. Another important feature of Superpave is that mechanical properties are measured on the asphalt binders at three conditions: unaged, short-term aged and long-term aged. The short and long-term aging is simulated in the laboratory using Rolling Thin Film Oven (RTFO) and Pressure Aging Vessel (PAV), respectively. The required mechanical properties at the three aging conditions both for high and low temperatures are specified in the Superpave specifications (MP1: Specification for Performance-Graded Asphalt Binder).

Table 5.2 Binder grades as specified in Superpave specifications

<b>High temperature Grade, °C</b>	<b>Low temperature Grade, °C</b>
PG 46	34, 40, 46
PG 52	10, 16, 22, 28, 34, 40, 46
PG 58	16, 22, 28, 34, 40
PG 64	10, 16, 22, 28, 34, 40
PG 70	10, 16, 22, 28, 34, 40
PG 76	10, 16, 22, 28, 34
PG 82	10, 16, 22, 28, 34, 40

The temperatures given in Table 5.2 correspond to the pavement temperature and can be estimated from the air temperature data collected over the years. Superpave defines the high and low temperatures by seven-day average maximum air and 1-day minimum air temperature. The seven-day average maximum temperature is defined as the average of highest air temperature for a period of seven consecutive days within a given year. The 1-day minimum temperature is defined as the lowest air temperature recorded in a given year. The data are collected over multiple years, and the design high and low pavement temperature values are then estimated using the average and standard deviations of the data collected for a desired reliability level.

## **5.4 Pavement Temperature by SHRP**

Several studies have been conducted to relate the air temperature to pavement temperature. Regression equations along with mathematical heat flow theories have been used for the correlation. Among these, models, based upon air temperature data, for the prediction of high and low pavement temperatures were established during the SHRP. Later SHRP established the LTPP program to support a broad range of pavement performance analysis, leading to improved engineering tools to design, construct, and manage pavements. The SMP, a task of LTPP, evaluated the effects of temperature variations on performance and validated the available models (Asi IM, 2007), this resulted in a new set of pavement temperature prediction models for the high and low temperature grade. Given below are the models developed under the SHRP and LTPP for high and low pavement temperature predictions.

### **5.4.1 High Temperature Models**

The SHRP high temperature model was developed from the results of theoretical heat transfer modeling (Brown, et al., 2001). Based upon the data collected from several sites throughout the United States, a regression model was developed for prediction of high pavement temperature as a function of depth. Superpave defines the high pavement design temperature at a depth of 20 mm below the pavement surface. Equation (1) represents the model



developed under the SHRP program, whereas Equation (2) is the revised LTPP high-temperature equation.

$$T_{pav,h} = (T_{air} - 0.00618Lat^2 + 0.2289Lat + 42.2)(0.9545) - 17.78 + \sigma_{air} \quad (5.1)$$

$$T_{pav,h,d} = 54.32 + 0.78T_{air} - 0.0025Lat^2 - 15.14 \log_{10}(d + 25) - z(9 + 0.61\sigma_{air}^2)^{1/2} \quad (5.2)$$

where

$T_{pav,h}$  = high AC pavement temperature at 20 mm from surface, (°C);

$T_{pav,h,d}$  = high AC pavement temperature at depth d from surface, (°C);

$T_{air}$  = high 7-day mean air temperature, (°C);

$Lat$  = latitude of the section, degrees;

$d$  = pavement depth, mm;

$\sigma_{air}$  = standard deviation of the 7-day maximum air temperature, (°C); and

$z$  = standard normal distribution value,  $z = 2.055$  for 98% reliability, and  $z = 0.0$  for 50% reliability.

#### 5.4.2 Low temperature models

SHRP considers the low air temperature as the design low pavement temperature (Brown, et al. 2001). The low pavement design temperature at the pavement surface is the same as the one-day minimum temperature since the air temperature is the same as the pavement surface temperature. This can be mathematically represented by the following relationship.

$$T_{pav,l} = T_{air} + 0.051d - 0.000063d^2 - z\sigma_{air}. \quad (5.3)$$

The LTPP low pavement temperature at the surface is presented in Equation (5.4) below.

$$T_{pav,l} = -1.56 + 0.72T_{air} - 0.004 * Lat^2 + 6.26 \log_{10}(d + 25) - z(4.4 + 0.52\sigma_{air}^2)^{1/2} \quad (5.4)$$

where

$T_{pav,l}$  = low AC pavement temperature, (°C);

$T_{air}$  = low air temperature, (°C);

$d$  = pavement depth,

$\sigma_{air}$  = standard deviation of the mean low air temperature, (°C);

$z$  = standard normal distribution value;

$z = 2.055$  for 98% reliability; and

$z = 0.0$  for 50%.

## 5.5 Temperature database for Libyan desert

In order to establish the PG for temperature conditions in the Libyan desert, temperature zoning for high and low pavement temperatures was first conducted. Using the above models, pavement temperature was estimated by making use of the air temperature data collected from the weather stations. Air temperature data from the eight weather stations across Libya were accumulated in a weather database created in Microsoft Excel. These weather station locations covered almost all the geographical areas of the Libya desert. The air temperature data was collected from two main sources that included:

1. Libya Metrological Department
2. Roads and Bridges Authority.

The temperatures of the asphalt layers for the eight stations for the years 2012–2013 were obtained from the work done by installing temperature sensors in the asphalt road layers in the locations. The database for the eight stations was expanded for an additional ten years (2000 to 2009) using the data from roads and bridges authority.

Table 5.3 summarizes the weather stations used for the development of pavement temperature zoning. The table has information on the weather station, latitude, and number of years of data collected and used for the analysis.

Table 5.3 Summary of weather stations

No.	Station	Latitude (degree)	Data availability (years) (Low/High)
1	Al Kufrah	24.28	5/2012-5/2013
2	Al Qatrun	24.93	5/2012-5/2013
3	Awbari	26.77	4/2012-3/2013
4	Brak	27.52	3/2012-3/2013
5	Awjilah	29.13	5/2012-4/2013
6	Ghat	24.96	4/2012-4/2013
7	Ghadamis	30.18	3/2012-3/2013
8	Al Joufra	29.03	5/2012-5/2013

## 5.6 Temperature data analysis

For all the locations, temperature data for one year were collected for air and pavement: at surface (C1) and depths of 3cm (C2), 8cm (C3), and 15 cm (C4). From these data, maximal and minimal daily temperatures were extracted for air and pavements at surface and depths of 3, 8, and 15 cm.

Then, for maximal temperatures, the seven day average of maximal daily temperature was calculated. In Table 5.4 the maximum of these seven day averages and minimums of minimal daily air and pavement temperatures for data registered during year 2012–2013 are given for all the locations. In Table 5.5 the maximums of maximal daily temperatures for registered data for the year 2012–2013 are given for all the locations.

Table 5.4 Maximum of seven day average of maximal daily temperatures and minimum of minimal daily temperatures for different locations, for year 2012–2013.

	Air_max_aver	C1_max_aver	C2_max_aver	C3_max_aver	C4_max_aver	Air_min	C1_min	C2_min	C3_min	C4_min
	Max					Min				
Al Jufroh	47,469	67,474	61,891	58,067	55,226	-0.95	3.320	4.120	6.380	7.780
Al Kufrah	45.345	65.037	59.682	54.341	47.892	0.91	4.200	7.210	10.440	12.62
Al Qatrun	48.177	67.164	62.278	59.430	57.018	0.31	4.160	6.180	4.700	4.980
Awbari	49.294	68.465	62.945	61.377	52.884	0.31	4.160	5.910	7.910	9.960
Awjilah	49.864	66.128	64.044	59.231	56.242	-0.01	3.990	4.560	6.970	6.970
Brak	47.185	66.077	62.785	60.600	55.031	2.2	10.82	6.820	7.600	9.710
Ghadamis	49.864	66.732	64.044	58.854	53.150	-1.61	2.040	3.610	4.460	6.120
Ghat	50.344	71.005	65.868	63.121	58.171	-0.52	3.860	4.540	6.270	7.100

Legend:

C1 – surface pavement temperature(°C);

C2 – 3cm pavement temperature(°C);

C3 – 8cm pavement temperature(°C);

C4 – 15cm pavement temperature(°C);

Air\_max\_aver – seven-day average of maximal daily air temperature(°C);

C1\_max\_aver – seven-day average of maximal daily surface (C1) pavement temperature(°C);

C2\_max\_aver – seven-day average of maximal daily (C2) pavement temperature(°C);

C3\_max\_aver – seven-day average of maximal daily (C3) pavement temperature(°C);

C4\_max\_aver – seven-day average of maximal daily (C4) pavement temperature(°C);

Air\_min – minimal daily air temperature(°C);

C1\_min – minimal daily surface (C1) pavement temperature(°C);

C2\_min – minimal daily (C2) pavement temperature(°C);

C3\_min – minimal daily (C3) pavement temperature(°C); and

C4\_min – minimal daily (C4) pavement temperature(°C).

Table 5.5 Maximum of maximal daily temperatures for different locations for the year 2012–2013.

	Air_max	C1_max	C2_max	C3_max	C4_max
	Max				
Al Jufroh	50,330	70,080	66,880	62,045	57,930
Al Kufrah	49,180	70,120	64,610	56,020	49,530
Al Qatrun	49,960	69,980	64,840	61,810	59,680
Awbari	53,360	70,890	66,010	64,660	55,470
Awjilah	50,930	66,990	64,800	59,840	56,980
Brak	50,100	69,060	65,230	62,720	56,630
Ghadamis	50,930	69,880	64,800	59,670	53,680
Ghat	52,580	72,460	66,810	64,020	60,460

Legend:

Air\_max – maximal daily air temperature(°C);

C1\_max – maximal daily surface (C1) pavement temperature(°C);

C2\_max – maximal daily (C2) pavement temperature(°C);

C3\_max – maximal daily (C3) pavement temperature(°C);

C4\_max – maximal daily (C4) pavement temperature(°C).

### 5.6.1 Project pavement temperature models based on data collected in 2012–2013

Using regression analysis, models for predicting maximal and minimal daily pavement temperatures at different distance including the surface, from maximal and minimal daily air temperatures, day of the year, latitude, wind speed and cumulative solar radiation were made. The best model appeared to be the model including maximal and minimal daily air temperatures, day of the year, latitude, and cumulative solar radiation.

Since data on cumulative solar radiation were not available for our research, we used the models including maximal and minimal daily air temperatures, day of the year, and latitude.

First we give models developed data from all eight locations.

#### 5.6.1.1 The models for the maximal daily pavement temperatures.

The following models based on data from all 8 eight locations, including latitude, for four different depths from the surface.

Surface:

$$T_{pav,surf}^{max} = 24.89776 + 0.70665T_{air}^{max} + 0.22056Day - 0.00061Day^2 - 0.48402Lat$$

3cm:

$$T_{pav,3cm}^{max} = 15.09352 + 0.74095T_{air}^{max} + 0.20191Day - 0.00056Day^2 - 0.26971Lat$$

8cm:

$$T_{pav,8cm}^{max} = 18.94276 + 0.73521T_{air}^{max} + 0.18249Day - 0.00050Day^2 - 0.46665Lat$$

15cm:

$$T_{pav,15cm}^{max} = 12.66080 + 0.66576T_{air}^{max} + 0.18439Day - 0.00050Day^2 - 0.30365Lat$$

where

$T_{pav,*}^{max}$  =maximal daily pavement temperature at certain depth,(°C);

$T_{air}^{max}$  = maximal daily air temperature, (°C);

$Day$  =day of the year;

$Day^2$  = square of the day of the year; and

$Lat$ = latitude of the section, (degrees).

### **5.6.1.2 The models for the minimal daily pavement temperatures**

The following models are based on data from all eight locations, including latitude, for four different depths from the surface.

Surface:

$$T_{pav,surf}^{min} = 1.525863 + 0.840662T_{air}^{min} + 0.037716Day - 0.000105Day^2 + 0.074524Lat$$

3cm:

$$T_{pav,3cm}^{min} = 9.203415 + 0.816427T_{air}^{min} + 0.055795Day - 0.000147Day^2 - 0.224462Lat$$

8cm:

$$T_{pav,8cm}^{min} = 13.08012 + 0.74673T_{air}^{min} + 0.07857Day - 0.00021Day^2 - 0.31927Lat$$

15cm:

$$T_{pav,15cm}^{min} = 13.73368 + 0.72050T_{air}^{min} + 0.08452Day - 0.00022Day^2 - 0.28861Lat$$

where

$T_{pav,*}^{min}$  =minimal daily pavement temperature at certain depth, (°C);

$T_{air}^{min}$  = minimal daily air temperature, (°C);

$Day$  =day of the year (number);

$Day^2$  = square of the day of the year;

$Lat$ = latitude of the section, (degrees).

### 5.6.1.3 Models including depth from the surface

The model to predict maximal daily pavement temperature at any depth from maximal daily air temperature, the day of the year, and latitude is:

$$T_{pav}^{max} = 22.20576 + 0.1973434T_{air}^{max} + 0.71214d - 0.00054Day - 0.38103Day^2Lat$$

where

$T_{pav}^{max}$  = maximal daily pavement temperature at depth  $d$ , in (°C);

$T_{air}^{max}$  = maximal daily air temperature, (°C);

$Lat$  = latitude of the section, (degrees); and

$d$  = pavement depth (cm).

The model to predict minimal daily pavement temperature from minimal daily air temperature, the day of the year, and latitude is:

$$T_{pav}^{min} = 7.723302 + 0.781078T_{air}^{min} + 0.255764d + 0.064150Day - 0.000172Day^2 - 0.189455Lat$$

where

$T_{pav}^{min}$  = minimal daily pavement temperature at depth  $d$ , in (°C);

$T_{air}^{min}$  = minimal daily air temperature, in (°C);

$Lat$  = latitude of the section, (degrees); and

$d$  = pavement depth (cm).

### 5.6.2 Project pavement temperatures predicted on air temperature data collected from year 2000 to year 2009

For each of the eight locations' data on daily maximum air sheltered temperature, °C and daily minimum sheltered air temperature in °C were collected for years from 2000 to 2009.

From these daily maximal (minimal) air temperatures, using regression models obtained in Chapter 4, predicted values for maximal (minimal) pavement temperatures for four depths were calculated.

We used models based on data from Libya, which we developed in chapter 4, and which include air temperature and day of the year, since data on solar radiation were not available. For calculating PG we used Superpave method as explained in chapter 2.

The seven-day average of maximal daily air and pavement temperatures was calculated.

Then:

- Yearly maximum for the seven-day average of maximal daily air and pavement temperatures was determined for each of the eight locations.
- Yearly minimum for minimal air and pavement temperatures was determined for each of the eight locations.
- Yearly maximum of maximal daily air and pavement temperatures was determined for each of the eight locations.

Next, for each location, we give formulas for regression models. For each of the years 2000–2009 we give the yearly maximum of the seven-day average of maximal daily air and pavement temperatures, the yearly minimum for minimal air and pavement temperatures, and the yearly maximum of maximal daily air and pavement temperatures.

### 5.6.2.1 Al Jufroh location

Table 5.6 Regression models for maximal pavement temperatures for the Al Jufroh location.

Surface	$T_{pav,surf}^{max} = 7.124206 + 0.841147T_{air}^{max} + 0.210048Day - 0.000577Day^2$
3cm	$T_{pav,3cm}^{max} = 5.635261 + 0.787060T_{air}^{max} + 0.189318Day - 0.000518Day^2$
8cm	$T_{pav,8cm}^{max} = 6.580602 + 0.716630T_{air}^{max} + 0.173635Day - 0.000481Day^2$
15cm	$T_{pav,15cm}^{max} = 5.599092 + 0.682433T_{air}^{max} + 0.181503Day - 0.000492Day^2$

Table 5.7 Regression models for minimal pavement temperatures for the Al Jufroh location.

Surface	$T_{pav,surf}^{min} = 1.618143 + 0.805014T_{air}^{min} + 0.066989Day - 0.000175Day^2$
3cm	$T_{pav,3cm}^{min} = 1.967646 + 0.827490T_{air}^{min} + 0.068178Day - 0.000180Day^2$
8cm	$T_{pav,8cm}^{min} = 4.332745 + 0.718193T_{air}^{min} + 0.088440Day - 0.000240Day^2$
15cm	$T_{pav,15cm}^{min} = 5.851072 + 0.733621T_{air}^{min} + 0.076956Day - 0.000207Day^2$

Table 5.8 Maximum of seven-day average of predicted maximal daily temperatures and minimum of minimal daily temperatures from year 2000 to year 2009, year 2012/2013, for the Al Joufroh location.

Al Jufroh		Predicted values					Predicted values				
Year	Air_max_aver	C1_max_aver	C2_max_aver	C3_max_aver	C4_max_aver	Air_min	C1_min	C2_min	C3_min	C4_min	
Max						Min					
2000	41,27	60,84	55,32	51,72	50,43	-0,50	2,49	2,85	5,23	6,87	
2001	42,17	61,23	55,68	52,05	50,74	-0,50	2,47	2,58	4,45	6,14	
2002	44,71	63,72	58,02	54,16	52,77	0,50	2,43	2,80	5,20	6,67	
2003	44,13	63,36	57,66	53,87	52,45	-1,10	2,19	2,29	4,26	5,92	
2004	42,30	60,91	55,43	51,74	50,52	-0,50	1,68	2,02	4,58	6,01	
2005	42,01	60,32	54,83	51,32	50,00	-0,60	1,95	2,30	4,91	6,31	
2006	42,29	60,64	55,20	51,51	50,30	-2,00	0,34	0,65	3,33	4,76	
2007	44,11	63,34	57,65	53,86	52,43	1,50	3,90	4,31	6,48	7,99	
2008	40,67	60,45	54,94	51,39	50,09	-0,50	2,65	3,01	5,69	7,03	
2009	42,74	62,17	56,56	52,85	51,50	1,30	4,44	4,85	7,35	8,71	
2012	47,469	67,474	61,891	58,067	55,226	-0,95	3,320	4,120	6,380	7,780	

Table 5.9 Maximum of predicted maximal daily temperatures for years 2000–2009 and 2012 for the Al Joufroh location.

Al Jufroh		Predicted values				
Year	Air_max	C1_max	C2_max	C3_max	C4_max	
Max						
2000	44,20	63,35	57,67	53,85	52,47	
2001	45,00	64,05	58,32	54,45	53,03	
2002	46,50	64,91	59,12	55,19	53,72	
2003	45,60	64,59	58,82	54,92	53,46	
2004	44,20	62,80	57,14	53,44	51,91	
2005	44,20	62,20	56,59	52,97	51,38	
2006	45,70	63,85	58,18	54,25	52,90	
2007	46,00	64,93	59,14	55,21	53,73	
2008	44,50	63,42	57,71	53,96	52,44	
2009	45,00	64,06	58,32	54,46	53,03	
2012	50,330	70,080	66,880	62,045	57,930	

For these data for 11 years, mean value, standard deviation maximum and minimum were calculated. To determine 50%, 85%, 95%, 98% and 99.9% level of reliability, we calculate intervals  $\text{Mean} \pm \text{SD}$ ,  $\text{Mean} \pm 1.65 \cdot \text{SD}$ ,  $\text{Mean} \pm 2 \cdot \text{SD}$ ,  $\text{Mean} \pm 3 \cdot \text{SD}$ . We use values of standard normal distribution presented in Table 5.11.



Table 5.10 Descriptive statistics for data for 11 years at the Al Jufroh location

Al Jufroh	Mean	Min	Max	Std.Dev	Mean ± SD		Mean ± 1.65*SD		Mean ± 2*SD		Mean ± 3*SD	
Air_max	45,57	44,20	50,33	1,76	43,80	47,33	42,65	48,48	42,04	49,10	40,27	50,86
C1_max_P	64,39	62,20	70,08	2,07	62,32	66,46	60,97	67,80	60,25	68,53	58,18	70,59
C2_max_P	58,90	56,59	66,88	2,76	56,14	61,66	54,34	63,46	53,37	64,43	50,61	67,19
C3_max_P	54,98	52,97	62,05	2,45	52,53	57,42	50,94	59,01	50,08	59,87	47,64	62,31
C4_max_p	53,27	51,38	57,93	1,71	51,56	54,98	50,45	56,09	49,86	56,69	48,15	58,40
Air_max_aver	43,08	40,67	47,47	1,91	41,17	44,99	39,93	46,23	39,26	46,90	37,35	48,81
C1_max_P_aver	62,22	60,32	67,47	2,15	60,07	64,37	58,67	65,77	57,92	66,52	55,77	68,67
C2_max_P_aver	56,65	54,83	61,89	2,10	54,56	58,75	53,20	60,11	52,46	60,84	50,37	62,94
C3_max_P_aver	52,96	51,32	58,07	2,01	50,95	54,96	49,65	56,27	48,94	56,97	46,94	58,98
C4_max_P_aver	51,50	50,00	55,23	1,60	49,90	53,10	48,85	54,14	48,29	54,70	46,69	56,30
Air_min	-0,30	-2,00	1,50	1,03	-1,34	0,73	-2,01	1,40	-2,37	1,76	-3,40	2,79
C1_min_P	2,53	0,34	4,44	1,10	1,43	3,63	0,71	4,35	0,33	4,74	-0,77	5,84
C2_min_P	2,89	0,65	4,85	1,18	1,71	4,07	0,94	4,84	0,52	5,25	-0,66	6,44
C3_min_P	5,26	3,33	7,35	1,15	4,11	6,41	3,36	7,16	2,96	7,56	1,80	8,72
C4_min_P	6,74	4,76	8,71	1,11	5,64	7,85	4,91	8,57	4,53	8,96	3,42	10,07

Legend:

C1 – surface pavement temperature (°C);

C2 – 3 cm pavement temperature (°C);

C3 – 8 cm pavement temperature (°C);

C4 – 15 cm pavement temperature (°C);

Air\_max\_aver – seven-day average of maximal daily air temperature(°C);

C1\_max\_aver – seven-day average of maximal daily surface (C1) pavement temperature(°C);

C2\_max\_aver – seven-day average of maximal daily (C2) pavement temperature(°C);

C3\_max\_aver – seven-day average of maximal daily (C3) pavement temperature(°C);

C4\_max\_aver – seven-day average of maximal daily (C4) pavement temperature(°C);

Air\_min – minimal daily air temperature(°C);

C1\_min – minimal daily surface (C1) pavement temperature(°C);

C2\_min – minimal daily (C2) pavement temperature(°C);

C3\_min – minimal daily (C3) pavement temperature(°C); and

C4\_min – minimal daily (C4) pavement temperature(°C).

C1\_max\_P – predicted maximal daily surface (C1) pavement temperature(°C);

C2\_max\_P – predicted maximal daily (C2) pavement temperature(°C);

C3\_max\_P – predicted maximal daily (C3) pavement temperature(°C);

C4\_max\_P – predicted maximal daily (C4) pavement temperature(°C);

C1\_max\_P – seven-day average of predicted maximal daily surface (C1) pavement temperature(°C);

C2\_max\_P – seven-day average of predicted maximal daily (C2) pavement temperature(°C);

C3\_max\_P – seven-day average of predicted maximal daily (C3) pavement temperature(°C);

C4\_max\_P – seven-day average of predicted maximal daily (C4) pavement temperature(°C);

C1\_min\_P – predicted minimal daily surface (C1) pavement temperature(°C);

C2\_min\_P – predicted minimal daily (C2) pavement temperature(°C);

C3\_min\_P – predicted minimal daily (C3) pavement temperature(°C);

C4\_min\_P – predicted minimal daily (C4) pavement temperature(°C).

Table 5.11 Values of standard normal distribution for 50%, 85%, 95%, 98% and 99.9% level of reliability.

<b>z - Standard normal distribution value</b>	<b>Reliability</b>
0	50%
1	85%
1.65	95%
2	98%
3	99,9%

Table 5.12 Reliability data for PG Al Jufroh

<b>Al Jufroh</b>	50% reliability Mean		85% reliability Mean ± SD		95% reliability Mean ± 1.65SD		98% reliability Mean ± 2SD		99,9% reliability Mean ± 3SD	
	Min	Max	Min	Max	Min	Max	Min	Max	Min	Max
C1	2,53	62,22	1,43	64,37	0,71	65,77	0,33	66,52	-0,77	68,67
C2	2,89	56,65	1,71	58,75	0,94	60,11	0,52	60,84	-0,66	62,94
C3	5,26	52,96	4,11	54,96	3,36	56,27	2,96	56,97	1,80	58,98
C4	6,74	51,50	5,64	53,10	4,91	54,14	4,53	54,70	3,42	56,30

Table 5.13 PG for different levels of reliability for the Al Jufroh location.

	<b>Al Jufroh</b>									
	PG 50% reliability		PG 85% reliability		PG 95% reliability		PG 98% reliability		PG 99,9% reliability	
	YY	XX	YY	YY	YY	XX	YY	XX	YY	XX
C1	64	-10	70	70	70	-10	70	-10	70	-10
C2	58	-10	64	64	64	-10	64	-10	64	-10
C3	58	-10	58	58	58	-10	58	-10	64	-10
C4	52	-10	58	58	58	-10	58	-10	58	-10

### 5.6.2.2 Al Kufrah location

Table 5.14 Regression models for maximal pavement temperatures for the Al Kufrah location.

Surface	$T_{pav,surf}^{max} = 13.68505 + 0.72857T_{air}^{max} + 0.20804Day - 0.00057Day^2$
3cm	$T_{pav,3cm}^{max} = 12.39437 + 0.63684T_{air}^{max} + 0.20451Day - 0.00056Day^2$
8cm	$T_{pav,8cm}^{max} = 11.25532 + 0.54622T_{air}^{max} + 0.20098Day - 0.00054Day^2$
15cm	$T_{pav,15cm}^{max} = 9.005746 + 0.454938T_{air}^{max} + 0.194789Day - 0.000519Day^2$

Table 5.15 Regression models for minimal pavement temperatures for the Al Kufrah location.

Surface	$T_{pav,surf}^{min} = 1.243982 + 0.808996T_{air}^{min} + 0.049696Day - 0.000127Day^2$
3cm	$T_{pav,3cm}^{min} = 3.728357 + 0.752792T_{air}^{min} + 0.064289Day - 0.000166Day^2$
8cm	$T_{pav,8cm}^{min} = 6.157240 + 0.724622T_{air}^{min} + 0.077079Day - 0.000199Day^2$
15cm	$T_{pav,15cm}^{min} = 7.485577 + 0.648677T_{air}^{min} + 0.093697Day - 0.000235Day^2$

Table 5.16 Maximum of seven-day average of predicted maximal daily temperatures and minimum of minimal daily temperatures from year 2000 to year 2009 and year 2012–2013, for the Al Kufrah location.

Al Kufrah		Predicted values				Predicted values				
Year	Air_max_aver	C1_max_aver	C2_max_aver	C3_max_aver	C4_max_aver	Air_min	C1_min	C2_min	C3_min	C4_min
Max						Min				
2000	40,64	61,79	56,52	51,81	45,48	2,00	3,72	6,34	8,93	10,39
2001	40,07	61,76	56,49	51,78	45,47	5,00	6,26	8,40	10,65	11,51
2002	42,69	63,33	57,83	52,96	46,44	3,00	3,82	6,18	8,56	9,71
2003	40,66	62,21	56,89	52,11	45,73	2,00	4,40	7,23	9,78	10,73
2004	42,50	62,87	57,38	52,30	45,71	3,00	4,92	7,30	9,73	10,90
2005	40,61	62,15	56,82	51,98	45,58	1,80	3,60	6,24	8,85	10,35
2006	41,93	62,65	57,22	52,22	45,80	3,00	5,42	8,10	10,60	11,84
2007	41,66	63,00	57,58	52,67	46,18	3,50	4,17	6,49	8,85	9,94
2008	44,04	64,44	58,80	53,62	46,90	1,30	3,01	5,63	8,21	9,68
2009	40,50	61,88	56,59	51,82	45,47	3,00	3,77	6,11	8,48	9,62
2012	45.345	65.037	59.682	54.341	47.892	0.91	4.200	7.210	10.440	12.62

Table 5.17 Maximum of predicted maximal daily temperatures for years 2000–2009 and 2012 for the Al Kufrah location.

Al Kufrah		Predicted values			
Year	Air_max	C1_max	C2_max	C3_max	C4_max
Max					
2000	42,00	63,24	57,78	52,89	46,39
2001	44,40	63,07	57,42	52,48	46,05
2002	43,50	63,99	58,44	53,44	46,84
2003	44,40	64,34	58,67	53,42	46,73
2004	45,60	65,09	59,31	53,95	47,08
2005	43,50	64,27	58,68	53,58	46,91
2006	44,50	64,15	58,49	53,53	46,88
2007	43,20	64,14	58,57	53,53	46,91
2008	45,40	65,51	59,74	54,44	47,60
2009	42,70	63,73	58,21	53,26	46,70
2012	49,180	70,120	64,610	56,020	49,530

For these data for 11 years, mean value, standard deviation maximum and minimum were calculated. To determine 50%, 85%, 95%, 98% and 99.9% level of reliability, we calculate intervals Mean  $\pm$  SD, Mean  $\pm$  1.65\*SD, Mean  $\pm$  2\*SD, Mean  $\pm$  3\*SD. We use values of standard normal distribution presented in Table 5.11.

Table 5.18 Descriptive statistics for data for 11 years at the Al Kufrah location.

Al Kufrah	Mean	Min	Max	Std.Dev	Mean $\pm$ SD		Mean $\pm$ 1.65*SD		Mean $\pm$ 2*SD		Mean $\pm$ 3*SD	
Air_max	44,40	42,00	49,18	1,92	42,47	46,32	41,22	47,57	40,55	48,25	38,63	50,17
C1_max_P	64,70	63,07	70,12	1,93	62,76	66,63	61,51	67,88	60,83	68,56	58,90	70,49
C2_max_P	59,08	57,42	64,61	1,94	57,14	61,02	55,88	62,28	55,20	62,96	53,27	64,90
C3_max_P	53,69	52,48	56,02	0,92	52,76	54,61	52,16	55,21	51,84	55,53	50,91	56,46
C4_max_p	47,06	46,05	49,53	0,91	46,15	47,96	45,56	48,55	45,24	48,87	44,34	49,78
Air_max_aver	41,88	40,07	45,35	1,66	40,22	43,54	39,14	44,62	38,56	45,20	36,89	46,86
C1_max_P_aver	62,83	61,76	65,04	1,08	61,74	63,91	61,04	64,62	60,66	65,00	59,58	66,08
C2_max_P_aver	57,44	56,49	59,68	1,01	56,42	58,45	55,77	59,11	55,41	59,46	54,40	60,48
C3_max_P_aver	52,51	51,78	54,34	0,83	51,68	53,34	51,14	53,88	50,85	54,17	50,02	55,00
C4_max_P_aver	46,06	45,47	47,89	0,76	45,30	46,82	44,80	47,31	44,54	47,58	43,78	48,34
Air_min	2,59	0,91	5,00	1,15	1,45	3,74	0,70	4,48	0,30	4,88	-0,84	6,03
C1_min_P	4,30	3,01	6,26	0,92	3,38	5,22	2,78	5,82	2,45	6,15	1,53	7,07
C2_min_P	6,84	5,63	8,40	0,88	5,96	7,72	5,39	8,29	5,09	8,59	4,21	9,47
C3_min_P	9,37	8,21	10,65	0,90	8,47	10,27	7,88	10,86	7,57	11,17	6,67	12,07
C4_min_P	10,66	9,62	12,62	0,98	9,68	11,65	9,04	12,28	8,70	12,63	7,72	13,61

Table 5.19 Reliability data for PG at the Al Kufrah location

Al Kufrah	50% reliability Mean		85% reliability Mean ± SD		95% reliability Mean ± 1.65SD		98% reliability Mean ± 2SD		99,9% reliability Mean ± 3SD	
	Min	Max	Min	Max	Min	Max	Min	Max	Min	Max
N=11 years										
C1	4,30	62,83	3,38	63,91	2,78	64,62	2,45	65,00	1.53	66.08
C2	6,84	57,44	5,96	58,45	5,39	59,11	5,09	59,46	4.21	60.48
C3	9,37	52,51	8,47	53,34	7,88	53,88	7,57	54,17	6.67	55.00
C4	10,66	46,06	9,68	46,82	9,04	47,31	8,70	47,58	7.72	48.34

Table 5.20 PG for different level of reliability for the Al Jufroh location

N=11 years	Al Kufrah									
	PG 50% reliability		PG 85% reliability		PG 95% reliability		PG 98% reliability		PG 99,9% reliability	
	YY	XX	YY	YY	YY	XX	YY	XX	YY	XX
C1	64	-10	64	-10	70	-10	70	-10	70	-10
C2	58	-10	64	-10	64	-10	64	-10	64	-10
C3	58	-10	58	-10	58	-10	58	-10	58	-10
C4	52	-10	52	-10	52	-10	52	-10	52	-10

### 5.6.2.3 Al Qatrun location

Table 5.21 Regression models for maximal pavement temperatures for the Al Qatrun location.

Surface	$T_{pav,surf}^{max} = 10.48413 + 0.59960T_{air}^{max} + 0.29049Day - 0.00080Day^2$
3cm	$T_{pav,3cm}^{max} = 8.387011 + 0.644196T_{air}^{max} + 0.244188Day - 0.000669Day^2$
8cm	$T_{pav,8cm}^{max} = 7.177688 + 0.627300T_{air}^{max} + 0.235079Day - 0.000648Day^2$
15cm	$T_{pav,15cm}^{max} = 8.403618 + 0.606931T_{air}^{max} + 0.209925Day - 0.000573Day^2$

Table 5.22 Regression models for minimal pavement temperatures for the Al Qatrun location.

Surface	$T_{pav,surf}^{min} = 2.839816 + 0.799698T_{air}^{min} + 0.046512Day - 0.000124Day^2$
3cm	$T_{pav,3cm}^{min} = 3.920201 + 0.819917T_{air}^{min} + 0.047829Day - 0.000127Day^2$
8cm	$T_{pav,8cm}^{min} = 2.482546 + 0.703822T_{air}^{min} + 0.102696Day - 0.000283Day^2$
15cm	$T_{pav,15cm}^{min} = 4.691829 + 0.721753T_{air}^{min} + 0.092263Day - 0.000253Day^2$

Table 5.23 Maximum of seven-day average of predicted maximal daily temperatures and minimum of minimal daily temperatures from year 2000 to year 2009, year 2012–2013, for the Al Qatrun location.

Al Qatrun		Predicted values					Predicted values				
Year	Air_max_aver	C1_max_aver	C2_max_aver	C3_max_aver	C4_max_aver	Air_min	C1_min	C2_min	C3_min	C4_min	
	Max					Min					
1999	40,64	60,81	56,42	53,57	51,90	2,0	5,236	6,379	5,647	7,714	
2000	40,07	61,74	56,36	53,49	51,85	5,00	7,70	8,97	6,13	8,63	
2001	42,69	63,33	57,66	54,74	53,12	3,00	5,38	6,52	4,90	7,13	
2002	40,66	62,21	56,79	53,93	52,24	2,00	5,65	6,86	4,89	7,28	
2003	42,50	62,83	57,10	54,30	52,59	3,00	6,45	7,62	6,04	8,39	
2004	40,61	62,17	56,73	53,89	52,18	1,80	5,12	6,26	5,60	7,65	
2005	41,93	62,65	57,04	54,22	52,50	3,00	6,63	7,87	5,39	7,82	
2006	41,66	63,00	57,49	54,62	52,90	3,50	5,73	6,89	5,15	7,40	
2007	44,04	64,41	58,64	55,77	54,00	1,30	4,55	5,67	4,87	6,96	
2008	40,50	61,88	56,50	53,66	51,96	3,00	5,33	6,48	4,80	7,04	
2012	48,177	67.164	62.278	59.430	57.018	0,31	4.160	6.180	4.700	4.980	

Table 5.24 Maximum of predicted maximal daily temperatures for years 2000–2009 and 2012 for the Al Qatrun location.

Al Qatrun		Predicted values			
Year	Air_max	C1_max	C2_max	C3_max	C4_max
	Max				
1999	42,00	63,24	57,70	54,81	53,10
2000	44,40	63,13	57,17	54,29	52,64
2001	43,50	63,99	58,36	55,46	53,72
2002	44,40	64,34	58,48	55,63	53,87
2003	45,60	65,05	59,05	56,20	54,43
2004	43,50	64,29	58,60	55,72	53,95
2005	44,50	64,15	58,24	55,29	53,73
2006	43,20	64,14	58,49	55,60	53,84
2007	45,40	65,48	59,61	56,71	54,90
2008	42,70	63,71	58,10	55,20	53,49
2012	49,96	69,98	64,84	61,81	59,68

For these data for 11 years, mean value, standard deviation maximum and minimum were calculated. To determine 50%, 85%, 95%, 98% and 99.9% level of reliability we calculate intervals  $\text{Mean} \pm \text{SD}$ ,  $\text{Mean} \pm 1.65 \cdot \text{SD}$ ,  $\text{Mean} \pm 2 \cdot \text{SD}$ ,  $\text{Mean} \pm 3 \cdot \text{SD}$ . We use values of standard normal distribution presented in Table 5.11.

Table 5.25 Descriptive statistics for data for 11 years at the Al Qatrun location.

Al Qatrun	Mean	Min	Max	Std.Dev	Mean ± SD		Mean ± 1.65*SD		Mean ± 2*SD		Mean ± 3*SD	
Air_max	44,47	42,00	49,96	2,12	42,35	46,59	40,97	47,97	40,23	48,71	38,10	50,83
C1_max_P	64,68	63,13	69,98	1,89	62,80	66,57	61,57	67,80	60,91	68,46	59,02	70,34
C2_max_P	58,97	57,17	64,84	2,05	56,92	61,02	55,59	62,35	54,87	63,07	52,82	65,12
C3_max_P	56,07	54,29	61,81	2,01	54,06	58,08	52,75	59,38	52,05	60,09	50,04	62,10
C4_max_p	54,30	52,64	59,68	1,88	52,42	56,18	51,20	57,41	50,54	58,07	48,66	59,95
Air_max_aver	42,13	40,07	48,18	2,33	39,80	44,47	38,28	45,99	37,46	46,80	35,13	49,14
C1_max_P_aver	62,93	60,81	67,16	1,69	61,24	64,61	60,14	65,71	59,55	66,30	57,86	67,99
C2_max_P_aver	57,55	56,36	62,28	1,70	55,84	59,25	54,73	60,36	54,14	60,96	52,43	62,66
C3_max_P_aver	54,69	53,49	59,43	1,70	52,99	56,40	51,88	57,50	51,29	58,10	49,59	59,80
C4_max_P_aver	52,93	51,85	57,02	1,50	51,44	54,43	50,46	55,40	49,94	55,93	48,44	57,42
Air_min	2,54	0,31	5,00	1,24	1,29	3,78	0,49	4,59	0,05	5,02	-1,19	6,27
C1_min_P	5,63	4,16	7,70	0,99	4,64	6,62	3,99	7,27	3,64	7,62	2,65	8,61
C2_min_P	6,88	5,67	8,97	0,94	5,94	7,82	5,34	8,43	5,01	8,76	4,07	9,69
C3_min_P	5,28	4,70	6,13	0,51	4,77	5,79	4,44	6,12	4,26	6,30	3,75	6,81
C4_min_P	7,36	4,98	8,63	0,95	6,41	8,32	5,79	8,94	5,46	9,27	4,50	10,22

Table 5.26 Reliability data for PG at the Al Qatrun location.

Al Qatrun	50% reliability Mean		85% reliability Mean ± SD		95% reliability Mean ± 1.65SD		98% reliability Mean ± 2SD		99,9% reliability Mean ± 3SD	
	Min	Max	Min	Max	Min	Max	Min	Max	Min	Max
N=11years										
C1	5,63	62,93	4,64	64,61	3,99	65,71	3,64	66,30	2,65	67,99
C2	6,88	57,55	5,94	59,25	5,34	60,36	5,01	60,96	4,07	62,66
C3	5,28	54,69	4,77	56,40	4,44	57,50	4,26	58,10	3,75	59,80
C4	7,36	52,93	6,41	54,43	5,79	55,40	5,46	55,93	4,50	57,42

Table 5.27 PG for different level of reliability for the Al Qatrun location.

N=1 1years	Al Qatrun									
	PG 50% reliability		PG 85% reliability		PG 95% reliability		PG 98% reliability		PG 99,9% reliability	
	YY	XX	YY	YY	YY	XX	YY	XX	YY	XX
C1	64	-10	70	-10	70	-10	70	-10	70	-10
C2	58	-10	64	-10	64	-10	64	-10	64	-10
C3	58	-10	58	-10	58	-10	64	-10	64	-10
C4	58	-10	58	-10	58	-10	58	-10	58	-10

#### 5.6.2.4 Awbari location

Table 5.28 Regression models for maximal pavement temperatures for the Awbari location.

Surface	$T_{pav,surf}^{max} = 18.74127 + 0.59894T_{air}^{max} + 0.20347Day - 0.00061Day^2$
3cm	$T_{pav,3cm}^{max} = 13.29718 + 0.64555T_{air}^{max} + 0.18942Day - 0.00055Day^2$
8cm	$T_{pav,8cm}^{max} = 11.92221 + 0.64533T_{air}^{max} + 0.18555Day - 0.00054Day^2$
15cm	$T_{pav,15cm}^{max} = 7.525291 + 0.530981T_{air}^{max} + 0.194371Day - 0.000539Day^2$

Table 5.29 Regression models for minimal pavement temperatures for the Awbari location.

Surface	$T_{pav,surf}^{min} = 0.963055 + 0.779732T_{air}^{min} + 0.075557Day - 0.000193Day^2$
3cm	$T_{pav,3cm}^{min} = 3.781358 + 0.836145T_{air}^{min} + 0.045412Day - 0.000117Day^2$
8cm	$T_{pav,8cm}^{min} = 7.451416 + 0.723849T_{air}^{min} + 0.068226Day - 0.000197Day^2$ ;
15cm	$T_{pav,15cm}^{min} = 8.526790 + 0.647124T_{air}^{min} + 0.095734Day - 0.000269Day^2$

Table 5.30 Maximum of seven-day average of predicted maximal daily temperatures and minimum of minimal daily temperatures from year 2000 to year 2009, year 2012–2013, for the Awbari location.

Awbari		Predicted values					Predicted values				
Year	Air_max_aver	C1_max_aver	C2_max_aver	C3_max_aver	C4_max_aver	Air_min	C1_min	C2_min	C3_min	C4_min	
	Max					Min					
2000	42,53	60,86	56,67	54,92	47,22	1,50	2,94	5,52	8,08	9,44	
2001	43,96	60,93	56,74	54,99	47,22	-5,00	-0,53	1,05	5,97	7,57	
2002	44,63	62,14	58,25	56,49	48,69	-2,00	0,47	3,05	6,99	8,31	
2003	44,59	62,21	58,30	56,54	48,71	-3,50	0,36	2,00	3,87	5,77	
2004	43,30	60,79	56,61	54,86	47,43	-2,00	-0,08	2,42	5,39	7,02	
2005	43,67	60,96	57,01	55,25	47,69	-3,30	-0,31	1,80	6,05	7,81	
2006	43,64	60,26	56,62	54,87	47,45	-1,30	0,25	2,87	6,78	8,06	
2007	43,59	61,69	57,70	55,94	48,19	-1,50	0,17	2,75	6,70	8,03	
2008	44,33	62,24	58,16	56,41	48,40	-2,50	0,17	2,39	6,68	8,37	
2009	43,53	61,50	57,57	55,81	48,13	1,10	3,39	5,64	8,70	10,52	
2012	49.294	68.465	62.945	61.377	52.884	0.31	4.160	5.910	7.910	9.960	



Table 5.31 Maximum of predicted maximal daily temperatures for years 2000–2009 and 2012 for the Al Joufroh location.

Awbari		Predicted values			
Year	Air_max	C1_max	C2_max	C3_max	C4_max
Max					
2000	44,50	62,07	58,03	56,27	48,54
2001	45,30	62,36	58,30	56,55	48,72
2002	47,50	63,26	59,49	57,73	49,77
2003	46,90	63,57	59,78	58,02	49,93
2004	44,50	62,12	58,06	56,31	48,37
2005	45,50	62,24	58,42	56,66	48,86
2006	45,70	62,22	58,28	56,52	48,68
2007	45,60	62,86	58,98	57,22	49,26
2008	46,40	63,49	59,52	57,77	49,54
2009	45,10	62,66	58,71	56,95	48,99
2012	53,36	70,89	66,01	64,66	55,47

For these data for 11 years, mean value, standard deviation maximum and minimum were calculated. To determine 50%, 85%, 95%, 98% and 99.9% level of reliability, we calculate intervals  $\text{Mean} \pm \text{SD}$ ,  $\text{Mean} \pm 1.65*\text{SD}$ ,  $\text{Mean} \pm 2*\text{SD}$ ,  $\text{Mean} \pm 3*\text{SD}$ . We use values of standard normal distribution presented in Table 5.11.

Table 5.32 Descriptive statistics for data for 11 years at the Al Jufroh location.

Awbari	Mean	Min	Max	Std.Dev	Mean $\pm$ SD		Mean $\pm$ 1.65*SD		Mean $\pm$ 2*SD		Mean $\pm$ 3*SD	
Air_max	46,40	44,50	53,36	2,49	43,9	48,89	42,29	50,50	41,42	51,37	38,93	53,86
C1_max_P	63,43	62,07	70,89	2,53	60,9	65,96	59,25	67,61	58,36	68,50	55,83	71,03
C2_max_P	59,42	58,03	66,01	2,27	57,1	61,69	55,67	63,16	54,87	63,96	52,60	66,23
C3_max_P	57,70	56,27	64,66	2,39	55,3	60,09	53,75	61,64	52,92	62,48	50,53	64,87
C4_max_p	49,65	48,37	55,47	2,00	47,6	51,64	46,35	52,94	45,65	53,64	43,66	55,64
Air_max_aver	44,28	42,53	49,29	1,77	42,5	46,05	41,36	47,20	40,74	47,82	38,97	49,59
C1_max_P_aver	62,00	60,26	68,47	2,24	59,7	64,25	58,30	65,70	57,52	66,49	55,28	68,73
C2_max_P_aver	57,87	56,61	62,95	1,81	56,0	59,68	54,88	60,86	54,24	61,50	52,43	63,31
C3_max_P_aver	56,13	54,86	61,38	1,87	54,2	58,00	53,06	59,21	52,40	59,86	50,54	61,73
C4_max_P_aver	48,36	47,22	52,88	1,60	46,7	49,96	45,73	51,00	45,17	51,56	43,57	53,16
Air_min	-1,65	-5,00	1,50	2,00	-	0,34	-4,95	1,64	-5,64	2,34	-7,64	4,33
C1_min_P	1,00	-0,53	4,16	1,65	-	2,65	-1,73	3,73	-2,31	4,30	-3,96	5,96
C2_min_P	3,22	1,05	5,91	1,68	1,54	4,90	0,44	5,99	-0,15	6,58	-1,83	8,26
C3_min_P	6,65	3,87	8,70	1,35	5,30	7,99	4,43	8,87	3,96	9,34	2,61	10,68
C4_min_P	8,26	5,77	10,52	1,34	6,92	9,60	6,05	10,47	5,58	10,94	4,24	12,28

Table 5.33 Reliability data for PG at the Awbari location.

Awbari	50% reliability Mean		85% reliability Mean ± SD		95% reliability Mean ± 1.65SD		98% reliability Mean ± 2SD		99,9% reliability Mean ± 3SD	
	Min	Max	Min	Max	Min	Max	Min	Max	Min	Max
N=11years										
C1	1,00	62,00	-0,65	64,25	-1,73	65,70	-2,31	66,49	-3,96	68,73
C2	3,22	57,87	1,54	59,68	0,44	60,86	-0,15	61,50	-1,83	63,31
C3	6,65	56,13	5,30	58,00	4,43	59,21	3,96	59,86	2,61	61,73
C4	8,26	48,36	6,92	49,96	6,05	51,00	5,58	51,56	4,24	53,16

Table 5.34 PG for different level of reliability for the Awbari location.

N=11 years	Awbari									
	PG 50% reliability		PG 85% reliability		PG 95% reliability		PG 98% reliability		PG 99,9% reliability	
	YY	XX	YY	YY	YY	XX	YY	XX	YY	XX
C1	64	-10	70	-10	70	-10	70	-10	70	-10
C2	58	-10	64	-10	64	-10	64	-10	64	-10
C3	58	-10	64	-10	64	-10	64	-10	64	-10
C4	52	-10	52	-10	52	-10	52	-10	58	-10

### 5.6.2.5 Awjilah location

Table 5.35 Regression models for maximal pavement temperatures for the Awjilah location.

Surface	$T_{pav,surf}^{max} = 9.318178 + 0.835453T_{air}^{max} + 0.174614Day - 0.000489Day^2$
3cm	$T_{pav,3cm}^{max} = 5.047061 + 0.823319T_{air}^{max} + 0.195413Day - 0.000544Day^2$
8cm	$T_{pav,8cm}^{max} = 6.223817 + 0.759976T_{air}^{max} + 0.160414Day - 0.000452Day^2$
15cm	$T_{pav,15cm}^{max} = 4.877254 + 0.703914T_{air}^{max} + 0.170250Day - 0.000459Day^2$

Table 5.36 Regression models for minimal pavement temperatures for the Awjilah location.

Surface	$T_{pav,surf}^{min} = 9.440062 + 0.657306T_{air}^{min} + 0.032589Day - 0.000133Day^2$
3cm	$T_{pav,3cm}^{min} = 3.294963 + 0.794512T_{air}^{min} + 0.053131Day - 0.000144Day^2$
8cm	$T_{pav,8cm}^{min} = 4.284102 + 0.761828T_{air}^{min} + 0.058534Day - 0.000152Day^2$
15cm	$T_{pav,15cm}^{min} = 4.356681 + 0.763559T_{air}^{min} + 0.060234Day - 0.000157Day^2$

Table 5.37 Maximum of seven-day average of predicted maximal daily temperatures and minimum of minimal daily temperatures from year 2000 to year 2009, year 2012–2013, for the Awjilah location.

Awjilah		Predicted values					Predicted values				
Year	Air_max_aver	C1_max_aver	C2_max_aver	C3_max_aver	C4_max_aver	Air_min	C1_min	C2_min	C3_min	C4_min	
	Max					Min					
2000	40.63	58.52	55.73	51.02	49.04	2.50	8.08	6.33	7.35	7.46	
2001	40.52	58.68	55.89	51.17	49.17	3.60	3.60	6.94	7.24	8.77	
2002	44.23	60.97	58.08	53.21	51.22	3.50	7.28	6.44	7.35	7.44	
2003	41.79	59.80	56.99	52.20	50.07	2.50	6.56	6.84	7.79	7.90	
2004	40.44	58.59	55.79	51.08	49.10	2.70	5.39	5.65	7.46	7.49	
2005	41.80	58.90	55.93	51.41	48.92	2.50	5.90	5.68	6.57	6.65	
2006	41.19	58.55	55.70	51.01	49.17	3.00	6.04	6.20	7.12	7.21	
2007	43.30	61.08	58.24	53.36	51.11	3.00	6.68	6.87	7.71	7.79	
2008	42.16	59.97	57.11	52.37	50.06	2.50	8.28	6.94	7.90	8.01	
2009	40.40	58.65	55.84	51.15	49.05	2.80	7.87	5.63	6.53	6.61	
2012	49.86	66.12	64.04	59.23	56.24	-0.01	3.99	4.56	6.97	6.97	

Table 5.38 Maximum of predicted maximal daily temperatures for years 2000–2009 and 2012 for the Al Joufroh location.

Awjilah		Predicted values				
Year	Air_max	C1_max	C2_max	C3_max	C4_max	
	Max					
2000	43,50	59,95	57,14	52,33	50,23	
2001	46,00	61,94	59,09	54,13	51,91	
2002	48,00	64,04	61,09	56,00	53,81	
2003	45,50	61,85	58,96	54,02	51,94	
2004	44,50	61,80	58,96	54,00	51,81	
2005	45,50	62,08	59,07	54,30	51,61	
2006	47,00	63,29	60,36	55,32	53,17	
2007	45,60	63,00	60,14	55,11	52,74	
2008	45,00	62,30	59,39	54,48	51,99	
2009	45,00	62,43	59,57	54,57	52,33	
2012	50,93	66,99	64,80	59,84	56,98	

For these data for 11 years, mean value, standard deviation maximum and minimum were calculated. To determine 50%, 85%, 95%, 98% and 99.9% level of reliability, we calculate intervals  $\text{Mean} \pm \text{SD}$ ,  $\text{Mean} \pm 1.65 \cdot \text{SD}$ ,  $\text{Mean} \pm 2 \cdot \text{SD}$ ,  $\text{Mean} \pm 3 \cdot \text{SD}$ . We use values of standard normal distribution presented in Table 5.11.

Table 5.39 Descriptive statistics for data for 11 years at the Al Jufroh location.

Awjilah	Mean	Min	Max	Std.Dev	Mean ± SD		Mean ± 1.65*SD		Mean ± 2*SD		Mean ± 3*SD	
Air_max	46,05	43,50	50,93	2,01	44,0	48,06	42,73	49,37	42,03	50,07	40,02	52,08
C1_max_P	62,70	59,95	66,99	1,76	60,9	64,46	59,80	65,60	59,18	66,21	57,42	67,97
C2_max_P	59,87	57,14	64,80	1,92	57,9	61,79	56,71	63,03	56,03	63,71	54,12	65,62
C3_max_P	54,92	52,33	59,84	1,88	53,0	56,80	51,82	58,02	51,16	58,67	49,29	60,55
C4_max_p	52,59	50,23	56,98	1,72	50,8	54,31	49,76	55,43	49,15	56,03	47,43	57,75
Air_max_aver	42,39	40,40	49,86	2,77	39,6	45,16	37,83	46,96	36,86	47,93	34,09	50,69
C1_max_P_aver	59,98	58,52	66,12	2,25	57,7	62,24	56,27	63,70	55,48	64,49	53,23	66,74
C2_max_P_aver	57,21	55,70	64,04	2,45	54,7	59,67	53,16	61,26	52,30	62,12	49,85	64,58
C3_max_P_aver	52,47	51,01	59,23	2,41	50,0	54,88	48,51	56,44	47,66	57,28	45,26	59,69
C4_max_P_aver	50,29	48,92	56,24	2,14	48,1	52,43	46,75	53,82	46,00	54,57	43,86	56,72
Air_min	2,60	-0,01	3,60	0,95	1,65	3,55	1,03	4,17	0,70	4,50	-0,25	5,45
C1_min_P	6,33	3,60	8,28	1,56	4,77	7,90	3,76	8,91	3,21	9,46	1,65	11,02
C2_min_P	6,19	4,56	6,94	0,75	5,44	6,94	4,95	7,43	4,69	7,69	3,94	8,44
C3_min_P	7,27	6,53	7,90	0,45	6,82	7,73	6,52	8,02	6,36	8,18	5,91	8,63
C4_min_P	7,48	6,61	8,77	0,63	6,85	8,11	6,44	8,53	6,22	8,75	5,58	9,38

Table 5.40 Reliability data for PG at the Awjilah location.

Awjilah	50% reliability Mean		85% reliability Mean ± SD		95% reliability Mean ± 1.65SD		98% reliability Mean ± 2SD		99,9% reliability Mean ± 3SD	
	Min	Max	Min	Max	Min	Max	Min	Max	Min	Max
N=11years										
C1	6,33	59,98	4,77	62,24	3,76	63,70	3,21	64,49	1,65	66,74
C2	6,19	57,21	5,44	59,67	4,95	61,26	4,69	62,12	3,94	64,58
C3	7,27	52,47	6,82	54,88	6,52	56,44	6,36	57,28	5,91	59,69
C4	7,48	50,29	6,85	52,43	6,44	53,82	6,22	54,57	5,58	56,72

Table 5.41 PG for different levels of reliability for the Al Jufroh location.

N=11 years	Awjilah									
	PG 50% reliability		PG 85% reliability		PG 95% reliability		PG 98% reliability		PG 99,9% reliability	
	YY	XX	YY	YY	YY	XX	YY	XX	YY	XX
C1	64	-10	64	-10	64	-10	70	-10	70	-10
C2	58	-10	64	-10	64	-10	64	-10	70	-10
C3	58	-10	58	-10	58	-10	58	-10	64	-10
C4	52	-10	58	-10	58	-10	58	-10	58	-10

### 5.6.2.6 Brak location

Table 5.42 Regression models for maximal pavement temperatures for the Al Jufroh location.

Surface	$T_{pav,surf}^{max} = 13.40893 + 0.62822T_{air}^{max} + 0.23666Day - 0.00065Day^2$
3cm	$T_{pav,3cm}^{max} = 7.188584 + 0.710666T_{air}^{max} + 0.225349Day - 0.000613Day^2$
8cm	$T_{pav,8cm}^{max} = 6.005975 + 0.686538T_{air}^{max} + 0.222403Day - 0.000603Day^2$
15cm	$T_{pav,15cm}^{max} = 4.639623 + 0.609187T_{air}^{max} + 0.212552Day - 0.000572Day^2$

Table 5.43 Regression models for minimal pavement temperatures for the Al Jufroh location.

Surface	$T_{pav,surf}^{min} = 9.216318 + 0.627141T_{air}^{min} + 0.061208Day - 0.000170Day^2$
3cm	$T_{pav,3cm}^{min} = 2.544214 + 0.815841T_{air}^{min} + 0.068388Day - 0.000179Day^2$
8cm	$T_{pav,8cm}^{min} = 3.116924 + 0.803832T_{air}^{min} + 0.077218Day - 0.000203Day^2$
15cm	$T_{pav,15cm}^{min} = 4.682006 + 0.760949T_{air}^{min} + 0.101335Day - 0.000274Day^2$

Table 5.44 Maximum of seven-day average of predicted maximal daily temperatures and minimum of minimal daily temperatures from year 2000 to year 2009, year 2012–2013, for the Brak location.

Brak		Predicted values				Predicted values				
Year	Air_max_aver	C1_max_aver	C2_max_aver	C3_max_aver	C4_max_aver	Air_min	C1_min	C2_min	C3_min	C4_min
	Max					Min				
2000	41,77	60,98	57,37	54,99	49,66	1,50	10,71	4,45	5,03	6,60
2001	42,79	60,83	57,20	54,82	49,51	1,00	10,15	3,70	4,30	5,94
2002	44,81	62,94	59,62	57,17	51,60	-1,00	8,95	2,13	2,77	4,52
2003	44,39	62,83	59,44	56,98	51,42	-1,90	8,15	2,54	3,22	4,40
2004	42,71	60,74	57,36	54,98	49,65	0,20	9,76	3,18	3,81	5,53
2005	42,27	61,14	57,55	55,16	49,81	0,60	10,41	4,14	4,85	6,41
2006	42,80	61,00	57,60	55,21	49,86	0,00	9,46	2,81	3,42	5,08
2007	43,84	62,45	59,03	56,59	51,08	-2,00	7,78	2,13	2,77	3,84
2008	44,04	62,36	58,91	56,45	50,90	-3,00	9,40	2,65	3,35	4,98
2009	42,43	61,58	58,04	55,63	50,23	2,00	12,11	7,17	7,69	9,07
2012	47.16	66.08	62.79	60.6	55.0	2.2	10.82	6.820	7.60	9.710

Table 5.45 Maximum of predicted maximal daily temperatures for years 2000–2009 and 2012 for the Brak location.

Brak		Predicted values			
Year	Air_max	C1_max	C2_max	C3_max	C4_max
Max					
2000	44,00	62,03	58,56	56,14	50,68
2001	44,10	62,41	58,99	56,56	51,05
2002	47,00	63,95	60,78	58,29	52,60
2003	44,70	63,03	59,67	57,20	51,61
2004	44,70	62,90	59,51	57,04	51,43
2005	44,10	62,34	58,99	56,56	51,06
2006	45,20	62,36	59,17	56,74	51,21
2007	46,00	63,80	60,56	58,07	52,39
2008	46,40	63,81	60,56	58,04	52,30
2009	44,50	62,85	59,49	57,04	51,48
2012	50,10	69,06	65,23	62,72	56,63

For these data for 11 years, mean value, standard deviation maximum and minimum were calculated. To determine 50%, 85%, 95%, 98% and 99.9% level of reliability, we calculate intervals Mean  $\pm$  SD, Mean  $\pm$  1.65\*SD, Mean  $\pm$  2\*SD, Mean  $\pm$  3\*SD. We use values of standard normal distribution presented in Table 5.11.

Table 5.46 Descriptive statistics for data for 11 years at the Brak location.

Brak	Mean	Min	Max	Std.Dev	Mean $\pm$ SD		Mean $\pm$ 1.65*SD		Mean $\pm$ 2*SD		Mean $\pm$ 3*SD	
Air_max	45,53	44,00	50,10	1,82	43,71	47,3	42,53	48,52	41,89	49,16	40,08	50,98
C1_max_P	63,50	62,03	69,06	1,96	61,55	65,4	60,27	66,73	59,59	67,42	57,63	69,37
C2_max_P	60,14	58,56	65,23	1,84	58,30	61,9	57,10	63,17	56,46	63,81	54,62	65,65
C3_max_P	57,67	56,14	62,72	1,81	55,86	59,4	54,68	60,66	54,05	61,30	52,23	63,11
C4_max_p	52,04	50,68	56,63	1,64	50,40	53,6	49,33	54,75	48,76	55,32	47,12	56,96
Air_max_aver	43,55	41,77	47,16	1,53	42,01	45,0	41,01	46,08	40,48	46,62	38,94	48,15
C1_max_P_aver	62,08	60,74	66,08	1,56	60,52	63,6	59,51	64,66	58,96	65,21	57,40	66,77
C2_max_P_aver	58,63	57,20	62,79	1,64	56,99	60,2	55,92	61,34	55,34	61,91	53,70	63,55
C3_max_P_aver	56,23	54,82	60,60	1,68	54,55	57,9	53,46	59,01	52,87	59,60	51,18	61,29
C4_max_P_aver	50,79	49,51	55,00	1,59	49,20	52,3	48,17	53,41	47,62	53,97	46,03	55,56
Air_min	-0,04	-3,00	2,20	1,73	-1,77	1,70	-2,90	2,83	-3,51	3,43	-5,24	5,17
C1_min_P	9,79	7,78	12,11	1,25	8,55	11,0	7,74	11,85	7,30	12,28	6,06	13,53
C2_min_P	3,79	2,13	7,17	1,76	2,04	5,55	0,89	6,69	0,28	7,31	-1,48	9,06
C3_min_P	4,44	2,77	7,69	1,75	2,68	6,19	1,54	7,33	0,93	7,95	-0,83	9,70
C4_min_P	6,01	3,84	9,71	1,88	4,13	7,88	2,91	9,10	2,25	9,76	0,38	11,64

Table 5.47 Reliability data for PG at the Brak location

Brak	50% reliability Mean		85% reliability Mean ± SD		95% reliability Mean ± 1.65SD		98% reliability Mean ± 2SD		99,9% reliability Mean ± 3SD	
	Min	Max	Min	Max	Min	Max	Min	Max	Min	Max
N=11years										
C1	9,79	62,08	8,55	63,65	7,74	64,66	7,30	65,21	6,06	66,77
C2	3,79	58,63	2,04	60,27	0,89	61,34	0,28	61,91	-1,48	63,55
C3	4,44	56,23	2,68	57,92	1,54	59,01	0,93	59,60	-0,83	61,29
C4	6,01	50,79	4,13	52,38	2,91	53,41	2,25	53,97	0,38	55,56

Table 5.48 PG for different levels of reliability for the Brak location

N=11 years	Brak									
	PG 50% reliability		PG 85% reliability		PG 95% reliability		PG 98% reliability		PG 99,9% reliability	
	YY	XX	YY	YY	YY	XX	YY	XX	YY	XX
C1	64	-10	64	-10	70	-10	70	-10	70	-10
C2	64	-10	64	-10	64	-10	64	-10	64	-10
C3	58	-10	58	-10	64	-10	64	-10	64	-10
C4	52	-10	58	-10	58	-10	58	-10	58	-10

### 5.6.2.7 Ghadamis location

Table 5.49 Regression models for maximal pavement temperatures for the Ghadamis location.

Surface	$T_{pav,surf}^{max} = 5.705109 + 0.827308T_{air}^{max} + 0.200932Day - 0.000546Day^2$
3cm	$T_{pav,3cm}^{max} = 2.785780 + 0.919918T_{air}^{max} + 0.168052Day - 0.000461Day^2$
8cm	$T_{pav,8cm}^{max} = 0.130674 + 0.866552T_{air}^{max} + 0.161649Day - 0.000441Day^2$
15cm	$T_{pav,15cm}^{max} = -1.86996 + 0.73224T_{air}^{max} + 0.18756Day - 0.00051Day^2$

Table 5.50 Regression models for minimal pavement temperatures for the Ghadamis location.

Surface	$T_{pav,surf}^{min} = 0.008911 + 0.751131T_{air}^{min} + 0.079117Day - 0.000204Day^2$
3cm	$T_{pav,3cm}^{min} = 1.559759 + 0.823675T_{air}^{min} + 0.058969Day - 0.000154Day^2$
8cm	$T_{pav,8cm}^{min} = 2.254005 + 0.815608T_{air}^{min} + 0.069928Day - 0.000182Day^2$
15cm	$T_{pav,15cm}^{min} = 5.453641 + 0.811387T_{air}^{min} + 0.056728Day - 0.000132Day^2$

Table 5.51 Maximum of seven-day average of predicted maximal daily temperatures and minimum of minimal daily temperatures from year 2000 to year 2009, year 2012–2013, for the Ghadamis location.

Ghadamis		Predicted values					Predicted values				
Year	Air_max_aver	C1_max_aver	C2_max_aver	C3_max_aver	C4_max_aver	Air_min	C1_min	C2_min	C3_min	C4_min	
	Max					Min					
2000	43,01	59,76	57,64	52,20	46,85	0,00	1,00	2,56	3,28	6,43	
2001	45,20	61,49	59,58	54,03	48,38	-2,50	0,46	1,33	2,38	5,20	
2002	46,47	62,61	60,81	55,19	49,37	-1,60	-0,89	0,57	1,28	4,48	
2003	46,21	62,42	60,61	54,99	49,21	-2,20	0,70	1,35	2,37	5,40	
2004	45,27	60,81	58,98	53,48	47,74	-1,40	0,63	1,52	2,51	5,90	
2005	46,50	62,39	60,62	55,01	49,17	-2,20	-0,65	0,67	1,44	4,57	
2006	44,66	60,90	58,93	53,40	47,86	-1,60	-0,73	0,59	1,36	4,49	
2007	45,46	61,78	59,91	54,32	48,65	-0,50	0,85	2,37	3,10	6,25	
2008	45,36	61,68	59,78	54,21	48,55	0,10	2,27	3,22	4,28	7,84	
2009	45,53	61,85	59,97	54,39	48,70	1,00	1,83	3,23	4,08	7,09	
2012	49,86	66,73	64,04	58,85	53,15	-1,61	2,04	3,61	4,46	6,12	

Table 5.52 Maximum of predicted maximal daily temperatures for years 2000–2009 and 2012 for the Al Joufroh location.

Ghadamis		Predicted values			
Year	Air_max	C1_max	C2_max	C3_max	C4_max
	Max				
2000	45,50	61,80	59,91	54,34	48,66
2001	47,40	63,28	61,58	55,91	49,97
2002	48,00	63,76	62,11	56,41	50,39
2003	47,00	63,07	61,33	55,67	49,79
2004	46,00	61,28	59,54	54,00	48,15
2005	47,50	63,22	61,54	55,88	49,91
2006	46,30	61,58	59,73	54,18	48,47
2007	46,50	62,65	60,87	55,23	49,42
2008	47,00	63,01	61,26	55,61	49,73
2009	47,00	63,06	61,32	55,66	49,78
2012	50,93	69,88	64,80	59,67	53,68

For these data for 11 years, mean value, standard deviation maximum and minimum were calculated. To determine 50%, 85%, 95%, 98% and 99.9% levels of reliability we calculate intervals  $\text{Mean} \pm \text{SD}$ ,  $\text{Mean} \pm 1.65 \cdot \text{SD}$ ,  $\text{Mean} \pm 2 \cdot \text{SD}$ ,  $\text{Mean} \pm 3 \cdot \text{SD}$ . We use values of standard normal distribution presented in Table 5.11.



Table 5.53 Descriptive statistics for data for 11 years at the Ghadamis location

Ghadamis	Mean	Min	Max	Std.Dev	Mean ± SD		Mean ± 1.65*SD		Mean ± 2*SD		Mean ± 3*SD	
Air_max	47,19	45,50	50,93	1,43	45,76	48,62	44,84	49,55	44,33	50,05	42,91	51,48
C1_max_P	63,33	61,28	69,88	2,31	61,02	65,64	59,51	67,14	58,70	67,95	56,39	70,26
C2_max_P	61,27	59,54	64,80	1,44	59,83	62,71	58,90	63,65	58,39	64,15	56,95	65,59
C3_max_P	55,69	54,00	59,67	1,54	54,15	57,22	53,15	58,22	52,61	58,76	51,08	60,30
C4_max_p	49,81	48,15	53,68	1,46	48,35	51,28	47,40	52,23	46,89	52,74	45,43	54,20
Air_max_aver	45,78	43,01	49,86	1,66	44,11	47,44	43,03	48,52	42,45	49,10	40,78	50,77
C1_max_P_aver	62,04	59,76	66,73	1,76	60,27	63,80	59,13	64,95	58,51	65,57	56,74	67,33
C2_max_P_aver	60,08	57,64	64,04	1,60	58,48	61,68	57,44	62,72	56,88	63,28	55,27	64,88
C3_max_P_aver	54,55	52,20	58,85	1,67	52,89	56,22	51,80	57,30	51,22	57,88	49,55	59,55
C4_max_P_aver	48,88	46,85	53,15	1,60	47,28	50,47	46,24	51,51	45,68	52,07	44,08	53,67
Air_min	-1,14	-2,50	1,00	1,12	-2,26	-0,01	-2,99	0,72	-3,39	1,11	-4,51	2,23
C1_min_P	0,68	-0,89	2,27	1,10	-0,42	1,78	-1,13	2,50	-1,52	2,88	-2,62	3,98
C2_min_P	1,91	0,57	3,61	1,13	0,78	3,04	0,04	3,78	-0,36	4,18	-1,49	5,31
C3_min_P	2,78	1,28	4,46	1,17	1,61	3,94	0,85	4,70	0,45	5,11	-0,72	6,27
C4_min_P	5,80	4,48	7,84	1,10	4,70	6,89	3,99	7,61	3,60	7,99	2,51	9,09

Table 5.54 Reliability data for PG at the Ghadamis location.

Ghadamis	50% reliability Mean		85% reliability Mean ± SD		95% reliability Mean ± 1.65SD		98% reliability Mean ± 2SD		99,9% reliability Mean ± 3SD	
	Min	Max	Min	Max	Min	Max	Min	Max	Min	Max
N=11years										
C1	0,68	62,04	-0,42	63,80	-1,13	64,95	-1,52	65,57	-2,62	67,33
C2	1,91	60,08	0,78	61,68	0,04	62,72	-0,36	63,28	-1,49	64,88
C3	2,78	54,55	1,61	56,22	0,85	57,30	0,45	57,88	-0,72	59,55
C4	5,80	48,88	4,70	50,47	3,99	51,51	3,60	52,07	2,51	53,67

Table 5.55 PG for different level of reliability for the Ghadamis location.

N=11 years	Ghadamis									
	PG 50% reliability		PG 85% reliability		PG 95% reliability		PG 98% reliability		PG 99,9% reliability	
	YY	XX	YY	YY	YY	XX	YY	XX	YY	XX
C1	64	-10	64	-10	70	-10	70	-10	70	-10
C2	64	-10	64	-10	64	-10	64	-10	70	-10
C3	58	-10	58	-10	58	-10	58	-10	64	-10
C4	52	-10	52	-10	52	-10	58	-10	58	-10

### 5.6.2.8 Ghat location

Table 5.56 Regression models for maximal pavement temperatures for the Ghat location.

Surface	$T_{pav,surf}^{max} = 15.60502 + 0.66044T_{air}^{max} + 0.21938Day - 0.00061Day^2$
3cm	$T_{pav,3cm}^{max} = 7.277605 + 0.810461T_{air}^{max} + 0.180809Day - 0.000506Day^2$
8cm	$T_{pav,8cm}^{max} = 12.42993 + 0.60993T_{air}^{max} + 0.20173Day - 0.00055Day^2$
15cm	$T_{pav,15cm}^{max} = 8.213704 + 0.572258T_{air}^{max} + 0.213122Day - 0.000583Day^2$

Table 5.57 Regression models for minimal pavement temperatures for the Ghat location.

Surface	$T_{pav,surf}^{min} = 3.429364 + 0.788663T_{air}^{min} + 0.056234Day - 0.000150Day^2$
3cm	$T_{pav,3cm}^{min} = 4.117598 + 0.813228T_{air}^{min} + 0.051351Day - 0.000138Day^2$
8cm	$T_{pav,8cm}^{min} = 5.329680 + 0.706210T_{air}^{min} + 0.089516Day - 0.000235Day^2$
15cm	$T_{pav,15cm}^{min} = 6.236562 + 0.647014T_{air}^{min} + 0.106429Day - 0.000285Day^2$

Table 5.58 Maximum of seven-day average of predicted maximal daily temperatures and minimum of minimal daily temperatures from year 2000 to year 2009, year 2012–2013, for the Ghat location.

Ghat		Predicted values					Predicted values				
Year	Air_max_aver	C1_max_aver	C2_max_aver	C3_max_aver	C4_max_aver	Air_min	C1_min	C2_min	C3_min	C4_min	
	Max					Min					
2000	43,14	63,68	58,26	57,17	52,29	0,50	4,21	4,88	6,30	7,29	
2001	42,19	62,79	57,20	56,36	51,53	0,50	4,42	4,93	7,13	7,54	
2002	44,21	64,44	59,17	57,85	52,94	-8,00	-1,67	-1,28	1,61	3,36	
2003	42,79	63,56	58,08	57,02	52,17	-4,50	1,57	2,00	4,85	5,67	
2004	41,71	62,28	56,67	55,92	51,08	-1,00	3,24	3,71	5,68	6,56	
2005	43,50	63,61	58,28	57,15	52,24	-1,50	2,36	3,00	4,45	5,48	
2006	42,00	62,65	56,95	56,16	51,36	-1,00	3,19	3,80	5,50	6,63	
2007	43,73	64,03	58,74	57,41	52,54	-7,00	-1,70	-1,22	1,00	2,44	
2008											
2009	43,20	63,81	58,39	57,26	52,39	-1,50	3,41	3,96	6,13	7,47	
2012	50.344	71.005	65.868	63.121	58.171	-0.52	3.860	4.540	6.270	7.100	

Table 5.59 Maximum of predicted maximal daily temperatures for years 2000–2009 and 2012 for the Ghat location

Ghat		Predicted values			
Year	Air_max	C1_max	C2_max	C3_max	C4_max
Max					
2000	44,70	64,75	59,55	58,14	53,21
2001	44,00	64,20	58,95	57,51	52,62
2002	45,80	65,49	60,46	58,82	53,85
2003	44,70	64,81	59,61	58,18	53,26
2004	44,00	63,96	58,62	57,31	52,44
2005	44,50	64,30	59,12	57,79	52,84
2006	43,50	63,72	58,27	57,15	52,30
2007	46,00	65,70	60,70	58,98	54,01
2008					
2009	44,90	64,98	59,82	58,29	53,37
2012	52,580	72,460	66,810	64,020	60,460

For these data for 11 years, mean value, standard deviation maximum and minimum were calculated. To determine 50%, 85%, 95%, 98% and 99.9% level of reliability, we calculate intervals Mean  $\pm$  SD, Mean  $\pm$  1.65\*SD, Mean  $\pm$  2\*SD, Mean  $\pm$  3\*SD. We use values of standard normal distribution presented in Table 5.11.

Table 5.60 Descriptive statistics for data for 11 years at the Ghat location

Ghat	Mean	Min	Max	Std.Dev	Mean $\pm$ SD		Mean $\pm$ 1.65*SD		Mean $\pm$ 2*SD		Mean $\pm$ 3*SD	
Air_max	45,47	43,50	52,58	2,62	42,85	48,08	41,15	49,78	40,24	50,70	37,62	53,32
C1_max_P	65,44	63,72	72,46	2,55	62,89	67,98	61,23	69,64	60,34	70,53	57,79	73,08
C2_max_P	60,19	58,27	66,81	2,45	57,74	62,64	56,15	64,23	55,30	65,08	52,85	67,53
C3_max_P	58,62	57,15	64,02	1,99	56,63	60,61	55,33	61,90	54,64	62,60	52,65	64,59
C4_max_p	53,84	52,30	60,46	2,40	51,44	56,23	49,88	57,79	49,05	58,63	46,65	61,02
Air_max_aver	43,68	41,71	50,34	2,47	41,21	46,15	39,60	47,76	38,74	48,62	36,27	51,10
C1_max_P_aver	64,19	62,28	71,01	2,49	61,70	66,67	60,08	68,29	59,21	69,16	56,73	71,65
C2_max_P_aver	58,76	56,67	65,87	2,62	56,14	61,38	54,44	63,09	53,52	64,00	50,90	66,63
C3_max_P_aver	57,54	55,92	63,12	2,05	55,49	59,59	54,16	60,92	53,44	61,64	51,39	63,69
C4_max_P_aver	52,67	51,08	58,17	2,02	50,66	54,69	49,35	56,00	48,64	56,70	46,63	58,72
Air_min	-2,40	-8,00	0,50	3,03	-5,44	0,63	-7,41	2,60	-8,47	3,67	-	6,70
C1_min_P	2,29	-1,70	4,42	2,26	0,03	4,54	-1,43	6,01	-2,22	6,80	-4,48	9,06
C2_min_P	2,83	-1,28	4,93	2,32	0,51	5,15	-1,00	6,66	-1,81	7,48	-4,14	9,80
C3_min_P	4,89	1,00	7,13	2,04	2,85	6,93	1,52	8,26	0,81	8,98	-1,23	11,02
C4_min_P	5,95	2,44	7,54	1,77	4,19	7,72	3,04	8,87	2,42	9,49	0,65	11,26

Table 5.61 Reliability data for PG at the Ghat location.

Ghat	50% reliability Mean		85% reliability Mean $\pm$ SD		95% reliability Mean $\pm$ 1.65SD		98% reliability Mean $\pm$ 2SD		99,9% reliability Mean $\pm$ 3SD	
	Min	Max	Min	Max	Min	Max	Min	Max	Min	Max
N=11years										
C1	2,29	64,19	0,03	66,67	-1,43	68,29	-2,22	69,16	-4,48	71,65
C2	2,83	58,76	0,51	61,38	-1,00	63,09	-1,81	64,00	-4,14	66,63
C3	4,89	57,54	2,85	59,59	1,52	60,92	0,81	61,64	-1,23	63,69
C4	5,95	52,67	4,19	54,69	3,04	56,00	2,42	56,70	0,65	58,72

Table 5.62 PG for different level of reliability for the Ghat location.

N=11 years	Ghadamis									
	PG 50% reliability		PG 85% reliability		PG 95% reliability		PG 98% reliability		PG 99,9% reliability	
	YY	XX	YY	YY	YY	XX	YY	XX	YY	XX
C1	70	-10	70	-10	70	-10	70	-10	76	-10
C2	64	-10	64	-10	64	-10	70	-10	70	-10
C3	64	-10	64	-10	64	-10	64	-10	64	-10
C4	58	-10	58	-10	58	-10	58	-10	64	-10

### 5.6.3 Libyan Desert road PG mapping

Table 5.63 PG for pavement temperatures at the surface, for eight locations.

	C1, surface			
	PG 98% reliability		PG 99,9% reliability	
	YY	XX	YY	XX
Al Jufroh	70	-10	70	-10
Al Kufrah	70	-10	70	-10
Al Qatrun	70	-10	70	-10
Awbari	70	-10	70	-10
Awjilah	70	-10	70	-10
Brak	70	-10	70	-10
Ghadamis	70	-10	70	-10
Ghat	70	-10	76	-10

Table 5.64 PG for pavement temperatures at 3cm depth for eight locations.

	<b>C2, 3cm</b>			
	<b>PG 98% reliability</b>		<b>PG 99,9% reliability</b>	
	<b>YY</b>	<b>XX</b>	<b>YY</b>	<b>XX</b>
Al Jufroh	64	-10	64	-10
Al	64	-10	64	-10
Al Qatrun	64	-10	64	-10
Awbari	64	-10	64	-10
Awjilah	64	-10	70	-10
Brak	64	-10	64	-10
Ghadamis	64	-10	70	-10
Ghat	70	-10	70	-10

Table 5.65 PG for pavement temperatures at 8cm depth for eight locations.

	<b>C3, 8 cm</b>			
	<b>PG 98% reliability</b>		<b>PG 99,9% reliability</b>	
	<b>YY</b>	<b>XX</b>	<b>YY</b>	<b>XX</b>
Al Jufroh	58	-10	64	-10
Al	58	-10	58	-10
Al Qatrun	64	-10	64	-10
Awbari	64	-10	64	-10
Awjilah	58	-10	64	-10
Brak	64	-10	64	-10
Ghadamis	58	-10	64	-10
Ghat	64	-10	64	-10

Table 5.66 PG for pavement temperatures at 15cm depth for eight locations.

	<b>C4, 15cm</b>			
	<b>PG 98% reliability</b>		<b>PG 99,9% reliability</b>	
	<b>YY</b>	<b>XX</b>	<b>YY</b>	<b>XX</b>
Al Jufroh	58	-10	58	-10
Al	52	-10	52	-10
Al Qatrun	58	-10	58	-10
Awbari	52	-10	58	-10
Awjilah	58	-10	58	-10
Brak	58	-10	58	-10
Ghadamis	58	-10	58	-10
Ghat	58	-10	64	-10

## **5.7 Determination of the performance grade of Libyan bitumen**

This section presents the performance grade of natural bitumen and modified bitumen according to the modified bitumen that is used on Libya's desert roads. Generally, the bitumen, with viscosity class 60/70 (AC-20), is used in Libyan road specification for binder course layer, also rubber modified bitumen is using for wearing course layer. To find the PG of bitumen and modified bitumen some tests were carried out.

### **5.7.1 Tests**

For the calculation of the performance grade, the determination of the following values was carried out on the unmodified bitumen and rubber modified bitumen:

- determination of complex shear modulus and phase angle - Dynamic Shear Rheometer (DSR) -in accordance with the European Standard EN 14770;
- determination of flexural creep stiffness—Bending Beam Rheometer (BBR) - in accordance with the European Standard EN 14771.

These tests were carried out in the accredited laboratory Niveelt Labor Praha spol.

### **5.7.2 Test results**

Test results of binders are described below:

- Asphalt binder bitumen 60/70 from Libyan production;
- Rubber modified binder can be qualified in accordance with the Superpave method as follows:
  - Binder bitumen 60/70: PG 64-22
  - Rubber modified binder: PG 76-16.

## Chapter 6 SUMMARY AND CONCLUSIONS

The performance of asphalt pavements is greatly influenced by environmental conditions. One of the most important environmental factors that significantly affects the mechanical properties of asphalt mixtures is temperature. Thus, accurate prediction of the temperature distribution within the pavement structure is important. This study has proposed regression models to predict flexible pavement temperature profile and measured values for air temperature, wind speed, and solar radiation at different pavement stations located at the Libya Desert Accelerated Pavement Facility. Data were collected for 365 days, air and pavement temperature, wind speed and solar radiation was recorded every fifteen minutes. For all eight locations, temperature data for one year were collected for air and pavement at four layers: at surface (C1) and depths of 3 cm (C2), 8 cm (C3), and 15 cm (C4). From these data, maximal and minimal daily temperatures were extracted for air and pavements at surface and depths of 3, 8, and 15 cm.

Based on maximal and minimal daily temperatures for air and four layers of pavement, using regression analysis, models for maximum and minimum daily temperatures were obtained. Regression was used to develop the maximal and minimal daily pavement models using air temperature, the day of the year, solar radiation and wind speed as independent variables. Several regression models based on daily maximal and minimal air temperatures, day of the year, wind speed and daily cumulative solar radiation were determined, in order to find the best model.

The best model appeared to be the model including the air temperature, daily cumulative solar radiation and the day of the year.

Regression models based on daily maximal and minimal air temperatures, day of the year, wind speed, daily cumulative solar radiation and distance from the surface were also determined. The best model appeared to be the model including the air temperature, daily cumulative solar radiation, distance from the surface and the day of the year.

After that similar model for predicting maximal (minimal) daily pavement temperature for three deeper layers (C2, C3, C4) including surface maximal (minimal) daily pavement temperature instead of maximal (minimal) daily air temperatures were determined.

For each of eight locations, data on daily maximum air sheltered temperature °C and daily minimum air sheltered temperature in °C were collected for years from 2000 to 2009. Maximal values of these sheltered air temperatures in °C were lower than maximal air temperatures measured in 2012–2013 for all eight locations.

From data for maximal (minimal) daily air temperatures for years from 2000 to 2009, using regression models obtained in Chapter 4, predicted values for maximal (minimal) daily pavement

temperatures for four layers were calculated for each year, and for each of eight locations. Although the best model appeared to be the model including the air temperature, daily cumulative solar radiation and the day of the year, since data on daily cumulative solar radiation were not available, the model including the air temperature, and the day of the year was used. The seven-day average of maximal daily air and predicted pavement temperatures was calculated.

Then:

- Yearly maximum for the seven-day average of maximal daily air and pavement temperatures was determined for each of the years from 2000 to 2009, for each of eight locations.
- Yearly minimum for minimal air and pavement temperatures was determined for each of the years from 2000 to 2009, for each of eight locations.
- Yearly maximum of maximal daily air and pavement temperatures was determined for each of the years from 2000 to 2009, for each of eight locations.

These maximums and minimum were used to determine PG grades for each of eight locations with 50%, 85%, 95%, 98% and 99.9% reliability.

Data were analyzed using the statistical package Statistica 12 (StatSoft Inc., Tulsa, OK, USA), university license for Novi Sad University.

## **6.1 Findings -temperature**

Based on the extensive field work conducted locally, the following can be stated:

1. Extreme asphalt pavement surface measured temperatures in the study area in Libya environment ranged between 2.04°C and 72.46°C in the year of the study (2012–2013). For predicted values these extremes range is from -1.7°C and 65.7°C in the years 2000–2009.
2. The maximum pavement temperature at a surface is generally higher than the maximum pavement temperature of other three layers and the maximum air temperature during the summer months. The same phenomenon is observed to a lesser degree in the winter months.
3. The minimum pavement temperature at a depth of 15cm is generally higher than the minimum pavement temperature of other three layers and the minimum air temperature (measured off-site) during the summer months. The same phenomenon is observed to a lesser degree in the winter months.
4. The difference between the maximum pavement temperature at a surface and the maximum pavement temperature of other three layers temperature is greatest during the summer months when the solar radiation is at its highest.



5. The maximum (or minimum) temperature in each layer occurs at different times from the maximum (or minimum) surface temperature with a time lag that increases with increasing depth from the surface.
6. Mean values of maximal daily temperatures are higher for pavement temperatures than air temperatures. Mean value of maximal daily surface temperature is the highest for four examined depths. Mean values of maximal daily temperatures for four depths decrease with distance from the surface. Same is for maximums of maximal daily air and pavement temperatures. Minimums of maximal daily air and pavement temperatures decrease with distance from the surface. Standard deviation of maximal air temperature is the lowest. Standard deviation of maximal surface temperature is the highest of four layers. Standard deviations of maximal daily temperatures for four layers decrease with distance from the surface, indicating less variation in deeper layers.
7. Mean values of minimal daily temperatures are higher for pavement temperatures than air temperatures. Mean value of minimal daily surface temperature is the lowest for four depths. Mean values of minimal daily temperatures for four depths increase with distance from the surface. Same is for maximums of minimal daily air and pavement temperatures. Minimums of minimal daily air and pavement temperatures increase with distance from the surface. Standard deviation of minimal air temperature is the lowest. Standard deviation of minimal C3 layer temperature is the highest of four depths. Standard deviations of minimal daily temperatures for C4 layer is the lowest of four depths, indicating less variation in deeper layers.
8. Standard deviations of maximal daily air and pavement temperatures are higher than standard deviations of maximal daily air and pavement temperatures indicating less variation in minimal than maximal temperatures.
9. A linear relationship exists between the maximal (and minimal) daily air temperature and the maximal (and minimal) daily pavement temperature at each of layers. Maximal (and minimal) daily pavement temperatures increase as maximal (and minimal) daily air temperature increase.
10. A linear relationship exists between the daily maximum (and minimum) surface temperature and the daily maximum (and minimum) pavement temperature of three deeper layers. Maximal (and minimal) daily pavement temperatures of three deeper layers increase as maximal (and minimal) daily surface temperature increase.
11. Maximal (minimal) daily pavement temperatures decrease with increase of latitude, decrease with increase of wind speed, and increase with increase of daily cumulative solar radiation.
12. Standard errors of estimate for maximal daily temperature for four depths are higher than standard errors of estimate for minimal temperatures, indicating less variation. Standard errors of estimate for maximal daily temperature are smaller for deeper layers, indicating less variation. Such pattern does not exist for minimal daily pavement temperatures.

13. Adjusted  $R^2$  are higher for minimal temperatures than for maximal temperatures, indicating better fit to the data.
14. The peak daily cumulative solar radiation was found to vary significantly with the month. Maximal and minimal daily pavement temperature can be predicted from local air temperature, day of the year, and cumulative solar radiation for any location. In addition, if the solar radiation measurement is not available, it may be calculated from local air temperature and the day of the year.
15. Comparison with the SHRP and LTPP models was made. SHRP and LTPP model overestimates maximal and underestimate minimal daily surface pavement temperatures both for the measured values and for predicted temperatures by the developed models. Therefore, the developed model is more representative of Libya's climatic conditions. SHRP and LTPP models would be expected to result in a different selection of the PG binder.

## 6.2 Findings - PG

Based on extensive field work conducted locally, the following can be stated:

1. The use of a 99% level of reliability provides additional safety margin against high traffic levels and uncontrolled loadings. No additional bumping of grade is needed as is recommended by AASHTO MP1 specifications since it will result in excessively stiff binder.
2. PG grading has been achieved on the basis of 50% , 85%, 95%,98% and 99% level of reliability. But practically 99.9% reliability is the most suitable to counter uncontrolled heavy loadings and slow moving vehicles.
3. Libya's desert area for wearing course layer of asphalt road pavement is divided into two temperature zones requiring PG 64-10 in zone 1 and PG 70-10 in zone 2, (Figure 6.3).
4. Libya's desert area for binder course layer of asphalt road pavement is divided into two temperature zones requiring PG 58-10 in zone 1 and PG 64-10 in zone 2, (Figure 6.4.)

## 6.3 Conclusions – temperature

Using regression analysis, models for predicting daily maximal and minimal pavement temperatures at different depths from air temperatures, day of the year, latitude, wind speed and cumulative solar radiation were made. Project pavement temperature models were based on data collected in 2012–2013.

1. The best model appeared to be the model including the air temperature, cumulative solar radiation and the day of the year.

a) The models for the maximal daily pavement temperatures at different depths.

Models are based on data from all eight locations and are dependent on latitude and four different depths from the surface.

Surface	$T_{pav,surf}^{max} = 24,14976 + 0,70367T_{air}^{max} + 0,21415Day - 0,00060Day^2 + 0,00004Cum\_SR - 0,47821Lat$
3cm	$T_{pav,3cm}^{max} = 14,33569 + 0,73859T_{air}^{max} + 0,19575Day - 0,00054Day^2 + 0,00004Cum\_SR - 0,26281Lat$
8cm	$T_{pav,8cm}^{max} = 19,04707 + 0,73432T_{air}^{max} + 0,18398Day - 0,00051Day^2 - 0,00001Cum\_SR - 0,46720Lat$
15cm	$T_{pav,15cm}^{max} = 11,37024 + 0,66200T_{air}^{max} + 0,17297Day - 0,00047Day^2 + 0,00007Cum\_SR - 0,29282Lat$

where

$T_{pav}^{max}$  =maximal pavement temperature, at certain depth °C;

$T_{air}^{max}$  = maximal daily air temperature, °C;

$Day$  =day of the year;

$Cum\_SR$ = cumulative solar radiation (W/m<sup>2</sup>); and

$Lat$ = latitude of the section, degrees.

b) The models for the minimal daily pavement temperatures at different depths.

Models are based on data from all eight locations and are dependent on latitude and four different depths from the surface.

Surface	$T_{pav,surf}^{min} = 1,013228 + 0,840467T_{air}^{min} + 0,033665Day - 0,000093Day^2 + 0,000026Cum\_SR + 0,079158Lat$
3cm	$T_{pav,3cm}^{min} = 8,947653 + 0,818129T_{air}^{min} + 0,053455Day - 0,000141Day^2 + 0,000012Cum\_SR - 0,221149Lat$
8cm	$T_{pav,8cm}^{min} = 13,31895 + 0,74725T_{air}^{min} + 0,08071Day - 0,00022Day^2 - 0,00001Cum\_SR - 0,32083Lat$
15cm	$T_{pav,15cm}^{min} = 13,77346 + 0,72141T_{air}^{min} + 0,08497Day - 0,00023Day^2 - 0,00000Cum\_SR - 0,28800Lat$

where

$T_{pav}^{min}$  =minimal pavement temperature, at certain depth(°C);

$T_{air}^{min}$ = minimal daily air temperature, (°C);

$Day$  =day of the year;

$Cum\_SR$ = cumulative solar radiation (W/m<sup>2</sup>); and

$Lat$  = latitude of the section, degrees.

The models which include depth from the surface.

The model to predict maximal daily pavement temperature at any depth from maximal daily air temperature, cumulative solar radiation, the day of the year, and latitude is:

$$T_{pav,d}^{max} = 24,14976 + 0,70972T_{air}^{max} - 0,66265d + 0,19170Day - 0,00053Day^2 + 0,00004Cum\_SR - 0,37526Lat$$

where

$T_{pav}^{max}$  = maximal pavement temperature at depth  $d$ , in (°C);

$T_{air}^{max}$  = maximal daily air temperature, (°C);

$Lat$  = latitude of the section, degrees;

$Cum\_SR$  = cumulative solar radiation (W/m<sup>2</sup>); and

$d$  = distance from the surface (cm).

The model to predict minimal daily pavement temperature from minimal daily air temperature, cumulative solar radiation, the day of the year and latitude is:

$$T_{pav,d}^{min} = 7,600962 + 0,781816T_{air}^{min} + 0,255748d + 0,063198Day - 0,000169Day^2 + 0,000005Cum\_SR - 0,187706Lat$$

where

$T_{pav}^{min}$  = minimal pavement temperature at depth  $d$ , in (°C);

$T_{air}^{min}$  = minimal daily air temperature, in (°C);

$Lat$  = latitude of the section, degrees;

$Cum\_SR$  = cumulative solar radiation (W/m<sup>2</sup>); and

$d$  = distance from the surface (cm).

2. Comparison with the SHRP and LTPP models was made. SHRP and LTPP model overestimates maximal and underestimate minimal daily surface pavement temperatures both for the measured values and for predicted temperatures by the developed models. Therefore, the developed model is more representative of Libya's climatic conditions. SHRP and LTPP models would be expected to result in a different selection of the PG binder.

## 6.4 Conclusions – PG

Based on the information collected from eight weather stations, high and low pavement temperatures were estimated for 98% and 99.9% level of reliability using prediction models based on collected data. Figures 6.3 and 6.4 presents PG grading which was determined in the analysis.

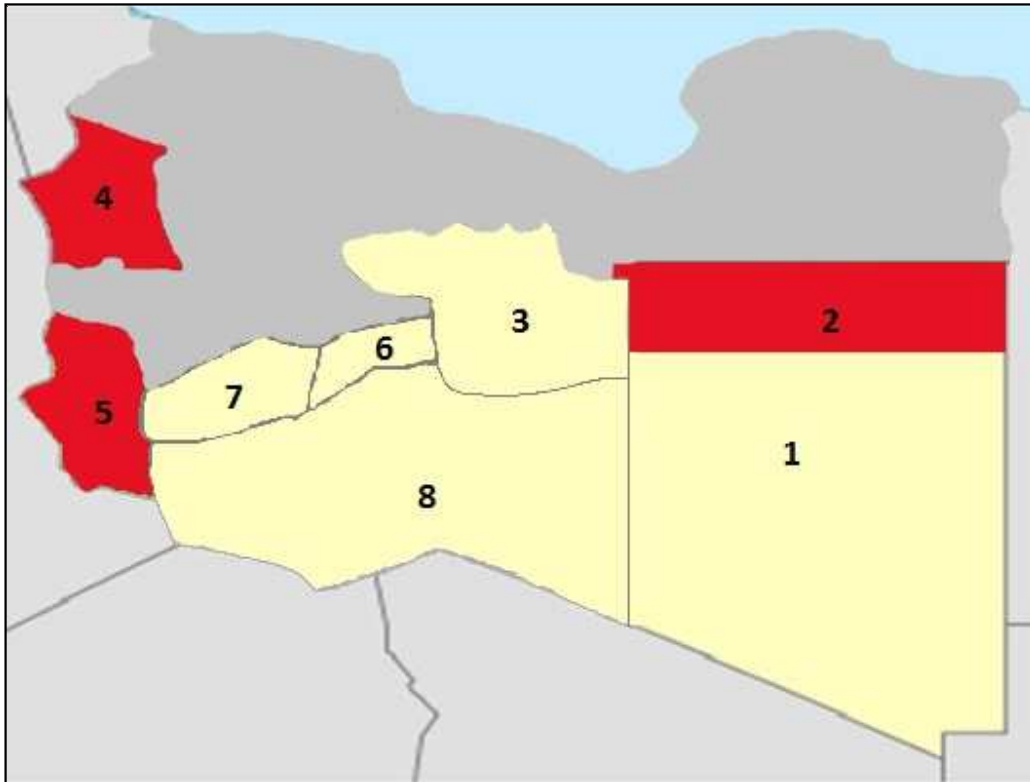


Figure 6.1 PG temperature zoning across Libya's desert area for wearing course layer

Legend:

PG 99.9% reliability		
1	Al Kufrah	64-10
3	Al Jufroh	64-10
6	Brak	64-10
7	Awbari	64-10
8	Al Qatrun	64-10
2	Awjilah	70-10
4	Ghadamis	70-10
5	Ghat	70-10
		Zone 1
		Zone 2

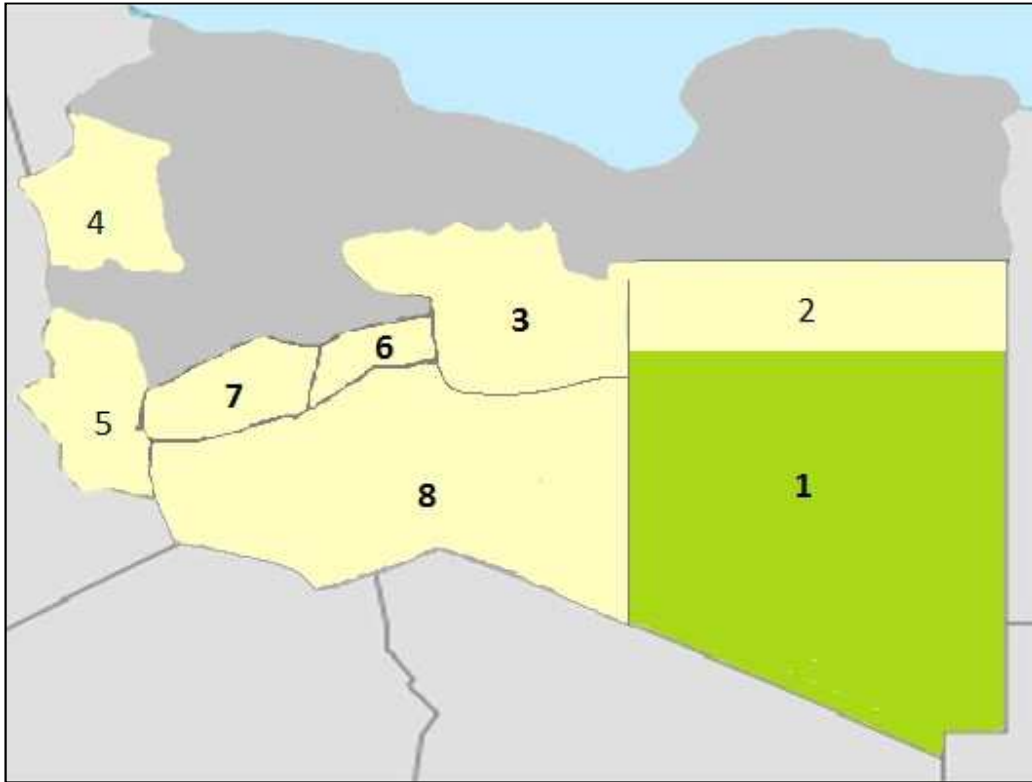


Figure 6.2 PG temperature zoning across Libya's desert area for binder course layer

Legend:

PG 99,9% reliability			
1	Al Kufrah	58-10	Zone 1
2	Awjilah	64-10	Zone 2
3	Al Jufroh	64-10	
4	Ghadamis	64-10	
5	Ghat	64-10	
6	Brak	64-10	
7	Awbari	64-10	
8	Al Qatrun	64-10	

## **Chapter 7 RECOMMENDATIONS**

Based on this study's results, the following recommendations are made:

The data set used to develop the model covered a period of 12 months. Incorporating data from a longer period of time is suggested to improve the accuracy of the developed models.

Additional weather stations should be established in different provinces of Libya for the collection of more comprehensive temperature data. This would result in a more ample performance grading system. Test sections should be constructed in different zones of the country using the proposed respective binder flavors to check their performance.

For the hotter zones of the country, asphalt should be modified using polymer to achieve PG 70-10, and PG 64-10; otherwise, problems of premature rutting and other pavement failures would continue by using conventional 60/70 grade binder.

Libya's asphalt refinery industry should adopt PG obtained in this study.

## REFERENCES

- Ahmed, A.Roffa, O., (2000) "The Evaluation of Pavement in Desert Region in Libya", 2<sup>nd</sup> Eurasphalt&Eurobitume Congress 2000, (The World Road Association, PIARC),Barcelona, Spain, 500-502.
- Ahmed, A.Roffa, O., (2002) "The Evaluation of Pavement in Desert Region in Libya", PhD, thesis, Brno, Czech Republic:90-96.
- Ahmed, A.Roffa, O., (2003) "Temperature Variation in Asphalt Pavement Layers in Libya", *Asfaltove Vozovky*, (Q-2003), Zilna, Slovak Republic, 46-51.
- Ahmed, A.Roffa, O., (2005)"Roads Construction in Libya", *Asfaltove Vozovky*, (Q-2005),Zilna, Slovak Republic, 53-58.
- Al-Abdul Wahhab, H.I. and Balghunaim, F.A., (1994) "Asphalt Pavement Temperature Related to Arid Saudi Environment," *J. of Materials in Civil Engineering*, American Society of Civil Engineers, 6 (1), pp. 1-14.
- Al-Abdul Wahhab, H.I., Asi, I.M., Al-Dubabe, A. and Ali, M.F., (1997) "Development ofPerformance Based Bitumen Specifications for the Gulf Countries," *Construction and Building Materials*, 11(1), pp.15-22.
- Ali, H. and A. Lopez, (1996) "Statistical Analysis of Temperature and Moisture Effects on Pavement Structural Properties Based on Seasonal Monitoring Data" *Transportation Research Record*, No. 1540, 48-55.
- Asi IM., (2007) "Performance evaluation of SUPERPAVE and Marshall Asphalt mix design to suit Jordan climatic and traffic conditions" *Constr Build Mater*; 21:1732–40.
- Andersland, O. B. and D. M. Anderson, (1978),"Geotechnical Engineering for ColdRegions". McGraw-Hill Co., New York, NY, 566p.
- Awadat H., Uzelac Dj., (2012) "Performance Evaluation Of Rubber Modified Asphalt Mixture In Hot Arid Climates", *ITC2012* (Oct 30- Nov 21, 2012, Kuala Lumpur, Malaysia).
- Awadat H., Matic D., Uzelac Dj., Matic B., (2014)"Temperature Zoning of Libya Desert for Asphalt Mix Design", *Applied Mechanics and Materials Vols. 638-640* (2014), pp. 1414-1426, Trans Tech Publications, Switzerland doi:10.4028/www.scientific.net/AMM.638-640.1414
- Awadat H., Matic D., Uzelac Dj., Lozanov-Crvenkovic Z., Matic B., (2014)"Development of a Model to Predict Pavement Temperature for Brak Region in Libya", *Applied Mechanics and Materials Vols. 638-640* (2014), pp. 1139-1148, Trans Tech Publications, Switzerland doi:10.4028/www.scientific.net/AMM.638-640.1139
- Awadat H., Uzelac Dj., Lozanov-Crvenkovic Z., (2014) "Development of a Model to Predict Pavement Temperature for Ghat Region in Libya", *Applied Mechanics and Materials Vols. 587-589* (2014), pp. 1115-1124, Trans Tech Publications, Switzerland doi:10.4028/www.scientific.net/AMM.587-589.1115
- Awadat H., Uzelac Dj., Lozanov-Crvenkovic Z., (2014) "Development of a model to predict



pavement temperature for Al Kufrah region in Libya" , 9<sup>th</sup> Asia Pacific conference on transportation and environment, Surilanka, 2014.

Brown R, Kandhal P, Zhang J., (2001)"Performance testing for hot mix asphalt, National Center for Asphalt Technology", Report No-05A, Auburn Univ., Alabama.

Barber, E. S., (1957) "Calculation of Maximum Pavement Temperatures from Weather Reports" Bulletin 168, Highway Research Board, National Research Council, 1-8.

Birgisson, B., J. Ovik, and D. E. Newcomb, (2000) "Analytical Predictions of Seasonal Variations in Flexible Pavements at the MnRoad Site" Transportation Research Record No. 1730, Transportation Research Board, 81-90.

Bosscher, P. J., Bahia, H. U., Thomas, S. and Russell, J. S., (1998) "The Relation Between Pavement Temperature and Weather Data: A Wisconsin Field Study to Verify the Superpave Algorithm," Transportation Research Record 1609, TRB, National Research Council, Washington, DC, pp. 1-11.

Christison, J. T., K. O. Anderson,(1972)"The Response of Asphalt Pavements to LowTemperature Climatic Environments", Proceedings of the 3rd International Conference on theStructural Design of Asphalt Pavements.

Diefenderfer, B.K., Al-Qadi, I.L., Reubush, S.D. and Freeman, T.E., (2002) "Development and Validation of A Model to Predict Pavement Temperature Profile," Presented at Transportation Research Board 82<sup>nd</sup> Annual Meeting, Washington DC.

Diefenderfer, B., (2002)"Moisture content determination and temperature profile modeling of flexible pavement structures", Doctor Dissertation, Faculty of the Virginia Polytechnic Institute and StateUniversity.

Geiger, R. (1965)"The Climate Near the Ground", Harvard University Press, Cambridge, MA, 611p.

Hermansson, A., (2000) "Mathematical Model for Calculation of Pavement Temperatures: Comparisons of Calculated and Measured Temperatures," Transportation Research Record 1699, TRB, National Research Council, Washington, DC, pp. 134-141.

Hermansson, A., (2001) "Mathematical Model for Calculation of Pavement Temperatures: Comparisons of Calculated and Measured Temperatures," Transportation Research Record 1764, TRB, National Research Council, Washington, DC, pp. 180-188.

Hsieh, C. K., C. Qin, E. E. Ryder.,(1989)"Development of Computer Modeling for Prediction of Temperature Distribution inside Concrete Pavements", Final Report to Florida Department of Transportation, Report Number FL/DOT/SMO/90-374.

Huber, G.A.,(1994)"Weather Database for the Superpave Mix Design System", SHRP-A-648A:139p

Huang, Y. H., (1993) "Pavement Analysis and Design" Prentice Hall, Englewood Cliffs, NJ, 805p

Inge, E.H., Jr., Y.R. Kim.,(1995)"Prediction of Effective Asphalt Layer Temperature" Transportation Research Record, 1473: 93-100.

- Kennedy T. et al., "Superior Performing Asphalt Pavements (Superpave): The product of the SHRP Asphalt Research Program", National Research Council, Washington, DC, 1994.
- Kreith, F. (1986) "Principles of Heat Transfer", 4<sup>th</sup> ed., Harper and Row, New York, NY, 700p.
- Liao, C.C., Department of Civil Engineering, National Central University, Jungli, Taiwan.
- Lukanen, E. O., Han, C. and Skok, E. L. Jr., (1998) "Probabilistic Method of Asphalt Binder Selection Based on Pavement Temperature", Transportation Research Record 1609, TRB, National Research Council, Washington, DC, pp. 12-20.
- Lytton, R. L., D. E. Pufahl, C. H. Michalak, H. S. Liang, and B. J. Dempsey, (1993) "An Integrated Model of the Climatic Effects on Pavements" FHWA Report RD-90-033, Federal Highway Administration, Washington DC, 304p.
- Mahoney, W.P. and W. Myers (2003) "Predicting Weather and Road Conditions: Integrated Decision Support Tool for Winter Maintenance Operations", Transportation Research Record, Journal of the Transportation Research Board 1824, pp. 98–105.
- Matić B., Tepić J., Sremac S., Radonjanin V., Matić D., Jovanović P., (2012) "Development and evaluation of the model for the surface pavement temperature prediction", Journal "Metalurgija", Croatian Metallurgical Society, Zagreb, Croatia, 51(2012)3, pp. 329-332, ISSN: 0543-5846.
- Matić B., Matić D., Radović N. (2012) "Model for pavement temperature prediction in Serbia", Building materials and structures No 54, Society for materials and structures testing of Serbia, Belgrade, ISSN: 0543-0798, UDK: 006.77:624.04.001.23:699.841(497.11+1) = 861, pp. 50-61.
- Matić, B., Awadat H., Matic D., Uzelac Dj., (2012) "Development and validation of a model to predict pavement temperature for winter maintenance operations in Serbia" 8<sup>th</sup> Asia Pacific conference on transportation and environment, Thailand.
- Matić, B., Matić, D., Ćosić Đ., Sremac S., Tepić G., Ranitović P., (2013) "A model for the pavement temperature prediction at specified depth". METABK 52(4) 505-508 (2013) UDC – UDK 62.001.57:536.5:625.144-111.
- Matić B., Radović N., Uzelac Đ., Matić D., (2013) "Modelling pavement temperature for optimum winter maintenance operations in Serbia", First International Scientific Professional Conference, "Modern Road Maintenance" Serbia, Arandelovac, November 7-9.
- Matić B., Matić D., Sremac S., Radović N., Viđikant P., (2014): A model for the pavement temperature prediction at specified depth using neural networks, Metalurgija, Journal "Metalurgija", Croatian Metallurgical Society, Zagreb, Croatia, 52(2013)4, pp. 505-508, ISSN: 0543-5846.
- Marshall, C., Meier, R.W. and Welsh, M., (2001) "Seasonal Temperature Effects on Flexible Pavements in Tennessee" Presented at Transportation Research Board 80th Annual Meeting, Washington, DC.
- Mohseni and Han., (1996) "LTPP Seasonal AC Pavement Temperature Models." FHWA-LTPP Division, McLean, VA.
- Mohseni, A., (1998) "LTPP Seasonal Asphalt Concrete (AC) Pavement Temperature Models,"

Report FHWA-RD-97-103, Federal Highway Administration, U.S. Department of Transportation, p. 71.

Mohseni, A. and Symons, M., (1998a) "Effect of Improved LTPP AC Pavement Temperature Models on Superpave Performance Grades," Presented at Transportation Research Board 77th Annual Meeting, Washington, D.C.

Mohseni, A. and Symons, M., (1998b) "Improved AC Pavement Temperature Models from LTPP Seasonal Data," Presented at Transportation Research Board 77th Annual Meeting, Washington, D.C.

Noss, P.M., (1973) "The Relationship Between Meteorological Factors and Pavement Temperature", Symposium on Frost Action on Roads Conference Paper, pp. 77-87.

Ovik, J. M., B. Birgisson, D. E. Newcomb, (1999) "Characterizing Seasonal Variations in Flexible Pavement Material Properties", Transportation Research Record No. 1684, Transportation Research Board, 1-7.

Park, D., N. Buch, K. Chatti, (2001) "Development of Effective Layer Temperature Prediction Model and Temperature Correction Using FWD Deflections", Presented at Transportation Research Board 80th Annual Meeting, Washington, DC, Jan.

Roberston, W.D., (1997) "Determining the Winter Design Temperature for Asphalt Pavements", Association of Asphalt Paving Technologists, Vol. 66, 312-343.

Roffa, A.A.O., Farhat Perma, link: <http://dx.doi.org/10.1061/9780784412671.0036> ASCE Subject Headings: Climates, Pavements, Deterioration, Libya © 2013 American Society of Civil Engineers.

Rumney, T. N. and R. A. Jimenez, (1969) "Pavement Temperatures in the Southwest." Highway Research Record No. 361, National Research Council, 1-13.

Solaimanian, M., Bolzan, P., (1993) "Analysis of the Integrated Model of Climatic Effects on Pavements: Sensitivity Analysis and Pavement Temperature Prediction" SHRP-A-637

Solaimanian, M. Kennedy, T.W., (1993) "Predicting Maximum Pavement Surface Temperature Using Maximum Air Temperature and Hourly Solar Radiation", Transportation Research Record 1417, TRB, National Research Council, Washington, DC, pp. 1-11.

Solaimanian, M., Kennedy, T.W., (1995) "Analysis of the Integrated Model of Climatic Effects on Pavements", SHRP-A-637: 158pp.

Shao, L., Park, S.W. and Kim, Y.R., (1997) "A Simplified Procedure for Prediction of Asphalt Pavement Subsurface Temperatures Based on Heat Transfer Theories", Transportation Research Record 1568, TRB, National Research Council, Washington, DC, pp. 114- 123.

Southgate, Deen, (1969) "An Evaluation of Temperature Distribution Within Asphalt Pavements and its Relationship to Pavement Deflection", 129pp.

Strategic Highway Research Program, National Research Council. Binder characterization and evaluation. Test methods. SHRP-A- 370, vol. 4, Washington, DC; 1994.

Straub, A. L., H.N. Schenck Jr., F.E. Przybycien (1968) "Bituminous Pavement Temperature Related to Climate", Highway Research Record, 256: 53-77.

Stoll, T. M. and Evstratov, G.I., (1987) "Building in hot climate", Mir Publishers, Moscow, pp. 9-13.

Thomas, Suwitho (1997) "Investigation of Modified Asphalt Performance Using SHRP Binder Specification", Master of Science Thesis, Civil and Environmental Engineering, University of Wisconsin-Madison.

Williamson, R.H.,(1972) Effects of Environment on Pavement Temperatures, International Conference on Structural Design Proceedings, pp. 144-158.

James, G., Witten, D., Hastie, T., Tibshirani, T., (2013) "An Introduction to Statistical Learning with Applications in R", Springer New York Heidelberg Dordrecht London.

Wolfe, R. K., G. L. Heath, D. C. Colony (1987)"Time-Temperature Model Laboratory and Field Validation", The University of Toledo, Report to The Ohio Department of Transportation.

Yavuzturk C., Ksaibati K., (2002)"Assesment of temperature fluctuations in asphalt pavements due to thermal environmental condition using a two-dimensional transient finite difference approach", Department of Civil and Architectural Engineering, University of Wyoming.

Yuan Xun Zheng et al., (2011), Advanced Materials Research, pp. 243-249, 506.

StatSoft Inc. STATISTICA (data analysis software system), v.12; 2012. Available from: [www.statsoft.com](http://www.statsoft.com).